UNIVERSIDAD AUTÓNOMA DE MADRID

DEPARTAMENTO DE BIOQUÍMICA

Identification of signaling pathways and specifically miRNAs altered in familial and sporadic forms of medullary thyroid tumors

Doctoral Thesis

Agnieszka Maliszewska

Madrid, 2012

BIOCHEMISTRY DEPARTMENT

FACULTY OF MEDICINE

AUTONOMA UNIVERSITY OF MADRID

Identification of signaling pathways and specifically miRNAs altered in familial and sporadic forms of medullary thyroid tumors

Agnieszka Maliszewska

Thesis co-directors

Dr. Mercedes Robledo Batanero

Dr. Xavier Matías-Guiu Guia

HEREDITARY ENDOCRINE CANCER GROUP

HUMAN CANCER GENETICS PROGRAMME

SPANISH NATIONAL CANCER RESEARCH CENTRE

La Dra. Mercedes Robledo Batanero, Jefe del grupo Cáncer Endocrino Hereditario del Centro Nacional de Investigaciones Oncológicas (CNIO), como Profesora Honoraria del Departamento de Biología Molecular de la Universidad Autónoma de Madrid

y

el Dr. Xavier Matías-Guiu Guia, Catedrático/ Jefe de Servicio de Anatomía Patológica/Director Científico de la Universidad de Lleida/Hospital Universitario Arnau de Vilanova/ Instituto de Investigación Biomédica de Lleida (IRBLLEIDA),

en calidad de co-Directores,

CERTIFICAN:

que la tesis doctoral titulada ***"Identification of signaling pathways and specifically miRNAs altered in familial and sporadic forms of medullary thyroid tumors"***, ha sido realizada en el Centro Nacional de Investigaciones Oncológicas y tutelada en el Departamento de Bioquímica de la Facultad de Medicina de la Universidad Autónoma de Madrid.

En nuestra opinión, la tesis realizada por **Agnieszka Maliszewska** reúne todas las condiciones requeridas por la legislación vigente y la originalidad y calidad científica para poder ser presentada y defendida con el fin de optar al grado de Doctor.

Y para que conste donde procesa, firman el presente certificado.

Madrid, 23 de Julio de 2012

V° B° de la co-Directora de la Tesis:
Dra. Mercedes Robledo Batanero

V° B° del co-Director de la Tesis:
Dr. Xavier Matías-Guiu Guia

Dra. Pilar Santisteban, Investigadora del Instituto de Investigaciones Biomédicas Investigaciones Biomédicas Alberto Sols, CSIC-UAM y como la Tutora de la Tesis

CERTIFICA:

Que Doña Agnieszka Maliszewska, ha realizado la presente Tesis Doctoral titulada **"*Identification of signaling pathways and specifically miRNAs altered in familial and sporadic forms of medullary thyroid tumors*"**, en el Centro Nacional de Investigaciones Oncológicas y que en su juicio, reúne plenamente todos los requisitos necesarios para optar al **Grado de Doctor**, a cuyos efectos será presentado en la Universidad Autónoma de Madrid.

Y para que conste se extiende el presente certificado,

Madrid, 23 de Julio de 2012

V^{o} B^{o} de la Tutora de la Tesis:
Dra. Pilar Santisteban

This thesis work was carried out at the Spanish National Cancer Research Centre (CNIO) in Madrid from 2008-2012; under the supervision of Dr. Mercedes Robledo-Batanero and Dr. Xavier Matías-Guiu Guia

The following fellowships and scientific projects have permitted the realization of this thesis.

- Fellowship for "la Caixa"/CNIO International PhD Programme in Biomedicine from 2008-2012
- Grant from the Fundación Mutua Madrileña (project AP2775/2008 to MR)
- Grant from the Fondo de Investigaciones Sanitarias (project PI080883 to MR),
- The Spanish Ministry of Science and Innovation MICINN (BFU2010-17628 to ME)
- Grants 2009SGR794, RD06/0020/1034 and the programa de intensificación de la investigación, Instituto Carlos III.

I wish to dedicate my PhD thesis to my parents and my lovely grandmother for their unconditional love and support

Acknowledgements

I would like to thank all the people thanks to whom I get so far and this PhD thesis was possible to defend and my parents for their unconditional love and support.

Table of Contents

Table of Contents

Abbreviations

3´UTR - 3´ Untranslated region

ARTN - artemin

ATA - American Thyroid Association

ATC - Anaplastic Thyroid Carcinoma

ATCC - American True Type Culture Collection

BAY 43-9006 - Sorafenib (Nexavar)

bp - base pairs (i.e. amplicon length)

BrdU - Bromodeoxyuridine (5-bromo-2'-deoxyuridine)

CAD - mouse neuroblastoma cell line

cAMP - cyclic adenosine monophosphate

***CD133 (PROM1)* / CD133 (PROM1)** - prominin 1 (gene/protein)

cDNA - complementary DNA

CEA - carcinogenic embryonic antigen

CLA - Cutaneous Lichen Amyloidosis

CMV - cytomegalovirus

cRNA - complementary RNA

CT - computed tomography

Cy3 - cyanine 5

Cy5 - cyanine 5

DEGs - differentially expressed genes

DKK4 - Dickkopf-4

DMEM - Dulbecco's Modified Eagle Medium

DNA -Deoxyribonucleic acid

dNTPs - deoxyribonucleotide triphosphateses

Dok1 - downstream of tyrosine kinase 1

dUTP - deoxyuridine triphosphate

EGFR - Epidermal growth factor receptor

EMT - epithelial-mesenchymal transition

ENS - enteric nervous system

Erk - Ras/extracelluar signal regulated kinase

ES - enrichment score

ESM1 **/ ESM1** - endothelial cell-specific molecule 1 (gene/protein)

FDA - Food and Drug Administration

FDR - False Discovery Rate (q value)

FFPE - formalin fixed paraffin embedded

FMTC - Familial Medullary Thyroid Carcinoma

FTA - Follicular Thyroid Adenoma

FTP - Follicular Thyroid Carcinoma

GAL - galanin 1

GAPDH - Glyceraldehyde 3-phosphate dehydrogenase

GDNF - gial cell line-derived neutrotropic factor

GEO - Gene Expression Omnibus

GEPAS - Gene Expression Profile Analysis Suite

GFRα1 **/ GFRα1** - GDNF family receptor alpha 1 (gene/protein)

GO - Gene Ontology

GSEA - Gene Set Enrichment Analysis

GUS - β-glucoronidase

H&E - haematoxylin-eosin

HPT - Hyperparathyroidism

HSCR - Hirschprung´s disease (Congenital Megacolon)

IHC - immunohistochemistry

IL1R - interleukin 1 receptor, type I

IPA - Ingenuity Pathway Analysis

IRS-1 - insulin receptor substrate-1

JAK - Janus kinase

JNK - c-Jun N-terminal kinase

KEGG - Kyoto Encyclopedia of Genes and Genomes

KREMEN2 - kringle containing transmembrane protein 2

LOXL2 - lysyl oxidase-like 2

MAGIA - MiRNA And Genes Integrated Analysis web tool

MAPK - Mitogen-activated protein kinase

MEN2 - Multiple Endocrine Neoplasia type 2

MEN2A - Multiple Endocrine Neoplasia type 2A (Sipple´s syndrome)

MEN2B - Multiple Endocrine Neoplasia type 2B

MET - hepatocyte growth factor receptor

miRNA - microRNA

MRI - contrast-enhanced magnetic resonance imaging

mRNA - messenger RNA

MTC - Medullary Thyroid Carcinoma

MTC^{WT} (S_WT) - sporadic MTC with no RET mutation

MTT - Dimethyl thiazolyl diphenyl tetrazolium salt

MZ-CRC-1 - MTC cell line harboring the M918T RET mutation

NES - normalized enrichment score

NFκB - nuclear factor kappa-light-chain-enhancer of activated B cells

NIH3T3 - mouse fibroblast cell line

NPR1 - natriuretic peptide receptor A/guanylate cyclase A

NTN - neurturin

oligo dT - a short single-stranded sequence of deoxythymine (dT)

ORF - open reading frame

p.M918T - specific mutation, a substitution of a Methionine to Threonine at 918 residue

P19 - mouse embryonal tumor cell line

p53 - protein 53

PC12 - rat pheocromocytoma cell lines

PCC - Pheochromocytoma

PDTC - Poorly Differentiated Thyroid Carcinoma

PET - positron emission tomography

PI3K - phosphatidylinositol 3-kinase

PITX2 - paired-like homeodomain 2

PLCγ - phospholipase C gamma

PPIA - peptidylprolyl isomerase A

PSP - persephin

PTC - Papillary Thyroid Carcinoma

RET **/RET** - REaranged during Transfection (gene/protein)

***RET*^{634} (F_634, MTC^{634})** - familial MTC with 634 RET mutation

***RET*^{918} (S_918, MTC^{918})** - sporadic MTC with somatic M918T RET mutation

RIN - RNA Integrity Number

RNA - Ribonucleic acid

RNAi - RNA interference

RPI-1 - RET inhibitor, Ras-cAMP Pathway Inhibitor

RPLP0 - 60S acidic ribosomal protein P0

RTK - receptor tyrosine kinase

RTN1 - reticulon 1

RT-qPCR - Real time quantitative PCR

SAM - Significance Analysis of Microarrays

SD - standard deviation

siRNA - short interfering RNA

sMTC - sporadic MTC

STAT - Signal Transducer and Activator of Transcription

SU11248 - Sunitinib (Sutent)

TGF-β - Transforming growth factor beta

TKI - tyrosine kinase inhibitor

Tm - melting temperature

TMA - tissue microarray

TNM - Classification of Malignant Tumours

TSCs - tumor stem cells

TT - MTC cell line harboring the RET634 mutation

XL184 - Cabozantinib (Exelixis)

ZD6474 -Vandetanib (Zactima)

Abstract/Resumen

Medullary thyroid carcinoma (MTC) accounts for around 2-5% of all thyroid malignancies. From these, around 25% are inherited forms attributable to germline *RET* mutations, and 75% are sporadic MTCs, with or without somatic mutation in the same *RET* proto-oncogene. Although the genotype-phenotype correlation related to specific germline *RET* mutations is well established, the knowledge of pathways specifically associated with each mutation, as well as to non-*RET* related sporadic MTC still remain largely unknown. Gene expression and microRNA patterns have provided a robust tool to identify molecular events related to specific tumor types and to different clinical features that could help to identify novel targets for therapy.

Based on gene expression and microRNA profiling from an outstanding series of tumors, it was possible to identify differences between sporadic and familial MTCs. Specifically, *PROM1 (*also called *CD133)*, *LOXL2*, *GFRA1* and *DKK4* over-expression were related to RET^{M918T}, while *GAL* was associated with RET^{634} mutation. Pathway enrichment analysis pointed to Wnt, Notch, NFκB, JAK/Stat and MAPkinase signaling as related to MTC^{M918T} group. The immunohistochemical assessment of ESM1, GFRA1 and CD133 only revealed a marginal association of the M918T group with CD133 protein over-expression. The lack of validation at protein level could be due to other underlying mechanism, such as posttranscriptional modifications conducted by microRNAs.

Based on the *in vitro* functional studies, we observed that PROM1 or CD133 is significantly expressed in MZ-CRC-1 cell lines harboring M918T *RET* mutation comparing to TT cell line model with RET^{634}. On the other hand, silencing CD133 by siRNA induced apoptosis in MZ-CRC-1. CD133 confers resistance to death by apoptosis, but does not imply a selective advantage on proliferation. To our knowledge this is the first time that PROM1 or CD133 overexpression is reported among primary tumors. This finding could lead to the identification of novel therapeutic targets.

The miRNome analysis revealed a downregulation of miR-30a, and miR-138 associated with MTC^{M918T} group, and miR-124 with MTC^{C634X}. These results were validated in independent series of frozen and FFPE series. Furthermore, mRNA-miRNA integration data on the same frozen MTC sample series pointed to inversely correlated miR-30a and *PROM1* among MTC^{M918T} group.

In summary, this study has allowed us to identify genes and microRNAs that could be used as markers related to specific genetic conditions in MTCs, and that could be taken into account as future therapeutic targets.

El Carcinoma Medular de Tiroides (CMT) representa el 2-5% de los carcinomas tiroideos. De éstos, en torno al 25% son formas familiares y atribuibles a mutaciones germinales en *RET*, y el 75% restante son esporádicos, con o sin mutación somática en el mismo gen. Aunque la correlación fenotipo-genotipo asociada a mutaciones germinales específicas de *RET* está bien establecida, no se conoce qué rutas están alteradas ante una mutación concreta en el tumor, ni tampoco aquellas implicadas en el desarrollo del tumor en ausencia de mutación somática en *RET*. El análisis de patrones de expresión génica y de microRNAs ha demostrado ser una herramienta robusta para identificar marcadores relacionados con subtipos tumorales o características clínicas, de modo que podría ayudar en la identificación de nuevas dianas terapéuticas.

En este trabajo, basándonos en el perfil transcripcional y de microRNAs de una colección sobresaliente de CMTs, fue posible identificar diferencias en los patrones moleculares de CMT familiares y esporádicos. En particular, la sobre-expresión de *PROM1 (*también llamado *CD133)*, *LOXL2*, *GFRA1* y *DKK4* se asoció a la mutación M918T, y la de *GAL* a mutaciones que afectaban el residuo 634. El análisis de enriquecimiento de rutas apuntaba a que la señalización dirigida por Wnt, Notch, NFκB, JAK/Stat y MAP-quinasas se relacionaba con los CMT^{M918T}. La evaluación inmunohistoquímica de ESM1, GFRA1 y CD133 reveló únicamente una asociación marginal entre sobre-expresión de CD133 y la presencia de la mutación M918T. La falta de validación podría deberse a modificaciones postranscripcionales llevadas a cabo por microRNAs.

Basándonos en estudios funcionales *in vitro*, se observó que PROM1 estaba significativamente expresado en la línea celular MZ-CRC-1, portadora de la mutación RET^{M918T}, en comparación con la línea celular TT, portadora de una mutación en RET^{634}. Por otro lado, se observó que el silenciamiento de CD133 con siRNAs inducía apoptosis en la línea MZ-CRC-1. Esto permitía concluir que la sobre-expresión de *CD133* confiere resistencia a apoptosis, y no implica ventaja selectiva en la proliferación. Esta es la primera vez que se describe sobre-expresión de *PROM1* en tumores primarios. PROM1 podría tenerse en cuenta como una nueva diana terapéutica.

El análisis del Miroma reveló una baja expresión del miR-30a y miR-138 asociada a CMT^{M918T}, y de miR-124 a CMT^{C634X}, y se validó en una serie independiente de CMTs. La integración mRNA-microRNA de los mismos tumores identificó una relación inversa entre el miR-30a y *PROM1* en los tumores con RET^{M918T}.

En resumen, hemos identificado genes y microRNAS que podrían ser utilizados como marcadores asociados a mutaciones específicas de *RET*, a tener en cuenta como futuras dianas terapéuticas.

Introduction

1. Thyroid carcinoma

Among endocrine system malignancies, thyroid tumors are the most common and they account for about 1% of all diagnosed cancer cases(Ferlay 2010). The thyroid carcinoma occurs between 20-50 years of age with incidence rate is from 0.5 to 10 cases per 100.000 individuals (DeLellis 2004). The thyroid gland is composed of two different types of cells: the follicular and the parafollicular or C-cells. Among the tumors derived from the former cells, the principal histological subtypes are papillary thyroid carcinoma (PTC), follicular thyroid carcinoma (FTP), poorly differentiated thyroid carcinoma (PDTC), anaplastic thyroid carcinoma (ATC), and the unique benign tumor, the follicular thyroid adenoma (FTA)(DeLellis 2004).

Medullary thyroid carcinoma (MTC), the subject of the present doctoral thesis, arises from C-cells, that have a neural-crest origin (DeLellis 2004) and produce calcitonin, a hormone that plays an important role in calcium blood homeostasis. C-cells producing calcitonin, whose levels are used as a diagnostic marker, account for only up to 1% of the thyroid mass, mainly concentrated in the posterior upper third of the gland (Khurana, et al. 2004b).

MTC is an infrequent neoplasia, which accounts for approximately 2-5% of all thyroid malignancies(Randolph 2000) and is characterized by a solid mass of polygonal shaped cells with frequently observed amyloid deposition. MTC disseminate locally in 50% of cases to cervical and mediastinal nodal groups and up to 20% to distant organs such as lungs, bones or liver (DeLellis 2004).

Around 75% of cases are sporadic in nature, while the remaining 25% are hereditary and associated with the multiple endocrine neoplasia type 2 syndrome (MEN 2, OMIM #171400). The major player in MTC development is the *RET* proto-oncogene, whose germline and somatic mutations are responsible for most of familial and sporadic cases respectively (Hofstra, et al. 1994; Mulligan, et al. 1993b), although recently there have also been cases reported with *BRAF* and *RAS* mutations (Goutas 2008; Moura, et al. 2011).

1.1 Multiple Endocrine Neoplasia type 2 (MEN 2) syndrome and general background

This disease has a prevalence of 1:30.000(Marsh 2002) and dominant autosomal inheritance, with a variable clinical expression pattern, and almost complete penetrance depending on the specific *RET* mutation, as will be further reviewed in this introduction. Inherited MTC cases are

characterized mainly by their multifocal and bilateral character. It manifests at an early age, and mostly accompanied by C-cell hyperplasia (CCH) (LiVolsi 1997). Sporadic forms emerge from unifocal clonal tumor cell population(Eng 1999), and are generally not associated with CCH(Hayashida, et al. 1993).

Until 1993, when the *RET* gene (REarranged during Transfection) was found to be specifically associated with MEN 2(Mulligan et al. 1993b), management and diagnosis of patients with hereditary MTC and their relatives were based on basal and stimulated levels of calcitonin. Nowadays genetic analysis is the most sensitive and specific tool in MEN 2 diagnostics and the risk of performing a prophylactic thyroidectomy in a normal individual is no longer a concern (Hoff, et al. 2010).

According to clinical presentation, MEN 2 syndrome can be subdivided into three different subtypes: multiple endocrine neoplasia type 2A (MEN 2A; OMIM #171400), multiple endocrine neoplasia type 2B (MEN 2B; OMIM#162300) and familial medullary thyroid carcinoma (FMTC; OMIM#155240). All of them (Table1) are associated with high risk of MTC development (in more than 90% of affected individuals). Pheochromocytoma (PCC) manifests in 50% of patients with MEN 2A and MEN 2B, while hyperparathyroidism (HPT), due to parathyroid hyperplasia or adenoma, occurs in approximately 20-30% in MEN 2A individuals(Eng, et al. 1996a). In addition to MTC and PCC, affected MEN 2B patients develop a typical phenotype that includes a marphanoid habitus, thickened lips, as well as ganglioneuromas in the mucosa and gastrointestinal tract(Skinner, et al. 1996).

MEN 2A. This subtype constitutes 70%-80% of cases of MEN 2, MTC generally being the first manifestation of this subtype. Up to 70% of patients develop cervical lymph node metastases(Cohen and Moley 2003). PCC in MEN 2A are diagnosed at an early age and have subtler symptoms, while HPT is typically mild with no symptoms(Brandi, et al. 2001). There are also some cases with MEN 2A having cutaneous lichen amyloidosis (CLA), located over the upper portion of the back and may appear before the onset of MTC(Seri, et al. 1997).

FMTC. This subtype constitutes approximately 10%-20% of cases of MEN 2. By definition MTC is the only clinical manifestation in this subtype. The age of onset of MTC is later in FMTC and the penetrance of the disease is lower than that observed in MEN 2A and MEN 2B (Eng et al. 1996a). In fact, after ATA (American Thyroid Association) recommendations in 2009, FMTC is typically

considered as a variant of MEN 2A with decreased penetrance of PCC and HPT, rather than an isolated subtype(Kloos 2009).

Table 1. Clinical features of MEN2 syndrome. Modified from (Pierotti, et al. 2004).

MEN 2 syndrome type	Characteristic features
MEN 2A	MTC (95%) PCC (50%) Parathyroid hyperplasia/adenoma (20-30%)
FMTC	MTC (100%)
MEN 2A with cutaneous lichen amyloidosis	MEN 2A and cutaneous lesions
MEN 2A/FMTC with Hirschprung´s disease	MEN 2A/FMTC with intestinal ganglionosis
MEN 2B	MTC (100%) PCC (50%) Intestinal/mucosal ganglioneuromatosis Habitus marfanoid

MEN 2B. The MEN 2B subtype constitutes around 5% of cases of MEN 2. It is characterized by the early age of the tumor development and shows the highest transforming capacity among all MTC forms(Skinner et al. 1996). Individuals with MEN 2B who do not undergo thyroidectomy at an early age (less than 1 year) are prone to develop metastatic MTC in childhood. PCC occur in 50% of the MEN 2B cases, while HPT is absent or very rare. Pediatric patients with MEN 2B are mostly identified in early childhood by the presence of mucosal neuromas on the anterior dorsal surface of the tongue, palate, or pharynx and a distinctive facial appearance.

2. *RET* proto-oncogene

RET (REarranged during Transfecion) is a receptor tyrosine kinase (RTK) implicated in nervous system development, kidney morphogenesis and spermatogenesis. It was originally identified as an oncogene activated by DNA rearrangement in a transformation experiment, were NIH3T3 cells were transfected with DNA from human T cell lymphoma(Takahashi 1985).

2.1 RET structure and protein

RET gene in humans is located on chromosome 10q11.2, is about 50 kb and contains 21 exons (Pasini, et al. 1995). Due to alternative splicing, there are three different RET isoforms, RET9, 43 and RET51, that differ at C-terminus. Only two of them are main products in vivo, RET9 and RET51 (Arighi et al., 2005). RET, being a typical receptor tyrosine kinase (RTK), is a single-pass transmembrane protein which comprises extracellular, transmembrane, and cytoplasmic domains (Figure 1). More specifically, it consists of two extracellular domains (four cadherin-like regions in tandem and a cystein-rich domain), one transmembrane, and two intracellular tyrosine kinase domains. RET is a functional receptor for neurotrophic ligands of the gial cell line-derived neutrotropic factor (GDNF) family (Figure 1), composed by GDNF, neurturin (NTN), artemin (ARTN) and persephin (PSP)(Santoro, et al. 2004a). These ligands require the recruitment of co-receptors with high-affinity [GFRα1-4] to be able to bind directly to the RET receptor for full activation and the signal transduction (Figure 1).

2.2 Activation mechanism of RET

To date, there are two accepted mechanisms for RET dependent pathways activation that involve the binding between GFL, GFRα and RET (Figure 1). The first suggests GFL association with the GFRα in the first turn to form a complex with one GFL molecule and a GFRα homodimer. This complex further recruits two RET molecules into the lipid raft leading to trans-phosphorylation of the tyrosine residues in RET and the signaling pathways are being triggered (Airaksinen et al., 1999). The second is based on the pre-associated complex between GFRα and RET being formed first and providing a docking site for the subsequent binding of the GFL (Manie et al., 2001).

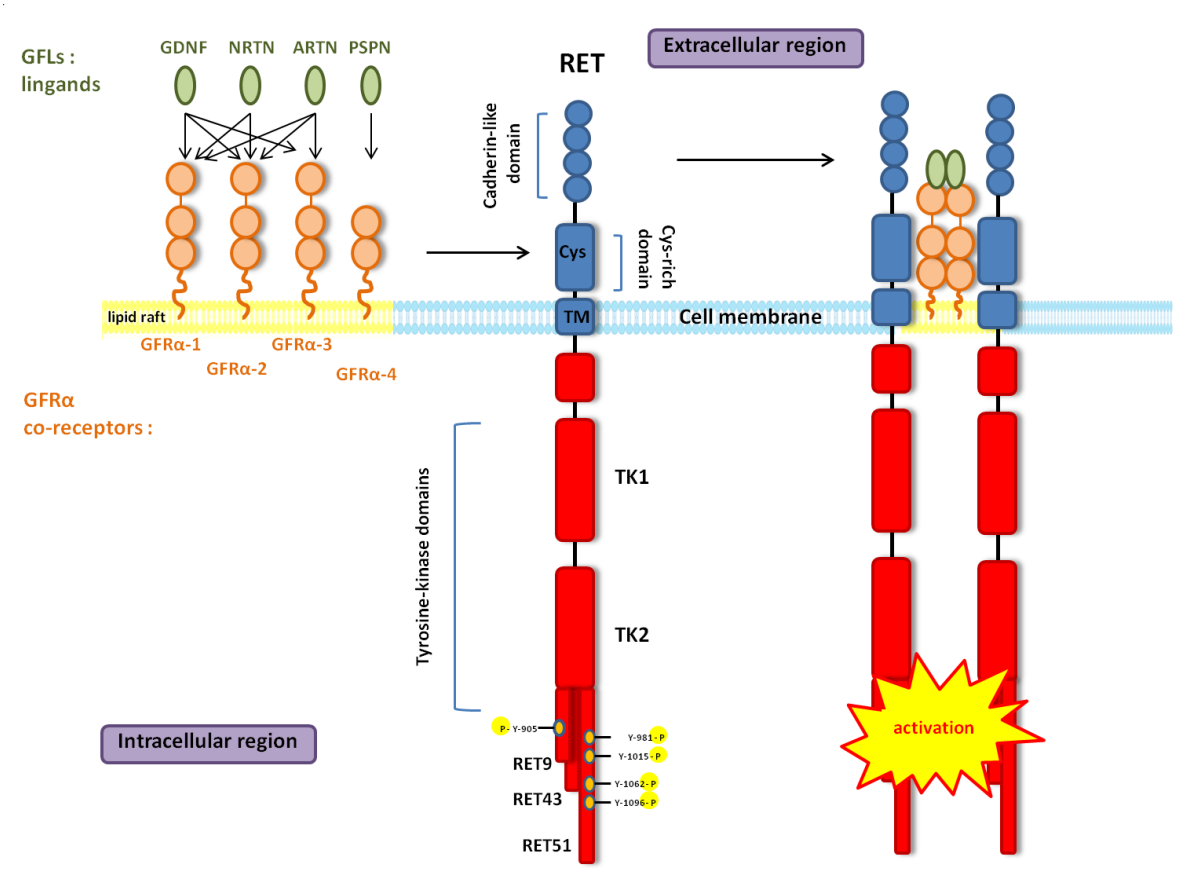

Figure 1. RET protein structure and mechanism of activation.

2.3 Signaling pathways

RET, similar to the other RTKs, is regulated by phosphorylation at specific tyrosine residues, which promotes the signal. Upon ligand stimulation and receptor association, RET undergo dimerization and trans-phosphorylation occurs on specific tyrosine residues, which serve as docking sites for other signaling proteins. Little is known regarding the specific *RET* mutation-driven signaling pathways and the molecular behavior of non-*RET* mutated (wild type) cases still remains unclear. Basically, wild-type RET, MEN 2A-related RET (RET/MEN 2A), FMTC-related RET (RET/FMTC), and MEN 2B-related RET (RET/MEN 2B) display differences in phosphorylation of docking sites and isoforms of the RET receptor, triggering specific intracellular signaling cascades (de Groot, et al. 2006).

It is known that RET can activate various well-known RTK pathways including those of Ras/extracelluar signal regulated kinase (Erk), phosphatidylinositol 3-kinase (PI3K)/Akt, p38 mitogen activated protein kinase (MAPK), c-Jun N-terminal kinase (JNK) and PLCγ(Arighi, et al. 2005a; Ichihara, et al. 2004). Activation of Ras/Erk pathways is important for neuronal survival and differentiation(Califano, et al. 2000). PI3K/Akt signaling pathway leads to the transformation potential of RET in Rat1 fibroblast cell line and plays role in cell survival and proliferation in neurons (Segouffin-Cariou and Billaud 2000). The JNK pathway contributes to the tumorigenic activity of RET in neuroblastoma tumor cell lines (Marshall, et al. 1997), while the PLCγ pathway is required for full oncogenic activation of RET in the mouse fibroblast cell line, NIH3T3 (Borrello, et al. 1996).

There are several sites recognized by adaptor proteins (Figure 1). Among them, phosphorylated Tyr905, 981, 1015, 1062 and 1096 are the most important ones(Encinas, et al. 2004; Ichihara et al. 2004). Tyr1096 is present only in RET43 and RET51 splicing variants, while Tyr1062 acts as the binding motifs of RET51 and RET9. Consequently the signaling cascades mediated by RET51 and RET9 will show discrepancy (Kurokawa, et al. 2003). Moreover, it has been shown that besides the tyrosine residues, phosphorylation at the serine 696 residue also plays a role in RET signaling (Fukuda, et al. 2002).

2.3.1 Tyrosine 1062 residue

Extensive studies have shown the importance of Tyr1062 in the cellular transformation capacity of RET, and as a docking site for the multiple adaptor proteins, including Shc, FRS2, downstream of tyrosine kinase 1(Dok1), Dok4/5, insulin receptor substrate-1 (IRS-1), enigma, and Rai, Shank3 and PKCα(Arighi et al. 2005a; Kurokawa et al. 2003).

Phosphorylated Tyr1062 interacting with Shc by recruiting Grb2/Sos (Besset, et al. 2000) or Grb2/Gab(Hayashi, et al. 2000) protein complexes underlay its dual function. Association with Grb2/Sos activates the Ras/Erk pathway(Besset et al. 2000), while connection of this phosphorylated tyrosine with Grb2/Gab triggers PI3K/Akt signaling pathway (Hayashi et al. 2000).

It was demonstrated that both, Ras/Erk and PI3K/Akt, are important for the activation of the transcription factors CREB and NFκB, respectively(Hayashi et al. 2000) and crucial for PC12 cells survival(De Vita, et al. 2000). Regarding another protein adaptor, Dok1, it was demonstrated that its binding leads to JNK pathway activation and at the same time suppresses the Ras/Erk signaling

pathway (Murakami, et al. 2002), while the Dok4/5 enhances it. IRS-1 competes with Shc to the Tyr1062 binding and triggers to the activation of PI3K/Akt pathway (Melillo, et al. 2001). A member of the Shc-like proteins family, Rai, was found to play an important role in Ras/Erk and PI3K/Akt signaling pathways activation (Pelicci, et al. 2002). The enigma protein, which interacts with RET9 (Borrello, et al. 2002) is required for the activation of Ras/Erk signaling pathway (Durick, et al. 1998). Shank3 mediates sustained Ras/Erk and PI3K/Akt signaling (Schuetz, et al. 2004). Finally and interestingly, PKCα is a negative regulator to the RET signaling as reduction in RET phosphorylation was demonstrated (Andreozzi, et al. 2003) upon co-expression of this protein.

2.3.2 Other Tyrosine residues: 905, 981, 1015, 1096 and Serine 696

Other well-studied Tyrosine phosphorylation sites of RET are Tyr905, 981, 1015 and 1096, being the docking sites for Grb7/10, Src, phospholipase C gamma (PLCγ) and Grb2, respectively (Borrello et al. 1996; Encinas et al. 2004). Interestingly, it has been demonstrated that serine phosphorylation is also involved in the RET signaling cascade. Phosphorylation at Ser696 of RET, in neuronal cells, has been shown to be mediated by GDNF up-regulation of the intracellular cyclic AMP (cAMP) level, while the mutation of this serine inhibits lamellipodia formation by GDNF in a human neuroblastoma cells(Fukuda et al. 2002). There is a possible relation between G-proteins signaling and RET, as the cAMP is a known key regulator of the G-coupled receptor mediated PKA pathways. The complete RET signaling network is detailed and summarized in Figure 2.

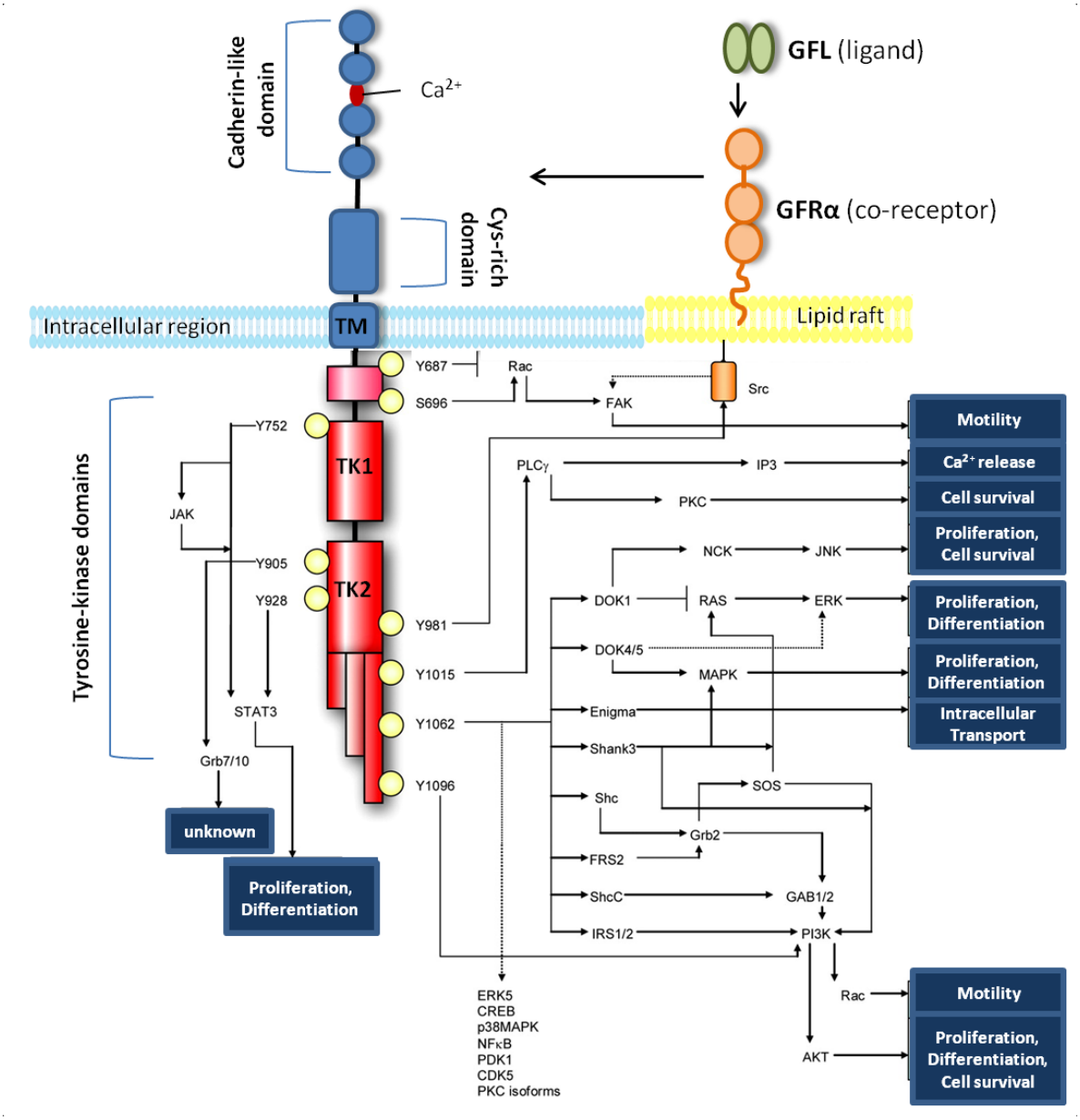

Figure 2. RET signaling network mediated by docking sites and their direct targets. Modified from (de Groot et al. 2006).

2.4 Function of RET

The RET receptor is important for gastrointestinal nervous system differentiation as well as sympathetic, neuroendocrine and renal development (Skinner, et al. 2008). The first *in vivo* study to reveal RET functions was based on mouse mutants harboring targeted homozygous mutation of

ret. These mice exhibited renal agenesis and severe dysgenesis, lacking enteric neurons throughout the digestive tract, and died within first days of their life (Schuchardt, et al. 1994). Monoisoformic RET51 mice, lacking the RET9 form, developed kidney hypodysplasia and lacked enteric ganglia from the colon(de Graaff, et al. 2001), which point to RET9 as highly important for kidney and enteric nervous system (ENS) development. In this regard, it has been demonstrated in another *in vivo* study that mice deficient in RET, GNDF, GFRα1 lacks all neurons in the gut, died immediately (for rewiev see(Manie, et al. 2001)). Interestingly, based on expression data, *RET* is expressed at the same moment than the ENS progenitors of neural crest origin entry into foregut mesenchyme(Durbec, et al. 1996) suggesting its implication at a very early stage of ENS development. One of the RET co-receptors, GFRα1, is expressed in all enteric neuron precursors and at an earlier stage compared to GFRα2(Enomoto 2005) which is present in a subpopulation of the precursors.

RET, its ligands, GFLs and co-receptors, GFRαs, are particularly important in sympathetic and parasympathetic nervous system development(Airaksinen and Saarma 2002; Sariola and Saarma 2003). In this regard, it has been observed that the GDNF/GFRα1/RET cascade is essential for the migration and proliferation of the cranial parasympathetic neuron precursors, whereas the NTN/GFRα2/RET signaling is required for nervous innervation to target organs (e.g. pancreas, reproductive organs) in the later developmental stages (Enomoto, et al. 2000; Rossi, et al. 2000).

RET is also implicated in kidney morphogenesis, as the GDNF/RET signaling is essential in nephron formation. It was suggested that this particular relation is controlled by negative feedback, where GDNF triggers RET signaling, promoting and maintaining high expression levels of Sprouty1 in the Wolffian duct, important in nephrogenesis. In response to that, the high level of Sprouty1 desensitizes RET towards GDNF resulting in Sprouty1 expression decrease(Basson, et al. 2005). Sprouty1 has been recently demonstrated, in another in vivo study, to play a role in medullary thyroid carcinoma as a tumor-suppressor gene(Macia, et al. 2011).

Moreover, *RET* implication has also been demonstrated in spermatogenesis, where GDNF/RET signaling has a crucial role in its early event. *RET* and *GFRα1* are expressed in a subset of undifferentiated spermatogonia and GDNF is derived from Sertoli cells, implicated in spermatogenesis regulation in a paracrine manner, and its overexpression inhibits the differentiation process (Sariola and Saarma 2003).

Finally, regarding the implication of *RET* in human disease, basically, the loss-of-function mutations result in congenital megacolon or Hirschprung´s disease (HSCR), whereas the gain-of-functions give rise to MEN 2 syndrome(Mulligan et al. 1993b). Other *RET* genetic changes have been demonstrated in papillary thyroid carcinoma (PTC), caused by different types of *RET* rearrangements and designated as RET/PTC, although this topic is not the issue of this thesis and it will not be further discussed.

3. Relation of *RET* with MEN2

3.1. Germline *RET* mutations

As already mentioned, germline *RET* mutations are related to MEN 2 syndrome development. A summary of *RET* mutations described so far is described in Table 2. Approximately 86%, 97% and almost 99% of patients with FMTC, MEN 2A and MEN 2B respectively carry activating mutations in *RET*. Those related to FMTC can be found in both extracellular and the tyrosine kinase domains of RET. The former include mainly substitutions of cysteines 609, 618, 620 (exon 10), 630 and 634 (exon11). The mutations affecting the tyrosine kinase domain include substitutions at residue 768, 790, 791 (exon 13), 804, 844 (exon 14), or 891 (exon15) (Alberti et al., 2003). Similarly to FMTC, the most common alterations related to MEN 2A are missense mutations in the extracellular domain. They mainly include changes affecting the cysteines 609, 611, 618, 620 (exon 10), 630 or 634 (exon 11). Among these mutations, the most common one found in MEN 2A patients is the substitution of Cys634, being involved in 80% of the cases (Alberti et al.,2003). RET/MEN 2A proteins display constitutive kinase activity due to ligand independent dimerization of the RET molecules (Alberti et al., 2003), which is a mechanism similar to that of FMTC. Two variants of MEN 2A are defined: MEN 2A associated with cutaneous lichen amyloidosis (CLA) and MEN 2A developing together with Hirschsprung's disease(Decker, et al. 1998). CLA is specifically associated with mutations involving codon 634 of exon 11, whereas MEN 2A associated with Hirschsprung's disease is linked to mutations involving codons 609, 611, 618, and 620. Patients with codon 634 mutation have an increased risk of lymph node metastasis at a young age (Machens, et al. 2003).The activation mechanism related to non-cysteine *RET* mutations occurring in the RET tyrosine kinase domain are still unknown.

MEN 2B is mainly associated with a specific mutation, a substitution of a Methionine to Threonine at 918 residue (p.M918T). Only a small portion (<5%) of the MEN2B patients carry another mutation (p.A883F). Tumors containing p.M918T often display a more aggressive phenotype (Alberti et al., 2003), very likely due to p.M918T causing constitutive activation of RET and transforming potential in a ligand-independent manner (Arighi et al., 2005). The p.M918T mutation does lead to constitutive dimerization like the cysteine mutations in FMTC and MEN 2A do (Alberti et al., 2003).

Information related to which specific mutation is responsible for the disease in a particular patient or family is critical due to there is a classification according to the transforming capacity associated with each mutation, and thus consequences for the clinical follow up. Hereditary MTCs are divided into three different risk categories (Brandi et al. 2001). The cases with highest risk, level 3, (Table 3) include mutations within the highest transforming capacities that are associated with MEN 2B syndrome. As these individuals develop the most severe form of MTC, they should undergo surgery during the first 6 months of life, and preferably during the first month. The second category within high risk includes mostly cases with 634 *RET* mutation carriers. For such patients total thyroidectomy is offered at the age of 5 years and for the other mutations affecting exon 10 might be performed later in life. In families with mutations in exons 13-15, which are included in an intermediate group risk and level 1 category, MTC clinically usually emerge with an indolent course in the second decade of life (de Groot et al. 2006).

Table 2. Germline *RET* mutations in MEN2 syndrome and somatic *RET* mutations in sporadic MTC (sMTC). Adapted from (Arighi et al. 2005a).

Exon	Codon number	Amino acid change	Phenotype
8	533	Gly → Cys	FMTC
	603	Lys → Gln	sMTC
	609	Cys → Ser	MEN 2A,
		Cys → Arg	MEN 2A, FMTC
		Cys → Tyr	MEN 2A

10	611	Cys → Tyr	MEN 2A
		Cys → Trp	MEN 2A, FMTC
		Cys → Ser	MEN 2A,
		Cys → Gly	FMTC
	618	Cys → Phe	MEN 2A
		Cys → Ser	MEN 2A, FMTC
		Cys → Gly	MEN 2A
		Cys → Arg	MEN 2A, FMTC
		Cys → Tyr	MEN 2A, FMTC
		Cys → Stop	MEN 2A
	620	Cys → Arg	MEN 2A, FMTC
		Cys → Tyr	MEN 2A
		Cys → Phe	MEN 2A
		Cys → Ser	MEN 2A
		Cys → Gly	MEN 2A
11	630	Cys → Phe	FMTC
		Cys → Arg	sMTC
	634	Cys → Tyr	MEN 2A, FMTC
		Cys → Arg	MEN 2A
		Cys → Phe	MEN 2A, FMTC
		Cys → Gly	MEN 2A
		Cys → Trp	MEN 2A
		Cys → Ser	MEN 2A, FMTC
		Cys → Arg	sMTC
	634 and 640	Cys → Arg and Ala→ Gly	De novo MEN 2A
	634 and 641	Cys → Ser and Ala→ Ser	MEN 2A
	634 and 640	Ala → Gly and Ala→ Arg	sMTC
13	768	Glu → Asp	FMTC/sMTC
	790	Leu → Phe	MEN 2A, FMTC
	791	Tyr → Phe	FMTC
14	804	Val → Leu	FMTC
		Val → Met	FMTC
	804 and 806	Val → Met and Tyr→ Cys	De novo MEN 2B
	778 and 804	Val → Ile and Val→ Met	FMTC
15	883	Ala → Phe	de novo MEN 2B
			sMTC
	891	Ser → Ala	FMTC
			FMTC and Pheo
16	918	Met → Thr	MEN 2B or sMTC
	922	Ser → Phe	sMTC

Table 3. Genotype-phenotype correlation. MTC risk levels according to mutated codon of *RET* proto-oncogene. Level 3 is the most severe. From (Brandi et al. 2001).

Mutated codons	Risk level	Syndrome(s)	Recommended actions
883, 918, 922	3	MEN 2B	Thyroidectomy within first 6 months of life
611, 618, 620, 634	2	MEN 2A, MEN 2B, FMTC	Thyroidectomy before age 5 years
609, 768, 790, 791,	1	MEN 2A, FMTC	Thyroidectomy between age 5 and 10 years.
804, 891	1	MEN 2A, FMTC	Periodic biochemical testing for MTC if thyroidectomy not performed

3.2 Somatic *RET* mutations

Around 40-50% of sporadic MTC harbor somatic *RET* mutations (Marsh 2002). The most common somatic mutation is the p.M918T change, the same one involved in MEN2B patients. Similarly to patients with germline mutations in this residue, the tumors with this mutation are considered to have the most aggressive clinical course(Schilling, et al. 2001). Somatic mutations at different codons such as 630, 634, 639, 641, 768, 883, 992 as well as deletion in codons 630 and 634 have also been identified(Bugalho 1997). However, the functional role of somatic *RET* mutations in MTC development still requires more investigation. It was shown by Eng and colleagues(Eng, et al. 1996b) that sporadic MTC cases with p.M918T *RET* mutations and their metastasis are heterogeneous. In this regard, this mutation can arise as a secondary event during progression from a metastatic clone or single tumor. A second possibility implies that MTC has polyclonal origin.

4. MTC management, detection and targeted therapies

As already mentioned, MTC disseminate locally in 50% of cases to cervical and mediastinal nodal groups and up to 20% to distant organs such as lungs, bones or liver(DeLellis 2004). When the disease is outside the thyroid gland, the chances of cure are reduced. Early diagnosis of tumors may affect the therapeutic strategy and chances of cure and may prolong survival. In case of

thyroid neoplasias, the fine needle aspiration biopsy is the routine method used to obtain prognostic information such as tumor aggressiveness, metastatic potential and response to the treatment.

Every patient with newly diagnosed MTC should be counseled about the possibility of familial disease and offered genetic testing. The serum calcitonin measurement, a sensitive marker for MTC, becomes useful in screening ¨at-risk¨ individuals and monitoring for disease recurrence in previously treated patients. Generally, complete preoperative evaluation of patients with possible MTC should consist of measurements of serum calicitonin, carcinogenic embryonic antigen (CEA), serum calcium and *RET* proto-oncogene mutational analysis. MTC in patients with palpable thyroid nodule could metastasize locally to the cervical lymph nodes as well as distant metastases to the bones, lungs or liver. In case of metastatic MTC diagnostics, imaging techniques such as computed tomography (CT) for lymph nodes and lungs (Giraudet, et al. 2007) or contrast-enhanced magnetic resonance imaging (MRI) and positron emission tomography (PET) for lung and liver metastases detection are widely used (Oudoux, et al. 2007). Surgery should then be personalized according to calcitonin levels, presence of palpable disease, imaging results, *RET* mutation screening and family history.

For primary MTC patients there are no alternatives except total thyroidectomy, while for metastatic advanced disease there is a great need for discovery of new molecular therapies. Previous clinical responses rates for chemotherapy in such patients have been disappointing, although there are currently some promising observations, as reviewed below. Classifying an individual or family by MEN 2 subtype is useful for determining prognosis and management.

4.1 Targeted therapies for MTC

Taking into account that there are currently several therapeutic approaches based on the use of tyrosine kinase inhibitors (TKIs), MTC patients may benefit from development of this particular field. In fact, targeted molecular therapies currently used in metastatic MTC management are based on inhibition of *RET* and other tyrosine kinase receptors that are involved in angiogenesis (Table 4).

Table 4. Summary of clinical trials in MTC patients with progressive disease. Adapted from (Almeida and Hoff 2012).

Target therapy	Target	Clinical phase	Type of MTC patients
Motesanib	VEGFR, RET	II	advanced MTC
Sorafenib (BAY 43-9006)	VEGFR, RET, BRAF	II	advanced MTC
Sunitinib (SU11248)	VEGFR, RET, BRAF	II	metastatic MTC
Axitinib	VEGFR,RET, RET/PTC	II	MTC
Vandetanib (ZD6474) (100 and 300mg)	VEGFR,RET, EGFR, RET/PTC	II & III	advanced & metastatic MTC
Cobazantanib(XL184)	VEGFR, MET, RET	I	hereditary & sporadic MTC

Very recently, in 2011, Vandetanib (ZD6474, Zactima), a potent inhibitor of EGFR, VEGFR2-3 and RET, was approved by the Food and Drug Administration (FDA) for progressive MTC treatment in adults. After phase II study with treatment of 300mg Vandetanib(Wells, et al. 2011a), and test for efficacy in a lower dose (100mg daily) in patients with advanced inherited MTC(Robinson, et al. 2011), this drug passed to phase III in clinical trials, showing therapeutic efficacy in the patients with advanced MTC(Wells, et al. 2011b).

Cabozantinib (XL184, Exelixis), is another small-molecule inhibitor of VEGFR1 and VEGFR2, hepatocyte growth factor receptor (MET) and RET. This drug was implemented in a phase I study conducted with 37 MTC patients(Kurzrock, et al. 2011). There is currently an ongoing phase III study (http://www.exelixis.com/investors-media/press-releases) performed on metastatic MTC comparing XL184 with placebo.

Sorafenib (BAY 43-9006, Nexavar), is another small-molecule TKI targeting VEGFR2 and VEGFR3, RET and BRAF. This drug was approved by the FDA for the treatment of advanced renal cell carcinoma and hepatocellular cancer. Sorafenib efficacy in metastatic MTC had been evaluated in the phase II study(Lam, et al. 2011).

Sunitinib (SU11248, Sutent), an inhibitor of the three VEGFRs, RET and RET/PTC subtypes 1 and 3, has been mostly associated with stable disease in MTC patients(Carr, et al. 2011) in a phase II study. Additionally, other phase II studies targeting VEGFRs are also being tested under commercial brands of Motesanib (Schlumberger, et al. 2009) or Axitinib, which did not block RET (Cohen, et al. 2008).

So far, clinical trials have included MTC patients as a minimal part of series of thyroid carcinoma patients. Thus, results and conclusions specifically related to MTC patients are scarce. In the next

few years, and after International Consortiums´ joint efforts to recruit metastatic and advanced MTC patients to be analyzed as a whole, we can probably expect robust conclusions with regards to the molecular features related to the success of their treatment.

5. Genomics

5.1 Transcriptomics

Although there is a well-established genotype-phenotype correlation for MEN2 patients, the mechanisms by which *RET*-mutations cause tumors, the development of sporadic MTC in the absence of *RET* mutations, and the specific oncogenic pathways involved, require further study. There is an urgent need to identify signaling pathways specifically related to familial and sporadic MTC using transcriptional profiling to gain new information about specific markers that could be used as potential therapeutic targets.

Transcriptional profiling has emerged as a robust tool to identify biomarkers related to the tumor differentiation stage and malignant behavior, among other features. Limitations related to this approach often arise from high quality RNA material requirements. Moreover, expression microarrays are based on freshly prepared mRNA extracts and show many difficulties with formalin fixed paraffin embedded (FFPE) tissue samples frequently containing degraded or low quality RNA material. Another pitfall is genomic data analysis, being mostly very time-consuming and often very complex in order to integrate all underlying information relevant to the biology of the specific disease. Despite many difficulties, these transcriptomic techniques compensate by retrieving a lot of information from a single experiment, including therapeutic targets and prognostic marker discoveries as well as many others such as sensitivity to specific treatments etc.

In fact, there are several studies focused on MTCs using this strategy (Ameur, et al. 2009; Jain, et al. 2004a; Lacroix, et al. 2005; Musholt, et al. 2005b; Watanabe, et al. 2002b) showing differences in gene expression according to specific *RET* mutation, although we are far from understanding the secondary processes involved in MTC pathogenesis.

5.2. microRNAs

MicroRNAs are small, around 20 nucleotide long, non-coding single-stranded RNA molecules regulating the expression of target genes by imperfect (in animals) binding to the 3´-UTR

(untranslated region) and possibly 5´-UTR of mRNA(Lytle, et al. 2007). To become mature form, miRNAs are processed by enzymatic complexes Dorsha and Dicer(Wiemer 2007), and they repress translation or lead to mRNA degradation of their target genes (Figure 3). Currently there are around 2000 human miRNA sequences annotated in the miRBase database version 18.0 (http://www.mirbase.org/) and this number is still growing. Regardless of the relatively small number of miRNAs, as each single miRNA targets several hundred genes and a single target gene can bind to multiple miRNAs(Lewis, et al. 2003) making the whole network very complex, it is believed that around 30% of all human genes are a target for miRNA regulation (Lewis, et al. 2005). There is also evidence that these small molecules are expressed in a tissue-/cell-specific manner, being restrictively reserved to specific cell type or ubiquitously associated within different human body compartments (Landgraf, et al. 2007).

It was previously demonstrated that dysfunctional expression of microRNAs is a frequent attribute of malignant behavior(Calin and Croce 2006). Nowadays, aberrant expression of specific microRNAs is associated with all cancer types. Germline and somatic mutations as well as polymorphisms in the mRNAs targeted by miRNAs can also lead to cancer predisposition and progression (Calin and Croce 2007). Growing evidence points to miRNA, being implicated in oncogenic processes, suggesting that miRNA expression profiling can distinguish tumors according to diagnosis and developmental cancer stages for more accurate studies than usually provided by traditional gene expression analyses(Lu, et al. 2005). Small non-coding RNAs can play a dual role in tumorigenesis, acting as oncogenes (e.g. miR-155 of miR-17-92 cluster family members), or tumor suppressors (e.g. miR-15a and miR-16). To date, there are three proposed mechanisms implicating miRNA deregulation in cancer. These processes involve chromosomal lesions at regions encoding miRNAs, failure in the their biosynthetic pathway machinery and finally epigenetic regulation(Lawrie 2008).

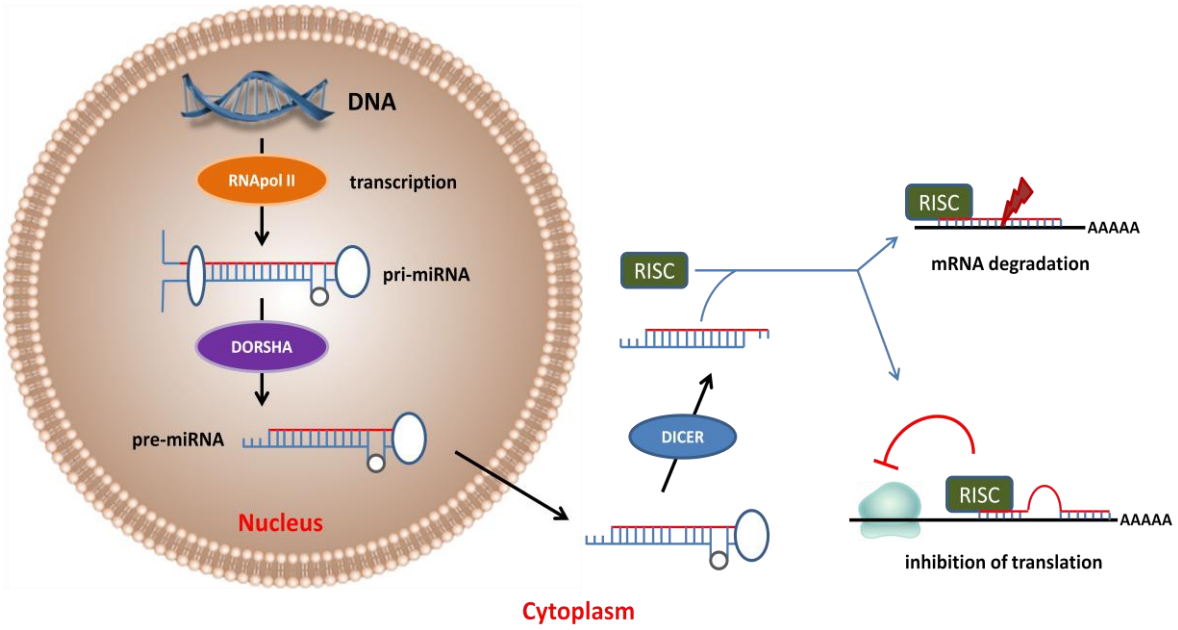

Figure 3. Biogenesis and microRNA function. miRNAs are transcribed in the nucleus by RNA polymerase II to form pri-miRNA which has to be processed to become functional mature form. This is possible due to RNAsas Dorsha and Dicer. The first processing is made in the nucleus by Dorsha and pre-miRNA is generated, which is transported to the cytoplasm and then Dicer processes the second part to obtain mature miRNA form. Then miRNA acts together with RISC complex which proceed the target gene silencing via two mechanisms: degradation of mRNA or inhibition of mRNA translation. Modified from (Bartel 2009).

Little is known regarding the studies based on the direct role of microRNAs implicated in MTC development. There are only two studies on miRNAs of MTC. The first one pointed to the miR-183 and miR-375 overexpression as lymph node metastasis prediction, although based on a small cohort of patients and not taking into account specific *RET* mutations in MTC development (Abraham, et al. 2011). The second one compares miRNA profiles of 2MTCs with unknown genetic background comparing them *versus* follicular-cell type origin thyroid carcinomas(Nikiforova, et al. 2008). Mian and colleagues have very recently could not validate the results of these mentioned studies (Mian, et al. 2012).

So far, apart from those above mentioned, there are no other miRNA profiling studies been performed on these rare tumors, offering a field to increase our understanding of this disease. The combination of both transcriptome and mirnome data can be a powerful tool to retrieve more relevant information underlying development and biology of the disease.

Resumen de la introducción

El Carcinoma Medular de tiroides (CMT) representa el 2-5% de los carcinomas tiroideos, y deriva de las células parafoliculares o células C, que secretan calcitonina, la hormona que regula los niveles de calcio en sangre. El CMT se disemina localmente a nódulos cervicales y mediastínicos en el 50% de los casos, y hasta en un 20% a órganos distantes como pulmón, huesos o hígado (DeLellis 2004).

La mayor parte son esporádicos (75%), desarrollándose el 25% restante en el contexto de una Neoplasia Endocrina Múltiple tipo (MEN2, OMIM #171400). De acuerdo a la presentación clínica, el síndrome MEN2 está subdividido en Neoplasia Endocrina Múltiple tipo 2A (MEN 2A; OMIM #171400), Neoplasia Endocrina Múltiple tipo 2B (MEN 2B; OMIM#162300) y Carcinoma Medular de Tiroides familiar (FMTC; OMIM#155240). Esta enfermedad presenta una prevalencia de 1:30.000(Marsh 2002), con una herencia autosómica domiante, expresión clínica variable, y una penetrancia casi completa dependiente de la mutación específica de *RET* responsable de la enfermedad en cada caso.

El gen responsable del desarrollo del CMT es el proto-oncogen *RET*, que codifica para un receptor tirosina-quinasa (RTK). Mutaciones activantes, tanto germinales como esporádicas, son responsables de la mayoría de los casos familiares o esporádicos respectivamente (Hofstra et al. 1994; Mulligan et al. 1993b), aunque recientemente han sido también descritas mutaciones en *BRAF* y *RAS* (Goutas 2008; Moura et al. 2011).

El gen *RET* está localizado en la banda cromosómica 10q11.2, está distribuido en 50kb y contiene 21 exones (Pasini et al. 1995). Existen tres isoformas diferentes, RET9, RET43 y RET51, como consecuencia de un proceso de *splicing* alternativo, que difieren en el extremo C-terminal. RET contiene dos dominios extracelulares (cuatro regiones "*cadherin-like*" en tandem, y un dominio rico en cisteínas), un dominio transmembrana, y dos dominios tirosina quinasa intracelulares. RET es el receptor para ligandos de la familia del factor derivado de las células de la glía (GDNF), compuesta por GDNF, neurturina (NTN), artemina (ARTN) y persephina (PSP)(Santoro et al. 2004a). Estos ligandos necesitan reclutar co-receptores para conseguir que se active la transducción de señales. Hasta la fecha hay dos mecanismos de activación dependiente de RET aceptados, que implican la unión entre GFL, GFRα y RET (Figura 1). El primero propone que se forma un complejo entre una molécula de GFL y una de GFRα, y el segundo plantea que se forma

un complejo entre GFRα y RET, que desencadena la aparición de un sitio de unión para GFL (Manie et al., 2001).

RET, al igual que otros RTKs, está regulado por fosforilación de residuos específicos de tirosina, lo que promueve la señal. Tras la estimulación del ligando y la asociación al receptor, RET se dimeriza y la trans-fosforilación ocurre en residuos intracelulares de tirosina concretos, que sirven como sitios de unión para otras proteínas que participan en la señalización. Se sabe muy poco sobre qué rutas de señalización se ven activadas ante mutaciones en *RET* particulares, así como de las implicadas cuando el tumor aparentemente no se desarrolla como consecuencia de una mutación en *RET* (de ahora en adelante *RET wild-type*).

Se sabe que RET puede activar varias rutas dependientes de RTKs bien conocidas, como la Erk, PI3K/Akt, MAPK, JNK y PLCγ(Arighi et al. 2005a; Ichihara et al. 2004). Hay varios sitios reconocidos como adaptadores de proteínas (Figure 1). Entre ellos, los más importantes son las tirosinas fosforiladas de las posiciones 905, 981, 1015, 1062 y 1096 (Encinas et al. 2004; Ichihara et al. 2004). Básicamente, lo que ocurre es que la proteína RET normal, las relacionadas con MEN2A, con MEN2B y con CMTf muestran diferencias en su fosforilación y por tanto en los sitios de unión a otras proteínas, que conducen a activar cascadas de señalización intercelular específicas en cada caso (de Groot et al. 2006).

En cuanto a la función de RET, se sabe que este receptor es importante en el desarrollo del sistema nervioso gastrointestinal, así como del simpático, neuroendocrino y renal (Skinner et al., 2008). Su implicación también ha sido demostrada en espermatogénesis, proceso para el cual la señalización dependiente de GDNF/RET tiene un papel crucial.

Con respecto al papel de *RET* en enfermedades humanas, es destacable que las mutaciones de pérdida de función conducen al desarrollo de la enfermedad de Hirschprung (HSCR), y las de ganancia de función a un MEN2 (Mulligan et al. 1993b). En carcinoma papilar de tiroides se ha demostrado la importancia de otro tipo de alteraciones genéticas que afectan a *RET*, caracterizadas por translocaciones cromosómicas con otros segmentos del genoma.

En relación con las mutaciones asociadas a MEN2, hay una correlación fenotipo-genotipo que estratifica dichas mutaciones en tres niveles de riesgo. Las clasificadas como nivel 1 de riesgo afectan a los residuos 609, 768, 790, 791, 804, y 891, y se asocian con desarrollo de CMT. Pacientes con mutaciones de nivel 2 (afectan a los residuos 611, 618, 620, y 634) tienen un mayor

riesgo, y se asocian a una mayor probabilidad de desarrollar metástasis del CMT. Mutaciones de nivel 3 (resíduos 883 y 918) tienen la capacidad transformante más elevada de todas, y conducen al desarrollo de CMTs con riesgo de metástasis a edades tempranas (Frank-Raue and Raue 2009). En torno al 40-50% de los CMT esporádicos presentan una mutación somática en *RET* (Marsh, et al. 1996). La más frecuente es la mutación p.M918T, que es la misma que está implicada en la mayor parte de los pacientes MEN2B, y se asocia a los cursos clínicos más agresivos (Schilling et al. 2001). La información relativa a qué mutación específica es la responsable de la enfermedad en un paciente o en una familia es crítica de cara a tener en cuenta el riesgo que tiene asociado, y por tanto con consecuencias para el seguimiento clínico.

El manejo de CMTs primarios pasa por una tiroidectomía realizada por expertos, mientras que para la enfermedad avanzada existe una necesidad real de descubrir nuevas dianas terapéuticas. Teniendo en cuenta que actualmente hay en marcha varios ensayos clínicos basados en el uso de inhibidores de tirosina quinasa, los pacientes con CMT podrían beneficiarse de este campo en particular. De hecho, las terapias moleculares dirigidas utilizadas en CMT metastásico están basadas en la inhibición de RET y de otros receptores tirosina quinasa implicados en angiogénesis. Hay una necesidad urgente de identificar rutas de señalización específicamente relacionadas con el carácter hereditario o esporádico de los tumores.

El análisis de perfiles de expresión génica ha sido utilizado como herramienta para identificar eventos moleculares asociados a subtipos tumorales, o procesos asociados concretos, como metástasis proliferación y angiogénesis(Glinsky 2006). Hay numerosos estudios que también han demostrado su potencial para identificar firmas moleculares asociadas a características clínicas(van de Vijver, et al. 2002) lo que podría ayudar a la identificación de nuevas dianas terapéuticas. De hecho, ya hay varios estudios enfocados en CMTs que han utilizado esta estrategia (Ameur et al. 2009; Jain, et al. 2004b; Lacroix et al. 2005; Musholt, et al. 2005a; Watanabe, et al. 2002a) y que muestran diferencias en el perfil de expresión génica de acuerdo a la mutación específica en *RET*, si bien estamos aún lejos de entender los procesos secundarios implicados en el desarrollo de un CMT.

Por otra parte, apenas se conoce el papel que los microRNAs puedan tener en el desarrollo de CMTs. Hasta la fecha hay solo dos estudios sobre el tema. El primero describe la sobre-expresión del miR-183 y del miR-375 asociada a la aparición de metastasis, aunque está basado en una cohorte de pacientes pequeña y no se tiene en cuenta qué mutaciones en *RET* caracterizaban cada

tumor (Abraham et al. 2011). El segundo estudio comparaba el perfil de microRNAs de dos CMTs con background genetic desconocido, con el mostrado por tumores tiroideos derivados de célula folicular (Nikiforova et al. 2008). Estos resultados no pudieron ser validados en un estudio reciente (Mian et al. 2012).

Objectives

The final goal of this work was to characterize the transcriptional and microRNA profiles specifically related to hereditary and sporadic MTC according to specific *RET* mutation, by using the same cohort of tumors. Due to there is a long list of unanswered questions regarding the signaling pathways associated with MTC development according to specific genetic condition, integration of these two OMIC approaches (gene expression and miRNA) might reveal an important input in deeper understanding of MTC biology. Therefore, the specific aims of this work were:

1) To define the transcriptome and mirnome of MTC cases according to the different individual genetic background. For that purpose it was consider the presence of the M918T *RET* mutation in sporadic MTC, sporadic MTC WT (no *RET* mutation) and hereditary MTC with germline *RET* mutation.

2) To identify biomarkers related to each genetic class included in the study, as well as pathways specifically altered, that could be the target of future therapeutic options.

Objetivos

El objetivo final de este trabajo fue caracterizar el perfil transcripcional y de microRNAs relacionados con el carácter esporádico y hereditario de los CMT, y relativos a mutaciones específicas en *RET,* utilizando para ello la misma coleción de tumores. Dado que hay una larga lista de preguntas sin respuesta relacionada con las rutas de señalización asociadas al desarrollo de CMTs bajo condiciones genéticas concretas, la integración de los resultados procedentes de estas dos plataformas (expresión génica y microRNAs) podría profundizar en el conocimiento de la biología del tumor. Los objetivos específicos de este trabajo fueron:

1) Definir el transcriptoma y el mirnoma del CMT, de acuerdo con el backgroung genetico individual del paciente. Para ello se consideraron 3 grupos de análisis: tumores esporádicos con la mutación M918T en *RET*, tumores esporádicos sin mutación detectable or Wild Type, y CMTs hereditarios pertenecientes a pacientes con mutaciones germinales en *RET*.

2) Identificar biomarcadores relacionados con cada una de las clases genéticas incluidas en el estudio, así como rutas específicamente alteradas, que pudiesen ser consideradas como futuras dianas terapéuticas.

Material and methods

1.1 Medullary Thyroid Carcinoma patients

Extracted DNA from peripheral blood samples of patients diagnosed with at least MTC was collected from 1996 to 2010 from Spanish hospitals. After obtaining consent from each patient, clinical information was collected through a questionnaire (supplementary annex 1), and when possible, the corresponding tumors used for further analysis. The genetic and general characteristics of the available tumors (frozen or FFPE) are detailed in Supplementary annex Table 1. Specific data such as gender, age at the diagnosis, the presence of metastasis (at the time of diagnosis or follow-up) and the existence of personal or family history of the disease were retrieved. Tumors were classified according to the molecular screening for *RET* proto-oncogene, and then this information was considered for further analyses.

1.2 Frozen MTC tissue samples

Sixty-nine frozen tumors from unrelated patients diagnosed with MTC were collected at the time of surgery from Spanish hospitals through the Spanish National Tumor Bank Network and from the Surgical Pathology Department of Medical and Surgical Sciences, Padova, Italy. Each frozen tissue sample was included in a matrix of polyvinyl (Tissue - Tek ® OCT™, Sakura, NL) and stored at -80 ° C until use for DNA or RNA extraction and hybridization onto arrays, or for *RET* mutational screening (in case that previous genetic information on the patient was not available). Staining with haematoxylin-eosin (H&E) was carried out for each of the tissues in order to assess the presence and abundance of tumor cells. All tissues were evaluated by two pathologists by hematoxylin and eosin staining; only samples with a high percentage (>80%) of tumor cells were included in the study. The protocol for staining with H&E of the frozen and paraffin tumor sections is detailed below:

1. Hydrate with absolute ethanol (2 minutes) and later with ethanol 95% (2 minutes).
2. Wash with distilled water (B. Braun Medical SA, Barcelona, Spain) for 2 minutes.
3. Stain with Mayer haematoxylin for 15 minutes.
4. Wash with distilled water for 2 minutes.
5. Stain with eosin for 2 minutes.
6. Remove the eosin remains, using 70% ethanol.
7. Dehydrate through successive washing with 96% ethanol (30 seconds), absolute ethanol (2 minutes) and xylol (2 washes, 2 minutes each).

8. Mount a cover objects in preparation with *Eukitt* (Electron Microscopy Sciences, Fort Washington, PA, USA).

Note: Staining of the frozen tissue sections did not require any previous step as the OCT™ does not interfere in the staining part nor in the nucleic acids (RNA and DNA) extraction.

1.3 Formalin fixed paraffin embedded (FFPE) samples and tissue microarray (TMA)

To validate results derived from gene expression and miRNA profiling study, an independent series of formalin fixed paraffin embedded tumors was available, composed of 38 MTC samples Supplementary annexes table 1 and 2, that were assessed by H&E staining (with a pre-step of de-paraffination with xylol).

Moreover, two 2 tissue microarrays (TMAs) constructed from 67 MTCs (molecularly characterized) were used for validation step with immunohistochemistry (IHC). For this purpose, representative tumor areas were selected and cylinders of 1mm in diameter included in a new block of paraffin with a 0,8mm separation between each tissue sample. MTC tumors included in the TMAs are detailed in Supplementary annexes table 3A and Table 3B, representing different mutations in the *RET* proto-oncogene as well as cases without detectable *RET* mutation. The first TMA (TMA-1), Supplementary annex Table 3A, contained 54 independent MTC tissues; of these, 12 carried a germline *RET* mutation in codon 634, 9 had a somatic M918T mutation, and 22 were classified as wild type (WT). This TMA also contained 4 other thyroid cancer types and 2 normal tissues used as controls, as well as the normal thyroid tissue of 13 MTC cases included in the TMA. TMA-2 (Supplementary annex Table 3B) was constructed with cores from matched FFPE material from 13 frozen samples used for profiling [6 MTCs from RET^{634} carriers, 4 with a RET^{918} somatic mutation, and 3 WT MTCs], as well as 2 MTCs not hybridized, 2 thyroid cancers of a different subtype and 12 normal thyroid tissues from the corresponding MTCs included in this TMA.

1.4 MTC cell line models

MZ-CRC-1 cells, derived from a metastatic MTC and harbor the M918T *RET* mutation (Cooley 1995; Santoro, et al. 1995), and TT cell line, harboring a mutation at residue 634 of RET were available.

2. DNA extraction

2.1 DNA extraction from peripheral blood

DNA extraction from the peripheral blood was performed following an automated method (*MagNa Pure* LC; Roche Diagnostics GmbH, Mannheim, Germany):

1. Starting from 1ml of peripheral blood, the system adds:

→ 0,115ml of *proteinase K* solution,

→ 0,84ml of lysis-union buffer to promote cell lysis and generate saline conditions suitable for the subsequent retention of DNA,

→ 0,54ml of the MGP reagent, which retains the DNA through magnetic crystalline particles.

2. Washing with 2,42ml of *Washing Solution I* to discard components not joined to the magnetic particles (proteins, cell membranes and inhibitors of amplification such as heparin).

3. Washing with 1,28ml of *Washing Solution II* to remove cell remains and to reduce the saline concentration.

4. Washing with 0,84ml of *Washing Solution III* to remove the remains of ethanol.

5. Finally, re-suspending purified DNA in 200µl of solution buffer previously pre-heated.

2.2 DNA extraction from frozen tumour material

DNA extraction from frozen tumour samples was carried out from 15-20 slide sections of 20µm thickness each cut using cryostat (Leica Microsystems, Barcelona, Spain). DNA Extraction was carried out with *Dneasy Tissue Kit* (Qiagen, Chatsworth, CA, USA) according to the manufacturer´s instructions with some modifications detailed below:

1. Immerse obtained cuts in O.C.T. (Tissue-Tek® O.C.T.™, Sakura, NL) material in 200µl of *ATL solution*.

2. Add 20µl *proteinase K* and mix vigorously, then incubate in a thermo cycler with agitation at 55°C until the material is completely digested. The incubation time can vary between 3 hours and overnight.

3. Stir again and add 200µl of *AL solution.* Mix and incubate at 70°C for 10 minutes.

4. Add 200µl of absolute ethanol and homogenize.

5. Pass the mixture to the column, supplied in the kit, and place in a collector tube. Centrifuge at 8,000 rpm for 1 minute. Discard the collector tube with the supernatant.

6. Place the column in a new collector tube and add 500µl of the *AW1 solution*. Centrifuge at 8000 rpm for 1 minute. Discard the collector tube with the supernatant.
7. Place the column in a third collector tube and add 500µl of the *AW2 solution*. Centrifuge at 13,000 rpm for 3 minutes to dry the membrane of the column completely. Discard the collector tube with the supernatant.
8. Place the column in a new clean tube and mark appropriately. Add 200µl of distilled water directly on the membrane and incubate at 15-20°C for 1 minute. Centrifuge for 1 minute to elute the DNA. Optionally, the elution can be performed using a lesser volume of water if expected to obtain little amounts of DNA.
9. Quantify 1µl DNA using NanoDrop ™ ND-1000 (NanoDrop Technologies, Wilmington, DE, USA) spectrophotometer. In those cases in which the concentration exceeding 1µg/µl, prepare a 1/10 dilution and use 1µl of this material to quantification, avoiding a possible saturation of the measurement. Freeze the remaining volume at -20°C until use.

2.3 DNA extraction from formalin fixed paraffin embedded (FFPE) material

Using a microtome (Leica Microsystems, Barcelona, Spain), 4 sections, each of 30µm thickness were obtained from each sample, and were introduced in 1.5ml tubes.

The extraction protocol used was similar to extraction from frozen tissue material but including the following previous steps for the deparaffination of the sample:

1. Place the paraffin cuts in a 1.5 or 2ml tube.
2. Add 600µl of xylol and mix vigorously.
3. Centrifuge at room temperature at 13,000 rpm for 5 minutes.
4. Remove the supernatant with a pipette without dragging the pellet.
5. Repeat the washing with xylol (steps 2 to 4).
6. Add 1000µl of absolute ethanol to the pellet to eliminate the residues of xylol and mix vigorously.
7. Centrifuging at room temperature at 13,000 rpm for 5 minutes.
8. Remove the ethanol with a pipette without dragging the pellet.
9. Repeat washing with ethanol (steps 6 to 8).
10. Incubate the pellet with the tube open at 37°C for 10-15 minutes (till the ethanol is evaporated).
11. Continue with Protocol DNA extraction of frozen material from step 1.

3. RNA extraction and analysis

3.1 RNA extraction from frozen material

Total RNA extraction from frozen tumour samples was carried out from 15-20 slide sections of 20µm thickness each cut using cryostat (Leica Microsystems, Barcelona, Spain). Extraction was followed by the TRI Reagent® Protocol (Molecular Research Centre, Cincinnati, OH, USA):

1. Homogenize tissue sections (50-100mg approximately) in 1ml of solution TRI Reagent. Leave at room temperature for 5-15 minutes.
2. Add 0,2ml of chloroform. Mix vigorously.
3. Centrifuge at 4°C and at 13,500 rpm for 15 minutes.
4. Recover the aqueous phase and add 0,5ml of isopropanol. Mix and leave overnight at -20ºC. Centrifuge at 4°C and at 13,500 rpm for 20 minutes.
5. Discard the supernatant and wash with 1ml of 75% aqueous ethanol. Centrifuge at 4°C and at 13,500 rpm for 5 minutes.
6. Dry pellets at 65°C for 3-5 minutes.
7. Re-suspend dried pellet in 12-15µl of RNAase free water.
8. Stir gently in a thermo cycler at 37°C for 20 minutes.
9. Use 1µl of the RNA obtained for its quantification using Nanodrop ND-1000 (Wilmington, DE, USA).

Simultaneously, 1µl of the RNA mixed with 4µl RNAase free water and 5µl of formamide (Applied Biosystems, Foster City, CA, US) in 1,5% agarose gel was tested. The remaining volume at -80°C was frozen until use.

Total RNA samples which presented degraded profile in an agarose gel electrophoresis (<500 mRNA bp), were extracted again in order to obtain good quality biological material.

3.2 RNA extraction from formalin fixed paraffin embedded (FFPE) material

Total RNA extraction from FFPE tissue was carried out using the *miRNeasy FFPE* (Qiagen, Chatsworth, CA, USA) kit following the Protocol according to the manufacturer´s instructions as specified below:

1. Cut4 sections of 30µm thickness each using microtome and deposit them in a 1,5ml tube.
2. Add 1ml of xylol and shake for 10 seconds at the room temperature.
3. Centrifuge at 13,000 rpm at 20-25°C for 2 minutes. Discard the supernatant, avoid touching the pellet.

4. Add 1ml of absolute ethanol and mix it vigorously.

5. Centrifuge again at 13,000 rpm at 20-25°C for 2 minutes. Remove the supernatant, avoid touching the pellet.

6. Incubate at 37°C with open tube for 10 minutes or until the residual ethanol has evaporated.

7. Re-suspend the pellet in 240µl of PDK solution and add 10µl of *proteinase K* and mix vigorously.

8. Incubate at 55°C for 15 minutes and then at 80°C for 15 minutes.

9. Add 500µl of RBC solution and mix vigorously.

10. Transfer the mixture to a column gDNA Eliminator spin (provided by the kit) and place it in a tube collector of 2ml. Centrifuge at 10,000 rpm for 30 seconds. Discard the column and keep the collected volume.

11. Add 1,750µl of absolute ethanol to the collected volume and mix with the pipette. Perform the next step immediately.

12. Transfer 700µl of the volume to the RNeasy MiniElute column, spin and place it in a tube collector of 2ml. Close the lid gently and centrifuge at 10,000 rpm for 15 seconds. Discard the supernatant. Repeat until the entire volume of the sample has gone through the column.

13. Add 500µl of RPE solution to the column. Close the lid gently and centrifuge at 10,000 rpm for 15 seconds to wash the membrane of the column. Discard the liquid elute.

14. Add 500µl of RPE solution to the column again. Close the lid gently and centrifuge at 10,000 rpm for 2 minutes.

15. Place the column in a tube collector of 2ml. Open the lid of the column and centrifuge at 13,000 rpm for 5 minutes. Discard the tube collector.

16. Place the column in a tube collector of 1,5ml. Add 14-30µl RNase-free water directly on the membrane of the column. Close the lid gently and centrifuge at 13,000 rpm for 1 minute. Keep the RNA obtained at -80°C until use.

3.3 RNA extraction from cell lines

Total RNA from MZ-CRC-1 and TT cells was extracted using the *RNAeasy* kit (QIAGEN, Alameda, CA) following the manufacturer´s instructions.

3.4 Analysis of RNA integrity and quality

For RNA samples obtained from frozen tissues that showed an optimal profile on the agarose gel, an evaluation of their integrity was carried out. Agilent 2100 Bioanalyzer (Agilent Technologies,

Palo Alto, CA, USA) was used for that purpose. This method estimates the integrity of RNA according to an algorithm called RNA Integrity Number (RIN), which corresponds to the quantified value of integrity by Agilent software. The RIN varies from 0 to 10, where 10 corresponds to the highest quality of RNA material. Only those samples with a value equal to or greater than 7 RIN (recommendation of the manufacturer) were selected for the gene expression and miRNA profiling study. In case of miRNAs, small RNA protocol was assessed to check RNA quality and miRNA content in a total RNA.

4. *RET* genetic screening

DNA extracted from peripheral blood as well as from frozen tumour material, when only available, was used for the genetic characterization of the MTC tumors. Point mutation screening included the specific coding regions (exons) of *RET* proto-gene (8, 10, 11, 13-16) associated with MTC development. The PCR conditions and primers used are described in table 5. A standard PCR procedure was used in a final volume of 25µl, which contained 100 ng of genomic DNA, 10% of the final volume of the 10XPCR solution (50mM KCl, 10mM Tris and 1,5mM $MgCl_2$), 200mM dNTPs (deoxyribonucleotide triphosphate) mix (dATP, aGTP, dCTP and dTTP; Fermentas-Life Sciences, Ontario, Canada), 20pmol of each specific primer and 1 unit of Taq polymerase. The reactions were carried out using Eppendorf thermocyclers (Eppedorf AG, Hamburg, Germany). Samples, once amplified, were tested by agarose gel electrophoresis at 2% dyed with ethidium bromide (0,5µg/ml) (Sigma-Alrdich, Alcobendas, Spain). The amplified products were purified and sequenced afterwards.

Table 5. Primers, amplicon length (bp) and melting temperature (Tm) of the *RET* mutational screening applied in the study**.**

***RET* gene primer pair**	**Primer pair sequence**	**Amplicon length (bp) & Tm (ºC)**
RET-EXON 8-FORWARD	GTGCTCCTGGCACTGTCTTT	Amplicon length : 438 bp Tm: 60ºC
RET-EXON 8-REVERSE	GCTATGCTGGCATCGAGAG	
RET-EXON 10-FORWARD	TATGCTTGCGACACCAGTTG	Amplicon length : 294 bp Tm: 62ºC
RET-EXON 10-REVERSE	CAGCAATTTCCTCCCTTGTT	
RET-EXON 11-FORWARD	CAGAGCATACGCAGCCTGTA	Amplicon length : 448 bp Tm: 62ºC
RET-EXON 11-REVERSE	CACAGACTGTCCCCACACAG	
RET-EXON 13-FORWARD	TGACCTGGTATGGTCATGGA	Amplicon length : 239 bp Tm: 58ºC
RET-EXON 13-REVERSE	GGAGAACAGGGCTGTATGGA	
RET-EXON 14-FORWARD	AAGACCCAAGCTGCCTGAC	Amplicon length : 328 bp Tm: 60ºC
RET-EXON 14-REVERSE	GCTGGGTGCAGAGCCATA	
RET-EXON 15-FORWARD	GTCTCACCAGGCCGCTAC	Amplicon length : 375 bp Tm: 62ºC
RET-EXON 15-REVERSE	TATCTTTCCTAGGCTTCCCAA	
RET-EXON 16-FORWARD	GCCTGGCCTTCTCCTTTAC	Amplicon length : 192 bp Tm: 60ºC
RET-EXON 16-REVERSE	TAACCTCCACCCCAAGAGAG	

Highlighted in blue: tumoral DNA screening for somatic *RET* mutations.

5. Gene expression characterization by using microarrays

The study of the expression profiles of MTC frozen tumors was carried out through a competitive hybridization between the tumor RNA (marked with a green fluorophore) and a universal reference RNA (marked with a red fluorophore) (Agilent Technologies, Palo Alto, CA, USA) on a commercially available platform of complementary DNA (cDNA) (Whole Human Genome Microarray format 4x44k). This platform contains 45,015 features with approximately 41,000 unique probes representing 22,000 genes that make up the complete human genome. Using this method, and starting from the total RNA, a fluorescent complementary RNA (cRNA) is generated which is further used for a competitive hybridization in which genes, that are over-expressed (red) or under-expressed (green), in the corresponding sample are detected. cRNA preparations, hybridizations, washes and detection were done as recommended by the supplier and generally following procedure is shown at Figure 4.

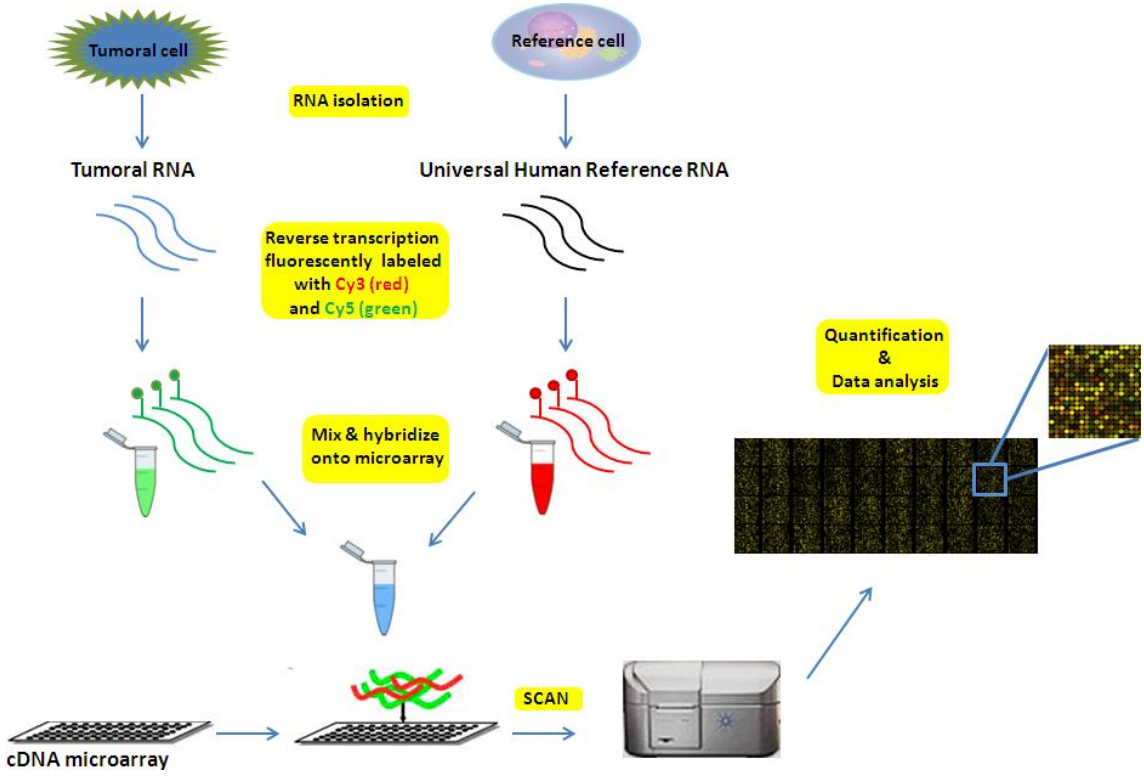

Figure 4 Schematic representation of Agilent data analysis procedure.

5.1 cDNA synthesis and cRNA labeling

Universal Human Reference RNA (Stratagene, La Jolla, CA, USA) was used as a control for all samples. Total RNA was amplified and labeled with cyanine 5 (Cy5)-conjugated dUTP for tumor samples, whereas cRNA from Universal Human Reference RNA was labeled with cyanine 3 (Cy3)-conjugated dUTP using Agilent's Low RNA Input Linear Amplification Kit (Agilent Technologies, Palo Alto, CA) following the manufacturer´s instructions.

Briefly, 500ng of total RNA was reversed transcribed to double-strand cDNA using a poly dT-T7 promoter primer. Firstly, template RNA and quality-control transcripts of known concentration and quality were first denatured at 65^0C for 10 min and incubated for 2 hours at 40^0C with 5x first strand Buffer, 0.1 M DTT, 10 mM dNTP, MMLV RT, and RNase-out. The MMLV RT enzyme was inactivated at 65^0C for 15 min. cDNA products were then used as templates for *in vitro* transcription to generate fluorescent cRNA. cDNA products were mixed with a transcription master mix in the presence of T7 RNA polymerase and Cy5 or Cy3 labeled-CTP and incubated at 40^0C for 2 hours. Labeled cRNAs were purified using QIAGEN's RNeasy mini spin columns and

eluted in 40ul of nuclease-free water. After amplification and labeling, cRNA quantity and cyanine incorporation were determined using a NanoDrop™ ND-1000 (NanoDrop Technologies, Wilmington, DE, USA). The following values were recorded: Cy3 or Cy5 dye concentration (pmol/µL), RNA absorbance ratio (260 nm/280 nm), cRNA concentration (ng/µL). To determine the cRNA yield and specific activity of each reaction we used the following equations: Concentration of cRNA * 40 µL (elution volume) / 1000 = µg of cRNA; (Concentration of Cy3/Cy5) / (Concentration of cRNA)*1000 = pmol Cy3 per µg cRNA. If the specific activity was <7.0 pmol Cy3 or Cy5 per µg cRNA I did not proceed to the hybridization step and repeated the cRNA preparation.

5.2 Hybridization

For each hybridization, 1µg of Cy3 labeled cRNA (reference) and 1µg of Cy5 labeled cRNA (tumor sample) were mixed, fragmented and hybridized onto Agilent Whole Human Genome (4x44K) Oligo Microarray. Briefly, 1µg of Cy3 labeled cRNA (reference) and 1µg of Cy5 labeled cRNA sample of interest were mixed along with 10x *Blocking Agent* and 25x *Fragmentation buffer* to a final volume of 45µl. After 30-minute incubation at 60^0C, the cRNA fragmentation step was stopped by adding 2x GE *Hybridization buffer HI-RPM*. Following the microarray handling tips from Agilent the hybridization assembly was prepared and the sample was placed in a hybridization oven set to 65^0C for 17 hours with rotation at 10 rpm.

5.3 Washing and scanning

The two-channel hybridized microarrays were disassembled at room temperature in *Agilent Gene Expression Wash Buffer 1* and washed in this solution for one minute. Then the microarray slides were moved into pre-heated (37°C) solution of *Gene Expression Wash Buffer 2* and were washed for one minute. Finally, moved into 100% acetonitrile at room temperature and incubated for one minute. After washing, microarrays were scanned using a fluorescent Agilent Microarray Scanner G2565 (Agilent Technologies, Palo Alto, CA, USA) in a special chamber free of ozone to omit possibility of Cy5 fluorophore degradation.

5.4 Data analysis - extraction, normalization and preprocessing

Two-channel arrays were hybridized and quantified using Agilent Feature Extraction software (version 9.5.3) and run on all array datasets using the GE2-v5_95_Feb07 protocol recommended for this platform. Reproducibility and reliability of each single microarray was assessed using

Quality Control report data. Microarray Background subtraction was done using the *normexp* (Ritchie, et al. 2007) method. The data set was normalized using *loess* within-array normalization and *quantile* between-array normalization. Normalization was performed using *limma* (Smyth, et al. 2005) package, publicly available in R (version 2.11.1, Bioconductor; www.bioconductor.org). Expression ratios were calculated (Cy5 processed signal was divided by Cy3 processed signal) and log2 transformed. Normalized data were preprocessed using GEPAS server (Montaner 2006). Inconsistent replicates (SD>1) were discarded, and consistent replicates were averaged. Finally, genes that exhibited flat patterns (SD≥0.8) across the set of samples were filtered and omitted in further comparisons. Microarray dataset from the set of tumors analyzed in this study is publicly available at GEO database (GEO accession number, GSE32662).

6. MicroRNA expression microarrays

For identifying the microRNA profiling 300 ng of total RNA was amplified, then labeled with Hy3 fluorescent dye and hybridized onto 1-color miRNA microarray (Exiqon, v.11.0 -hsa, mmu & rho) according to the manufacturer's instructions using miRCURY LNA™ microRNA Array kit (Exiqon). This array contains capture probes targeting 1084 human miRNAs annotated in the miRBASE database (www.mirbase.org).

6.1 Labeling and hybridization: miRCURY LNA™ microRNA Array

Prior to performing the labeling, the fluorescent dye (Hy3) and the spike-in miRNAs were dissolved by adding 29µL and 30µL of nuclease-free water, respectively, and incubated in ice for 30 min. The spike-in miRNAs were aliquoted to avoid repeated freeze/thawing.

The purified total RNA with preserved small RNAs and RIN above 7 was dissolved in RNAse-free water to a final amount of 300ng of RNA.

The labeling procedure was follow according manufacturer instructions:

1. Place all *miRCURY LNA™ microRNA Array Power Labeling kit* components on ice and thaw them for 15-20 minutes. Mix all components vigorously excluding the enzymes.
2. Add 1µL of *Spike-in miRNA kit*, 0,5µL of *CIP buffer* and 0,5µL of *CIP enzyme* to a 2µL of total RNA. Pipette all the reagents up and down and mix vigorously.
3. Incubate the mixture at 37^0C for 30 minutes using a PCR cycler with heated lid.

4. Stop the enzyme reaction and denature the RNA by incubation at 95^0C for 5 minutes followed by snap cooling on ice. Leave on ice between 2, to up to 15 minutes and then centrifuge the reaction after the incubation on ice briefly.

5. To avoid direct light exposure while performing this step, add 3µL of *Labeling buffer*, 1,5µL of *Fluorescent label* (Hy3™), 2µL of DMSO, 2µL of *Labeling enzyme* to a final volume of 4µL of the mixture from step 4.

6. Mix and centrifuge the reagents briefly and incubate them at 16^0C for 1h using a PCR cycler with heated lid. Protect reaction from light.

7. Incubate at 65^0C for 15 minutes and after stopping the labeling reaction, centrifuge and leave on ice. The labeled samples are ready for the hybridization part, on the array. Hybridization should preferably occur within next 1-2h.

The hybridization protocol was followed according to manufacturer´s instructions:

1. Adjust the volume of the sample from the Hy3 labeling reaction to 200µL by adding nuclease-free water.

2. Add 200µL of Hybridization buffer and denature the sample at 95^0C for 2 minutes. Leave on ice from 2 up to 15 minutes and then add 400µL to reservoir.

3. Incubate at 56^0C for 16h in a hybridization chamber with rotation.

6.2 Washing and scanning: miRCURY LNA™ microRNA Array

Further on the slides were washed during repetitively procedure as followed:

1. Wash in *buffer A* at 56^0C for 2 minutes.

2. Wash in *buffer B* at 23^0C for 2 minutes.

3. Wash in *buffer C* at 23^0C for 2 minutes.

4. Dry the slides in absolute ethanol by immersing for 1 minute.

After washing, microarrays were scanned using a fluorescent Agilent Microarray Scanner G2565 (Agilent Technologies, Palo Alto, CA, USA).

6.3 miRNA normalization and preprocessing

Fluorescence intensities on scanned one-color images were quantified using Feature Extraction v9.5 software (Agilent Technologies) using the modified Exiqon protocol. Background correction was carried out, and raw data were normalized by quantiles. Normalized data were preprocessed using GEPAS server(Montaner, et al. 2006). Differentially expressed miRNAs were identified by

applying linear models using the Bioconductor *limma* R package (Smyth 2005) (http://www.bioconductor.org). Microarray dataset is publicly available at GEO database.

7. Bioinformatic analysis of gene expression and miRNA data

7.1 Unsupervised clustering

MTC tumor samples were grouped according to their expression profiles by average linkage hierarchical clustering (Pearson correlation, uncentered metrics) using Gene Cluster 2.0 (Reich 2004) and Treeview (http://rana.stanford.edu/software) algorithms were used to obtain clustering of the data sets. Unsupervised clustering was implemented by a SOM algorithm. The level of expression of each gene in each sample, relative to the median level of expression of that gene across all the samples is represented using a green-black-red color scale. Green corresponds to expression value below median, black, to median and red above median. Only tumors exhibiting the 634 or the M918T *RET* mutation, and tumors classified as WT were used in further analysis.

7.2 Supervised clustering

To determine if there were genes and miRNAs differentially expressed between particular groups associated with specific *RET* mutations, supervised classification was performed with T-test with 200.000 permutations or with linear models (limma), implemented in the POMELO II tool (Morrissey and Diaz-Uriarte 2009), freely available in Asterias web server (http://asterias.bioinfo.cnio.es). T-test was also carried out using a T-Rex application from the GEPAS package and for differential expression analysis(Montaner et al. 2006). To account for multiple hypothesis testing, the estimated significance level (*p*-value) was adjusted using Benjamini's False Discovery Rate (FDR) correction (Benjamini, et al. 2001). Those genes with FDR <0.05 and miRNAs with FDR<0.15 and both with a fold-change>2 were considered as significantly differentially expressed and selected for the validation step. Moreover, alternatively, Significance Analysis of Microarrays (SAM) (Tusher, et al. 2001), was performed for analysis of miRNA/genes significantly different between two classes, comparing groups with specific genetic conditions, where T-test statistics was applied. SAM calculates a score for each miRNA/gene on the basis of the change in expression relative to the standard deviation (SD) of all measurements. A threshold of q-value of 0.01 (transcriptional profiling) and 0.15 (miRNA profiling) were used and 3000 permutations were applied. The missing values were excluded.

7.3 Functional profiling and pathways analysis

7.3.1. Gene Ontology analysis

Functional enrichment of gene ontologies (GOs) for differentially expressed genes (DEGs) was performed using the FatiGO tool (Al-Shahrour, et al. 2004) implemented in Babelomics software. Fisher's exact test was performed to obtain significant over-representation of GO terms in the DEGs list *versus* the rest of the genome. GO terms showing an FDR<0.05 were considered significant.

7.3.2. Gene Set Enrichment Analysis (GSEA)

Gene Set Enrichment Analysis (GSEA) (Subramanian, et al. 2005) was performed to gain insight into global molecular networks and canonical pathways related to MTC specific genetic condition-driven signature and translating differentially expressed genes into pathways between specific genetic groups. GSEA outcome is based on the study of the distribution of gene sets sharing functional annotations across a list of genes ranked according to differential expression. GSEA gene sets are defined based on prior biological knowledge, e.g., published information about biochemical pathways or co-expression in previous experiments. In our data analysis we have included the Biocarta (www.biocarta.com) and KEGG (www.genome.jp/kegg/) datasets as a source of pathway annotations. The ranking of all genes in the sets were determined and an enrichment score (ES) was calculated for each pathway as a measure of its relevance. This enrichment score value was further normalized in order to calculate the normalized enrichment score (NES) used for pathway evaluation. The ranking of genes was performed with T-test, with an absolute mode for gene list sorting. 1000 gene set permutations were done on the gene expression profiles to assess the statistical significance of the pathways. FDR (q value) is computed by GSEA program. Pathways within FDR <0.25, were considered significantly enriched between classes under comparison.

7.3.3. Ingenuity Pathway Analysis (IPA) 9.0

Once a list of significantly differentially expressed genes is obtained, interesting targets of miRNAs or molecular signatures originating from different MTC subtypes were explored by applying different tools for functional analysis. Their function is to analyze between/inter interaction of different genes implicated in the study. One of them, the Ingenuity Pathways Analysis (IPA -

Ingenuity Systems, Mountain View, California) is a network application, which allows us to analyze the biology of different list of genes at different levels, integrating data from various experimental platforms, allowing further in depth study of the molecular and chemical interactions, cellular phenotypes and related diseases. IPA was used to assess the enrichment of groups of genes associated with specific genetic conditions such as RET^{634}, RET^{918} and RET^{WT}, together with their implicated biological functions and signaling pathways. This computer-based programme was also used to identify the direct physical and functional interactions between proteins.

7.4. mRNA-miRNA expression integration and functional enrichment analysis

As miRNA and mRNA profiling data were available from the same tumor set, we performed an integration of both profiles assuming that increased or decreased expression of specific miRNA results in at least partially decreased or increased expression of corresponding target mRNAs respectively. Significantly differentially expressed miRNAs and mRNA from comparisons MTC^{634} *vs* MTC^{918} and MTC^{918} *vs* MTC^{WT} were used in the analysis.

Those significant miRNAs according to the Fisher's exact test (FDR<0.1) were selected on the basis of their non-random association with the gene expression signature of interest (FDR <0.05). The microRNA predicted targets were identified using miRBase Targets Release v5.0 and Target Scan. Then we researched the inverse correlation between upregulated expression of a microRNA and its predicted targets using MAGIA(Sales, et al. 2010) web tool applying the parametric linear Pearson correlation for all analyses. IPA 9.0 (www.ingenuity.com) was used to assess potential biological pathways, functions and networks for significant putative targets (FDR<0.25) of miRNAs revealed previously from miRNA-mRNA integration analysis.

8. Validation by quantitative RT-PCR

For the validation of microarray data, genes and significantly differentially expressed miRNAs among profiling results were selected to be assessed by RT qPCR. PCRs were done on an ABI Prism 7000 sequence detection system (Applied Biosystems, Foster City, CA, USA).

8.1. Validation of the results from gene expression profiling by quantitative RT-PCR

For gene expression results validation, the independent FFPE and frozen samples series were used. As endogenous references we used β-glucoronidase (*GUS)*, 60S acidic ribosomal protein P0 (*RPLP0*) and peptidylprolyl isomerase A (*PPIA*); *GUS* was used to normalize the quantification of mRNA expression. Reverse transcription was performed using 1µg total RNA and random hexamers (FFPE samples), or 0,5µg total RNA and oligoDT (frozen specimens), and M-MLV Reverse Transcriptase (Promega Corporation, Madison, WI, USA). PCRs were done on an ABI Prism 7600 sequence detection system (Applied Biosystems, Foster City, CA, USA) using the Universal Probe Library set (https://www.roche-applied-science.com) as described by the manufacturer. All analyses were performed in triplicate. The Kruskal-Wallis test (nonparametric ANOVA) for multiple class comparisons and the nonparametric Mann-Whitney test for two class comparisons were used to compare the genetic classes. Quantification data were calculated by the $2^{-\Delta\Delta CT}$ method.

8.2. Validation of the results from miRNA expression profiling by quantitative RT-PCR

Significantly differentially expressed miRNAs among profiling results were selected according to the mentioned criteria to be assessed by RT qPCR. Frozen and FFPE independent MTC series were used for validation. As endogenous references we used RNU-5G, SNORD48 and SNORA66 to normalize the quantification of miRNA expression. Reverse transcription was performed with miRCURY LNA™ Universal RT microRNA PCR system (Exiqon) using 20ng total RNA according to the manufacturer´s instructions. Samples (cDNAs) were diluted 1:80 and stored at -20°C until used for real-time PCR. PCRs were done on an ABI Prism 7900HT sequence detection system (Applied Biosystems, Foster City, CA, USA) using the LNA™ microRNA PCR primer/SYBR® Green mix (Exiqon) as described by the manufacturer. PCR reactions were performed in triplicates and negative controls were included. The Kruskal-Wallis test (nonparametric ANOVA) for multiple class comparison was assessed (P value<0.05) and was carried out using SPSS software package version 17.0 (SPSS, Inc., Chicago, IL). Quantification data were calculated by the $2^{-\Delta\Delta CT}$ method and qBase (Biogazelle) software was used(Hellemans, et al. 2007).

9. Immunohistochemistry (IHC)

Immunohistochemical staining was performed on both MTC tissue microarrays available. TMA blocks were sectioned at a thickness of 3µm and dried for 1h at 60ºC. Deparaffinization,

rehydration and epitope retrieval were achieved by heat treatment in a PT Link (Dako, Glostrup, Denmark) at pH 9. Before staining the sections, endogenous peroxidase was blocked. Primary antibodies used were anti-CD133 (1:500, ab19898 Abcam, Cambridge, MA, USA), anti-GFRα1 (1:500, C-20, Santa Cruz Biotechnology, Santa Cruz, CA, USA) and anti-ESM1, (1:500, clone 6D4 Santa Cruz Biotechnology, Santa Cruz, CA, USA); incubations with primary antibodies were according to the manufacturers' instructions. After incubation with anti-CD133, the reaction was visualized with EnVision™ FLEX (Dako, Glostrup, Denmark) using diaminobenzidine chromogen as a substrate; anti-GFRα1 binding was visualized with the LSAB+ Kit (Dako, Glostrup, Denmark) using diaminobenzidine chromogen as a substrate; anti-ESM1 binding was visualized with DAKO EnVision TM FLEX Mouse kit (Linker)(DAKO, Carpinteria, CA, USA), the sections were deparafinated, and made the recovery of the antibody to PH9 PT link (DAKO, Carpinteria, CA, USA) and AB incubation for 30 min. Sections were counterstained with hematoxylin. Appropriate positive and negative controls were also tested.

Immunoexpression was graded semi-quantitatively by considering the percentage and intensity of the staining. A histological score was obtained for each sample, which ranged from 0 (no immunoreaction) to 300 (maximum immunoreactivity). Interpretation was done as previously described (Gallel 2008). Since each TMA included two cores from each case, immunohistochemical evaluation was done after examining all samples.

10. MTC cell lines and *in vitro* functional studies on MTC cell lines (MZ-CRC-1 and TT)

MZ-CRC-1 cells, derived from a metastatic MTC and harbor the M918T *RET* mutation (Cooley 1995; Santoro et al. 1995), and TT cell line, harboring a mutation at residue 634 of RET were available.

10.1 Cell culture and nucleofection

MZ-CRC-1 cells were a generous gift from Dr. Robert F. Gagel (M.D. Anderson Cancer Center, University of Texas). TT cells were from the American True Type Culture Collection (ATCC). Both cell lines were maintained in DMEM medium supplemented with 10% inactivated fetal bovine serum, 1% pyruvate, 1% non essential amino acids, 100U/ml penicillin and streptomycin at 37ºC in 5% of CO2 in air. For nucleofection of MZ-CRC-1 cells, two million cells per condition were incubated with 2µM synthetic siRNAs (Sigma) directed against human CD133 in a buffer containing 150mM phosphate buffer, 100mM KCl and 10mM MgCl2. Cells were nucleofected using the A30

program of an Amaxa Nucleofector II device (Lonza). Rapidly after nucleofection, the cells were re-suspended in medium and seeded onto 6-well plates.

10.2 Lentivirus construction and infection

An expression cassette consisting of the cytomegalovirus (CMV) promoter followed by the human Pprominin1 open reading frame was cloned into a modified pDSL_hpUG vector (ATCC, cat # 10326371) lacking the Ubiquitin c-GFP cassette. Briefly, the Prominin1 open reading frame was first cloned into pcDNA3 (Invitrogen) by standard techniques. Using a construct such as a template, a PCR product consisting of the CMV promoter followed by the Prominin1 ORF and flanked by attB sites was generated. Finally, this product was sequentially cloned into pDONR221 entry vector (Invitrogen) and then moved to the final destination vector (FUSPA) via gateway recombination technology.

Lentiviral particles were produced essentially as described (Encinas, et al. 2008). Briefly, 293T cells were co-transfected by the calcium phosphate method with the above plasmid plus plasmids coding for the envelope and the packaging systems (VSV-G and Δ8.9, respectively). The day after, the transfection culture medium was replaced with fresh medium and left for additional 2-3 days to allow lentiviruses to be produced and released. Supernatants were then harvested, filtered through a 0.45 μm filter, and directly applied to TT cells. Typically, cells were infected overnight and experiments were conducted 4 to 5 days after infection.

10.3 Apoptosis assays

Three days after transfection, we analyzed the number of apoptotic nuclei by Hoechst staining. Cell-permeant Hoechst 33342 dye was directly added to cells at a final concentration of 0,5mg/ml, and incubated 15 minutes at 37ºC. Cells were then photographed under a fluorescence microscope (Olympus IX70). The percentage of apoptotic nuclei was scored in triplicate by a naïve observer. Five hundred to one thousand cells per condition were counted.

10.4 Real time quantitative PCR (RT-qPCR)

Total RNA from MZ-CRC-1 cells was extracted with the RNAeasy kit (QIAGEN, Alameda, CA) and reverse transcribed using the TaqMan® Reverse Transcription kit from Applied Biosystems (Foster City. CA). The relative mRNA levels of CD133 and GFRα1 were measured by real-time PCR using TaqMan® probes from Applied Biosystems (Hs01009250_m1 (CD133) and Hs00237133_m1

(GFRα1)). Probe Hs99999905_m1 (GAPDH) was used for data normalization. Results were calculated by the $2^{-\Delta\Delta CT}$ method.

11. Statistical analysis

Immunoexpression was analyzed in two different ways, as a continuous variable, and as a binary variable using the median as the cut-off. For the first analysis, Mann-Whitney U test was used, and for the second, difference in expression was tested with a Chi-squared or Fisher's exact test when appropriate. Statistical analyses were carried out using SPSS software package version 17.0 (SPSS, Inc., Chicago, IL). Nominal two-sided P-values less than 0.05 were considered statistically significant.

In order to identify statistically significant associations between differentially expressed microRNAs (FDR < 0.1) and gene expression signatures (FDR <0.05), the analysis of consistency of predicted microRNA-mRNA targeting pairs with the pair components inversely correlated. Those miRNAs and genes with significant FDR values were subjected to Fisher´s exact test and selected on the basis of their non-random association with their expression signature of interest. For multiclass comparisons with non-parametric ANOVA, the U-Kruskal-Wallis test was applied comparing three groups of MTC: MTC^{634}, MTC^{M918T}, MTC^{WT}.

Results

Results I. Gene expression profiling project.

1. Molecular genetic characteristics of the MTC tumors

Medullary thyroid carcinomas were classified according to their specific *RET* mutation. Forty-nine MTCs out of the 69 available passed the selection criteria (good RNA quality and high tumor percentage in the tissue, >80%) and were hybridized onto Agilent microarray platform. Among the 49 tumors used for profiling, 7 carried a germline *RET* mutation in codon 634, 14 carried the M918T *RET* mutation, and 20 were classified as WT. The remaining eight MTCs had 6 different germline mutations and 2 different somatic mutations in *RET* (supplementary appendix Table 1). These latter 8 tumors were not considered in clustering analysis. Twenty-tree out of the 38 additional independent formalin-fixed paraffin embedded (FFPE) MTCs (supplemental annex Tables 1 and 2) as well as those frozen tumors not considered for hybridization purposes were used for validation by RT-qPCR.

2. Data reveal differential expression profiles in inherited and sporadic MTC

Unsupervised hierarchical clustering, performed using standard correlation as a measure of similarity across all hybridized samples, showed a relatively low heterogeneity distributed over two principal branches (Figure 5).

An enrichment with familial MTC cases with germline *RET* mutations was observed in the second branch of the cluster, whereas the first one was enriched with sporadic MTC with somatic M918T *RET* mutations and WT cases. This observation led to us to do a supervised analysis based on the known mutations of each available tumor. Differential expression analysis was performed comparing $MTCs^{M918T}$ *vs* $MTCs^{WT}$, and $MTCs^{M918T}$ *vs* $MTCs^{634}$ (Figures 6A and 6B), obtaining a list of 360, and 18 significant genes (GEO accession number GSE32662) respectively.

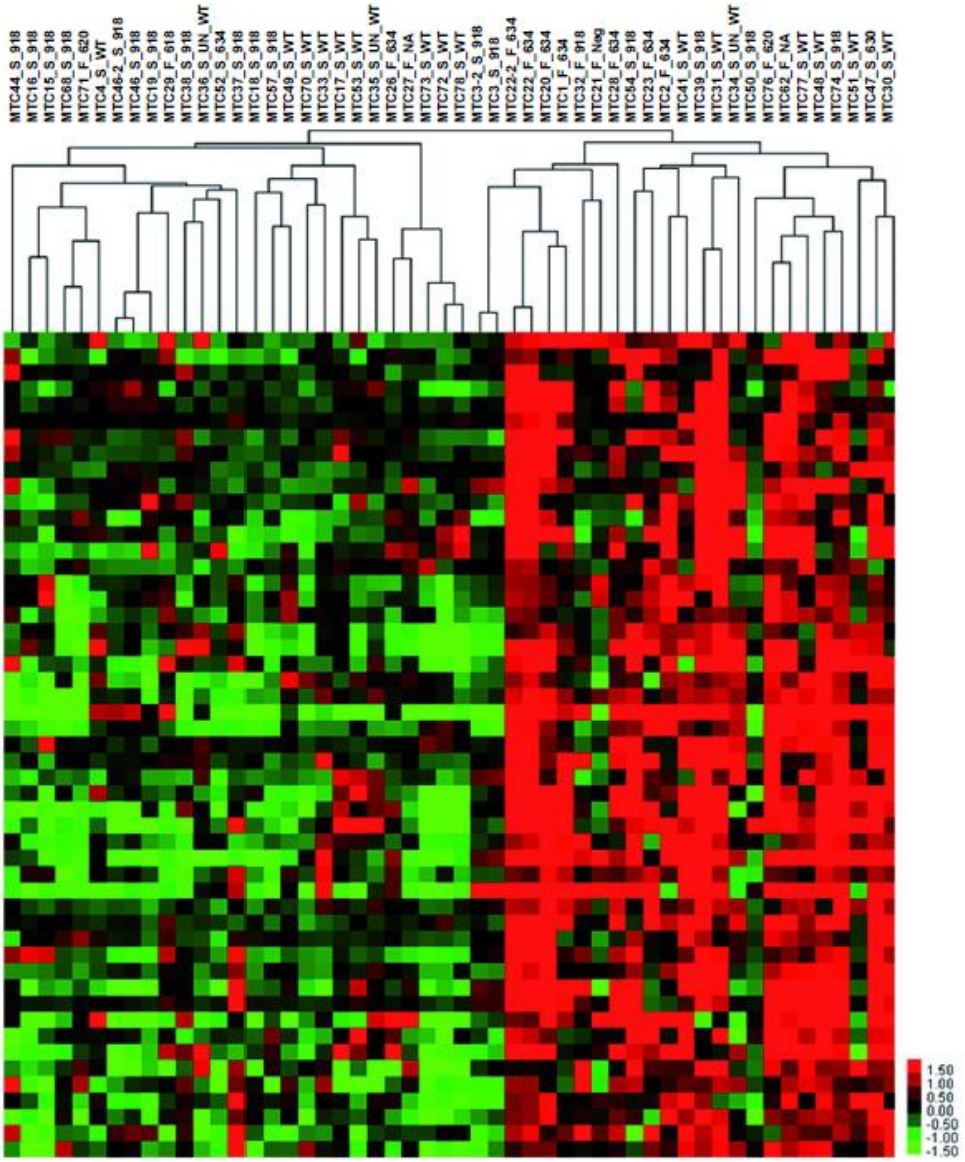

Figure 5. Unsupervised clustering of hybridized frozen MTC series. Partial heat map showing two principal branches after applying unsupervised clustering to the 49 MTCs. The first branch was enriched with MTC^{M918T} cases and the second with familial MTC cases, mostly with RET^{634} mutation. Color bar, green and red, represents relative under- and over expression levels respectively. MTC cases were named using ID case and extensions as: S_918 (sporadic MTC with somatic M918T *RET* mutation), F_634 (familial MTC with 634 *RET* mutation) and S_WT (sporadic MTC with no *RET* mutation), S_UN_WT (sporadic MTC with no data regarding somatic *RET* mutation).

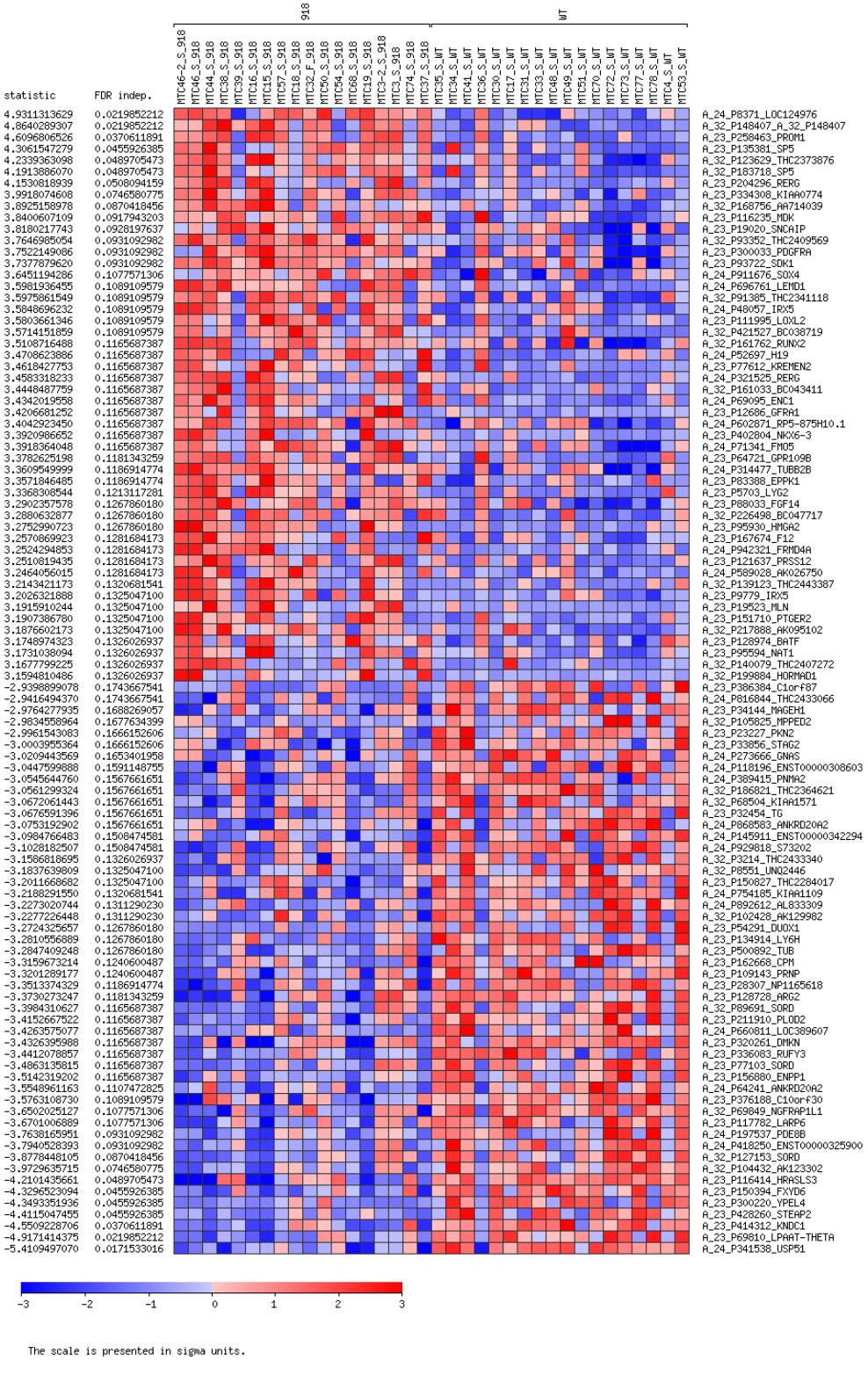

Figure 6A. Differential expression analysis of MTCs^{M918T} *vs* MTCs^{WT} using the GEPAS package. The first 100 genes with a false discovery rate (FDR) <0.05 are shown, including information about t statistic.

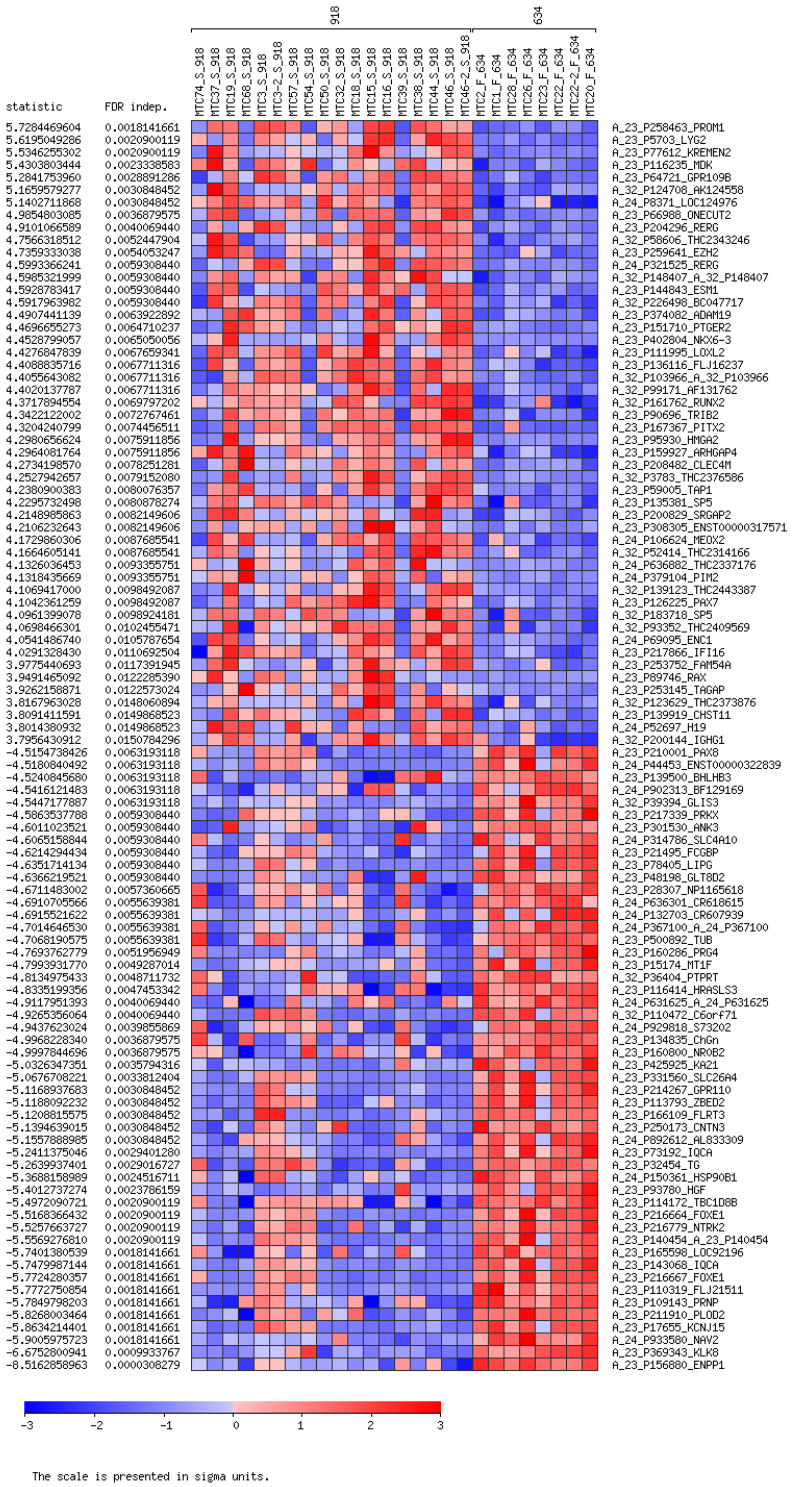

Figure 6B. Differential expression analysis of MTCs^{M918T} *vs* MTCs^{634} using the GEPAS package. The first 100 genes with a false discovery rate (FDR) <0.05 are shown, including information about t statistic.

Based on threshold-free methodology using GSEA, signaling pathways were identified as significantly differently expressed (FDR<25%) when comparing $MTCs^{M918T}$ *vs* $MTCs^{634}$ and $MTCs^{M918T}$ *vs* $MTCs^{WT}$ (Supplemental annex Tables 4A and 4B, respectively). The M918T cluster was correlated with several pathways related to malignant tumor behavior, such as the p53, caspase, cytokine, Wnt, NFκB, MAPK, IL1R, JAK/Stat, and Notch pathways.

Analyses of Gene Ontologies (GO) revealed significant biological processes in the M918T group associated as well with malignant behavior (shown in bold in supplementary annex Table 5). They were mainly associated with cell-cycle, cell adhesion and proliferation and anti-apoptotic activity pointing to aggressive course of this specific MTC group.

Further one, hierarchical clustering analysis of the most relevant FatiGO outputs for biological processes, revealed a long list of significant results associated specifically with MTC^{M918T}group. They again, pointed to the importance of cell adhesion, migration and proliferation ontologies (Supplementary annex Table 6).

FatiGO analysis (supplementary appendix Table 5) and GSEA analysis (supplementary appendix Tables 4A and 4B) revealed similar significant pathways associated with the M918T group.

3. Markers identified as specific of genetic condition

After applying the filtering criteria (FDR <0.05 and fold change greater than 2), five genes (*PROM1*, *GFRA1*, *LOXL2, GAL,* and *DKK4)* appeared to be markers of different genetic conditions and were selected for further validation at the mRNA level.

GAL was the only gene statistically significant found to be a specific marker for the germline *RET* mutation in codon 634. The expression of the other four genes was validated by quantitative RT-PCR as up-regulated markers among $MTCs^{M918T}$. Due to limited availability of RNA, it was only possible to validate *PROM1* and *LOXL2* in FFPE MTC samples. Figures 7A and 7B summarize these results in the independent frozen and FFPE series, respectively.

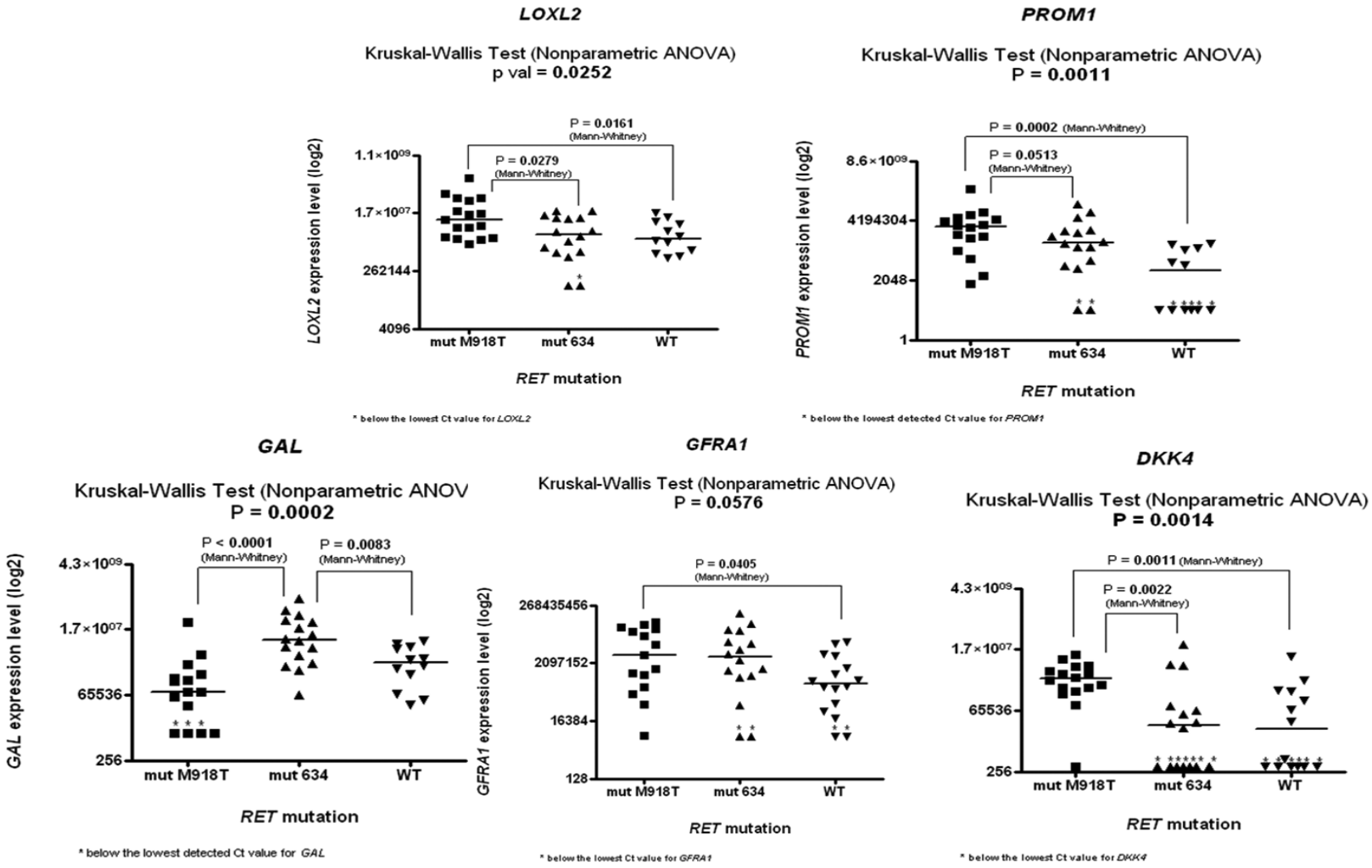

Figure 7A. Result from validation in frozen independent MTC series.

Although not selected for further validation, other genes differentially expressed among the three different genetic conditions considered herein had been reported to be involved in cancer of tissues derived from neural crest, and also in the RTK signaling pathway. Therefore, these previous findings were considered as a cross-validation of our results. Among these markers, the up-regulated genes associated with the M918T mutation were *ESM1*, *NPR1, PITX2, RTN1,* and *SHC1. ESM1* (endothelial cell-specific molecule 1) is associated with cell migration and proliferation, and its over-expression has been previously described in sporadic RET^{M918T} MTC cases (Ameur et al. 2009). *NPR1 (*natriuretic peptide receptor A/guanylate cyclase A) regulates the activation of ERK1/2(Deng 2010), as well as Ras/Raf/ERK and Wnt/β-cathenin pathways. *PITX2* (paired-like homeodomain 2) is involved in tumorigenesis and Wnt/β-cathenin signaling, and is expressed in neural crest cells (Zacharias 2010). *RTN1* (reticulon 1), overexpression of which leads to apoptosis of neuroblastoma cell lines, is involved in secretion or membrane trafficking in neuroendocrine cells as well as in tumorigenesis, and is expressed in neurons and neuroendocrine cells (Steiner 2004). Fibroblasts transformed by RET^{C634R} display constitutive RET-mediated phosphorylation of SHC which activates the RAS/MAPK signaling pathway (Ohiwa, et al. 1997).

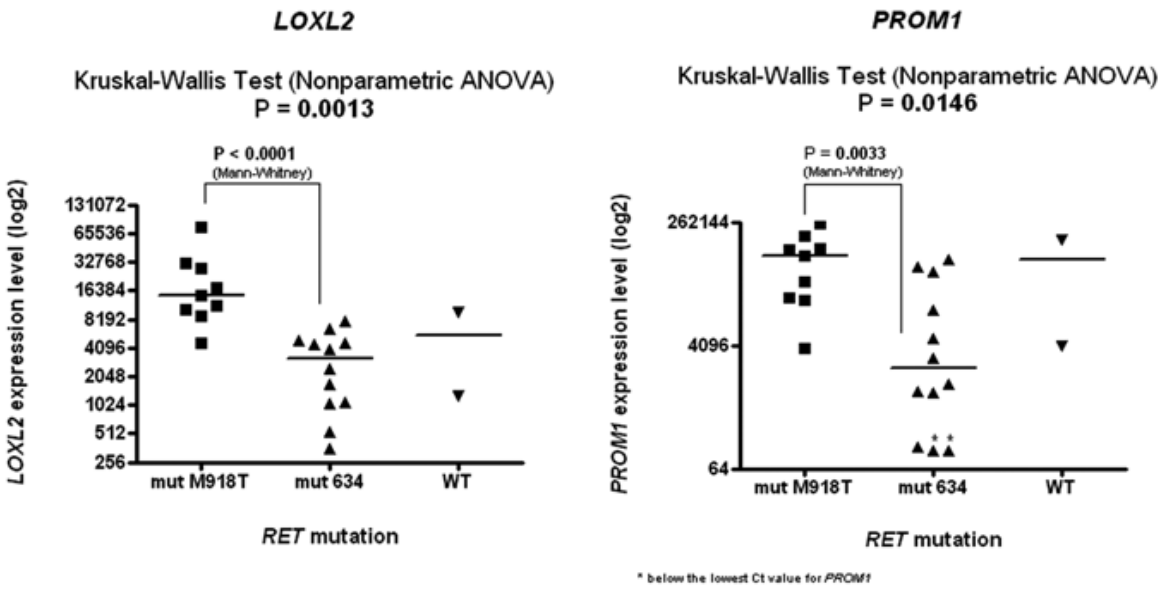

Figure 7B. RT-qPCR with Taqman probes of *LOXL2* and *PROM1* expression in an independent FFPE MTC validation series.

4. Immunohistochemical characterization

We performed immunohistochemistry (Figure 8) for GFRA1, ESM1 and CD133 (PROM1). Differences at the mRNA level were not validated at the protein level. GFRA1 and ESM1 protein levels were not significantly different among the groups. CD133 showed higher staining in MTCs^{M918T} than in MTCs^{634} (P=0.059), in agreement with mRNA detection (Table 6).

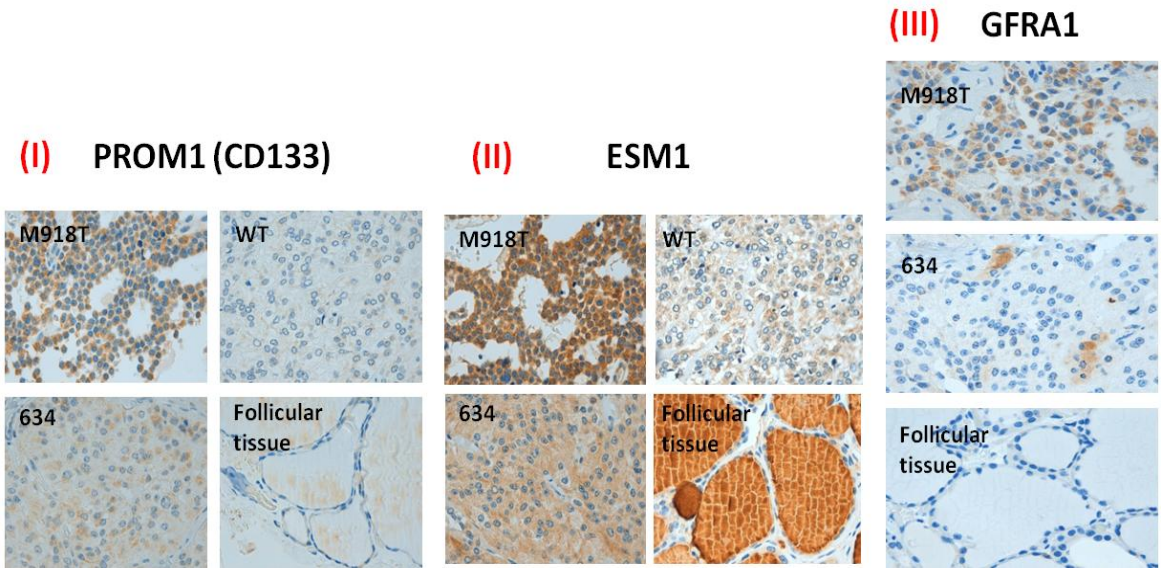

Figure 8. Representative microscopic images of immunohistochemical staining for PROM1 (CD133**) (I),** ESM1 **(II)** and GFRα1 **(III)** in medullary thyroid carcinoma.

Table 6. Statistical analysis of 3 different IHC markers: (A) PROM1 (CD133), (B) ESM1 and (C) GFRA1, respectively. Statistical analyses from three different comparisons: MTC^{634} *vs* MTC^{WT}, MTC^{634} *vs* MTC^{918} and MTC^{WT} *vs* MTC^{918}.

(A) **PROM1 (CD133)**

		number of cases			Total
		WT	634	M918T	
staining	low	13	8	6	27
	moderate	11	10	2	23
	high	11	2	5	18
Total		35	20	13	68

	P value
634 vs WT	0.161
634 vs 918	0.059
WT vs 918	0.539

(B) **ESM1**

		number of cases			
		WT	634	M918T	Total
staining	low	11	7	7	25
	moderate	13	4	3	20
	high	10	9	3	22
Total		34	20	13	67

	P value
634 vs WT	0.329
634 vs 918	0.420
WT vs 918	0.380

(C) **GFRA1**

		number of cases			
		WT	634	M918T	Total
staining	low	9	6	3	18
	moderate	8	4	4	16
	high	11	4	2	17
Total		28	14	9	51

	P value
634 vs WT	0.741
634 vs 918	0.723
WT vs 918	0.578

5. Silencing CD133 by siRNA induces apoptosis

We used the MZ-CRC-1 cell line nucleofected with two different synthetic siRNAs against human CD133 for *in vitro* validation. Knockdown efficiency was assessed in parallel dishes by RT-qPCR, and the number of apoptotic nuclei was scored as percentage of total nuclei. As shown in Figure 9 both siRNAs caused an increase in the number of apoptotic nuclei, suggesting that CD133 is necessary for the survival of these cells.

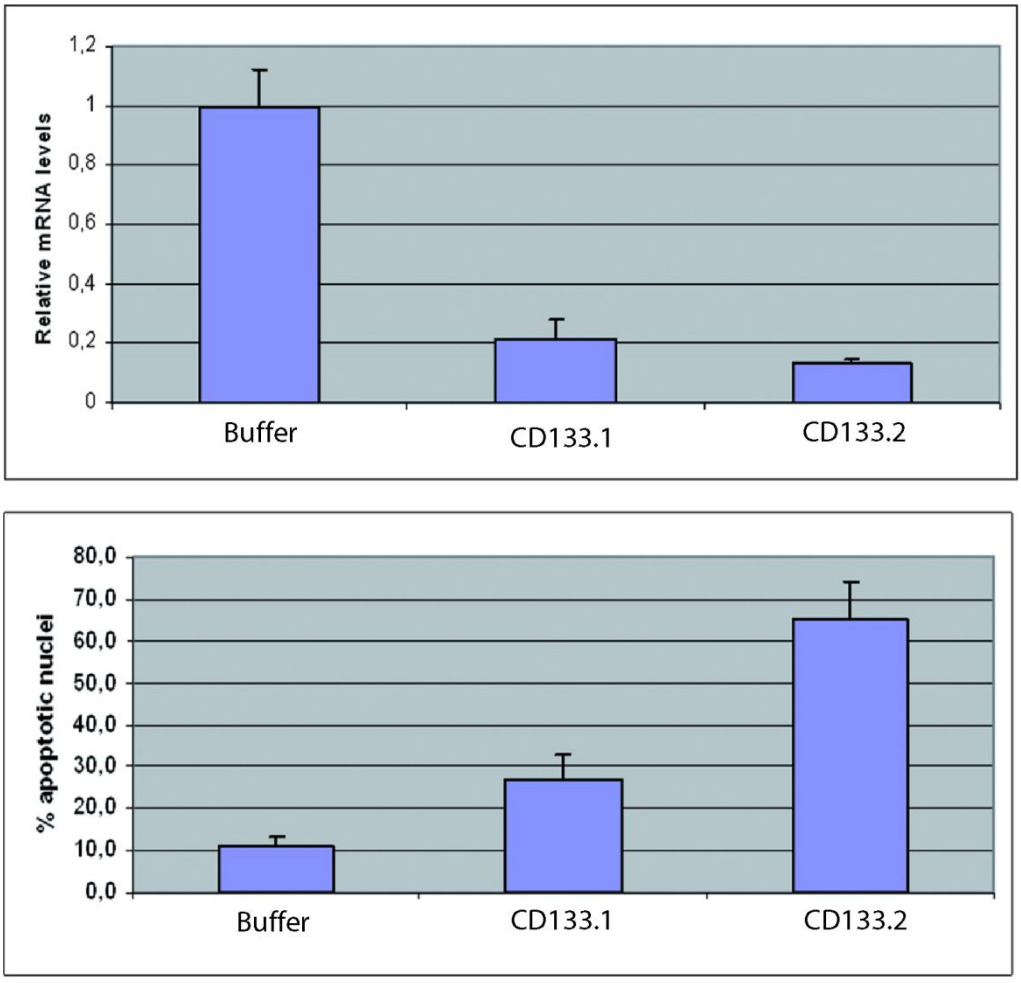

Figure 9. Top panel: Knockdown efficacy of two different siRNAs against human CD133. MZ-CRC-1 cells were nucleofected with either buffer or the indicated siRNAs against CD133 (CD133.1 and CD133.2). Three days later CD133 expression was assessed by real time RT-PCR. **Bottom panel**: Silencing of CD133 causes apoptotic death of MZ-CRC-1 cells. Cells were nucleofected as above and three days later the number of nuclei showing apoptotic morphology was scored.

6. PROM1 overexpression assay based on lentiviral approach and PROM1 clone formation.

6.1 CD133 overexpression in MZ-CRC-1 and TT cell lines.

We checked the CD133 mRNA levels using the quantitative RT-PCR experiment. PROM1 levels were higher in MZ-CRC-1 cell line comparing to TTs. The higher incorporation of BrdU in MZ-CRC-1 *vs* TT cells indicated a higher rate of cellular proliferation (Figure 10).

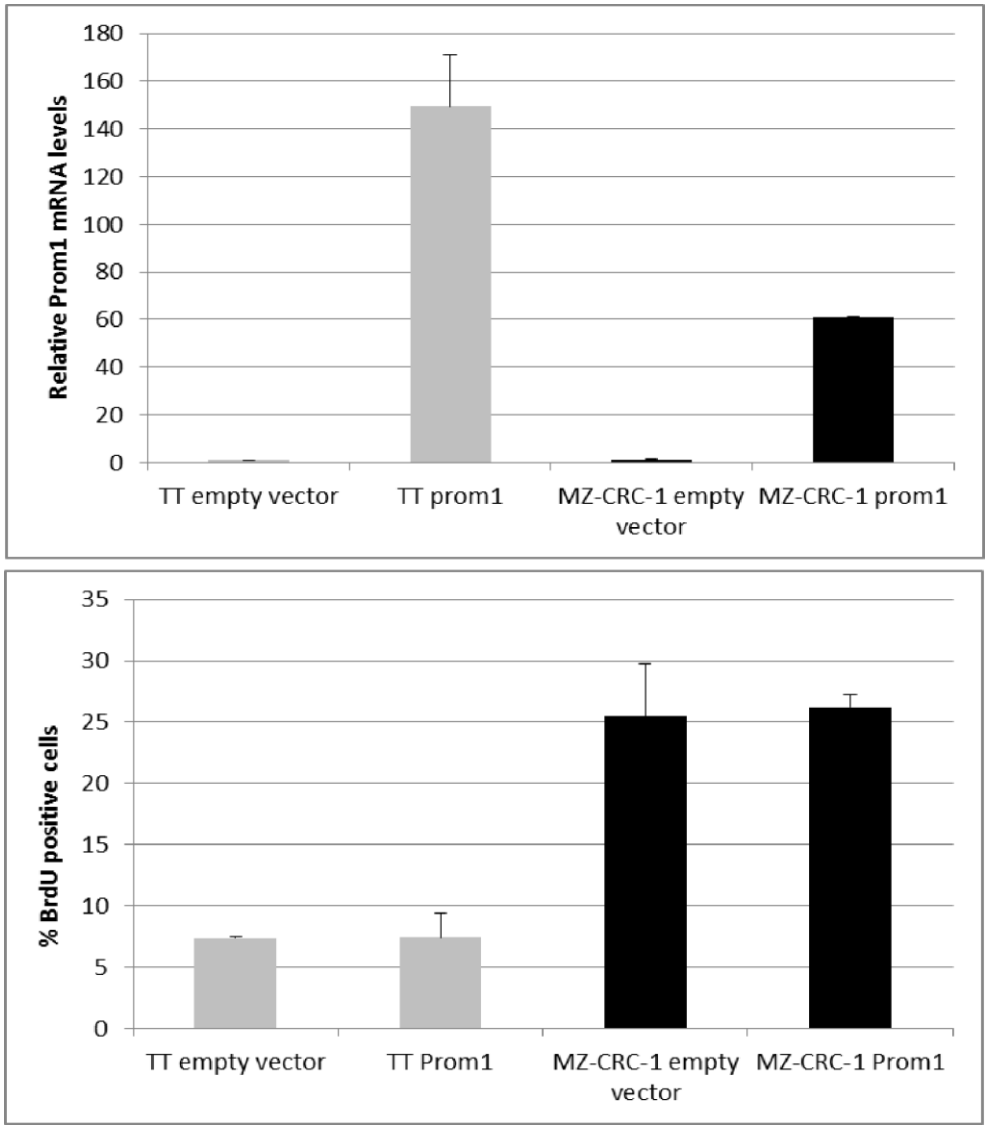

Figure 10. *PROM1* (CD133) levels in MZ-CRC-1 and TT cell lines.

According to these results, *PROM1* over-expression does not affect the proliferation of both, TT and MZ-CRC-1 cell lines. PROM1 over-expression seemed to be associated with the resistance to death by RPI-1 (well know RET inhibitor) in TT cell lines, although also it was observed in MZ-CRC-1. This was observed after 48h treatment conducted by reduction with MTT assay (Figure 11A), while there were not differences after 24h of treatment (Figure 11B).

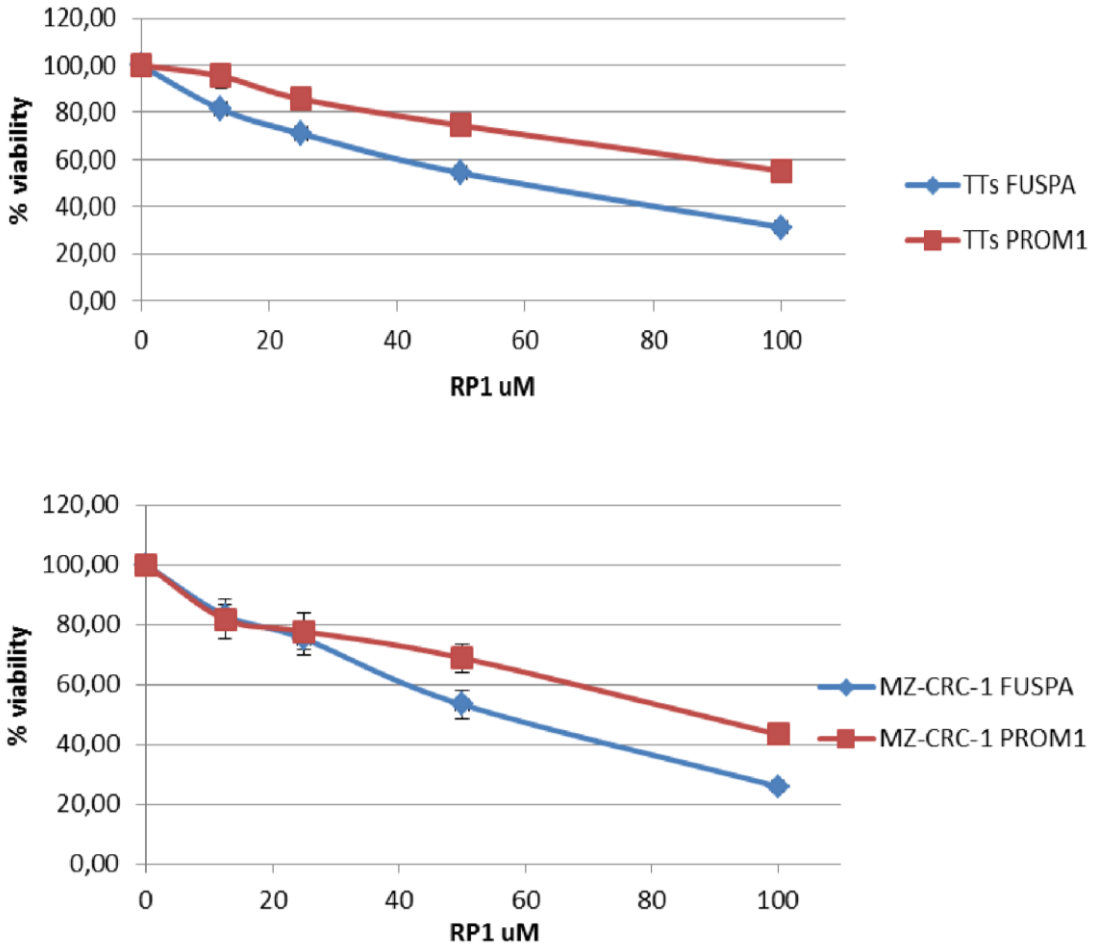

Figure 11A. 48h treatment with RPI-1 RET inhibitor in TT and MZ-CRC-1 cell lines.

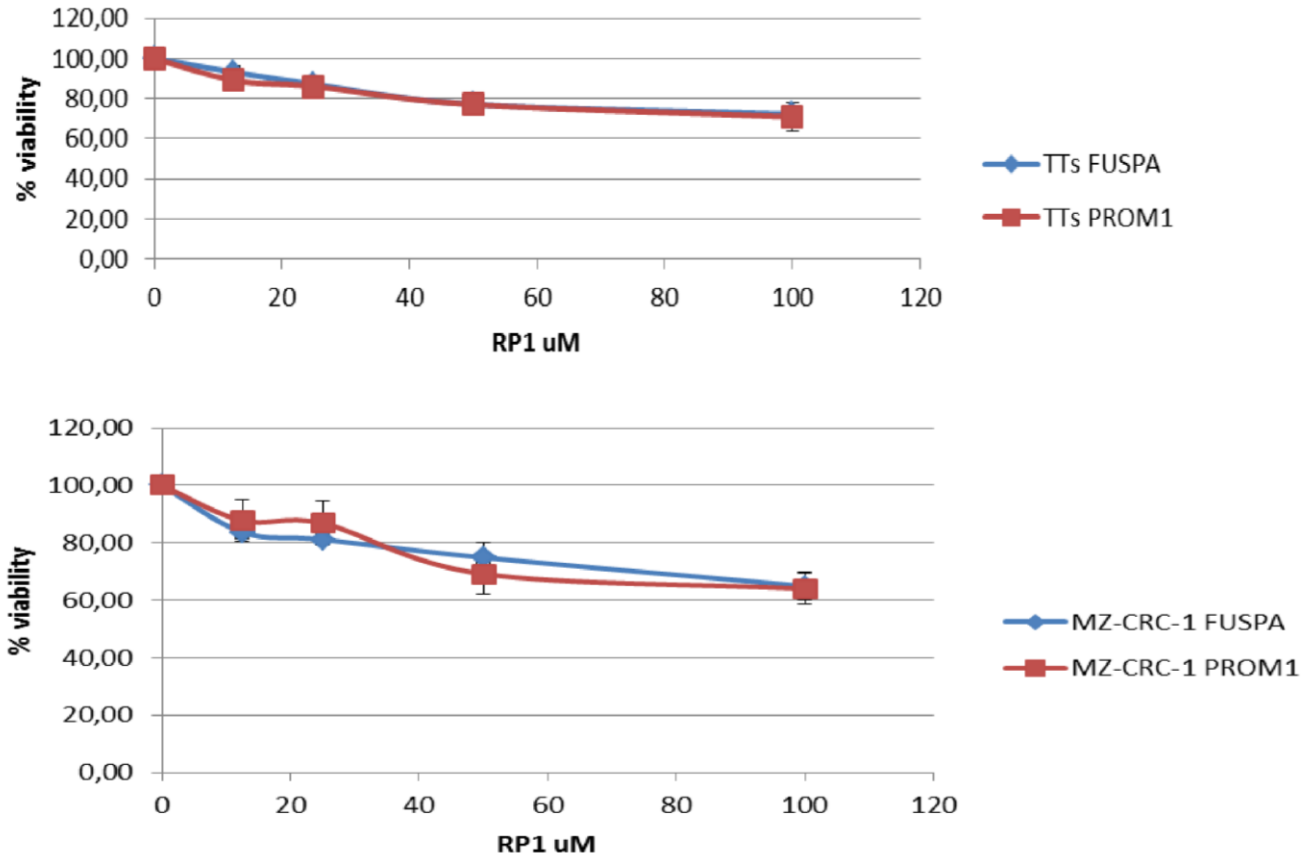

Figure 11B. 24h treatment with RPI-1 RET inhibitor in TT and MZ-CRC-1 cell lines.

7. Data reveal differential miRNA expression profiles in inherited and sporadic MTC

Unsupervised hierarchical clustering, performed using standard correlation as a measure of similarity across all hybridized samples, showed a relatively low heterogeneity distributed over two principal branches (Figure 12). An enrichment of MTC^{918} cases was observed in the second branch of the cluster, whereas the first branch was enriched with WT and MTC^{634} cases. The supervised analysis was performed comparing $MTCs^{918}$ *vs* $MTCs^{WT}$, and $MTCs^{918}$ *vs* $MTCs^{634}$ (Figure 13), obtaining a long lists of 602, and 276 significant miRs (GEO publicly available data) respectively.

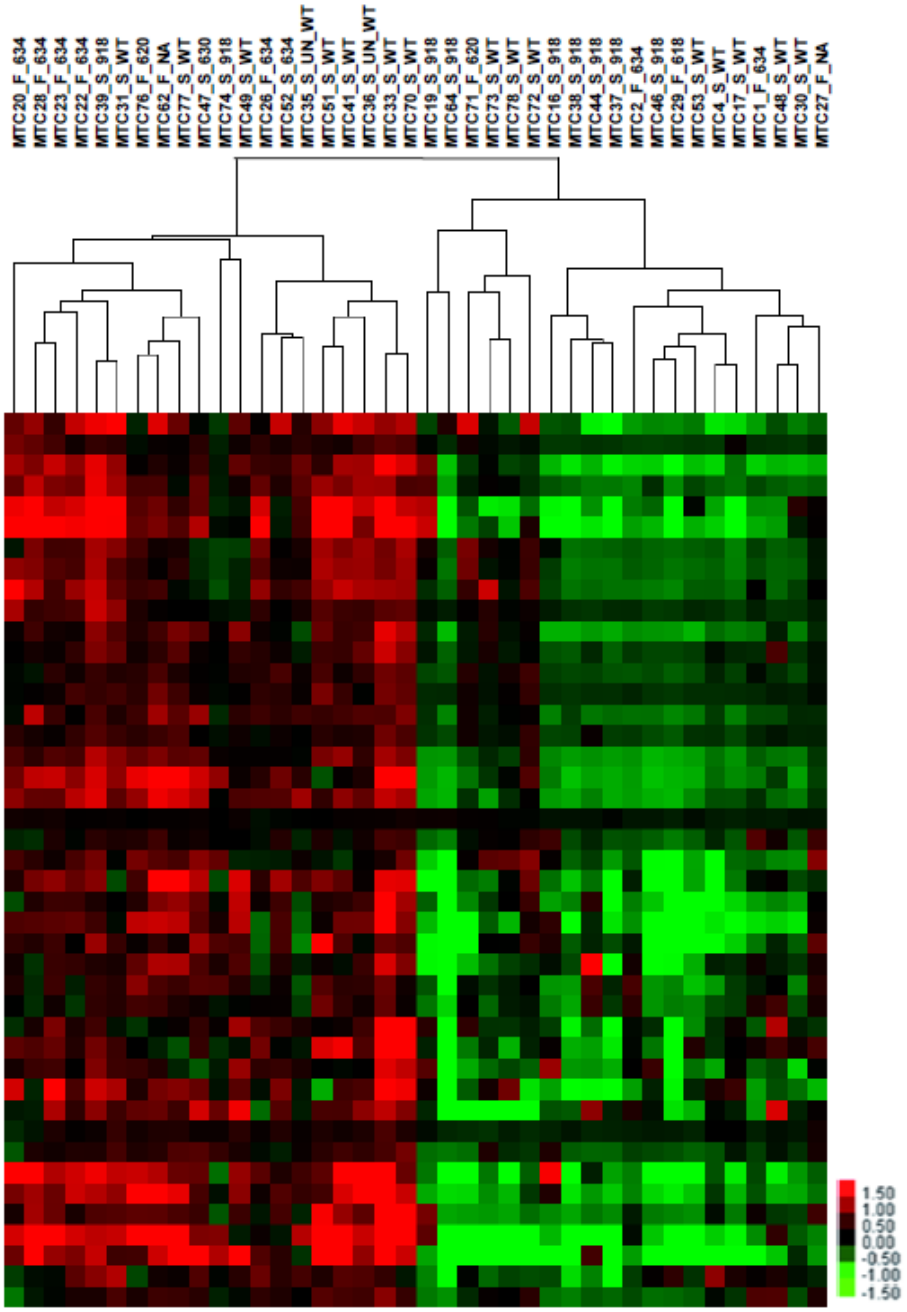

Figure 12. Unsupervised clustering of hybridized frozen MTC series. Partial heat map showing two principal branches after applying unsupervised clustering to the 49 MTCs. The first branch was enriched with MTC^{M918T} cases and the second with familial MTC cases, mostly with RET^{634} mutation. Color bar, green and red, represents relative under- and over expression levels respectively. MTC cases were named using ID case and extensions as: S_918 (sporadic MTC with somatic M918T *RET* mutation), F_634 (familial MTC with 634 *RET* mutation) and S_WT (sporadic MTC with no *RET* mutation).

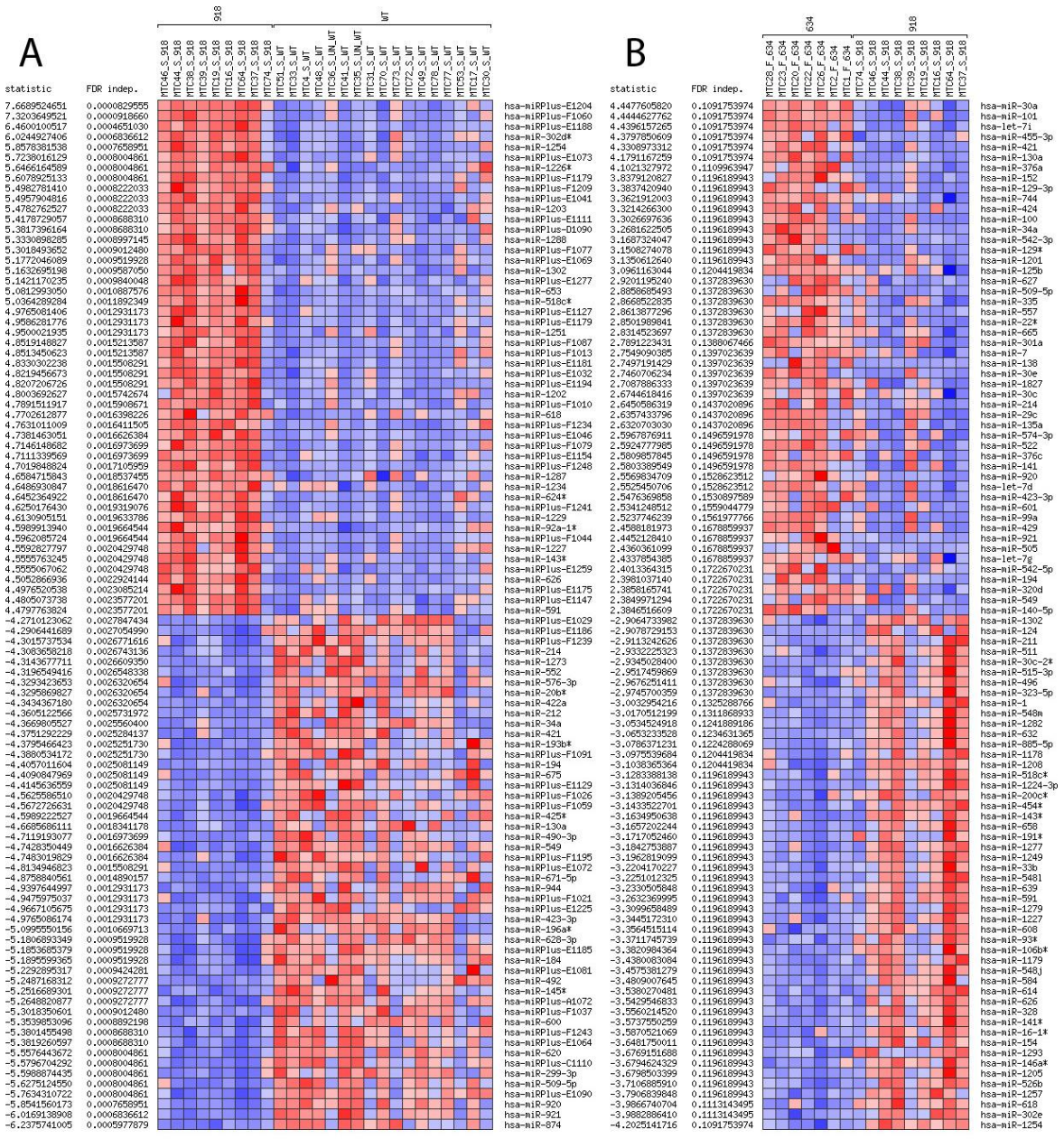

Figure 13. A. MiRNA differential expression analysis of MTCs^{M918T} *vs* MTCs^{WT} and **B.** MiRNA differential expression analysis of MTCs^{M918T} *vs* MTCs^{634} using the GEPAS package. The first 100 miRs with a false discovery rate (FDR) <0.05 are shown, including information about t statistic.

8. Biomarkers of specific genetic condition

Seven miRs common for two comparisons (hsa-miR-124, hsa-miR-1249, hsa-miR-129*, hsa-miR-129-3p, hsa-miR-205, hsa-miR-30a, hsa-miR-7) fit filtering criteria and hsa-miR-138 had significant FDR and almost reach fold change of 2. Five of them (hsa-miR-124, hsa-miR-129-3p, hsa-miR-138, hsa-miR-30a and hsa-miR-7) were selected for validation by RT-qPCR. Hsa-miR-30a and hsa-miR-138 were over-expressed and specific for the germline *RET*^{634} mutation, being down-regulated in MTC^{918} group. The expression of the hsa-miR-124 was validated by quantitative RT-PCR as up-regulated markers among MTCs^{918}. Due to limited availability of RNA from FFPE tumors; it was only possible to validate hsa-miR-138 in this material. Figure 14 summarizes these results in the independent frozen and FFPE series, respectively.

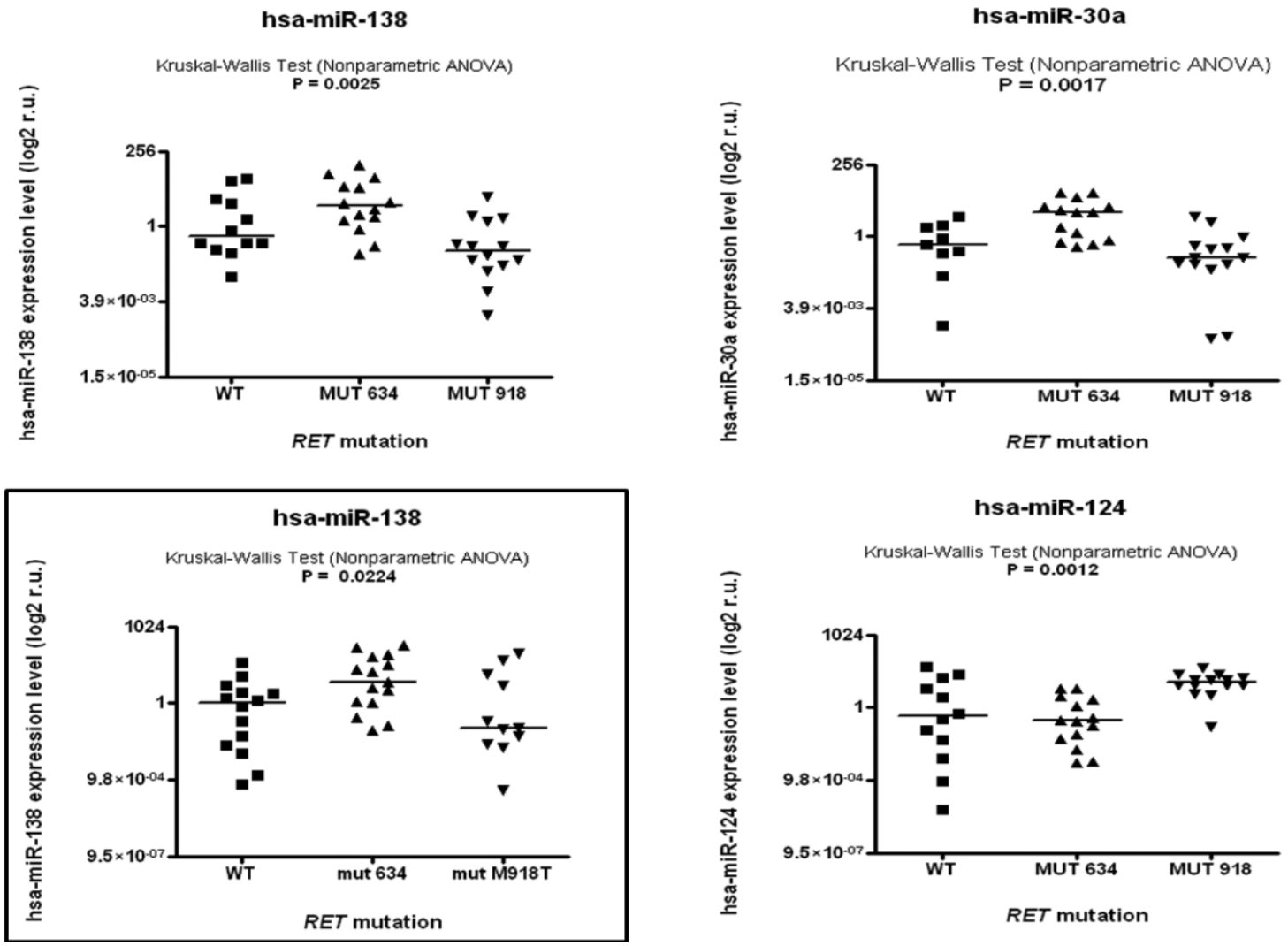

Figure 14. RT-qPCR with LNA™ microRNA PCR primer/SYBR® Green mix (Exiqon) of miR-124, miR-30a and miR-138 expression in an independent frozen and FFPE (in frame) MTC validation series.

9. mRNA-miRNA integration

In total 36 mRNA gene targets were deregulated and being co-regulated by the 26 miRNAs from comparison MTC^{918} *vs* MTC^{634},and 247 of genes 90 miRs negatively correlated from comparison MTC^{918} *vs* MTC^{WT}, respectively. The functions of identified mRNAs and the molecular pathways they potentially target were assessed by IPA and MAGIA softwares. IPA analysis was performed on the selected differentially expressed predicted mRNAs targets, retrieved from the MAGIA analysis. We obtained a list of the biological functions of putative miRNA target genes from MAGIA analysis performed by IPA analysis (Table 7). They point to cancer and cell death categories and functions related to malignant cell transformation.

NF-κB pathway revealed to be one of the most interesting one identified among the different genetic MTC groups., From the both comparisons MTC^{M918T} *vs* MTC^{634} and MTC^{M918T} *vs* MTC^{WT}, the most interesting findings were that the biological functions associated with MTC^{M918T} group were related to malignant behavior, metastatic potential and cell adhesion process, often implicated in tumorgenesis (Supplementary annex Table 7). IPA network analysis of the miRNA mRNA targets that were differentially expressed among MTC groups, highlighted “Cellular Growth and Proliferation”, “Cellular Development”, and “Tissue Morphology network” (Figure 15) as the most significant ones, involving 17 putative miRNA targets.

Table 7. IPA analysis of biological functions of putative miRNA target genes from MAGIA analysis.

Category	Functions	p-Value	Genes
Tissue Development	tissue development	2.16E-05	BMP2,CASR,CDH13,CSGALNACT1,ERBB4,ONECUT2,PAX8,PRNP,SGCD
Cellular Development	differentiation of mesenchymal cells	1.18E-04	BMP2,HMGA2
Embryonic Development	differentiation of mesenchymal cells	1.18E-04	BMP2,HMGA2
Cellular Growth and Proliferation	proliferation of tumor cell lines	2.58E-04	BMP2,CASR,CDH13,ERBB4,HMGA2,PRNP,PTGER2,TRIB2
Cell Death	cell viability of tumor cell lines	3.58E-04	BMP2,HMGA2,HSP90B1,PRNP
Cell Death	survival of superior cervical ganglion neurons	2.09E-03	BMP2
Cancer	metastasis of medulloblastoma	6.27E-03	ERBB4
Reproductive System Disease	metastasis of medulloblastoma	6.27E-03	ERBB4
Neurological Disease	metastasis of medulloblastoma	6.27E-03	ERBB4
Cell-To-Cell Signaling and Interaction	cell-cell adhesion	7.67E-03	CASR,CDH13
Cellular Growth and Proliferation	proliferation of cerebral cortex cells	8.35E-03	BMP2
Endocrine System Development and Function	thyroid gland development	8.35E-03	PAX8
Nervous System Development and Function	differentiation of astrocytes	1.04E-02	BMP2
Neurological Disease	bipolar disorder	1.13E-02	CDH13,HSP90B1,NR3C2,PROM1,SGCD,SLC26A7,ZNF365
Cancer	transformation of carcinoma cell lines	1.25E-02	BMP2
Cancer	carcinoma	1.84E-02	BMP2,CDH13,ERBB4,HLF,HMGA2,HSP90B1,NR3C2,PAX8,PRNP,PROM1,PTGER2,RELB
Cancer	adrenal cortex adenoma	1.87E-02	NR3C2
Cell Death	cell survival	1.98E-02	BMP2,ERBB4,HMGA2,HSP90B1,PRNP
Cellular Growth and Proliferation	proliferation of endothelial cells	2.18E-02	BMP2,CDH13
Cell Death	neuronal cell death	2.22E-02	BMP2,PRNP
Cell Death	cell viability of carcinoma cell lines	2.49E-02	BMP2
Cell Death	cell viability of neuroblastoma cell lines	2.49E-02	PRNP
Cellular Development	differentiation of mesenchymal stem cells	2.49E-02	BMP2
Cellular Growth and Proliferation	proliferation of carcinoma cell lines	2.61E-02	BMP2,TRIB2
Cell Death	cell death of neuroblastoma cells	3.10E-02	PRNP
Cellular Movement	invasion of epithelial cell lines	3.50E-02	PTGER2
Cell Morphology	morphology of carcinoma cell lines	3.50E-02	TRIB2
Cancer	hyperplasia	3.55E-02	HMGA2,NR3C2
Cancer	carcinoma in situ	4.31E-02	HMGA2,PROM1
Cellular Development	growth of neuroblastoma cell lines	4.31E-02	HMGA2
Cellular Growth and Proliferation	growth of neuroblastoma cell lines	4.31E-02	HMGA2

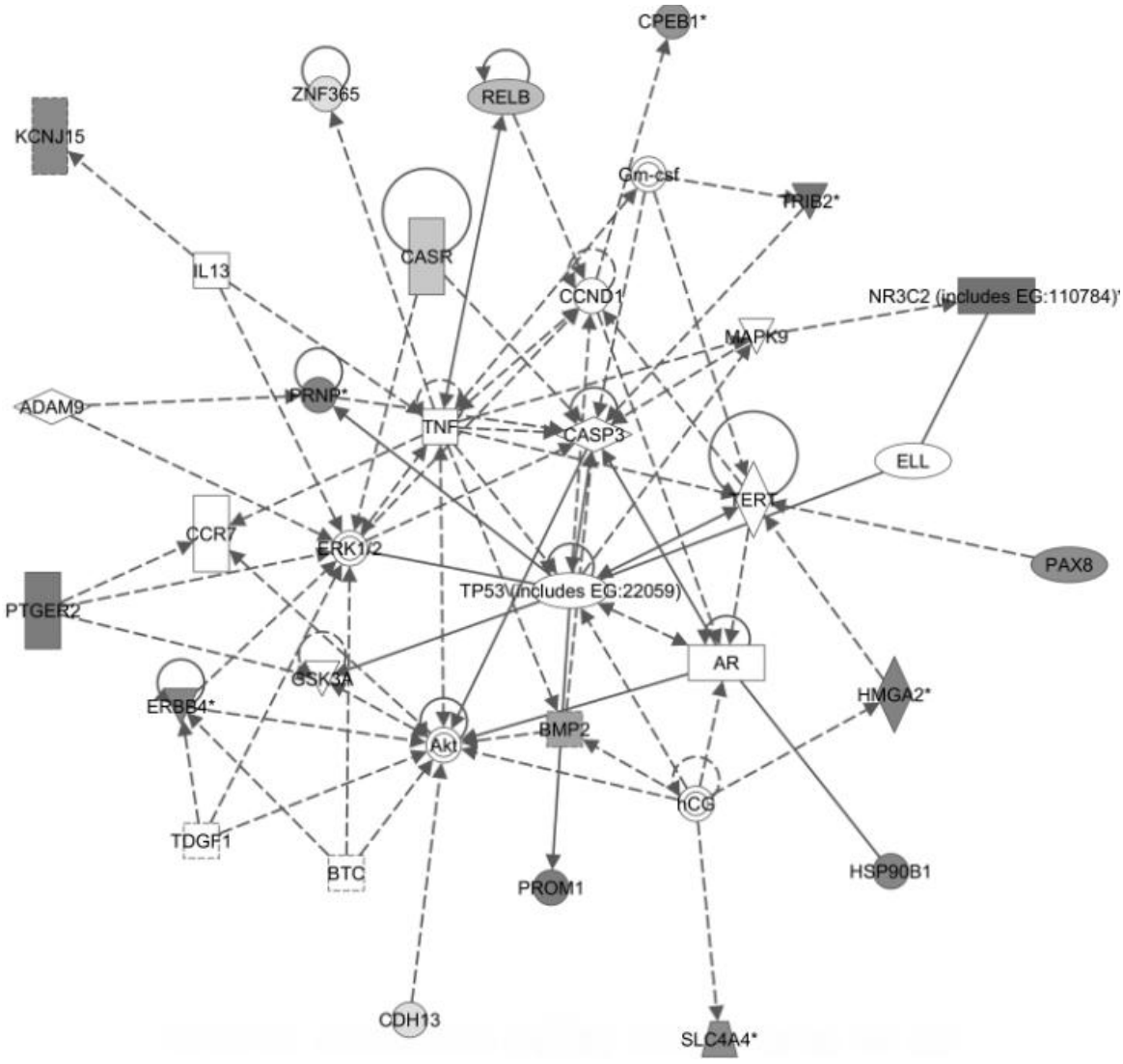

Figure 15. IPA network analysis based on putative miRNA targets from MAGIA analysis. Cellular Growth and Proliferation, Cellular Development, Tissue Morphology network.

Discussion

1. The power of high-throughput technologies

Approximately one third of the patients with MTC have recurrence after surgery. Metastasis development occurs more frequently in sporadic than in hereditary MTC. Thus, it is critical to perform the somatic *RET* mutations analysis in apparently sporadic cases, and to find out the biological effect that somatic mutations can have on the patients' health. Furthermore, since the biological effect of the different mutations is different in terms of signaling pathway activation, we should expect to find differences in the ages of MTC development or prognosis. For example, patients with mutations in codons 918 and 634 should expierience more aggressive evolution of the tumor than patients with genetic variants associated with mild/moderate transforming capacity in which clinical courses would be expected to be more indolent.

Treating MTC patients is not a trivial issue. Medullary thyroid carcinoma metastasizes during follow-up with low chances of survival. For the primary MTCs, total thyroidectomy is the only current approach and there are no other alternatives for the metastatic stages(Schlumberger 2008). Thus, there is a huge need to identify potential therapeutic targets. While a genotype-phenotype correlation has been well established for MEN2 cases, little is known about signaling pathways and biomarkers for specific germline and somatic *RET* mutations related to the MTC development.

High –throughput microarray techniques has become an effective tool to identify gene/miRNA sets with similar patterns of differential expression according to histological subtype, existence of metastatic disease, biomarker discovery etc. Although it is an efficient technique, it presents a series of difficulties, such as the need of following optimized protocols and applying careful data analysis of the complex underlying biological processes. After identifying specific biomarkers related to a concrete condition, their final application to the clinical setting has to include at least an immunostaining validation. The post-transcriptional modifications add complexity to the overall understanding of the process. Consequently it is difficult to translmit the obtained results to the clinic immediately. In recent years, several studies have been published on different types of solid tumors where the correlation between the expression profiles and the presence of the specific mutations have allowed identification of transcriptional changes associated with each genotype in breast cancer(Bertucci, et al. 2004), in melanoma(Pavey, et al. 2004), and in pheochromocytoma(Lopez-Jimenez, et al. 2010), among others. While there are numerous studies based on transcriptome characterization focused on follicular cell-derived thyroid cancer, those

related to MTC are scarce. In the case of the former thyroid tumors, a clear relation between the genotype and the specific changes in gene regulation has been identified (DeLellis 2004). In the case of MTC tumors, there are several difficulties which have contributed to the lack of studies. Firstly, comparisons of primary tumors *versus* normal C-cells are not possible due to the very low parafollicular cell representation (about 1%) in the thyroid cell mass (Khurana, et al. 2004a). Furthermore, it is challenging to obtain a sufficiently large series of frozen MTC tissues for genomic study due to the rarity of the tumor itself. This explains why only few studies on MTC profiling have been reported (Ameur et al. 2009; Jain et al. 2004b; Lacroix et al. 2005; Musholt et al. 2005a; Watanabe et al. 2002a). The work of this doctoral thesis was focused on identifying more accurate and additional information related to specific *RET* mutation through gene expression and microRNA profiling. Our interest pointed to the identification of specific genetic biomarkers, biological processes and network interactions associated with concrete germline and somatic *RET* mutations. The power of this study was the outstanding series of molecularly characterized series of tumors available. The unsupervised clustering demonstrated that this approach was able to cluster cases according to the specific *RET* mutation considered. Basically, we found that familial and sporadic cases were grouped in separated branches of the cluster as shown in figure 5. This finding is especially interesting due to the fact that some of the *RET* mutations are associated with higher transforming capacities, but knowledge about the underlying biological mechanisms is still lacking. After applying supervised analysis to MTC^{918}, MTC^{634} and MTC^{WT} groups, it was possible to select a list of genes as potential biomarkers to validate.

2. Biomarkers and pathways specifically related to each genetic class

Our study revealed concrete biomarkers associated to specific *RET* mutations, such as *PROM1* or *CD133*, *GFRA1*, *LOXL2, GAL,* and *DKK4* over-expression related to $MTCs^{M918T}$ group, or *GAL* over-expression related to mutations affecting the 634 residue. In agreement with the *GAL* over-expression associated with $MTCs^{634}$ described herein, *GAL* over-expression was previously observed in PC12 rat pheocromocytoma cell lines (Tofighi, et al. 2008). *GAL* is involved in neuropeptide signaling, tumorigenesis, nervous system development and the regulation of cell proliferation; it is expressed in neuroblastoma and pheochromocytoma cancer cell lines, and it activates MAPK and ERK signaling (Berger, et al. 2005; Hawes 2006; Sugimoto, et al. 2009; Tofighi et al. 2008). These findings suggest that *GAL* over-expression may be involved in the development

of the phenotype exhibited by MEN2A patients carrying a 634 germline *RET* mutation. These patients develop pheochromocytoma in at least 50% of cases (Eng 1996; Machens, et al. 2005).

GFRA1 (GDNF family receptor alpha 1), associated with MTCs^{M918T}, is a known co-receptor of RET which mediates its activation through the binding of RET ligands. These include ligands that are widely expressed and promote the survival of neurons during development. *GFRA1* has been previously reported as a genetic risk factor associated with susceptibility to developing sporadic MTC in a case-control study (Gimm 2001), and our results support its role in MTC development.

DKK4 (Dickkopf-4), another gene overexpressed in MTCs^{M918T}, was demonstrated to be significantly upregulated in colorectal cancer reflecting activation of the Wnt canonical pathway (Matsui 2009). Furthermore, *KREMEN2* (kringle containing transmembrane protein 2) co-operates with *DKK4* to regulate Wnt signaling (Mao and Niehrs 2003). *KREMEN2* was upregulated similarly to *DKK4* in M918T tumors included in our study. Deregulation of the Wnt pathway results in the development of cancer and other diseases, and Wnt/β-catenin signaling and JNK noncanonical pathways are implicated in RET signaling, which is activated in MTC. Deregulation of the Wnt pathway specifically associated with *RET*^{M918T} MTC could open new perspectives for treatment.

The most interesting results among the M918T group were the over-expression of *LOXL2* and *PROM1 (CD133),* which could partially explain the high rate of metastasis related to MTCs that carry this mutation. *LOXL2* (lysyl oxidase-like 2) activates Snail/E-cadherin and Src kinase/Focal adhesion kinase (Src/FAK) pathways, and is associated with tumor cell invasion. *LOXL2* is linked to epithelial-mesenchymal transition (EMT), which leads to metastasis and lower survival rates in epithelial and neuroendocrine tumors (Peinado 2005, 2008; Peng, et al. 2009; Ruckert, et al. 2010). Our results are in agreement with the increased expression of genes associated with EMT previously observed in MEN2B MTCs(Jain et al. 2004b).

PROM1 was the gene most significantly over-expressed among the MTCs^{M918T} included in our series of primary tumors. *PROM1* was recently reported by Zhu *et al.* (Zhu 2010) to be a cancer stem cell marker in MZ-CRC-1 cell lines harboring a M918T *RET* mutation. MTCs bearing the M918T *RET* mutation are resistant to treatment, and a high *PROM1* (*or CD133*) expression might be related to such resistance. In this regard, high expression of *CD133* is associated with neural crest-derived stem cells, and slowly differentiating cancer stem cells have proved resistant to irradiation and cytotoxic drugs (Zhu 2010). To our knowledge, ours is the first study based on primary tumors pointing to a *PROM1* over-expression associated with the M918T mutation. Another study recently showed an association of poor prognosis with a high expression of *CD133*

in medulloblastoma tumors, suggesting that it might be a more general prognostic marker (Raso, et al. 2011).

Immunohistochemical assessment of ESM1, GFRA1 and CD133 in the 71 FFPE MTCs only revealed a tendency towards association of the M918T group with PROM1 or CD133 protein over-expression. The lack of validation at protein level could be due to another underlying mechanism, such as posttranscriptional modifications conducted to microRNAs. Furthermore, after silencing *CD133* with two different siRNAs, we observed decreased levels of *CD133* mRNA which led to an increased number of apoptotic nuclei. This significant correlation between silencing of *CD133* and apoptosis led us to conclude that *CD133* is not only a specific biomarker for the M918T *RET* mutation, but its targeting seems feasible and might lead to apoptotic cell death. As already mentioned, usually the MTC^{M918T} is associated with greater aggressiveness and with the acquisition of resistance for variety of chemotherapeutics. Bearing this in mind, MTC patients could be stratified according to their genetic condition, since those with high CD133 protein expression could benefit from a targeted treatment.

Based on the significantly differentiated gene/miRNA target lists we performed further analyses in order to identify underlying signaling pathways and biological processes associated with the specific MTC groups. In this regard, GO biological function analyses using FatiGO/Babelomics revealed that important processes such as anti-apoptotic functions, proliferation, migration, cell cycle and adhesion were highly associated with the M918T group. To search for the genes related to each specific *RET* mutation, we used the whole gene expression profile in order to perform a pathway analysis. In that context, the GSEA tool was applied with Biocarta and KEGG as a source of pathway annotations and the IPA 9.0 software was used to find the top Biocarta/KEGG pathways significantly (FDR<25%) differentially expressed between different groups. Pathway enrichment analysis of the M918T group pointed to signaling cascades mainly involved in tumor invasion and metastasis (NFκB, interleukin, cytokine, p38MAPK, Wnt, JAK/Stat, Notch, MAPK or cell adhesion), which corresponds to what would be expected on the grounds of the clinical behavior of M918T-related MTCs. Among these pathways, the Notch pathway is known to play an important role in the normal development of neuroendocrine cells, including the calcitonin producing C-cells of the thyroid (Cook 2010).

The most recurrent terms were NfκB, TGF-β, focal adhesion and others related to remodeling of the cytoskeleton, which generally facilitate the EMT process allowing the tumors cells to spread to

distant organs causing metastasis. The TGF-β signaling pathway is a well known linker to the EMT process in the advanced stages of cancer development (Siegel and Massague 2003).In our series it was enriched in MTC^{M918T}, which exhibits the worst prognosis among all MTCs. EMT is a well-known process allowing dissemination of tumor cells that involves cell-cell interactions, tight junctions, matrix remodeling and cytoskeleton reorganizations together with cell polarity changes (loss in epithelial cells) (Grunert, et al. 2003).

TGF-β leads to fibrosis and, together with NF-kB, controls the inflammation processes. Snail, another main player in EMT, is related to decreased proliferation and has been found to be a main inducer of EGFR signaling. Important genes in EMT processes such as cadherins, chemokines, collagens and laminins were significantly differentially expressed among our MTC tumor series, suggesting these carcinomas had mesenchymal cell properties that were linked to tumor invasion.

In addition to NF-κB, MAPK/JNK pathways were also significantly activated. JNKs are a group of mitogen-activated protein kinases (MAPKs) being stimulated by multiple factors including cytokines, DNA-damaging agents and environmental stresses, and play a crucial role in programmed cell death or apoptosis control. The inhibition of JNKs has been shown to enhance chemotherapy-induced inhibition of tumor cell growth (Vasilevskaya and O'Dwyer 2003). These results required further functional validation in order to confirm discovery of specific pathways.

In summary, we identified specific biomarkers related to different genetic conditions by means of expression analysis. The over-expression of *LOXL2 and DKK4,* involved in the cell adhesion pathway and the EMT process, or the Wnt pathway respectively, as well as the fact that a decrease in *PROM1/CD133* expression was associated with an increased number of apoptotic nuclei, opening new therapeutic possibilities to improve MTC management. Prospective studies based on larger cohorts of MTC tumors with lower TNM stages would be necessary to assess the prognostic role of the genes which are responsible for the metastatic potential of such carcinomas.

3. The contribution of microRNAs to MTC development

Aberrant microRNA expression patterns have been described in various hematological and solid cancers, finding high correlation with progression and prognosis. Additionally, microRNA

expression profiles have been linked to the clinical features of several cancers, suggesting their usefulness as potential diagnostic and prognostic markers.

The biological significance as well as the oncogenic potential of miRNAs in MTC development has been poorly investigated. So far there are only two studies on miRNA data. The first one was based on a very small datasets of 2 MTC cases with unknown genetic background, which were compared with follicular cell-derived thyroid tumors (Nikiforova et al. 2008). The second one compared sporadic and hereditary MTC cases, not taking into account specific *RET* mutations associated with different transforming capacities(Abraham et al. 2011). Very recently, an Italian group from Padova was unable to validate the proposed biomarkers in these two previous reports (Mian et al. 2012). To our knowledge, there are no studies based on the specific *RET* mutational status as well as no studies assessing possible miRNA-regulated gene networks.

As previously discussed for mRNA profiling, our findings suggested that the miRNA expression profile was able to cluster MTCs according to underlying genetic conditions. In this regard, it was possible to obtain long lists of microRNAs related to each specific MTC mutational group, comparing the differentially expressed miRs between MTC^{918} *vs* MTC^{634} and MTC^{918} *vs* MTC^{WT} with a significant FDR value <0.15. Once again, this approach, applied on one of the largest series of primary MTCs described so far, pointed to differences in MTC biology associated with familial and sporadic nature of such tumors. In fact, three miRNA biomarkers were identified by microRNA profiling for sporadic and hereditary MTC with specific *RET* mutations, which were validated by RT-qPCR in an independent frozen and FFPE MTC series.

4. miRNAs specific to each genetic class. *PROM1* and miR-30a relation

According to our data, miR-124 was over-expressed in $MTCs^{918}$ and down-regulated in MTC^{634} cases, suggesting that the miR-124 could be acting as an oncomir in sporadic MTC tumorogenesis. In other words, acting on tumor suppressor genes and stimulating cancer development. This miR is involved in nervous system development and neuronal differentiation(Yu, et al. 2008), and it correlates with the neural-crest origin of MTCs. Interestingly, there have been previous reports the overexpression of miR-124 in a sub-population of gliobliastoma multiforme cells expressing neural crest stem cell marker CD133(Silber, et al. 2008), as well as its deregulation in meduloblastoma and glioblastoma multiforme (Li, et al. 2009; Pierson, et al. 2008). Up-regulation of miR-124 induces neuronal differentiation of mouse neuroblastoma cell lines CAD and Neuro2a and the

mouse embryonal tumor cell line P19(Makeyev, et al. 2007), suggesting miRNAs could be valuable therapeutic targets if they would act similarly in promoting differentiation of human tumor cells and tumor stem cells (TSCs). Taking into account that MTCs with M918T *RET* mutation also had high expression of *CD133* or *PROM1,* the miR-124 might be useful as a potential therapeutic target in MTC treatment.

MiR-30a and miR-138, downregulated in MTC^{918} group, are expressed in neurons and neuroendocrine cells (Steiner 2004), and associated with cell migration and proliferation. Their over-expression has been described as leading to apoptosis of neuroblastoma cell lines, and involved in secretion or membrane trafficking in neuroendocrine cells as well as in tumorigenesis.

MiR-138 is one of the most frequently down-regulated microRNA in tumors, and seems to be important in cancer progression in human metastatic tumors (Baffa, et al. 2009). Its downregulation is linked to EMT in squamous cell carcinoma cell lines (Jiang, et al. 2010; Liu, et al. 2011), which leads to metastasis. Its deregulation was also observed in thyroid carcinomas (Mitomo, et al. 2008; Yip, et al. 2011) associated with poor prognosis.

MiR-30a, which suppresses EMT by targeting Snai1, was found to be downregulated in non-small cell lung cancer(Kumarswamy, et al. 2011). In this regard, it is worth noting the increased expression of genes associated with EMT observed in $MTCs^{918}$ (Jain et al. 2004b). *PROM1,* a miR-30a putative target, was the gene most significantly over-expressed among the $MTCs^{918}$, observing a significant negative-inverse correlation between miR-30a and *PROM1*.

Among other miRNAs derived from our study, miR-885-5p was down-regulated in hereditary cases with the 634 *RET* mutation. In this regard, miR-885-5p has been previously demonstrated as being up-regulated in *RET* related-pheocromocytomas (Tombol, et al. 2010), and also found in neuroblastoma. Furthermore, the overexpression of miR-885-5p has been previously reported to be associated with malignant mesothelioma tissues(Guled, et al. 2009). Another marker, miR-154, already validated in Nikiforova study(Nikiforova et al. 2008), was up-regulated in MTC^{M918T} cases, pointing to another potential miRNA for functional validation.

5. MicroRNA-mRNA interactions: a way of understanding underlying biological mechanisms involved in MTC development

It is known that biological processes are not only regulated at a transcriptional level, but that posttranscriptional modifications of proteins also take place. Thus, microRNAs are key pieces for

the comprehensive understanding of the process. To highlight the role of significantly differentially expressed miRNAs associated with specific *RET* status and to discover processes modified by post-transcriptional regulation, *in silico* predicted miRNA-mRNA interactions were identified and pathway analysis of the targets was performed. To our knowledge, there have been no studies based on integration miRNA and gene expression data in MTC. This was possible in this study due in part to the microRNA profiling data and transcriptional data that were derived from the same MTC sample sets.

After identifying the entire list of interactions by MAGIA (supplementary annex Table 7), IPA analysis pointed out the NF-κB pathway as significantly activated in the MTC^{918} group. This result was in agreement with data obtained from gene expression data, where the GSEA retrieved it also among the top significant canonical pathways.

NF-κB is a ubiquitously expressed transcription factor involved in a wide spectrum of cellular functions including cell cycle control, stress adaptation, inflammation and control of apoptosis. Its activation has been found to be involved in the development of human malignancies, and it appears to be important for a cancer cell´s survival. It is also associated with more aggressive tumor phenotypes and resistance to drug therapies (Arlt, et al. 2003; Arlt, et al. 2001; Biswas, et al. 2003; Dong, et al. 1999). The fact of finding NF-kB pathways activated among MTC^{918} could partially explain the treatment resistance observed in these patients.

In summary, we identified specific biomarkers related to different genetic conditions by means of microRNA expression analysis. The over-expression of miR-124 and down-regulation of miR-138 and miR-30a in MTC^{918} were associated with the EMT process and malignant behavior, or the Nf-κB pathway respectively, opening new therapeutic possibilities to improve MTC management.

6. Clinical implications and molecular targeted therapies

One fundamental issue to consider when a new pharmaceutical/compound is intended to be introduced in a clinical trial is the selection of biomarkers. The OMIC technologies have become widely used to retrieve not only relevant information regarding complex cancer biology, but also to identify specific biomarkers associated with treatment resistance.

Regarding the available alternative solutions for MTC patients, it has been previously shown that different *RET* mutants show different affinities to specific tyrosine kinase inhibitors (TKIs). For

instance, resistance to inhibitors such as PP1-2 and vandetanib was observed for V804M *RET* mutant in contrast to RET^{C634R} (Santoro, et al. 2004b) , whilst sorafenib was effective in both *RET* mutants(Carlomagno, et al. 2006; Plaza-Menacho, et al. 2007). Despite the progress and effort made recently in the field, alternative treatments to the conventional therapies have failed to provide significant improvements in the prognosis of the patients with MTCs. Therefore, more focussed analyses taking into account the genetic background are required. With respect to this, little is known about additional mechanisms that can modify the treatment response, such as miRNA regulation dependent on *RET* mutational status. Taking advantage of the same cohort of patients, the integration of gene expression and miRNA data could facilitate the identification of molecular pathways and miRNA biomarkers which underlie the biology of MTC development, and thereby facilitate the design of new and effective therapeutic solutions. It was especially interesting that a *PROM1* (*CD133*) over-expression was found among MTC harboring M918T *RET* mutation. Such a result could explain the tumor recurrence frequently associated with this specific mutation, as this gene is a neural crest stem cell marker. Cancer stem cells have the capacity of self-renewal; an over-expression of the *PROM1* gene could indicate the existence of a higher proportion of neural crest stem cell, and explain the association between the presence of this mutation and recurrence. Furthermore, according to predictions available, PROM1 is a predicted target of miR-30a. This result could point to new targets, such as miRs for a future MTC therapeutic option, based on specific *RET* mutation status.

Conclusions

1) Both transcriptome and mirnome characterization of MTCs revealed specific molecular signatures according to the primary *RET* mutation.

2) Over-expression of *PROM1*, *LOXL2*, *DKK4* and *GFRA1* was related to the M918T *RET* mutation, and over-expression of *GAL* to mutation affecting 634 residue in *RET*.

3) Pathway enrichment analysis of gene expression profile linked to the M918T group pointed to signaling cascades mainly involved in tumor invasion and metastasis (NFκB, interleukin, cytokine, p38MAPK, Wnt, JAK/Stat, Notch, MAPK or cell adhesion).

4) Silencing CD133 by siRNA led to an increased number of apoptotic nuclei. CD133 confers resistance to death by apoptosis. It is not only a specific biomarker for the M918T *RET* mutation, but also a good candidate for future therapeutic options.

5) The downregulation of miR-30a, and miR-138 was associated with MTC^{M918T} group, and miR-124 with MTC^{C634X}, and could be considered as potential specific biomarkers.

6) The integration of miRNA and mRNA profiles revealed an over-expression of PROM1 (CD133) and a down-regulation of has-miR-30a as inversely correlated in MTC^{M918T} group. According to the relation from the former to neural crest stem cell, these findings suggest this correlation could be linked with the clinical resistance to chemotherapy observed in this specific group of patients.

Conclusiones

1. Los perfiles de expression génica y los de microRNAs identificados en CMT difieren de acuerdo a la mutación de *RET* presente en estos tumores.

2. La sobre-expresión de *PROM1*, *LOXL2*, *DKK4* y *GFRA1* se asocial a la presencia de la mutación M918T en *RET*, y la sobre-expresión de *GAL* a mutaciones en el residuo 634.

3. El análisis de enriquecimiento de rutas a partir de resultados de perfiles de expression permitió identificar una asociación significativa entre la mutación M918T y cascadas de señalización relacionadas con invasión y metástasis. Entre ellas destacaron NFκB, interleuquinas, citoquinas, p38MAPK, Wnt, JAK/Stat, Notch, MAPK or adhesión celular.

4. La ablación de CD133 mediante el uso de ARN de interferencia conduce a un incremento en el número de núcleos apoptóticos. CD133 no solo es un marcador de la mutación M918T en *RET*, sino que podría ser considerado como diana terapéutica en un futuro.

5. La baja expression del miR-30a y del miR-138 se asoció con la presencia de la mutación M918T en *RET*, y la del miR-124 con el grupo caracterizado por mutaciones en 634. Al menos estos microRNAs podrían considerarse biomarcadores específicos de mutación.

6. El análisis integrado de los resultados derivados de ambas plataformas, perfiles de expression génica y de microRNAs, reveló que PROM1 (CD133) y el has-miR-30a estaban inversamente correlacionados en los CMT con la mutación M918T en *RET*. De acuerdo con la relación del primero con la existencia de células progenitoras de cresta neural, estos hallazgos sugieren que esta relación podría explicar la resistencia a quimioterapia observada en este grupo de pacientes.

References

Abraham D, Jackson N, Gundara JS, Zhao J, Gill AJ, Delbridge L, Robinson BG & Sidhu SB 2011 MicroRNA profiling of sporadic and hereditary medullary thyroid cancer identifies predictors of nodal metastasis, prognosis, and potential therapeutic targets. Clin Cancer Res 17 4772-4781.

Airaksinen MS & Saarma M 2002 The GDNF family: signalling, biological functions and therapeutic value. Nat Rev Neurosci 3 383-394.

Al-Shahrour F, Diaz-Uriarte R & Dopazo J 2004 FatiGO: a web tool for finding significant associations of Gene Ontology terms with groups of genes. Bioinformatics 20 578-580.

Almeida MQ & Hoff AO 2012 Recent advances in the molecular pathogenesis and targeted therapies of medullary thyroid carcinoma. Curr Opin Oncol 24 229-234.

Ameur N, Lacroix L, Roucan S, Roux V, Broutin S, Talbot M, Dupuy C, Caillou B, Schlumberger M & Bidart JM 2009 Aggressive inherited and sporadic medullary thyroid carcinomas display similar oncogenic pathways. Endocrine-Related Cancer 16 1261-1272.

Andreozzi F, Melillo RM, Carlomagno F, Oriente F, Miele C, Fiory F, Santopietro S, Castellone MD, Beguinot F, Santoro M, et al. 2003 Protein kinase Calpha activation by RET: evidence for a negative feedback mechanism controlling RET tyrosine kinase. Oncogene 22 2942-2949.

Arighi E, Borrello MG & Sariola H 2005 RET tyrosine kinase signaling in development and cancer. Cytokine Growth Factor Rev 16 441-467.

Arlt A, Gehrz A, Muerkoster S, Vorndamm J, Kruse ML, Folsch UR & Schafer H 2003 Role of NF-kappaB and Akt/PI3K in the resistance of pancreatic carcinoma cell lines against gemcitabine-induced cell death. Oncogene 22 3243-3251.

Arlt A, Grobe O, Sieke A, Kruse ML, Folsch UR, Schmidt WE & Schafer H 2001 Expression of the NF-kappa B target gene IEX-1 (p22/PRG1) does not prevent cell death but instead triggers apoptosis in Hela cells. Oncogene 20 69-76.

Baffa R, Fassan M, Volinia S, O'Hara B, Liu C-G, Palazzo JP, Gardiman M, Rugge M, Gomella LG, Croce CM, et al. 2009 MicroRNA expression profiling of human metastatic cancers identifies cancer gene targets. The Journal of Pathology 219 214-221.

Ball D, Baylin SB, De Butros AC 2000. Medullary thyroid carcinoma, Braverman LE, Utiger RD, eds. Werner and Ingbar's the thyroid. 8th ed. Philadelphia: Lippincott Williams and Wilkins 930-943.

Bartel DP 2009 MicroRNAs: target recognition and regulatory functions. Cell 136 215-233.

Basson MA, Akbulut S, Watson-Johnson J, Simon R, Carroll TJ, Shakya R, Gross I, Martin GR, Lufkin T, McMahon AP, et al. 2005 Sprouty1 is a critical regulator of GDNF/RET-mediated kidney induction. Dev Cell 8 229-239.

Benjamini Y, Drai D, Elmer G, Kafkafi N & Golani I 2001 Controlling the false discovery rate in behavior genetics research. Behav Brain Res 125 279-284.

Berger A, Santic R, Hauser-Kronberger C, Schilling FH, Kogner P, Ratschek M, Gamper A, Jones N, Sperl W & Kofler B 2005 Galanin and galanin receptors in human cancers. Neuropeptides 39 353-359.

Bertucci F, Finetti P, Birnbaum D & Viens P 2004 Gene expression profiling of inflammatory breast cancer. Cancer 116 2783-2793.

Besset V, Scott RP & Ibanez CF 2000 Signaling complexes and protein-protein interactions involved in the activation of the Ras and phosphatidylinositol 3-kinase pathways by the c-Ret receptor tyrosine kinase. J Biol Chem 275 39159-39166.

Biswas DK, Martin KJ, McAlister C, Cruz AP, Graner E, Dai SC & Pardee AB 2003 Apoptosis caused by chemotherapeutic inhibition of nuclear factor-kappaB activation. Cancer Res 63 290-295.

Borrello MG, Alberti L, Arighi E, Bongarzone I, Battistini C, Bardelli A, Pasini B, Piutti C, Rizzetti MG, Mondellini P, et al. 1996 The full oncogenic activity of Ret/ptc2 depends on tyrosine 539, a docking site for phospholipase Cgamma. Mol Cell Biol 16 2151-2163.

Borrello MG, Mercalli E, Perego C, Degl'Innocenti D, Ghizzoni S, Arighi E, Eroini B, Rizzetti MG & Pierotti MA 2002 Differential interaction of Enigma protein with the two RET isoforms. Biochem Biophys Res Commun 296 515-522.

Brandi ML, Gagel RF, Angeli A, Bilezikian JP, Beck-Peccoz P, Bordi C, Conte-Devolx B, Falchetti A, Gheri RG, Libroia A, et al. 2001 CONSENSUS: Guidelines for Diagnosis and Therapy of MEN Type 1 and Type 2. Journal of Clinical Endocrinology & Metabolism 86 5658-5671.

Bugalho M, Frade JP, Santos JR, Limbert E, Sobrinho L,. 1997 Molecular analysis of the RET proto-oncogene in patients with sporadic medullary thyroid carcinoma: a novel point mutation in the extracellular cysteine-rich domain. Eur J Endocrinol 136 423-426.

Califano D, Rizzo C, D'Alessio A, Colucci-D'Amato GL, Cali G, Bartoli PC, Santelli G, Vecchio G & de Franciscis V 2000 Signaling through Ras is essential for ret oncogene-induced cell differentiation in PC12 cells. J Biol Chem 275 19297-19305.

Calin GA & Croce CM 2006 MicroRNA signatures in human cancers. Nat Rev Cancer 6 857-866.

Calin GA & Croce CM 2007 Chromosomal rearrangements and microRNAs: a new cancer link with clinical implications. J Clin Invest 117 2059-2066.

Carlomagno F, Anaganti S, Guida T, Salvatore G, Troncone G, Wilhelm SM & Santoro M 2006 BAY 43-9006 inhibition of oncogenic RET mutants. J Natl Cancer Inst 98 326-334.

Carr LL, Mankoff DA, Goulart BH, Eaton KD, Capell PT, Kell EM, Bauman JE & Martins RG 2011 Phase II study of daily sunitinib in FDG-PET-positive, iodine-refractory differentiated thyroid cancer and metastatic medullary carcinoma of the thyroid with functional imaging correlation. Clin Cancer Res 16 5260-5268.

Cohen EE, Rosen LS, Vokes EE, Kies MS, Forastiere AA, Worden FP, Kane MA, Sherman E, Kim S, Bycott P, et al. 2008 Axitinib is an active treatment for all histologic subtypes of advanced thyroid cancer: results from a phase II study. J Clin Oncol 26 4708-4713.

Cohen MS & Moley JF 2003 Surgical treatment of medullary thyroid carcinoma*. Journal of Internal Medicine 253 616-626.

Cook M, Yu, XM, Chen, H 2010 Notch in the development of thyroid C-cells and the treatment of medullary thyroid cancer. Am J Transl Res 10 119-125.

Cooley L, Elder, FF, Knuth, A, Gagel, R.F. 1995 Cytogenetic characterization of three human and three rat medullary thyroid carcinoma cell lines. Cancer Genet Cytogenet 80 138-149.

Dabir T, Hunter S, Russell C, McCall D & Morrison P 2006 The RET Mutation E768D Confers a Late-onset Familial Medullary Thyroid Carcinoma – Only Phenotype with Incomplete Penetrance: Implications for Screening and Management of Carrier Status. Familial Cancer 5 201-204.

de Graaff E, Srinivas S, Kilkenny C, D'Agati V, Mankoo BS, Costantini F & Pachnis V 2001 Differential activities of the RET tyrosine kinase receptor isoforms during mammalian embryogenesis. Genes Dev 15 2433-2444.

de Groot JW, Links TP, Plukker JT, Lips CJ & Hofstra RM 2006 RET as a diagnostic and therapeutic target in sporadic and hereditary endocrine tumors. Endocr Rev 27 535-560.

De Vita G, Melillo RM, Carlomagno F, Visconti R, Castellone MD, Bellacosa A, Billaud M, Fusco A, Tsichlis PN & Santoro M 2000 Tyrosine 1062 of RET-MEN2A mediates activation of Akt (protein kinase B) and mitogen-activated protein kinase pathways leading to PC12 cell survival. Cancer Res 60 3727-3731.

Decker RA, Peacock ML & Watson P 1998 Hirschsprung disease in MEN 2A: increased spectrum of RET exon 10 genotypes and strong genotype-phenotype correlation. Hum Mol Genet 7 129-134.

DeLellis R, Lloyd, RV , Heitz, PU, C. Eng C. 2004 World Health Organization classification of tumours: pathology and genetics of tumours of endocrine organs. Chapter 2: tumour of the thyroid and parathyroid. Lyon: IARC Press. IARC WHO Classification of Tumours 86-91.

Deng Y, Nagae, G, Midorikawa, Y, Yagi, K, Tsutsumi, S, Yamamoto, S, Hasegawa, K, Kokudo, N, Aburatani, H, Kaneda, A 2010 Identification of genes preferentially methylated in hepatitis C virus-related hepatocellular carcinoma. Cancer Sci 101 1501-1510.

Dong G, Chen Z, Kato T & Van Waes C 1999 The host environment promotes the constitutive activation of nuclear factor-kappaB and proinflammatory cytokine expression during metastatic tumor progression of murine squamous cell carcinoma. Cancer Res 59 3495-3504.

Drosten M & Putzer BM 2006 Mechanisms of Disease: cancer targeting and the impact of oncogenic RET for medullary thyroid carcinoma therapy. Nat Clin Prac Oncol 3 564-574.

Durbec PL, Larsson-Blomberg LB, Schuchardt A, Costantini F & Pachnis V 1996 Common origin and developmental dependence on c-ret of subsets of enteric and sympathetic neuroblasts. Development 122 349-358.

Durick K, Gill GN & Taylor SS 1998 Shc and Enigma are both required for mitogenic signaling by Ret/ptc2. Mol Cell Biol 18 2298-2308.

Encinas M, Crowder RJ, Milbrandt J & Johnson EM, Jr. 2004 Tyrosine 981, a novel ret autophosphorylation site, binds c-Src to mediate neuronal survival. J Biol Chem 279 18262-18269.

Encinas M, Rozen EJ, Dolcet X, Jain S, Comella JX, Milbrandt J & Johnson EM, Jr. 2008 Analysis of Ret knockin mice reveals a critical role for IKKs, but not PI 3-K, in neurotrophic factor-induced survival of sympathetic neurons. Cell Death Differ 15 1510-1521.

Eng C 1999 RET Proto-Oncogene in the Development of Human Cancer. Journal of Clinical Oncology 17 380.

Eng C, Clayton D, Schuffenecker I, Lenoir G, Cote G, Gagel RF, van Amstel HK, Lips CJ, Nishisho I, Takai SI, et al. 1996a The relationship between specific RET proto-oncogene mutations and disease phenotype in multiple endocrine neoplasia type 2. International RET mutation consortium analysis. Jama 276 1575-1579.

Eng C, Clayton D, Schuffenecker I, Lenoir G, Cote G, Gagel RF, van Amstel HKP, Lips CJM, Nishisho I, Takai S-I, Marsh DJ, Robinson BG, Frank-Raue K, Raue F, Xue F, Noll WW, Romei C, Pacini F, Fink M, Niederle B, Zedenius J, Nordenskjold M, Komminoth P, Hendy GN, Gharib H, Thibodeau SN, Lacroix A, Frilling A, Ponder BAJ, Mulligan LM 1996 The relationship between specific RET proto-oncogene mutations and disease phenotype in multiple endocrine neoplasia type 2. International RET mutation consortium analysis. Journal of the American Medical Association 276 1575-1579.

Eng C, Mulligan LM, Healey CS, Houghton C, Frilling A, Raue F, Thomas GA & Ponder BA 1996b Heterogeneous mutation of the RET proto-oncogene in subpopulations of medullary thyroid carcinoma. Cancer Res 56 2167-2170.

Enomoto H 2005 Regulation of neural development by glial cell line-derived neurotrophic factor family ligands. Anat Sci Int 80 42-52.

Enomoto H, Heuckeroth RO, Golden JP, Johnson EM & Milbrandt J 2000 Development of cranial parasympathetic ganglia requires sequential actions of GDNF and neurturin. Development 127 4877-4889.

Ferlay J, Shin, HR, Bray, F, Forman, D, Mathers, C, Parkin, DM. 2010 Estimates of worldwide burden of cancer in 2008: GLOBOCAN 2008. Int J Cancer.

Frank-Raue K & Raue F 2009 Multiple endocrine neoplasia type 2 (MEN 2). European Journal of Cancer 45 267-273.

Fukuda T, Kiuchi K & Takahashi M 2002 Novel mechanism of regulation of Rac activity and lamellipodia formation by RET tyrosine kinase. J Biol Chem 277 19114-19121.

Gallel P, Pallares, J, Dolcet, X, Llobet, D, Eritja, N, Santacana, M, Yeramian, A, Palomar-Asenjo, V, Lagarda, H, Mauricio, D, Encinas, M, Matias-Guiu, X 2008 Nuclear factor-kappaB activation is associated with somatic and germ line RET mutations in medullary thyroid carcinoma. In Hum Pathol., pp 994-1001.

Gimm O, Dziema, H, Brown J, Hoang-Vu C, Hinze R, Dralle H, Mulligan LM and Eng C 2001 Over-representation of a germline variant in the gene encoding RET co-receptor GFR alpha-1 but not GFR alpha-2 or GFR alpha-3 in cases with sporadic medullary thyroid carcinoma. Oncogene 20 2161-2170.

Giraudet AL, Vanel D, Leboulleux S, Auperin A, Dromain C, Chami L, Ny Tovo N, Lumbroso J, Lassau N, Bonniaud G, et al. 2007 Imaging medullary thyroid carcinoma with persistent elevated calcitonin levels. J Clin Endocrinol Metab 92 4185-4190.

Glinsky GV 2006 Genomic models of metastatic cancer: functional analysis of death-from-cancer signature genes reveals aneuploid, anoikis-resistant, metastasis-enabling phenotype with altered cell cycle control and activated Polycomb Group (PcG) protein chromatin silencing pathway. Cell Cycle 5 1208-1216.

Goutas N, Vlachodimitropoulos D, Bouka M, Lazaris AC, Nasioulas G, Gazouli M. 2008 BRAF and K-RAS Mutation in a Greek Papillary and Medullary Thyroid Carcinoma Cohort. Anticancer Research 28 305-308.

Grunert S, Jechlinger M & Beug H 2003 Diverse cellular and molecular mechanisms contribute to epithelial plasticity and metastasis. Nat Rev Mol Cell Biol 4 657-665.

Guled M, Lahti L, Lindholm PM, Salmenkivi K, Bagwan I, Nicholson AG & Knuutila S 2009 CDKN2A, NF2, and JUN are dysregulated among other genes by miRNAs in malignant mesothelioma -A miRNA microarray analysis. Genes Chromosomes Cancer 48 615-623.

Hawes J, Narasimhaiah, R, Picciotto, MR 2006 Galanin and galanin-like peptide modulate neurite outgrowth via protein kinase C-mediated activation of extracellular signal-related kinase. Eur J Neurosci 23 2937-2946.

Hayashi H, Ichihara M, Iwashita T, Murakami H, Shimono Y, Kawai K, Kurokawa K, Murakumo Y, Imai T, Funahashi H, et al. 2000 Characterization of intracellular signals via tyrosine 1062 in RET activated by glial cell line-derived neurotrophic factor. Oncogene 19 4469-4475.

Hayashida CY, Alves VA, Kanamura CT, Ezabella MC, Abelin NM, Nicolau W, Bisi H & Toledo SP 1993 Immunohistochemistry of medullary thyroid carcinoma and C-cell hyperplasia by an affinity-purified anti-human calcitonin antiserum. Cancer 72 1356-1363.

Hellemans J, Mortier G, De Paepe A, Speleman F & Vandesompele J 2007 qBase relative quantification framework and software for management and automated analysis of real-time quantitative PCR data. Genome Biology 8 R19.

Hoff AO, Camacho C, Maciel RMB, Yao JC & Hoff PM 2010 Hereditary and Sporadic Medullary Thyroid Carcinoma Neuroendocrine Tumors. pp 177-193: Humana Press.

Hofstra RM, Fattoruso, O, Quadro, L, Wu, Y, Libroia, A, Verga, U, Colantuoni,V and Buys, C.H. 1997 A novel point mutation in the intracellular domain of the ret protooncogene in a family with medullary thyroid carcinoma. Journal of Clinical Endocrinology and Metabolism 82 4176-4178.

Hofstra RM, Landsvater RM, Ceccherini I, Stulp RP, Stelwagen T, Luo Y, Pasini B, Hoppener JW, van Amstel HK, Romeo G, et al. 1994 A mutation in the RET proto-oncogene associated with multiple endocrine neoplasia type 2B and sporadic medullary thyroid carcinoma. Nature 367 375-376.

Ichihara M, Murakumo Y & Takahashi M 2004 RET and neuroendocrine tumors. Cancer Lett 204 197-211.

Jain S, Watson M, DeBenedetti M, Hiraki Y, Moley J & Milbrandt J 2004 Expression profiles provide insights into early malignant potential and skeletal abnormalities in multiple endocrine neoplasia type 2B syndrome tumors. Cancer Res 64 3907 - 3913.

Jiang L, Liu X, Kolokythas A, Yu J, Wang A, Heidbreder CE, Shi F & Zhou X 2010 Downregulation of the Rho GTPase signaling pathway is involved in the microRNA-138-mediated inhibition of cell migration and invasion in tongue squamous cell carcinoma. International Journal of Cancer 127 505-512.

Khurana R, Agarwal A, Bajpai VK, Verma N, Sharma AK, Gupta RP & Madhusudan KP 2004 Unraveling the amyloid associated with human medullary thyroid carcinoma. Endocrinology 145 5465-5470.

Kloos R, Eng C, Evans DB, Francis GL, Gagel R F, Gharib H, Moley JF, Pacini F, Ringel MD, Schlumberger M, and Wells Jr SA. 2009 Medullary Thyroid Cancer: Management Guidelines of the American Thyroid Association. Thyroid 19 565-612.

Kodama Y, Asai, N, Kawai, K, Jijiwa, M, Murakumo, Y, Ichihara, M, Takahashi, M. 2005 The RET proto-oncogene: a molecular therapeutic target in thyroid cancer. Cancer Sci 96 143-148.

Kumarswamy R, Mudduluru G, Ceppi P, Muppala S, Kozlowski M, Niklinski J, Papotti M & Allgayer H 2011 MicroRNA-30a inhibits epithelial-to-mesenchymal transition by targeting Snai1 and is downregulated in non-small cell lung cancer. International Journal of Cancer n/a-n/a.

Kurokawa K, Kawai K, Hashimoto M, Ito Y & Takahashi M 2003 Cell signalling and gene expression mediated by RET tyrosine kinase. Journal of Internal Medicine 253 627-633.

Kurzrock R, Sherman SI, Ball DW, Forastiere AA, Cohen RB, Mehra R, Pfister DG, Cohen EE, Janisch L, Nauling F, et al. 2011 Activity of XL184 (Cabozantinib), an oral tyrosine kinase inhibitor, in patients with medullary thyroid cancer. J Clin Oncol 29 2660-2666.

Lacroix L, Lazar V, Michiels S, Ripoche H, Dessen P, Talbot M, Caillou B, Levillain JP, Schlumberger M & Bidart JM 2005 Follicular thyroid tumors with the PAX8-PPAR gamma 1 rearrangement display characteristic genetic alterations. American Journal of Pathology 167 223-231.

Lam ET, Ringel MD, Kloos RT, Prior TW, Knopp MV, Liang J, Sammet S, Hall NC, Wakely PE, Jr., Vasko VV, et al. 2011 Phase II clinical trial of sorafenib in metastatic medullary thyroid cancer. J Clin Oncol 28 2323-2330.

Landgraf P, Rusu M, Sheridan R, Sewer A, Iovino N, Aravin A, Pfeffer S, Rice A, Kamphorst AO, Landthaler M, et al. 2007 A mammalian microRNA expression atlas based on small RNA library sequencing. Cell 129 1401-1414.

Lawrie CH 2008 MicroRNA expression in lymphoid malignancies: new hope for diagnosis and therapy? J Cell Mol Med 12 1432-1444.

Lewis BP, Burge CB & Bartel DP 2005 Conserved seed pairing, often flanked by adenosines, indicates that thousands of human genes are microRNA targets: Cell. 2005 Jan 14;120(1):15-20.

Lewis BP, Shih IH, Jones-Rhoades MW, Bartel DP & Burge CB 2003 Prediction of mammalian microRNA targets. Cell 115 787-798.

Li KKW, Pang JC-s, Ching AK-k, Wong CK, Kong X, Wang Y, Zhou L, Chen Z & Ng H-k 2009 miR-124 is frequently down-regulated in medulloblastoma and is a negative regulator of SLC16A1. Human Pathology 40 1234-1243.

Liu X, Wang C, Chen Z, Jin Y, Wang Y, Kolokythas A, Dai Y & Zhou X 2011 MicroRNA-138 suppresses epithelialâ€“mesenchymal transition in squamous cell carcinoma cell lines. Biochemical Journal 440 23-31.

LiVolsi VA 1997 C Cell Hyperplasia/Neoplasia. J Clin Endocrinol Metab 82 39-41.

Lopez-Jimenez E, Gomez-Lopez G, Leandro-Garcia LJ, Munoz I, Schiavi F, Montero-Conde C, de Cubas AA, Ramires R, Landa I, Leskela S, et al. 2010 Research resource: Transcriptional profiling reveals different pseudohypoxic signatures in SDHB and VHL-related pheochromocytomas. Mol Endocrinol 24 2382-2391.

Lu J, Getz G, Miska EA, Alvarez-Saavedra E, Lamb J, Peck D, Sweet-Cordero A, Ebert BL, Mak RH, Ferrando AA, et al. 2005 MicroRNA expression profiles classify human cancers. Nature 435 834-838.

Lytle JR, Yario TA & Steitz JA 2007 Target mRNAs are repressed as efficiently by microRNA-binding sites in the 5' UTR as in the 3' UTR. Proc Natl Acad Sci U S A 104 9667-9672.

Machens A, Brauckhoff M, Holzhausen H-Jr, Thanh PN, Lehnert H & Dralle H 2005 Codon-Specific Development of Pheochromocytoma in Multiple Endocrine Neoplasia Type 2. Journal of Clinical Endocrinology & Metabolism 90 3999-4003.

Machens A, Niccoli-Sire P, Hoegel J, Frank-Raue K, van Vroonhoven TJ, Roeher H-D, Wahl RA, Lamesch P, Raue F, Conte-Devolx B, et al. 2003 Early Malignant Progression of Hereditary Medullary Thyroid Cancer. New England Journal of Medicine 349 1517-1525.

Macia A, Gallel P, Vaquero M, Gou-Fabregas M, Santacana M, Maliszewska A, Robledo M, Gardiner JR, Basson MA, Matias-Guiu X, et al. 2011 Sprouty1 is a candidate tumor-suppressor gene in medullary thyroid carcinoma. Oncogene 2011 556.

Makeyev EV, Zhang J, Carrasco MA & Maniatis T 2007 The MicroRNA miR-124 Promotes Neuronal Differentiation by Triggering Brain-Specific Alternative Pre-mRNA Splicing. Molecular Cell 27 435-448.

Manie S, Santoro M, Fusco A & Billaud M 2001 The RET receptor: function in development and dysfunction in congenital malformation. Trends Genet 17 580-589.

Mao B & Niehrs C 2003 Kremen2 modulates Dickkopf2 activity during Wnt/LRP6 signaling. Gene 302 179-183.

Marsh D, Zori R. 2002 Genetic insights into familial cancers-update and recent discoveries. Cancer Lett 181 125-164.

Marsh DJ, Learoyd DL, Andrew SD, Krishnan L, Pojer R, Richardson AL, Delbridge L, Eng C & Robinson BG 1996 Somatic mutations in the RET proto-oncogene in sporadic medullary thyroid carcinoma. Clin Endocrinol 44 249-257.

Marshall GM, Peaston AE, Hocker JE, Smith SA, Hansford LM, Tobias V, Norris MD, Haber M, Smith DP, Lorenzo MJ, et al. 1997 Expression of multiple endocrine neoplasia 2B RET in neuroblastoma cells alters cell adhesion in vitro, enhances metastatic behavior in vivo, and activates Jun kinase. Cancer Res 57 5399-5405.

Marx SJ 2005 Molecular genetics of multiple endocrine neoplasia types 1 and 2. Nat Rev Cancer 5 367-375.

Matsui A, Yamaguchi, T, Maekawa, S, Miyazaki, C, Takano, S, Uetake, T, Inoue, T, Otaka, M, Otsuka, H, Sato, T, Yamashita, A, Takahashi, Y, Enomoto, N 2009 DICKKOPF-4 and -2 genes are upregulated in human colorectal cancer. Cancer Sci 100 1923-1930.

Melillo RM, Carlomagno F, De Vita G, Formisano P, Vecchio G, Fusco A, Billaud M & Santoro M 2001 The insulin receptor substrate (IRS)-1 recruits phosphatidylinositol 3-kinase to Ret: evidence for a competition between Shc and IRS-1 for the binding to Ret. Oncogene 20 209-218.

Mian C, Pennelli G, Fassan M, Balistreri M, Barollo S, Cavedon E, Galuppini F, Pizzi M, Vianello F, Pelizzo MR, et al. 2012 microRNA profiles in familial and sporadic medullary thyroid carcinoma: preliminary relationships with RET status and outcome. Thyroid 2012 3.

Mitomo S, Maesawa C, Ogasawara S, Iwaya T, Shibazaki M, Yashima-Abo A, Kotani K, Oikawa H, Sakurai E, Izutsu N, et al. 2008 Downregulation of miR-138 is associated with overexpression of human telomerase reverse transcriptase protein in human anaplastic thyroid carcinoma cell lines. Cancer Science 99 280-286.

Montaner D, Tarraga J, Huerta-Cepas J, Burguet J, Vaquerizas JM, Conde L, Minguez P, Vera J, Mukherjee S, Valls J, et al. 2006 Next station in microarray data analysis: GEPAS. Nucleic Acids Res 34 W486-491.

Morrissey ER, Diaz-Uriarte, R. 2009 Pomelo II: finding differentially expressed genes. Nucleic Acids Res 37 W581-W586.

Moura MM, Cavaco BM, Pinto AE & Leite V 2011 High prevalence of RAS mutations in RET-negative sporadic medullary thyroid carcinomas. J Clin Endocrinol Metab 96 E863-868.

Mulligan L, Eng C, Healey CS, Clayton D, Kwok JB, Gardner E, Ponder MA, Frilling A, Jackson CE, Lehnert H, Neumann HPH, Thibodeau SN and Ponder BAJ 1994 Specific mutations of the RET proto-oncogene are related to disease phenotype in MEN 2A and FMTC. Nature Genetics 6 70-74.

Mulligan LM, Kwok JB, Healey CS, Elsdon MJ, Eng C, Gardner E, Love DR, Mole SE, Moore JK, Papi L, et al. 1993 Germ-line mutations of the RET proto-oncogene in multiple endocrine neoplasia type 2A. Nature 363 458-460.

Murakami H, Yamamura Y, Shimono Y, Kawai K, Kurokawa K & Takahashi M 2002 Role of Dok1 in cell signaling mediated by RET tyrosine kinase. J Biol Chem 277 32781-32790.

Musholt TJ, Hanack J, Brehm C, von Wasielewski R & Musholt PB 2005 Searching for non-RET molecular alterations in medullary thyroid carcinoma: Expression analysis by mRNA differential display. World Journal of Surgery 29 472-482.

Nikiforova MN, Tseng GC, Steward D, Diorio D & Nikiforov YE 2008 MicroRNA expression profiling of thyroid tumors: biological significance and diagnostic utility. J Clin Endocrinol Metab 93 1600-1608.

Ohiwa M, Murakami H, Iwashita T, Asai N, Iwata Y, Imai T, Funahashi H, Takagi H & Takahashi M 1997 Characterization of Ret-Shc-Grb2 complex induced by GDNF, MEN 2A, and MEN 2B mutations. Biochem Biophys Res Commun 237 747-751.

Oudoux A, Salaun PY, Bournaud C, Campion L, Ansquer C, Rousseau C, Bardet S, Borson-Chazot F, Vuillez JP, Murat A, et al. 2007 Sensitivity and prognostic value of positron emission tomography with F-18-fluorodeoxyglucose and sensitivity of immunoscintigraphy in patients with medullary thyroid carcinoma treated with anticarcinoembryonic antigen-targeted radioimmunotherapy. J Clin Endocrinol Metab 92 4590-4597.

Pachnis V, Mankoo B, and Costantini F 1993 Expression of the c-ret proto-oncogene during mouse embryogenesis. Development 119 1005-1017.

Pasini B, Hofstra RM, Yin L, Bocciardi R, Santamaria G, Grootscholten PM, Ceccherini I, Patrone G, Priolo M, Buys CH, et al. 1995 The physical map of the human RET proto-oncogene. Oncogene 11 1737-1743.

Pavey S, Johansson P, Packer L, Taylor J, Stark M, Pollock PM, Walker GJ, Boyle GM, Harper U, Cozzi SJ, et al. 2004 Microarray expression profiling in melanoma reveals a BRAF mutation signature. Oncogene 23 4060-4067.

Peinado H, Del Carmen Iglesias-de la Cruz, M, Olmeda, D, Csiszar, K, Fong, KS, Vega, S, Nieto, MA, Cano, A, Portillo, F 2005 A molecular role for lysyl oxidase-like 2 enzyme in snail regulation and tumor progression. EMBO J 24 3446-3458.

Peinado H, Moreno-Bueno, G, Hardisson, D, Perez-Gomez, E, Santos, V, Mendiola, M, de Diego, JI, Nistal, M, Quintanilla, M, Portillo, F, Cano, A 2008 Lysyl oxidase-like 2 as a new poor prognosis marker of squamous cell carcinomas. Cancer Res 68 4541-4550.

Pelicci G, Troglio F, Bodini A, Melillo RM, Pettirossi V, Coda L, De Giuseppe A, Santoro M & Pelicci PG 2002 The neuron-specific Rai (ShcC) adaptor protein inhibits apoptosis by coupling Ret to the phosphatidylinositol 3-kinase/Akt signaling pathway. Mol Cell Biol 22 7351-7363.

Peng L, Ran YL, Hu H, Yu L, Liu Q, Zhou Z, Sun YM, Sun LC, Pan J, Sun LX, et al. 2009 Secreted LOXL2 is a novel therapeutic target that promotes gastric cancer metastasis via the Src/FAK pathway. Carcinogenesis 30 1660-1669.

Pierotti MA, Arighi E, Degl'innocenti D & Borrello MG 2004 RET activation in medullary carcinomas. Cancer Treat Res 122 389-415.

Pierson J, Hostager B, Fan R & Vibhakar R 2008 Regulation of cyclin dependent kinase 6 by microRNA 124 in medulloblastoma. Journal of Neuro-Oncology 90 1-7.

Plaza-Menacho I, Mologni L, Sala E, Gambacorti-Passerini C, Magee AI, Links TP, Hofstra RM, Barford D & Isacke CM 2007 Sorafenib functions to potently suppress RET tyrosine kinase activity by direct enzymatic inhibition and promoting RET lysosomal degradation independent of proteasomal targeting. J Biol Chem 282 29230-29240.

Randolph G, Maniar D. 2000 Medullary carcinoma of the thyroid. Cancer Control 7 253-261.

Raso A, Mascelli S, Biassoni R, Nozza P, Kool M, Pistorio A, Ugolotti E, Milanaccio C, Pignatelli S, Ferraro M, et al. 2011 High levels of PROM1 (CD133) transcript are a potential predictor of poor prognosis in medulloblastoma. Neuro Oncol 13 500-508.

Reich M, Ohm K, Angelo M, Tamayo P, Mesirov JP 2004 GeneCluster 2.0 :an advanced toolset for bioarray analysis. Bioinformatics 20 1797-1798.

Ritchie M, Silver J, Oshlack A, Holmes M, Diyagamam D, Holloway A, Smyth GK 2007 A comparison of background correction methods for two-colour microarrays. Bioinformatics 23 2700-2707.

Robinson BG, Paz-Ares L, Krebs A, Vasselli J & Haddad R 2011 Vandetanib (100 mg) in patients with locally advanced or metastatic hereditary medullary thyroid cancer. J Clin Endocrinol Metab 95 2664-2671.

Rossi J, Tomac A, Saarma M & Airaksinen MS 2000 Distinct roles for GFRalpha1 and GFRalpha2 signalling in different cranial parasympathetic ganglia in vivo. Eur J Neurosci 12 3944-3952.

Ruckert F, Joensson P, Saeger HD, Grutzmann R & Pilarsky C 2010 Functional analysis of LOXL2 in pancreatic carcinoma. International Journal of Colorectal Disease 25 303-311.

Sales G, Coppe A, Bisognin A, Biasiolo M, Bortoluzzi S & Romualdi C 2010 MAGIA, a web-based tool for miRNA and Genes Integrated Analysis. Nucleic Acids Research 38 W352-W359.

Santoro M, Carlomagno F, Melillo RM & Fusco A 2004a Oncogenic protein tyrosine kinases. Cellular and Molecular Life Sciences 61 2954-2964.

Santoro M, Carlomagno F, Romano A, Bottaro DP, Dathan NA, Grieco M, Fusco A, Vecchio G, Matoskova B, Kraus MH, et al. 1995 Activation of RET as a dominant transforming gene by germline mutations of MEN2A and MEN2B. Science 267 381-383.

Santoro M, Melillo RM, Carlomagno F, Vecchio G & Fusco A 2004b Minireview: RET: normal and abnormal functions. Endocrinology 145 5448-5451.

Sariola H & Saarma M 2003 Novel functions and signalling pathways for GDNF. J Cell Sci 116 3855-3862.

Schilling T, Burck J, Sinn HP, Clemens A, Otto HF, Hoppner W, Herfarth C, Ziegler R, Schwab M & Raue F 2001 Prognostic value of codon 918 (ATG-->ACG) RET proto-oncogene mutations in sporadic medullary thyroid carcinoma. Int J Cancer 95 62-66.

Schlumberger M, Carlomagno, F, Baudin, E, Bidart, JM, Santoro, M 2008 New therapeutic approaches to treat medullary thyroid carcinoma. Nat Clin Pract End Met 4 22-32.

Schlumberger MJ, Elisei R, Bastholt L, Wirth LJ, Martins RG, Locati LD, Jarzab B, Pacini F, Daumerie C, Droz JP, et al. 2009 Phase II study of safety and efficacy of motesanib in patients with

progressive or symptomatic, advanced or metastatic medullary thyroid cancer. J Clin Oncol 27 3794-3801.

Schuchardt A, D'Agati V, Larsson-Blomberg L, Costantini F & Pachnis V 1994 Defects in the kidney and enteric nervous system of mice lacking the tyrosine kinase receptor Ret. Nature 367 380-383.

Schuetz G, Rosario M, Grimm J, Boeckers TM, Gundelfinger ED & Birchmeier W 2004 The neuronal scaffold protein Shank3 mediates signaling and biological function of the receptor tyrosine kinase Ret in epithelial cells. J Cell Biol 167 945-952.

Segouffin-Cariou C & Billaud M 2000 Transforming ability of MEN2A-RET requires activation of the phosphatidylinositol 3-kinase/AKT signaling pathway. J Biol Chem 275 3568-3576.

Seri M, Celli I, Betsos N, Claudiani F, Camera G & Romeo G 1997 A Cys634Gly substitution of the RET proto-oncogene in a family with recurrence of multiple endocrine neoplasia type 2A and cutaneous lichen amyloidosis. Clin Genet 51 86-90.

Siegel PM & Massague J 2003 Cytostatic and apoptotic actions of TGF-beta in homeostasis and cancer. Nat Rev Cancer 3 807-821.

Silber J, Lim D, Petritsch C, Persson A, Maunakea A, Yu M, Vandenberg S, Ginzinger D, James CD, Costello J, et al. 2008 miR-124 and miR-137 inhibit proliferation of glioblastoma multiforme cells and induce differentiation of brain tumor stem cells. BMC Medicine 6 14.

Skinner MA, DeBenedetti MK, Moley JF, Norton JA & Wells Jr SA 1996 Medullary thyroid carcinoma in children with multiple endocrine neoplasia types 2A and 2B. Journal of Pediatric Surgery 31 177-182.

Skinner MA, Safford SD, Reeves JG, Jackson ME & Freemerman AJ 2008 Renal aplasia in humans is associated with RET mutations. Am J Hum Genet 82 344-351.

Smyth GK, Michaud J & Scott HS 2005 Use of within-array replicate spots for assessing differential expression in microarray experiments. Bioinformatics 21 2067-2075.

Steiner P, Kulangara, K, Sarria, JCF, Glauser, L, Regazzi, R and Hirling, H, 2004 Reticulon 1-C/neuroendocrine-specific protein-C interacts with SNARE proteins. Journal of Neurochemistry 89 569-580.

Subramanian A, Tamayo P, Mootha VK, Mukherjee S, Ebert BL, Gillette MA, Paulovich A, Pomeroy SL, Golub TR, Lander ES, et al. 2005 Gene set enrichment analysis: a knowledge-based approach for interpreting genome-wide expression profiles. Proc Natl Acad Sci U S A 102 15545-15550.

Sugimoto T, Seki N, Shimizu S, Kikkawa N, Tsukada J, Shimada H, Sasaki K, Hanazawa T, Okamoto Y & Hata A 2009 The galanin signaling cascade is a candidate pathway regulating oncogenesis in human squamous cell carcinoma. Genes Chromosomes Cancer 48 132-142.

Takahashi M, Ritz J, and Cooper GM 1985 Activation of a novel human transforming gene, ret, by DNA rearrangement. Cell 42 581-588.

Tofighi R, Joseph B, Xia S, Xu ZQ, Hamberger B, Hokfelt T & Ceccatelli S 2008 Galanin decreases proliferation of PC12 cells and induces apoptosis via its subtype 2 receptor (GalR2). Proc Natl Acad Sci U S A 105 2717-2722.

Tombol Z, Eder K, Kovacs A, Szabo PM, Kulka J, Liko I, Zalatnai A, Racz G, Toth M, Patocs A, et al. 2010 MicroRNA expression profiling in benign (sporadic and hereditary) and recurring adrenal pheochromocytomas. Mod Pathol 23 1583-1595.

Tusher VG, Tibshirani R & Chu G 2001 Significance analysis of microarrays applied to the ionizing radiation response. Proc Natl Acad Sci U S A 98 5116-5121.

van de Vijver MJ, He YD, van't Veer LJ, Dai H, Hart AA, Voskuil DW, Schreiber GJ, Peterse JL, Roberts C, Marton MJ, et al. 2002 A gene-expression signature as a predictor of survival in breast cancer. N Engl J Med 347 1999-2009.

Vasilevskaya I & O'Dwyer PJ 2003 Role of Jun and Jun kinase in resistance of cancer cells to therapy. Drug Resist Updat 6 147-156.

Watanabe T, Ichihara M, Hashimoto M, Shimono K, Shimoyama Y, Nagasaka T, Murakumo Y, Murakami H, Sugiura H, Iwata H, et al. 2002 Characterization of gene expression induced by RET with MEN2A or MEN2B mutation. American Journal of Pathology 161 249-256.

Weber T, Schilling, T, Buchler, MW 2006 Thyroid carcinoma. Curr Opin Oncol 18 30-35.

Wells SA, Jr., Gosnell JE, Gagel RF, Moley J, Pfister D, Sosa JA, Skinner M, Krebs A, Vasselli J & Schlumberger M 2011 Vandetanib for the treatment of patients with locally advanced or metastatic hereditary medullary thyroid cancer. J Clin Oncol 28 767-772.

Wiemer EA 2007 The role of microRNAs in cancer: no small matter. Eur J Cancer 43 1529-1544.

Yip L, Kelly L, Shuai Y, Armstrong M, Nikiforov Y, Carty S & Nikiforova M 2011 MicroRNA Signature Distinguishes the Degree of Aggressiveness of Papillary Thyroid Carcinoma. Annals of Surgical Oncology 18 2035-2041.

Yu J-Y, Chung K-H, Deo M, Thompson RC & Turner DL 2008 MicroRNA miR-124 regulates neurite outgrowth during neuronal differentiation. Experimental Cell Research 314 2618-2633.

Zacharias A, Gage, PJ 2010 Canonical Wnt/beta-catenin signaling is required for maintenance but not activation of Pitx2 expression in neural crest during eye development. Dev Dyn 239 3215-3225.

Zhu W, Hai, T, Ye, L, Cote, GJ 2010 Medullary thyroid carcinoma cell lines contain a self-renewing CD133+ population that is dependent on ret proto-oncogene activity. J Clin Endocrinol Metab 95 439-444.

Appendix I

Supplementary material

Supplementary annex 1. Clinical information retrieved from related patients suspected to MEN2 development.

MEN2 and Pheocromocytoma questionnaire

Name(s) and Surname(s) .....
Hospital .....
Responsible MD (Telephone / e-mail) .....
Biopsy number .....
Gender
Male ☐ Female ☐
Date of birth .....
Raze .....

Medullary Thyroid Carcinoma

- Date of diagnosis .....
- C-cell Hyperplasia (CCH) ☐
- Monotypic localization ☐
- Multiple localization ☐
- Major Tumor size (major diameter in cm) .....
- Lymph node metastasis
  - At diagnosis ☐
  - During the evolution (follow-up) ☐ (date) .....
- Hepatic metastasis
  - At diagnosis ☐
  - During the evolution (follow-up) ☐ (date) .....
- Other lung and bone metastasis ☐ (date) .....

Pheochromocytoma

- Date of diagnosis .....
- Unilateral ☐
- Bilateral ☐
- Metastasis ☐
  Localization and date .....

Primary Hyperthyroidism (PHPT)

- Date of diagnosis .....
- C-cell Hyperplasia (CCH) ☐
- Unique tumor yes ☐ no ☐
- Unknown ☐
- Metastasis (date and localization) .....

Other related lesions

- Neuromas ☐
- Marfanoid habitus ☐
- Hirschsprung disease ☐
- Cutaneous lichen amyloidosis ☐

Familial antecedents (family tree, specifying the MEN2 manifestations and age of onset).

Supplementary annex Table 1. Clinical and genetic information of the frozen and FFPE MTC series.

Nº	ID	miRNA Array*	cDNA Array	Frozen[a,b]/ FFPE	MTC+	Gender	Year of birth	Antec.	Germline mutation	Somatic mutation	Classification
1	MTC20	yes	yes	Frozen[a,b]	Fam	F	1936	no	C634R	-	¨634¨
2	MTC23	yes	yes	Frozen[a,b]	Fam	F	1986	yes	C634R	-	¨634¨
3	MTC26	yes	yes	Frozen[a,b]	Fam	M	1966	yes	C634R	-	¨634¨
4	MTC28	yes	yes	Frozen[a,b]	Fam	M	1957	yes	C634R	-	¨634¨
5	MTC1	yes	yes	Frozen[a,b]	Fam	F	1988	yes	C634S	-	¨634¨
6	MTC2	yes	yes	Frozen[a,b]	Fam	M	1943	yes	C634S	-	¨634¨
7	MTC22	yes	yes	Frozen[a,b]	Fam	M	1973	yes	C634Y	-	¨634¨
8	MTC71	yes	yes	Frozen[a,b]	Fam	F	1955	yes	C620G	-	-
9	MTC76	yes	yes	Frozen[a,b]	Fam	F	1965	yes	C620G	-	-
10	MTC29	yes	yes	Frozen[a,b]	Fam	M	1968	yes	C618S	-	-
11	MTC27	yes	yes	Frozen[a,b]	Fam	M	1944	yes	NA	NA	-
12	MTC62	yes	yes	Frozen[a,b]	Fam	M	1967	yes	NA	-	-
13	MTC44	yes	yes	Frozen[a,b]	S	M	1944	no	Neg	M918T	¨918¨
14	MTC38	yes	yes	Frozen[a,b]	S	M	1924	no	Neg	M918T	¨918¨
15	MTC39	yes	yes	Frozen[a,b]	S	F	1979	no	Neg	M918T	¨918¨
16	MTC46	yes	yes	Frozen[a,b]	S	M	1949	no	Neg	M918T	¨918¨
17	MTC19	yes	yes	Frozen[a,b]	S	M	1949	no	Neg	M918T	¨918¨
18	MTC16	yes	yes	Frozen[a,b]	S	F	1948	no	Neg	M918T	¨918¨
19	MTC64	yes	no	Frozen[b]	S	M	1947	no	Neg	M918T	¨918¨
20	MTC37	yes	yes	Frozen[a,b]	S	M	1954	no	Neg	M918T	¨918¨
21	MTC74	yes	yes	Frozen[a,b]	S	M	1941	no	Neg	M918T	¨918¨
22	MTC31	yes	yes	Frozen[a,b]	S	F	1944	no	Neg	Neg	¨WT¨
23	MTC41	yes	yes	Frozen[a,b]	S	M	1926	no	Neg	Neg	¨WT¨
24	MTC48	yes	yes	Frozen[a,b]	S	M	1968	no	Neg	Neg	¨WT¨
25	MTC49	yes	yes	Frozen[a,b]	S	M	1958	no	Neg	Neg	¨WT¨
26	MTC51	yes	yes	Frozen[a,b]	S	M	1939	no	Neg	Neg	¨WT¨
27	MTC4	yes	yes	Frozen[a,b]	S	F	1953	no	Neg	Neg	¨WT¨
28	MTC53	yes	yes	Frozen[a,b]	S	M	1955	no	Neg	Neg	¨WT¨
29	MTC17	yes	yes	Frozen[a,b]	S	F	1951	no	Neg	Neg	¨WT¨
30	MTC30	yes	yes	Frozen[a,b]	S	F	1963	no	Neg	Neg	¨WT¨
31	MTC70	yes	yes	Frozen[a,b]	S	F	2001	no	Neg	E-16 Neg	¨WT¨
32	MTC72	yes	yes	Frozen[a,b]	S	F	1946	no	Neg	E-16 Neg	¨WT¨
33	MTC73	yes	yes	Frozen[a,b]	S	M	1920	no	Neg	E-16 Neg	¨WT¨
34	MTC77	yes	yes	Frozen[a,b]	S	M	1937	no	Neg	E-16 Neg	¨WT¨
35	MTC78	yes	yes	Frozen[a,b]	S	F	1959	no	Neg	E-16 Neg	¨WT¨
36	MTC35	yes	yes	Frozen[a,b]	S	F	1922	no	Neg	unkown	¨WT¨
37	MTC36	yes	yes	Frozen[a,b]	S	M	1937	no	Neg	unkown	¨WT¨
38	MTC33	yes	yes	Frozen[a,b]	S	F	1936	no	Neg	unkown	¨WT¨
39	MTC52	yes	yes	Frozen[a,b]	S	M	1944	no	Neg	C634R	¨634¨
40	MTC47	yes	yes	Frozen[a,b]	S	M	1963	no	Neg	C630G	-
41	MTC34	no	yes	Frozen[a]	S	F	1942	no	Neg	unknown	¨WT¨
42	MTC15	no	yes	Frozen[a]	S	F	1948	no	Neg	M918T	¨918¨
43	MTC18	no	yes	Frozen[a]	S	M	1968	no	Neg	M918T	¨918¨
44	MTC50	no	yes	Frozen[a]	S	F	1949	no	Neg	M918T	¨918¨

45	MTC54	no	yes	Frozen[a]	S	M	1961	no	Neg	M918T	¨918¨
46	MTC57	no	yes	Frozen[a]	S	M	1938	no	Neg	M918T	¨918¨
47	MTC68	no	yes	Frozen[a]	S	M	1979	no	Neg	M918T	¨918¨
48	MTC3	no	yes	Frozen[a]	S	F	1929	no	Neg	M918T	¨918¨
49	MTC32	no	yes	Frozen[a]	Fam	F	1976	no	M918T	-	¨918¨
50	MTC21	no	yes	Frozen[a]	Fam	F	1936	yes	E 11, 10 Neg	-	-
51	MTC81	no	no	Frozen	Fam	F	1947	unknown	C634Y	-	¨634¨
52	MTC82	no	no	Frozen	Fam	F	1966	yes	C634Y	-	¨634¨
53	MTC83	no	no	Frozen	Fam	F	1979	yes	C634Y	-	¨634¨
54	MTC7	no	no	Frozen	Fam	F	1970	yes	C634Y	-	¨634¨
55	MTC9	no	no	Frozen	Fam	M	1963	yes	C634Y	-	¨634¨
56	MTC13	no	no	Frozen	Fam	M	1972	yes	C634Y	-	¨634¨
57	MTC10	no	no	Frozen	Fam	M	1971	yes	C634Y	-	¨634¨
58	MTC87	no	no	Frozen	Fam	F	1970	yes	C634S	-	¨634¨
59	MTC88	no	no	Frozen	Fam	F	1969	yes	C634R	-	¨634¨
60	MTC89	no	no	Frozen	Fam	F	1993	yes	C634R	-	¨634¨
61	MTC56	no	no	Frozen	S	M	1958	no	Neg	M918T	¨918¨
62	MTC11	no	no	Frozen	S	M	1962	no	Neg	M918T	¨918¨
63	MTC90	no	no	Frozen	S	M	1981	no	Neg	M918T	¨918¨
64	MTC43	no	no	Frozen	S	F	1938	no	E 11, 10 Neg	Neg	¨WT¨
65	MTC40	no	no	Frozen	S	M	1933	no	Neg	-	¨WT¨
66	MTC66	no	no	Frozen	S	F	1971	no	Neg	E-16 Neg	¨WT¨
67	MTC67	no	no	Frozen	S	M	1942	no	Neg	E-16 Neg	¨WT¨
68	MTC79	no	no	Frozen	S	F	1958	unknown	E 11, 10 Neg	Neg	¨WT¨
69	MTC80	no	no	Frozen	S	F	1944	no	E 11, 10 Neg	Neg	¨WT¨
70	MTC91	no	no	FFPE	Fam	M	1978	yes	C634W	-	¨634¨
71	MTC92	no	no	FFPE	Fam	F	1944	yes	C634Y	-	¨634¨
72	MTC93	no	no	FFPE	Fam	F	1973	yes	C634Y	-	¨634¨
73	MTC94	no	no	FFPE	Fam	M	1982	yes	C634Y	-	¨634¨
74	MTC95	no	no	FFPE	Fam	F	1952	yes	C634W	-	¨634¨
75	MTC96	no	no	FFPE	Fam	M	1948	yes	C634Y	-	¨634¨
76	MTC97	no	no	FFPE	Fam	F	1917	yes	C634R	-	¨634¨
77	MTC98	no	no	FFPE	Fam	M	1958	yes	C634Y	-	¨634¨
78	MTC99	no	no	FFPE	Fam	M	1948	yes	C634R	-	¨634¨
79	MTC100	no	no	FFPE	Fam	M	1960	yes	C634Y	-	¨634¨
80	MTC101	no	no	FFPE	Fam	F	1965	yes	C634Y	-	¨634¨
81	MTC102	no	no	FFPE	Fam	F	1959	yes	C634R	-	¨634¨
82	MTC128	no	no	FFPE	Fam	F	1969	yes	C634R	-	¨634¨
83	MTC129	no	no	FFPE	Fam	F	1993	yes	C634R	-	¨634¨
84	MTC127	no	no	FFPE	Fam	F	1970	yes	C634S	-	¨634¨
85	MTC104	no	no	FFPE	S	F	1954	no	-	M918T	¨918¨
86	MTC105	no	no	FFPE	S	F	1937	no	-	M918T	¨918¨
87	MTC106	no	no	FFPE	S	F	1949	no	-	M918T	¨918¨
88	MTC107	no	no	FFPE	S	M	1928	no	-	M918T	¨918¨

89	MTC108	no	no	FFPE	S	F	1931	no	-	M918T	¨918¨
90	MTC109	no	no	FFPE	S	M	1948	no	-	M918T	¨918¨
91	MTC110	no	no	FFPE	S	M	1949	no	-	M918T	¨918¨
92	MTC111	no	no	FFPE	S	F	1961	no	-	M918T	¨918¨
93	MTC124	no	no	FFPE	S	F	1932	no	-	M918T	¨918¨
94	MTC126	no	no	FFPE	S	M	1952	no	-	M918T	¨918¨
95	MTC114	no	no	FFPE	S	M	NA	no	Neg	Neg	¨WT¨
96	MTC115	no	no	FFPE	S	F	1936	no	Neg	Neg	¨WT¨
97	MTC112	no	no	FFPE	S	M	1951	no	Neg	Neg	¨WT¨
98	MTC116	no	no	FFPE	S	M	1926	no	Neg	Neg	¨WT¨
99	MTC113	no	no	FFPE	S	M	1952	no	Neg	Neg	¨WT¨
100	MTC117	no	no	FFPE	S	M	1967	no	Neg	Neg	¨WT¨
101	MTC118	no	no	FFPE	S	F	1929	no	Neg	Neg	¨WT¨
102	MTC119	no	no	FFPE	S	M	1961	no	Neg	Neg	¨WT¨
103	MTC120	no	no	FFPE	S	F	NA	no	Neg	Neg	¨WT¨
104	MTC121	no	no	FFPE	S	M	1951	no	Neg	Neg	¨WT¨
105	MTC122	no	no	FFPE	S	F	1976	no	Neg	Neg	¨WT¨
106	MTC123	no	no	FFPE	S	M	1952	no	Neg	Neg	¨WT¨
107	MTC125	no	no	FFPE	S	M	1974	no	Neg	Neg	¨WT¨

[*] Indicate if the sample was or not hybridized onto miRCURY LNA™ microRNA Array. Those not used for hybridization purposes, were used for independent validation through RT-qPCR using LNA™ microRNA PCR primer/SYBR® Green mix (Exiqon).[†] Indicate the familial or the sporadic nature of the tumor, according to germline or somatic *RET* mutation status, as well as the existence of personal or familiar antecedents. [a] Frozen MTC tumor hybridized onto Agilent 4X44K Whole Human Genome Array.[b] Frozen MTC tumor hybridized onto miRCURY LNA™ microRNA Array.

Abbreviations: Gender: F, female; M, male; Antec- antecedents (personal or familiar); NA- not available; Neg – negative; E-10, E-11, E-16 : exon 10, exon 16 and exon 11, respectively. Fam- Familial, S- Sporadic.

Supplementary annex Table 2. FFPE MTC series for independent validation.

Nº	ID case	Gender	Year of birth	MTC*	*RET* mutation	Classification
1	MTC91	M	1978	Familial	C634W	¨634¨
2	MTC92	F	1944	Familial	C634Y	¨634¨
3	MTC93	F	1973	Familial	C634Y	¨634¨
4	MTC94	M	1982	Familial	C634Y	¨634¨
5	MTC95	F	1952	Familial	C634W	¨634¨
6	MTC96	M	1948	Familial	C634Y	¨634¨
7	MTC97	F	1917	Familial	C634R	¨634¨
8	MTC98	M	1958	Familial	C634Y	¨634¨
9	MTC99	M	1948	Familial	C634R	¨634¨
10	MTC100	M	1960	Familial	C634Y	¨634¨
11	MTC101	F	1965	Familial	C634Y	¨634¨
12	MTC102	F	1959	Familial	C634R	¨634¨
13	MTC145	F	1962	Sporadic	M918T	¨918¨
14	MTC104	F	1954	Sporadic	M918T	¨918¨
15	MTC105	F	1937	Sporadic	M918T	¨918¨
16	MTC106	F	1949	Sporadic	M918T	¨918¨

17	MTC107	M	1928	Sporadic	M918T	¨918¨
18	MTC108	F	1931	Sporadic	M918T	¨918¨
19	MTC109	M	1948	Sporadic	M918T	¨918¨
20	MTC110	M	1949	Sporadic	M918T	¨918¨
21	MTC111	F	1961	Sporadic	M918T	¨918¨
22	MTC112	M	1951	Sporadic	Negative	WT
23	MTC113	M	1952	Sporadic	Negative	WT

* Indicate the familial or the sporadic nature of the tumor, according to germline or somatic *RET* mutation status, as well as the existence of personal or familiar antecedents. Abbreviations. Gender: F, female; M, male;

Supplementary annex Table 3A. Genetic information of the TMA-1.

Nº	ID	Tumor/tissue	Somatic mutation	Germinal mutation	Normal thyroid	Classification
1	MTC134	MTC	-	C618F		not used
2	MTC150	MTC	-	C618F		not used
3	MTC154	MTC	-	C618F		not used
4	MTC99	MTC	-	C634R		¨634¨
5	MTC98	MTC	-	C634R	yes	¨634¨
6	MTC102	MTC	-	C634R		¨634¨
7	MTC97	MTC	-	C634R		¨634¨
8	MTC94	MTC	-	C634W	yes	¨634¨
9	MTC91	MTC	-	C634W	yes	¨634¨
10	MTC95	MTC	-	C634W		¨634¨
11	MTC93	MTC	-	C634Y		¨634¨
12	MTC151	MTC	-	C634Y		¨634¨
13	MTC92	MTC	-	C634Y		¨634¨
14	MTC100	MTC	-	C634Y		¨634¨
15	MTC101	MTC	-	C634Y	yes	¨634¨
16	MTC137	MTC	-	S891A	yes	not used
17	MTC106	MTC	M918T	Neg	yes	¨918¨
18	MTC107	MTC	M918T	Neg		¨918¨
19	MTC145	MTC	M918T	Neg		¨918¨
20	MTC108	MTC	M918T	Neg		¨918¨
21	MTC136	MTC	M918T	Neg		¨918¨
22	MTC109	MTC	M918T	Neg		¨918¨
23	MTC105	MTC	M918T	Neg		¨918¨
24	MTC110	MTC	M918T	Neg		¨918¨
25	MTC104	MTC	M918T	Neg	yes	¨918¨
26	MTC135	MTC	C618R	Neg		not used
27	MTC156	MTC	C620F	Neg		not used
28	MTC149	MTC	C634R	Neg		not used
29	MTC155	MTC	C634S	Neg		not used
30	MTC159	MTC	A883F	Neg		not used
31	MTC113	MTC	E 10, 11, 15, 16 neg	Neg		¨WT¨
32	MTC112	MTC	E 10, 11, 15, 16 neg	Neg		¨WT¨
33	MTC117	MTC	E 10, 11, 15, 16 neg	Neg	yes	¨WT¨

34	MTC132	MTC	E 10, 16 neg	Neg		¨WT¨
35	MTC152	MTC	E 15, 16 neg	Neg		¨WT¨
36	MTC146	MTC	E 11, 16 neg	Neg		¨WT¨
37	MTC147	MTC	E 11, 16 neg	Neg		¨WT¨
38	MTC148	MTC	E 11, 16 neg	Neg		¨WT¨
39	MTC143	MTC	E 11, 16 neg	Neg		¨WT¨
40	MTC140	MTC	E 11, 16 neg	Neg	yes	¨WT¨
41	MTC138	MTC	E 16 neg	Neg		¨WT¨
42	MTC139	MTC	E 16 neg	Neg		¨WT¨
43	MTC142	MTC	E 16 neg	Neg	yes	¨WT¨
44	MTC131	MTC	E 16 neg	Neg	yes	¨WT¨
45	MTC141	MTC	E 16 neg	Neg	yes	¨WT¨
46	MTC144	MTC	E 16 neg	Neg		¨WT¨
47	MTC133	MTC	E 16 neg	NA	yes	¨WT¨
48	MTC115	MTC	Neg	Neg		¨WT¨
50	MTC157	MTC	Neg	Neg		¨WT¨
51	MTC116	MTC	Neg	Neg		¨WT¨
52	MTC114	MTC	Neg	Neg		¨WT¨
53	MTC130	MTC	Neg	Neg		¨WT¨
54	MTC153	MTC	NA	Neg		not used
55	MTC158	MTC	NA	Neg		not used
57	PDTC1	PDTC				control
58	PTC1	PTC				control
59	PTC2	PTC				control
60	PTC3	PTC				control
61	MC	medulla cortex				control
62	PL	placenta				control

Abbreviations: NA- not available; Neg – negative; E-10, E-11, E-15, E-16 : exon 10, exon 11, exon 15 and exon 16, respectively.

Supplementary annex Table 3B. Genetic information of the TMA-2 .

Nº	ID	Tumor	Somatic mutation	Germline mutation	Normal thyroid	Classification
1	MTC20_P	MTC	-	C634R	Yes	¨634¨
2	MTC23_P	MTC	-	C634R	Yes	¨634¨
3	MTC28_P	MTC	-	C634R	Yes	¨634¨
4	MTC22_P	MTC	-	C634Y	Yes	¨634¨
5	MTC24_P*	MTC	-	C634Y	Yes	¨634¨
6	MTC25_P*	MTC	-	C634R	Yes	¨634¨
7	MTC18_P	MTC	M918T	Neg	Yes	¨918¨
8	MTC19_P	MTC	M918T	Neg	No	¨918¨
9	MTC46_P	MTC	M918T	Neg	No	¨918¨
10	MTC16_P	MTC	M918T	Neg	No	¨918¨
11	MTC17_P	MTC	WT	E 10, 11 Neg	Yes	¨WT¨
12	MTC31_P	MTC	WT	E 10, 11 Neg	Yes	¨WT¨
13	MTC21_P	MTC	Unkown	E 10, 11 Neg	Yes	¨WT¨

14	MTC27_P	MTC	Unkown	Unkown	Yes	not used
15	MTC29_P	MTC	-	C618S	Yes	Not used
16	HCN1	Hürthle cell neoplasm				control
17	FTC1	FTC				control

*tumors not hybridized due to lack of RNA.
Abbreviations: FTC- Follicular Thyroid Carcinoma; Neg – negative. P:FFPE sample code associated to MTC frozen samples code.

Supplementary annex Table 4A. GSEA analysis of MTC^{M918T} *vs* MTC^{634}. Enriched pathways in M918T group.

BIOCARTA PATHWAY NAME	NES	NOM p-val*	FDR q-val†
TCRPATHWAY	1,766	0,002	0,053
NKTPATHWAY	1,830	0,000	0,055
HIVNEFPATHWAY	1,784	0,002	0,056
INFLAMPATHWAY	1,768	0,005	0,058
ATRBRCAPATHWAY	1,788	0,005	0,060
STEMPATHWAY	1,833	0,004	0,066
DEATHPATHWAY	1,732	0,005	0,066
NO2IL12PATHWAY	1,793	0,006	0,068
NTHIPATHWAY	1,709	0,011	0,077
NFKBPATHWAY	1,845	0,000	0,079
BCRPATHWAY	1,678	0,011	0,086
IL1RPATHWAY	1,688	0,009	0,086
RELAPATHWAY	1,667	0,017	0,087
LAIRPATHWAY	1,640	0,013	0,103
CASPASEPATHWAY	1,849	0,004	0,110
DCPATHWAY	1,906	0,000	0,115
TH1TH2PATHWAY	1,605	0,024	0,127
TNFR1PATHWAY	1,576	0,030	0,151
CTLA4PATHWAY	1,556	0,041	0,155
IL12PATHWAY	1,562	0,038	0,155
NKCELLSPATHWAY	1,531	0,032	0,175
FMLPPATHWAY	1,513	0,033	0,189
AMIPATHWAY	1,484	0,057	0,212
TNFR2PATHWAY	1,476	0,063	0,212
ERYTHPATHWAY	1,489	0,054	0,215
ETSPATHWAY	1,443	0,070	0,234
P38MAPKPATHWAY	1,414	0,052	0,237
CSKPATHWAY	1,446	0,071	0,239
WNTPATHWAY	1,422	0,069	0,240
CCR5PATHWAY	1,415	0,068	0,243
IL2PATHWAY	1,405	0,078	0,243
CYTOKINEPATHWAY	1,425	0,068	0,244
MAPKPATHWAY	1,447	0,021	0,246
KEGG PATHWAY NAME	**NES**	**NOM p-val***	**FDR q-val†**

NATURAL KILLER CELL MEDIATED CYTOTOXICITY	2,276	0,000	0,001
P53 SIGNALING PATHWAY	2,142	0,000	0,002
TYPE I DIABETES MELLITUS	2,067	0,000	0,002
ASTHMA	1,917	0,000	0,010
CYTOKINE-CYTOKINE RECEPTOR INTERACTION	1,880	0,000	0,012
APOPTOSIS	1,837	0,000	0,016
NATURAL KILLER CELL MEDIATED CYTOTOXICITY	1,802	0,000	0,022
HEMATOPOIETIC CELL LINEAGE	1,801	0,000	0,019
CELL CYCLE	1,794	0,000	0,018
ONE CARBON POOL BY FOLATE	1,777	0,004	0,019
DNA REPLICATION	1,765	0,005	0,020
TOLL-LIKE RECEPTOR SIGNALING PATHWAY	1,732	0,005	0,027
T CELL RECEPTOR SIGNALING PATHWAY	1,629	0,009	0,063
JAK-STAT SIGNALING PATHWAY	1,520	0,042	0,105
B CELL RECEPTOR SIGNALING PATHWAY	1,519	0,021	0,140
LEUKOCYTE TRANSENDOTHELIAL MIGRATION	1,506	0,014	0,145
NOTCH SIGNALING PATHWAY	1,505	0,030	0,135
PATHOGENIC ESCHERICHIA COLI INFECTION-EHEC	1,485	0,021	0,148
PYRIMIDINE METABOLISM	1,461	0,009	0,166
COMPLEMENT AND COAGULATION CASCADES	1,458	0,029	0,159

[*] NOM p-value is the significance of the normalized enrichment score (NES); [†]FDR q-val is the false discovery rate (FDR), the estimated probability that a gene set with a given NES represents a false positive finding; The GSEA analysis report highlights enriched gene sets with an FDR of less than 25%.

Supplementary annex Table 4B. GSEA analysis of MTC^{M918T} *vs* MTC^{WT}. Enriched pathways in M918T group.

BIOCARTA PATHWAY NAME	NES	NOM p-val[*]	FDR q-val[†]
CYTOKINEPATHWAY	2,153	0,000	0,000
COMPPATHWAY	2,139	0,000	0,001
DCPATHWAY	2,090	0,000	0,005
LAIRPATHWAY	2,020	0,000	0,008
INFLAMPATHWAY	1,998	0,000	0,007
NKTPATHWAY	1,990	0,000	0,006
ERYTHPATHWAY	1,931	0,002	0,014
STEMPATHWAY	1,797	0,004	0,053
NKCELLSPATHWAY	1,715	0,015	0,100
GCRPATHWAY	1,697	0,013	0,105
FMLPPATHWAY	1,651	0,008	0,132
RAC1PATHWAY	1,611	0,025	0,164
CXCR4PATHWAY	1,593	0,019	0,172
TH1TH2PATHWAY	1,590	0,024	0,164
IL1RPATHWAY	1,527	0,030	0,233
SPPAPATHWAY	1,517	0,037	0,233
KEGG PATHWAY NAME	**NES**	**NOM p-val[*]**	**FDR q-val[†]**
COMPLEMENT AND COAGULATION CASCADES	2,430	0,000	0,000
ASTHMA	2,160	0,000	0,001
TYPE I DIABETES MELLITUS	2,118	0,000	0,001

PROTEASOME	1,923	0,000	0,013
HEMATOPOIETIC CELL LINEAGE	1,772	0,000	0,045
PORPHYRIN AND CHLOROPHYLL METABOLISM	1,771	0,002	0,037
CYTOKINE-CYTOKINE RECEPTOR INTERACTION	1,732	0,000	0,047
PATHOGENIC ESCHERICHIA COLI INFECTION	1,728	0,000	0,042
PYRIMIDINE METABOLISM	1,698	0,000	0,047
P53 SIGNALING PATHWAY	1,680	0,002	0,049
ANDROGEN AND ESTROGEN METABOLISM	1,673	0,002	0,047
PENTOSE AND GLUCURONATE INTERCONVERSIONS	1,664	0,013	0,047
NICOTINATE AND NICOTINAMIDE METABOLISM	1,607	0,018	0,071
CELL CYCLE	1,603	0,004	0,068
MAPK SIGNALING PATHWAY	1,614	0,012	0,092
TOLL-LIKE RECEPTOR SIGNALING PATHWAY	1,550	0,004	0,098
APOPTOSIS	1,500	0,007	0,132
DNA REPLICATION	1,498	0,030	0,126
ARGININE AND PROLINE METABOLISM	1,493	0,039	0,124
CELL ADHESION MOLECULES (CAMS)	1,445	0,041	0,153
RENIN-ANGIOTENSIN SYSTEM	1,433	0,074	0,174
PARKINSON'S DISEASE	1,398	0,080	0,210
GAP JUNCTION	1,389	0,031	0,212
LONG-TERM DEPRESSION	1,360	0,031	0,244
CITRATE CYCLE (TCA CYCLE)	1,355	0,095	0,242

*NOM p-value is the significance of the normalized enrichment score (NES); †FDR q-val is the false discovery rate (FDR), the estimated probability that a gene set with a given NES represents a false positive finding. The GSEA analysis report highlights enriched gene sets with an FDR of less than 25%. Pathways are ranked by the FRD q-value.

Supplementary annex Table 5. FatiGo/Babelomics analysis of GO biological processes.

Nº	Term (GO)	M918T gene list	odds_ratio_log	pvalue	adj_pvalue
1	muscle organ development (GO:0007517)	*FAM65B,TNNI3,SPIB,MEOX2,EZH2,PAX7*	1,92	3,85E-04	2,88E-02
2	organ morphogenesis (GO:0009887)	*TNNI3,SPIB,CDH13,HOXC8,TNF,PDGFRA,CHST11, MEOX2,ONECUT2,RUNX2,PITX2,SHC1*	1,78	3,23E-06	1,50E-03
3	tissue development (GO:0009888)	*TNNI3,SPIB,IKZF1,TNF,CHST11,NRTN,MEOX2, ONECUT2,RUNX2,EZH2,PAX7*	1,67	2,08E-05	4,36E-03
4	negative regulation of cytokine production (GO:0001818)	*SPIB,TNF,CIDEA*	3,08	4,68E-04	3,26E-02
5	chondrocyte differentiation (GO:0002062)	*SPIB,CHST11,RUNX2*	3,04	5,24E-04	3,33E-02
6	myeloid leukocyte differentiation (GO:0002573)	*SPIB,IKZF1,TNF,RELB,IFI16*	3,01	8,59E-06	2,10E-03
7	DNA metabolic process (GO:0006259)	*SPIB,FANCI,PDGFRA,ESCO2,CIDEA,TYMS,SHC1,TERT*	1,55	5,13E-04	3,33E-02
8	DNA replication (GO:0006260)	*SPIB,PDGFRA,TYMS,SHC1,TERT*	1,95	1,01E-03	4,83E-02
9	protein amino acid phosphorylation (GO:0006468)	*SPIB,NEK2,GSG2,TNF,PIM2,TRIB2,ADRA2A,STK17B, PDGFRA,SHC1*	1,43	3,05E-04	2,70E-02
10	**anti-apoptosis (GO:0006916)**	***SPIB,CDH13,TNF,IL2RB,PIM2,PAX7,TERT***	**2,31**	**1,24E-05**	**2,79E-03**

11	induction of apoptosis (GO:0006917)	*SPIB,TNF,CASP4,STK17B,BID,CIDEA,IFI16*	2,15	3,18E-05	5,82E-03
12	cellular component movement (GO:0006928)	*SPIB,CDH13,TNF,ADRA2A,PDGFRA,NRTN,ONECUT2 ,MTSS1*	1,44	1,07E-03	4,94E-02
13	cytoskeleton organization (GO:0007010)	*SPIB,NEK2,CXCL1,ADRA2A,ARHGAP4,MTSS1,SHC1*	1,61	8,24E-04	4,26E-02
14	**cell cycle (GO:0007049)**	***SPIB,NEK2,GSG2,TNF,PIM2,FANCI,GAS2L1,ESCO2, HMGA2***	**1,34**	**1,04E-03**	**4,92E-02**
15	**cell adhesion (GO:0007155)**	***SPIB,SIRPG,CDH13,SDK1,TNF,ONECUT2,CLEC4M, MTSS1,SHC1,LOXL2***	**1,41**	**3,68E-04**	**2,83E-02**
16	leukocyte adhesion (GO:0007159)	*SPIB,TNF,CLEC4M*	3,14	3,93E-04	2,88E-02
17	enzyme linked receptor protein signaling pathway (GO:0007167)	*SPIB,CDH13,STAP1,PDGFRA,CHST11,CIDEA,NRTN ,ONECUT2,RUNX2,MTSS1,SHC1*	2,19	1,64E-07	1,60E-04
18	**transmembrane receptor protein tyrosine kinase signaling pathway (GO:0007169)**	***SPIB,CDH13,STAP1,PDGFRA,NRTN,RUNX2,MTSS1, SHC1***	**2,25**	**4,62E-06**	**1,50E-03**
19	**transforming growth factor beta receptor signaling pathway (GO:0007179)**	***SPIB,CHST11,CIDEA,ONECUT2***	**2,56**	**3,56E-04**	**2,83E-02**
20	**protein kinase cascade (GO:0007243)**	***SPIB,GSG2,TNF,ADRA2A,STK17B,NRTN,HMGA2,SHC 1***	**1,67**	**2,41E-04**	**2,28E-02**
21	**Rho protein signal transduction (GO:0007266)**	***SPIB,CDH13,ADRA2A,ARHGAP4***	**2,24**	**1,12E-03**	**4,95E-02**
22	pattern specification process (GO:0007389)	*SPIB,MFNG,RAX,HOXC8,MEOX2,PAX7,PITX2*	2,16	2,99E-05	5,82E-03
23	**aging (GO:0007568)**	***SPIB,SHC1,TERT,LOXL2***	**2,33**	**8,30E-04**	**4,26E-02**
24	positive regulation of cell proliferation (GO:0008284)	*SPIB,SIRPG,CDH13,TNF,ADRA2A,PDGFRA,RUNX2,SH C1*	1,91	5,07E-05	7,81E-03
25	negative regulation of cell proliferation (GO:0008285)	*SPIB,SIRPG,CDH13,CXCL1,TNF,RERG*	1,73	1,00E-03	4,83E-02
26	apoptotic mitochondrial changes (GO:0008637)	*SPIB,PIM2,BID*	3,21	3,26E-04	2,73E-02
27	negative regulation of metabolic process (GO:0009892)	*SPIB,IKZF1,HOXC8,TNF,IGF2BP2,CIDEA,RUNX2,HMG A2*	1,43	1,09E-03	4,94E-02
28	positive regulation of metabolic process (GO:0009893)	*SPIB,IKZF1,CDH13,TNF,IL2RB,PDGFRA,ONECUT2,RU NX2,SHC1*	1,38	7,97E-04	4,24E-02
29	regulation of signal transduction (GO:0009966)	*SPIB,CDH13,TNF,DKK4,TRIB2,ADRA2A,CHST11,CIDEA ,ONECUT2, RUNX2,HMGA2,SHC1*	1,68	8,33E-06	2,10E-03
30	negative regulation of signal transduction (GO:0009968)	*SPIB,DKK4,CHST11,CIDEA,ONECUT2,RUNX2,HMGA2*	2,42	6,16E-06	1,80E-03
31	positive regulation of cell death (GO:0010942)	*SPIB,TNF,CASP4,STK17B,BID,CIDEA,IFI16*	1,83	2,27E-04	2,28E-02
32	peptide transport (GO:0015833)	*SPIB,CPLX3,TNF,TAP1,CLEC4M*	2,67	4,07E-05	6,61E-03
33	**cell-cell adhesion (GO:0016337)**	***SPIB,SIRPG,CDH13,TNF,CLEC4M,SHC1***	**1,93**	**3,66E-04**	**2,83E-02**
34	regulation of cell-cell adhesion (GO:0022407)	*SPIB,SIRPG,TNF*	3,26	2,85E-04	2,61E-02
35	positive regulation of cell-cell adhesion (GO:0022409)	*SPIB,SIRPG,TNF*	3,75	7,30E-05	1,02E-02
36	cell projection assembly	*SPIB,CDH13,ONECUT2,MTSS1*	2,39	6,52E-04	3,74E-02

	(GO:0030031)				
37	myeloid cell differentiation (GO:0030099)	*SPIB,IKZF1,TNF,RELB,IFI16*	2,28	2,40E-04	2,28E-02
38	**regulation of cell adhesion (GO:0030155)**	***SPIB,SIRPG,CDH13,TNF,ONECUT2***	**2,45**	**1,08E-04**	**1,27E-02**
39	**positive regulation of cell migration (GO:0030335)**	***SPIB,CDH13,PDGFRA,ONECUT2***	**2,51**	**4,32E-04**	**3,08E-02**
40	cellular response to DNA damage stimulus (GO:0034984)	*SPIB,FANCI,ESCO2,CIDEA,IFI16,TYMS*	1,73	9,90E-04	4,83E-02
41	**regulation of growth (GO:0040008)**	***SPIB,IKZF1,CDH13,ESM1,HMGA2,RERG,SHC1***	**1,99**	**8,81E-05**	**1,17E-02**
42	**regulation of cell proliferation (GO:0042127)**	***SPIB,SIRPG,CDH13,CXCL1,TNF,ADRA2A,PDGFRA,CHST11,RUNX2,RERG,PTGER2,SHC1***	**1,76**	**3,91E-06**	**1,50E-03**
43	vitamin D biosynthetic process (GO:0042368)	*SPIB,TNF*	4,07	7,38E-04	4,06E-02
44	odontogenesis of dentine-containing tooth (GO:0042475)	*SPIB,PDGFRA,RUNX2*	2,83	9,42E-04	4,75E-02
45	regulation of apoptosis (GO:0042981)	*SPIB,CDH13,TNF,IL2RB,PIM2,CASP5,CASP4,STK17B,CHST11,BID,CIDEA,PAX7,IFI16,TERT*	1,94	8,91E-08	1,45E-04
46	positive regulation of apoptosis (GO:0043065)	*SPIB,TNF,CASP4,STK17B,BID,CIDEA,IFI16*	1,84	2,08E-04	2,25E-02
47	**negative regulation of apoptosis (GO:0043066)**	***SPIB,CDH13,TNF,IL2RB,PIM2,CHST11,CIDEA,PAX7,TERT***	**2,13**	**3,18E-06**	**1,50E-03**
48	regulation of programmed cell death (GO:0043067)	*SPIB,CDH13,TNF,IL2RB,PIM2,CASP5,CASP4,STK17B,CHST11,BID,CIDEA,PAX7,IFI16,TERT*	1,93	9,90E-08	1,45E-04
49	positive regulation of programmed cell death (GO:0043068)	*SPIB,TNF,CASP4,STK17B,BID,CIDEA,IFI16*	1,84	2,17E-04	2,27E-02
50	negative regulation of programmed cell death (GO:0043069)	*SPIB,CDH13,TNF,IL2RB,PIM2,CHST11,CIDEA,PAX7,TERT*	2,12	3,44E-06	1,50E-03
51	positive regulation of DNA replication (GO:0045740)	*SPIB,PDGFRA,SHC1*	3,06	4,96E-04	3,30E-02
52	positive regulation of cell adhesion (GO:0045785)	*SPIB,SIRPG,CDH13,TNF*	2,84	1,27E-04	1,43E-02
53	smooth muscle cell proliferation (GO:0048659)	*SPIB,CDH13,TNF,SHC1*	2,89	1,06E-04	1,27E-02
54	regulation of smooth muscle cell proliferation (GO:0048660)	*SPIB,CDH13,TNF,SHC1*	2,93	9,23E-05	1,17E-02
55	positive regulation of smooth muscle cell proliferation (GO:0048661)	*SPIB,CDH13,TNF,SHC1*	3,19	3,44E-05	5,92E-03
56	skeletal system morphogenesis (GO:0048705)	*SPIB,HOXC8,PDGFRA,CHST11,RUNX2*	2,58	5,97E-05	8,74E-03
57	cytokine secretion (GO:0050663)	*SPIB,TNF,CIDEA*	3,02	5,53E-04	3,37E-02
58	regulation of developmental process (GO:0050793)	*SPIB,IKZF1,CDC42SE1,CDH13,TNF,IL2RB,PIM2,CHST11,CIDEA,RUNX2,EZH2,PAX7,TERT*	1,67	4,49E-06	1,50E-03
59	cartilage development (GO:0051216)	*SPIB,CHST11,RUNX2,PAX7*	2,59	3,22E-04	2,73E-02
60	negative regulation of protein transport (GO:0051224)	*SPIB,TNF,CIDEA*	2,91	7,49E-04	4,06E-02

61	positive regulation of cellular component movement (GO:0051272)	*SPIB,CDH13,PDGFRA,ONECUT2*	2,44	5,50E-04	3,37E-02
62	centrosome separation (GO:0051299)	*SPIB,NEK2*	4,16	6,34E-04	3,71E-02
63	negative regulation of amino acid transport (GO:0051956)	*SPIB,TNF*	3,85	1,10E-03	4,94E-02
64	palate development (GO:0060021)	*SPIB,PDGFRA,MEOX2*	3,06	4,96E-04	3,30E-02
65	limb development (GO:0060173)	*SPIB,RAX,CHST11,MEOX2*	2,39	6,70E-04	3,77E-02
66	positive regulation of calcidiol 1- (GO:0060559)	SPIB,TNF	4,16	6,34E-04	3,71E-02

Supplementary annex Table 6. Biocarta pathways in M918T group compared to Agilent Whole Genome: Biocarta significant terms (pvalue<0.05) from FatiGo analysis.

Nº	Term (Biocarta Pathway)	M918T gene list	odds_ratio_log	pvalue	adj_pvalue
1	Angiotensin II mediated activation of JNK Pathway via Pyk2 dependent signaling(h_At1rPathway)	*SPIB,SHC1*	3,302	3,07E-03	2,57E-02
2	BCR Signaling Pathway (h_bcrPathway)	*SPIB,SHC1*	3,028	5,06E-03	3,28E-02
3	Bioactive Peptide Induced Signaling Pathway (h_biopeptidesPathway)	*SPIB,SHC1*	3,202	3,68E-03	2,57E-02
4	CBL mediated ligand-induced downregulation of EGF receptors (h_cblPathway)	*SPIB,PDGFRA*	4,168	6,78E-04	2,11E-02
5	Cadmium induces DNA synthesis and proliferation in macrophages (h_cdMacPathway)	*SPIB,TNF*	3,945	9,89E-04	2,11E-02
6	Apoptotic Signaling in Response to DNA Damage (h_chemicalPathway)	*SPIB,BID*	3,682	1,56E-03	2,12E-02
7	Cytokine Network (h_cytokinePathway)	*SPIB,TNF*	3,762	1,36E-03	2,12E-02
8	Induction of apoptosis through DR3 and DR4/5 Death Receptors (h_deathPathway)	*SPIB,BID*	3,156	4,01E-03	2,66E-02
9	Phospholipids as signalling intermediaries (h_edg1Pathway)	*SPIB,PDGFRA*	3,302	3,07E-03	2,57E-02
10	EGF Signaling Pathway (h_egfPathway)	*SPIB,SHC1*	3,414	2,52E-03	2,57E-02
11	EPO Signaling Pathway (h_epoPathway)	*SPIB,SHC1*	3,682	1,56E-03	2,12E-02
12	Role of Erk5 in Neuronal Survival (h_erk5Pathway)	*SPIB,SHC1*	3,849	1,17E-03	2,11E-02
13	Fc Epsilon Receptor I Signaling in Mast Cells (h_fcer1Pathway)	*SPIB,SHC1*	2,845	7,06E-03	4,17E-02
14	Growth Hormone Signaling Pathway (h_ghPathway)	*SPIB,SHC1*	3,202	3,68E-03	2,57E-02
15	Adhesion and Diapedesis of Granulocytes (h_granulocytesPathway)	*SPIB,TNF*	3,945	9,89E-04	2,11E-02
16	Calcium Signaling by HBx of Hepatitis B virus (h_HBxPathway)	*SPIB,SHC1*	5,149	1,53E-04	1,04E-02
17	Role of ERBB2 in Signal Transduction and Oncology (h_her2Pathway)	*SPIB,SHC1*	3,251	3,37E-03	2,57E-02
18	HIV-I Nef (h_HivnefPathway)	*SPIB,TNF,BID*	2,949	6,98E-04	2,11E-02
19	Stress Induction of HSP Regulation (h_hsp27Pathway)	*SPIB,TNF*	3,945	9,89E-04	2,11E-02
20	IGF-1 Signaling Pathway (h_igf1Pathway)	*SPIB,SHC1*	3,539	2,01E-03	2,38E-02
21	Multiple antiapoptotic pathways from IGF-1R signaling lead to BAD phosphorylation (h_igf1rPathway)	*SPIB,SHC1*	3,302	3,07E-03	2,57E-02
22	Signal transduction through IL1R (h_il1rPathway)	*SPIB,TNF*	3,202	3,68E-03	2,57E-02

23	IL 2 signaling pathway (h_il2Pathway)	*SPIB,IL2RB,SHC1*	4,025	3,87E-05	1,02E-02
24	Cytokines and Inflammatory Response (h_inflamPathway)	*SPIB,TNF*	3,302	3,07E-03	2,57E-02
25	Insulin Signaling Pathway (h_insulinPathway)	*SPIB,SHC1*	3,539	2,01E-03	2,38E-02
26	Integrin Signaling Pathway (h_integrinPathway)	*SPIB,SHC1*	3,156	4,01E-03	2,66E-02
27	Keratinocyte Differentiation (h_keratinocytePathway)	*SPIB,TNF*	2,879	6,63E-03	4,01E-02
28	NF-kB Signaling Pathway (h_nfkbPathway)	*SPIB,TNF*	3,682	1,56E-03	2,12E-02
29	Nerve growth factor pathway (NGF) (h_ngfPathway)	*SPIB,SHC1*	3,357	2,79E-03	2,57E-02
30	p38 MAPK Signaling Pathway (h_p38mapkPathway)	*SPIB,SHC1*	3,202	3,68E-03	2,57E-02
31	PDGF Signaling Pathway (h_pdgfPathway)	*SPIB,PDGFRA,SHC1*	3,773	7,48E-05	1,02E-02
32	Regulation of transcriptional activity by PML (h_pmlPathway)	*SPIB,TNF*	3,849	1,17E-03	2,11E-02
33	Links between Pyk2 and Map Kinases (h_pyk2Pathway)	*SPIB,SHC1*	3,302	3,07E-03	2,57E-02
34	Acetylation and Deacetylation of RelA in The Nucleus (h_RELAPathway)	*SPIB,TNF*	4,168	6,78E-04	2,11E-02
35	SODD/TNFR1 Signaling Pathway (h_soddPathway)	*SPIB,TNF*	4,301	5,43E-04	2,11E-02
36	Sprouty regulation of tyrosine kinase signals (h_spryPathway)	*SPIB,SHC1*	3,762	1,36E-03	2,12E-02
37	TNF/Stress Related Signaling (h_stressPathway)	*SPIB,TNF*	3,608	1,78E-03	2,30E-02
38	T Cell Receptor Signaling Pathway (h_tcrPathway)	*SPIB,SHC1*	2,879	6,63E-03	4,01E-02
39	Chaperones modulate interferon Signaling Pathway (h_tidPathway)	*SPIB,TNF*	4,301	5,43E-04	2,11E-02
40	TNFR1 Signaling Pathway (h_tnfr1Pathway)	*SPIB,TNF*	3,251	3,37E-03	2,57E-02
41	TPO Signaling Pathway (h_TPOPathway)	*SPIB,SHC1*	3,357	2,79E-03	2,57E-02
42	Trka Receptor Signaling Pathway (h_trkaPathway)	*SPIB,SHC1*	3,849	1,17E-03	2,11E-02
43	VEGF, Hypoxia, and Angiogenesis (h_vegfPathway)	*SPIB,SHC1*	3,202	3,68E-03	2,57E-02
44	Wnt/LRP6 Signalling (h_wnt-lrp6Pathway)	*SPIB,KREMEN2*	5,149	1,53E-04	1,04E-02
45	IL-2 Receptor Beta Chain in T cell Activation (h_il2rbPathway)	*IL2RB,SHC1*	2,879	6,63E-03	4,01E-02
46	Erk1/Erk2 Mapk Signaling pathway (h_erkPathway)	*PDGFRA,SHC1*	3,251	3,37E-03	2,57E-02

Supplementary annex Table 7. MAGIA analysis: Predicted mRNA-miRNA interactions from comparisons MTC^{634} *vs* MTC^{M918T} and MTC^{M918T} *vs* MTC^{WT}.

Enterez Gene	Gene name	miR	correlation	FDR (q value)
9480	ONECUT2	hsa-mir-125b	-0.900615	0.005203759
4306	NR3C2	hsa-mir-124	-0.885968	0.005383238
28951	TRIB2	hsa-mir-125b	-0.818175	0.017458032
169792	GLIS3	hsa-mir-302d	-0.796912	0.021492096
64398	MPP5	hsa-mir-1	-0.779456	0.022991975
9515	STXBP5L	hsa-mir-302e	-0.777011	0.022991975
744	MPPED2	hsa-mir-141	-0.774109	0.023004278
54885	TBC1D8B	hsa-mir-106b	-0.758083	0.030524416
5732	PTGER2	hsa-mir-421	-0.749074	0.034589338
8842	PROM1	hsa-mir-30a	-0.739228	0.03736597
744	MPPED2	hsa-mir-130a	-0.737102	0.03736597
9480	ONECUT2	hsa-mir-421	-0.737086	0.03736597
6652	SORD	hsa-mir-141	-0.724767	0.039988874
169792	GLIS3	hsa-mir-373	-0.719444	0.039988874
6652	SORD	hsa-mir-124	-0.718376	0.039988874
115111	SLC26A7	hsa-mir-33b	-0.717388	0.039988874
8091	HMGA2	hsa-mir-421	-0.697004	0.049128681
9515	STXBP5L	hsa-mir-373	-0.690512	0.052788223
5621	PRNP	hsa-mir-130b	-0.687524	0.053367903
169792	GLIS3	hsa-mir-302e	-0.682627	0.054631478
2066	ERBB4	hsa-mir-302e	-0.674599	0.057150195
9480	ONECUT2	hsa-mir-30a	-0.67303	0.057150195
7184	HSP90B1	hsa-mir-1	-0.669585	0.057150195
55790	CSGALNACT1	hsa-mir-106b	-0.668637	0.057150195
64398	MPP5	hsa-mir-302e	-0.66721	0.057150195
55906	ZC4H2	hsa-mir-143	-0.665929	0.057150195
169792	GLIS3	hsa-mir-211	-0.653154	0.065632625
3772	KCNJ15	hsa-mir-141	-0.6497	0.065632625
23767	FLRT3	hsa-mir-124	-0.644254	0.067284525
8671	SLC4A4	hsa-mir-503	-0.632385	0.074603249
7849	PAX8	hsa-mir-330-5p	-0.628353	0.07552454
169792	GLIS3	hsa-mir-204	-0.62614	0.07552454
83543	AIF1L	hsa-mir-124	-0.625643	0.07552454
55906	ZC4H2	hsa-mir-146a	-0.615194	0.082943549
64506	CPEB1	hsa-mir-124	-0.610239	0.08654631
169792	GLIS3	hsa-mir-106b	-0.606023	0.08884981
5621	PRNP	hsa-mir-130a	-0.605228	0.08884981
6444	SGCD	hsa-mir-33b	-0.602476	0.090286984
6444	SGCD	hsa-mir-124	-0.595484	0.096298872
4306	NR3C2	hsa-mir-204	-0.587725	0.099859503

28951	TRIB2	hsa-mir-542-3p	-0.585097	0.099910539
9515	STXBP5L	hsa-mir-363	-0.583478	0.099910539
83543	AIF1L	hsa-mir-1	-0.582013	0.099910539
650	BMP2	hsa-mir-106b	-0.572396	0.107280427
25840	METTL7A	hsa-mir-204	-0.571048	0.107369429
3131	HLF	hsa-mir-130b	-0.561305	0.115736873
6444	SGCD	hsa-mir-211	-0.533626	0.144119051
167410	LIX1	hsa-mir-124	-0.529892	0.145747581
2066	ERBB4	hsa-mir-130b	-0.5289	0.145747581
5971	RELB	hsa-mir-7	-0.527095	0.146482325
846	CASR	hsa-mir-503	-0.515015	0.15941972
64398	MPP5	hsa-mir-373	-0.514058	0.15941972
64506	CPEB1	hsa-mir-130a	-0.505009	0.166834939
9480	ONECUT2	hsa-mir-542-3p	-0.503921	0.166834939
64506	CPEB1	hsa-mir-363	-0.499269	0.171853335
25840	METTL7A	hsa-mir-211	-0.496498	0.173093396
57282	SLC4A10	hsa-mir-363	-0.492046	0.173093396
64398	MPP5	hsa-mir-302d	-0.483665	0.176682702
6444	SGCD	hsa-mir-15b	-0.482773	0.176682702
3131	HLF	hsa-mir-133a	-0.480058	0.17896112
64506	CPEB1	hsa-mir-1	-0.464598	0.197060889
8671	SLC4A4	hsa-mir-15b	-0.463235	0.197362073
9515	STXBP5L	hsa-mir-130a	-0.461183	0.198744182
63876	PKNOX2	hsa-mir-30b	-0.453458	0.206429496
4306	NR3C2	hsa-mir-211	-0.451365	0.206429496
9480	ONECUT2	hsa-mir-424	-0.451271	0.206429496
744	MPPED2	hsa-mir-130b	-0.450511	0.206429496
1012	CDH13	hsa-mir-30a	-0.4434	0.212275458
2066	ERBB4	hsa-mir-146a	-0.438634	0.218085345
1534	CYB561	hsa-mir-30b	-0.435728	0.220948217
8091	HMGA2	hsa-mir-424	-0.434243	0.22151914
22891	ZNF365	hsa-mir-130b	-0.432074	0.223204951
8671	SLC4A4	hsa-mir-211	-0.427753	0.228418439
8671	SLC4A4	hsa-mir-106b	-0.4214	0.237089903
64506	CPEB1	hsa-mir-130b	-0.416151	0.242104302

Appendix II

Publications derived from the thesis

Manuscript submitted for publication

Title: Differential gene expression of Medullary Thyroid Carcinoma reveals specific markers associated with genetic conditions.

Authors: Agnieszka Maliszewska, MSc.[1], Luis Javier Leandro-Garcia, MSc.[1], Esmeralda Castelblanco, MSc.[2], Gonzalo Goméz-López, PhD[3], Lucía Inglada-Pérez, MSc.[1,4], Cristina Álvarez-Escolá, MD, PhD[5], Anna Macià, MSc.[6], Leticia De la Vega, B.S.[1], Rocío Letón, B.S.[1], Álvaro Gómez-Graña, B.S. [1], Iñigo Landa, PhD[1], Aguirre de Cubas, MSc.[1], Alberto Cascón, PhD[1,5], Cristina Rodríguez-Antona, PhD[1,5], Salud Borrego, MD, PhD[7,4], Mariangela Zane, PhD[8], Francesca Schiavi, PhD[9], Isabella Merante-Boschin, MD, PhD[8], Mario Encinas, PhD[6], Maria Rosa Pelizzo, MD[8], David G. Pisano, PhD[3], Giuseppe Opocher, MD, PhD[8,9], Xavier Matias-Guiu MD, PhD [2], and Mercedes Robledo, PhD[1,4]*.

Affiliations: [1]Hereditary Endocrine Cancer Group , CNIO, Madrid; [2]Department of Pathology and Molecular Genetics, Hospital Universitari Arnau de Vilanova, University of Lleida, IRBLLEIDA, Lleida, Spain; [3]Bioinformatics Unit, Structural Biology Programme, CNIO, Madrid; [4]Centro de Investigación Biomédica en Red de Enfermedades Raras (CIBERER), Spain; [5]Endocrinology Service, Hospital Universitario La Paz, Madrid, Spain; [6]Neuronal Signaling Unit, Universitat de Lleida/Institut de Recerca Biomèdica de Lleida, Lleida, Spain; [7]Unidad de Gestión Clínica de Genética, Reproducción y Medicina Fetal, Instituto de Biomedicina de Sevilla (IBIS), Hospital Universitario Virgen del Rocío/CSIC/Universidad de Sevilla, Sevilla, Spain; [8]Department of Medical and Surgical Sciences, University of Padova, Padova, Italy; [9]Familial Cancer Clinic and Endocrine Oncology, Veneto Institute of Oncology, Padova, Italy.

Short running head: MTC biomarkers identified by genomics.

Fundings: This work was supported in part by the Fundación Mutua Madrileña (project AP2775/2008 to MR), the Fondo de Investigaciones Sanitarias (project PI080883 to MR), the Spanish Ministry of Science and Innovation MICINN (BFU2010-17628 to ME), and by grants 2009SGR794, RD06/0020/1034 and the programa de intensificación de la investigación, Instituto Carlos III. Agnieszka Maliszewska and Aguirre de Cubas are predoctoral fellows of the "la Caixa"/CNIO international PhD program. Lucía Inglada-Pérez is predoctoral fellow of the CIBERER. Luis Javier Leandro-Garcia is a predoctoral fellow of the Fondo de Investigaciones Sanitarias. Esmeralda Castelblanco holds a predoctoral fellowship from Fundació Alicaia Cuello de Merigó, and AGAUR 2010FI-B01057.

Corresponding Autor: Mercedes Robledo. Hereditary Endocrine Cancer Group, Human Cancer Genetics Programme. Centro Nacional de Investigaciones Oncológicas, Melchor Fernández Almagro 3, 28029 Madrid, Spain

Phone: +34-91-732 8000 Ext 3320; Fax: +34-91-224 69 23

e-mail: mrobledo@cnio.es

Abstract

Medullary thyroid carcinoma accounts for 2-5% of thyroid malignancies. Around 75% of them are sporadic, and the remaining 25% are hereditary and related to Multiple Endocrine Neoplasia type 2 syndrome. Although it is well established a genotype-phenotype correlation related to specific germline *RET* mutations, the knowledge of pathways specifically associated with each mutation, as well as to non-*RET* mutated sporadic MTC still remain largely unknown. Gene expression patterns have provided a tool to identify molecular events related to specific tumor types and to different clinical features that could help to identify novel targets for therapy. Using an outstanding series of 68 frozen MTC

classified accordingly to *RET* mutation, we identified *PROM1*, *LOXL2*, *GFRA1*, *DKK4* as related to RET^{M918T}, while *GAL* was associated with RET^{634} mutation respectively. According to pathway enrichment analysis and GO biological processes, genes associated with MTC^{M918T} group were mainly involved in proliferative, cell adhesion and general malignant metastatic effects and Wnt, Notch, NFκB, JAK/Stat and MAPkinase signaling pathways. Assays based on silencing PROM1 by siRNAs performed in MZ-CRC-1 cell line, harboring RET^{M918T}, caused an increase in apoptotic nuclei, suggesting that PROM1 is necessary for the survival of these cells. To our knowledge this is the first time that PROM1 overexpression is reported among primary tumors. This finding could lead to the identification of novel therapeutic targets.

Introduction

Medullary Thyroid Carcinoma (MTC) is a rare malignancy derived from calcitonin-producing parafollicular thyroid cells or thyroid C-cells; it constitutes 5% to 10% of all thyroid neoplasias (Ball 2000). Approximately 25% of all MTCs are hereditary as part of multiple endocrine neoplasia type 2 (MEN2; MIM#17140014), a rare cancer syndrome (1:30,000) that follows an autosomal dominant inheritance pattern and shows a variable clinical expression.

MEN2 is subdivided into MEN2A, MEN2B and FMTC (familial medullary thyroid carcinoma), according to the clinical features exhibited by the patients. Specific activating point mutations in the *RET* proto-oncogene are responsible for the three forms of MEN2. *RET* encodes a tyrosine kinase receptor (RTK) implicated in neural crest tissue development and differentiation (Pachnis 1993), that activates a variety of signaling pathways. Ret signaling mainly takes place through autophosphorylation of Ret tyrosine residues which, once phosphorylated, trigger the recruitment of several intercellular adapters, leading to the activation of several cascades.

MEN2A patients commonly carry *RET* mutations in codon 634 encoding cysteine (Eng 1996) , and less frequently in the cysteine-encoding codons 609, 611, 618, 620, and 630 (Mulligan 1994; Mulligan, et al. 1993a). Patients with a mutated codon 634 have a high risk of lymph node metastasis and a more than 40% increased risk of developing the disease by age 20 (Machens et al. 2003). FMTC cases mainly carry *RET* mutations affecting highly conserved cysteine regions, such as codons 609, 611, 618 and 620, as well as other infrequent mutations in residues of the intracellular domain in e.g. exons 13 (Dabir, et al. 2006) and 15 (Hofstra 1997). *RET* mutation M918T in exon 16 correlates with an aggressive disease(Drosten and Putzer 2006; Kodama 2005; Marx 2005), and is found as a germline mutation in the majority of MEN2B patients (94%) and as a somatic mutation in 30-50% of sporadic MTC cases (Marx 2005). This mutation lead to constitutive activation of RET and transforming potential in a lignad independent manner (Arighi, et al. 2005b).

MTC progresses slowly and metastasizes to cervical and mediastinal nodal groups in up to 50% of cases. It also metastasizes to distant organs such as lungs, liver and bones in 20% of patients. Total

thyroidectomy remains the only effective treatment, but once metastatic disease has spread there is no effective therapy available (Weber 2006).

Although there is a well-established genotype-phenotype correlation for MEN2 patients, the mechanisms by which *RET*-mutations cause tumors, the development of sporadic MTC in the absence of *RET* mutations, and the specific oncogenic pathways involved require further study. Our main aim was to identify signaling pathways specifically related to familial and sporadic MTC using transcriptional profiling to gain new information about specific markers that could be used as potential therapeutic targets.

Material and Methods

Human MTC Tissue samples and cell lines

Sixty-eight tumors from unrelated patients diagnosed with MTC were collected at the time of surgery from Spanish hospitals through the Spanish National Tumor Bank Network and from the Surgical Pathology Department of Medical and Surgical Sciences, Padova, Italy. Tissue samples were embedded in Tissue-Tek® OCT compound (Sakura, Torrance, CA, USA), frozen in liquid nitrogen, and stored at -80ºC until they were used for RNA extraction and hybridization onto arrays, or for *RET* mutational screening (in case previous genetic information on the patient was absent). All tissues were evaluated by pathologists by hematoxylin and eosin staining; only samples with a high percentage (> 80%) of tumor cells were included in the study.

After obtaining consent of each patient, clinical information was collected by questionnaire. The genetic and general characteristics of the cases are detailed in Supplementary Table 1.

Two Tissue Microarrays (TMAs) were available for further analysis. The first TMA (TMA-1) contained 54 independent molecularly characterized formalin-fixed, paraffin-embedded (FFPE) MTC tissues; of these, 12 carried a germline *RET* mutation in codon 634, 9 had a somatic M918T mutation, and 22 were classified as WT if no mutations were found. This TMA also contained 4 other thyroid cancer types and 2 normal tissues used as controls, as well as normal thyroid tissue of

13 MTC cases included in the TMA (Supplementary Table 2A). TMA-2 (Supplementary Table 2B) was constructed with cores from the corresponding paraffin-embedded material from 13 frozen samples used for profiling purposes as well as 2 MTCs which were not hybridized and 2 thyroid cancer of different subtype and 12 normal thyroid tissues from the corresponding MTCs. This TMA contained MTCs from patients carrying a germline *RET* mutation in codon 634 and somatic *RET* mutations affecting codon 918, as well as MTCs from patients classified as WT.

Twenty-three additional independent FFPE MTCs were available to validate expression profiling through RT-qPCR (Supplementary Table 3).

MZ-CRC-1 cells are derived from a metastatic MTC and harbor the M918T *RET* mutation (Cooley 1995; Santoro et al. 1995).

Molecular characterization of tumors

Screening of *RET* was performed by direct sequencing of exons 10, 11, and 13-16 in DNA extracted from peripherial blood samples (when available), and if negative, from tumor specimens. Genomic tumor DNA was obtained following the manufacturer's instructions using the DNeasy kit (Qiagen Inc., Valencia, CA, USA).

RNA isolation

Total RNA from 68 frozen MTC tissues was obtained following the manufacturer's instructions using the TriReagent kit (MRC, Cincinnati, OH, USA). RNA purity and integrity was assessed using an Agilent 2100 Bioanalyzer (Agilent Technologies, Palo Alto, CA, USA). RNA of nineteen cases was degraded (RNA Integrity Number below 7) and discarded for hybridization assays, but considered in the RT-qPCR validation step. Total RNA from 23 independent FFPE MTCs was isolated following the manufacturer's instructions using the RNeasy FFPE kit (Qiagen, Valencia, CA, USA). Concentration was determined using a Nanodrop ND-1000 spectrophotometer. These FFPE tumors were used for validation by RT-qPCR. After this first quality filter, 49 MTCs were used for hybridization assays, and 42 (19 frozen and 23 FFPE) samples for validation purposes.

Total RNA from MZ-CRC-1 cells was extracted using the RNAeasy kit (QIAGEN, Alameda, CA).

cDNA synthesis, labeling, hybridization, and detection

For each of the 49 MTC tumors used for profiling, 500 ng of total RNA was amplified according to the manufacturer's instructions by double strand cDNA synthesis, followed by T7-based in vitro transcription. Universal Human Reference RNA (Stratagene, La Jolla, CA, USA) was used as a control for all samples. Amplified complementary RNA (cRNA) was labeled with cyanine 5 (Cy5)-conjugated dUTP, whereas cRNA from Universal Human Reference RNA was labeled with cyanine 3 (Cy3)-conjugated dUTP. The Agilent Whole Human Genome Array (4x44K) was used for competitive hybridization and the slides were washed, dried, and scanned in an Agilent microarray scanner (Agilent Technologies, Palo Alto, CA, USA).

Normalization and preprocessing

Two-channel arrays were hybridized and quantified using Feature Extraction v9.5 software. Microarray background substraction was done using the *normexp* method (Ritchie 2007). The data set was normalized using *loess* within-array normalization and quantile between-array normalization. Differentially expressed genes were identified by applying linear models using the Bioconductor limma R package (Smyth 2005) (http://www.bioconductor.org). Normalized data were preprocessed using GEPAS server (Montaner 2006). Inconsistent replicates (SD>1) were discarded, and consistent replicates were averaged. Finally, genes that exhibited flat patterns (SD$\geq$0.8) across the set of samples were filtered and omitted in further comparisons.

Unsupervised and supervised analysis

Tumor samples were grouped according to their expression profiles by means of unsupervised clustering using GeneCluster 2.0 (Reich 2004). Unsupervised clustering was implemented by a SOM algorithm. Only tumors exhibiting the 634 or the M918T mutation, and tumors classified as WT were used in further analysis.

Gene expression profiling and gene ontology analysis

T-test was carried out using POMELOII (Morrissey 2009), and T-Rex from the GEPAS package was used for differential expression analysis (Montaner 2006). To account for multiple hypothesis

testing, the estimated significance level (*p*-value) was adjusted using Benjamini's False Discovery Rate (FDR) correction (Benjamini et al. 2001). Genes with an FDR<0.05 and with a fold-change > 2 were selected for the validation step.

Functional enrichment of gene ontologies (GOs) for differentially expressed genes (DEGs) was performed using the FatiGO tool (Al-Shahrour et al. 2004) implemented in Babelomics software. Fisher's exact test was performed to obtain significant over-representation of GO terms in the DEGs list *versus* the rest of the genome. GO terms showing an FDR<0.05 were considered significant.

Gene Set Enrichment Analysis (GSEA) (Subramanian 2005) using Biocarta and KEGG annotations was applied. Gene expression values were ranked based on the t statistic. Gene sets showing an FDR<0.25 were considered enriched between classes under comparison.

Validation by quantitative RT-qPCR

For validation of microarray data, five genes significantly differentially expressed among profiling results were selected to be assesed by RT qPCR. Thirty-two MTCs out of 49 previously hybridized samples, and 42 available MTCs from an independent series (19 frozen MTC tissues not used in profiling and 23 FFPE tumors), were used for validation. As endogenous references we tested β-glucoronidase (*GUS)*, 60S acidic ribosomal protein P0 (*RPLP0*) and peptidylprolyl isomerase A (*PPIA*); *GUS* was used to normalize the quantification of mRNA expression.

Reverse transcription was performed using 1 μg total RNA and random hexamers (FFPE samples), or 0.5 μg total RNA and oligodT (frozen specimens), and M-MLV Reverse Transcriptase (Promega Corporation, Madison, WI, USA).

PCRs were done on an ABI Prism 7900 sequence detection system (Applied Biosystems, Foster City, CA, USA) using the Universal Probe Library set (https://www.roche-applied-science.com) as described by the manufacturer. PCR reactions were performed in triplicates. The Kruskal-Wallis test (nonparametric ANOVA) for multiple class comparisons and the nonparametric Mann-Whitney test for two class comparisons were used to compare the genetic classes.

For MZ-CRC-1 cells, total RNA was reverse transcribed using the TaqMan® Reverse Transcription kit from Applied Biosystems (Foster City, CA). The relative mRNA level of PROM1 was measured by RT-qPCR using TaqMan® probes from Applied Biosystems (Hs01009250_m1; PROM1). Probe Hs99999905_m1 (GAPDH) was used for data normalization. Quantification data were calculated by the $2^{-\Delta\Delta CT}$ method.

Cell culture and nucleofection

MZ-CRC-1 cells were maintained in DMEM supplemented with 10% heat-inactivated fetal bovine serum, 1% pyruvate, 1% non-essential amino acids, 100U/ml penicillin and streptomycin at 37ºC in 5% CO_2 in air. For nucleofection, $2x10^6$ cells per condition were incubated with 2μM synthetic siRNAs (Sigma) directed against human PROM1 in a solution containing 100mM phosphate buffer, 100mM KCl and 10mM $MgCl_2$. Cells were nucleofected using the A30 program of an Amaxa Nucleofector II device (Lonza). Immediately after nucleofection, cells were resuspended in medium and seeded onto 6-well plates.

Apoptosis assay

Three days after transfection, the number of apoptotic nuclei was analyzed. Cell-permeant Hoechst dye 33342 was directly added to cells at a final concentration of 0.5mg/ml and incubation was continued for 15 minutes at 37ºC. Cells were then photographed under a fluorescence microscope (Olympus IX70). The percentage of apoptotic nuclei was scored in triplicate. Five hundred to one thousand cells per condition were counted.

Immunohistochemistry

Immunohistochemical staining was performed on both MTC tissue microarrays available. TMA blocks were sectioned at a thickness of 3 μm and dried for 1 h at 60ºC. Deparaffinization, rehydration and epitope retrieval were achieved by heat treatment in a PT Link (Dako, Glostrup, Denmark) at pH 9. Before staining the sections, endogenous peroxidase was blocked. Primary antibodies used were anti-PROM1 (1:500, ab19898 Abcam, Cambridge, MA, USA) and anti-GFRA1 (1:500, C-20, Santa Cruz Biotechnology, Santa Cruz, CA, USA); incubations with primary

antibodies were according to the manufacturers' instructions. After incubation with anti-PROM1, the reaction was visualized with EnVision™ FLEX (Dako, Glostrup, Denmark) using diaminobenzidine chromogen as a substrate; anti-GFRA1 binding was visualized with the LSAB+ Kit (Dako, Glostrup, Denmark) using diaminobenzidine chromogen as a substrate. Sections were counterstained with hematoxylin. Appropriate positive and negative controls were also tested.

Immunoexpression was graded semi-quantitatively by considering the percentage and intensity of the staining. A histological score was obtained for each sample, which ranged from 0 (no immunoreaction) to 300 (maximum immunoreactivity). Interpretation was done as previously described (Gallel 2008). Since each TMA included two cores from each case, immunohistochemical evaluation was done after examining all samples.

Statistical analysis

Immunoexpression was analyzed in two different ways, as a continuous variable, and as a binary variable using the median as the cut-off. For the first analysis , Mann-Whitney U test was used, and for the second one, difference in expression was tested with a Chi-squared or Fisher's exact test when appropriated. Statistical analyses were carried out using SPSS software package version 17.0 (SPSS, Inc., Chicago, IL). Nominal two-sided P-values less than 0.05 were considered statistically significant.

Results

Molecular genetic characteristics of the MTC tumors

Tumors were classified according to their specific *RET* mutation. Among the 49 tumors available for profiling, 7 carried a germline *RET* mutation in codon 634, 14 carried the M918T *RET* mutation (1 germline and 13 somatic mutations), and 20 were classified as WT. The remaining eight MTCs had 6 different germline mutations and 2 different somatic mutations in *RET* (Supplementary Table 1). These last 8 tumors were not considered in clustering analysis.

Data reveal differential expression profiles in inherited and sporadic MTC

Unsupervised hierarchical clustering, performed using standard correlation as a measure of similarity across all hybridized samples, showed a relatively low heterogeneity distributed over two principal branches (Figure 1). An enrichment of familial MTC cases with various germline *RET* mutations was observed in the second branch of the cluster, whereas the first branch was enriched for sporadic MTC with somatic M918T *RET* mutations and WT cases. This observation led to us to do a supervised analysis based on the known mutations of each available tumor. Differential expression analysis was performed comparing $MTCs^{M918T}$ *vs* $MTCs^{WT}$, and $MTCs^{M918T}$ *vs* $MTCs^{634}$ (Figures 2A and 2B), obtaining a list of 360, and 18 significant genes (GEO accession number GSE32662) respectively.

Based on threshold-free methodology using GSEA, signaling pathways were identified as significantly differently expressed (FDR<25%) when comparing $MTCs^{M918T}$ *vs* $MTCs^{634}$ and $MTCs^{M918T}$ *vs* $MTCs^{WT}$ (Supplementary Tables 4A and 4B, respectively). The M918T cluster was correlated with several pathways related to malignant tumor behavior, such as the p53, caspase, cytokine, Wnt, NFκB, MAPK, IL1R, JAK/Stat, and Notch pathways.

Analyses of Gene Ontologies (GO) revealed significant biological processes in the M918T group associated as well with malignant behavior (shown in bold in Supplementary Table 5). Hierarchical clustering analysis of the most relevant FatiGO outputs for biological processes pointed to the importance of cell adhesion, migration and proliferation ontologies (data not shown).

FatiGO analysis (Supplementary Table 6) and GSEA analysis (Supplementary Tables 4A and 4B) revealed similar significant pathways associated with the M918T group.

Biomarkers of specific genetic condition.

After applying the filtering criteria, five genes (*PROM1*, *GFRA1*, *LOXL2*, *GAL*, and *DKK4)* appeared to be biomarkers of different genetic conditions and were selected for further validation at the mRNA level.

GAL was the only gene statistically significant found to be a specific marker for the germline *RET* mutation in codon 634. The expression of the other four genes was validated by quantitative RT-PCR as up-regulated markers among MTCs^{M918T}. Due to limited availability of RNA, it was only possible to validate *PROM1* and *LOXL2* in FFPE MTC samples. Supplementary Figures 1A and 1B summarize these results in the independent frozen and FFPE series, respectively.

Although not selected for further validation, other genes differentially expressed among the three different genetic conditions considered here have been reported to be involved in cancer of tissues derived from the same neural crest origin as MTC, and also in the RTK signaling pathway. Therefore, these previous findings were considered as a cross-validation of our results. Among these markers, the up-regulated genes associated with the M918T group were *ESM1*, *NPR1*, *PITX2*, *RTN1*, and *SHC1*. *ESM1* (endothelial cell-specific molecule 1) is associated with cell migration and proliferation, and its over-expression has been previously described in sporadic *RET*^{M918T} MTC cases (Ameur et al. 2009). *NPR1 (*natriuretic peptide receptor A/guanylate cyclase A) regulates the activation of ERK1/2 (Deng 2010), as well as Ras/Raf/ERK and Wnt/β-cathenin pathways. *PITX2* (paired-like homeodomain 2) is involved in tumorigenesis and Wnt/β-cathenin signaling, and is expressed in neural crest cells (Zacharias 2010). *RTN1* (reticulon 1), overexpression of which leads to apoptosis of neuroblastoma cell lines, is involved in secretion or membrane trafficking in neuroendocrine cells as well as in tumorigenesis, and is expressed in neurons and neuroendocrine cells (Steiner 2004). Fibroblasts transformed by *RET*^{C634R} display constitutive RET-mediated phosphorylation of SHC which activates the RAS/MAPK signaling pathway (Ohiwa et al. 1997).

Immunohistochemistry

We performed immunohistochemistry for GFRA1 and PROM1. Results were evaluated following uniform pre-established criteria.

Differences at the mRNA level were not observed at the protein level. GFRA1 protein levels were not significantly different among the groups. PROM1 showed higher staining in $MTCs^{M918T}$ than in $MTCs^{634}$ (P=0.059), in agreement with mRNA detection.

Silencing PROM1 by siRNA induces apoptosis

We used the MZ-CRC-1 cell line nucleofected with two different synthetic siRNAs against human PROM1 for *in vitro* validation. Knockdown efficiency was assessed in parallel dishes by RT-qPCR, and the number of apoptotic nuclei was scored as percentage of total nuclei. As shown in Figure 3 both siRNAs caused an increase in the number of apoptotic nuclei, suggesting that PROM1 is necessary for the survival of these cells.

Discussion

MTC patients show relatively low survival if their carcinomas metastasize (Schlumberger 2008). Surgery is the primary treatment for MTC and there is a lack of alternatives for tumors with poor response to either conventional chemotherapy or radiotherapy (Schlumberger 2008). Thus, there is a pressing need to identify potential therapeutic targets. Although a genotype-phenotype correlation has been established for MEN2 cases and it is known that clinical behavior differs according to specific germline and somatic *RET* mutations, the signaling pathways involved in the clinical behavior are largely unknown. Therefore, it is important to identify pathways related to non-*RET*-dependent sporadic MTC and to the most frequent pathogenic *RET* mutations, in order to reveal prognostic markers. Although this need is well recognized, there are several difficulties which have contributed to the lack of studies on MTC tumors. Firstly, comparisons of primary tumors *versus* normal C-cells are not possible due to the very low parafollicular cell representation (about 1%) in the thyroid cell mass(Khurana et al. 2004b). Besides these difficulties, it is a challenge to obtain a sufficiently large series of frozen MTC tissues for genomic study due to the rarity of MTC. This

explains why only few studies on MTC profiling were reported(Ameur et al. 2009; Jain et al. 2004b; Lacroix et al. 2005; Musholt et al. 2005a; Watanabe et al. 2002a). Our study, based on one of the largest series of primary MTCs described so far, was focussed on finding differences among expression profiles according to the genetic condition of the MTC samples.

Biomarkers and pathways specific to each genetic class

In agreement with our finding in MTCs^{634}, *GAL* over-expression was previously observed in PC12 rat pheocromocytoma cell lines (Tofighi et al. 2008). *GAL* is involved in neuropeptide signaling, tumorigenesis, nervous system development and the regulation of cell proliferation; it is expressed in neuroblastoma and pheochromocytoma cancer cell lines, and it activates MAPK and ERK signaling (Berger et al. 2005; Hawes 2006; Sugimoto et al. 2009; Tofighi et al. 2008). The findings of the present study suggest that *GAL* over-expression may be involved in the development of the phenotype exhibited by MEN2A patients carrying a 634 germline *RET* mutation, who develop pheochromocytoma in at least 50% of cases (Eng 1996; Machens et al. 2005).

GFRA1 (GDNF family receptor alpha 1), associated with MTCs^{M918T}, is a known co-receptor of RET which mediates its activation through the binding of RET ligands. These include ligands that are widely expressed and promote the survival of neurons during development. *GFRA1* has been previously reported as a genetic risk factor associated with susceptibility to developing sporadic MTC in a case-control study (Gimm 2001), and our results support its role in MTC development.

DKK4 (Dickkopf-4), another gene overexpressed in MTCs^{M918T}, was demonstrated to be significantly upregulated in colorectal cancer, and this upregulation reflected activation of the Wnt canonical pathway (Matsui 2009). Furthermore, *KREMEN2* (kringle containing transmembrane protein 2) co-operates with *DKK4* to regulate Wnt signaling (Mao and Niehrs 2003). *KREMEN2* was upregulated similar to *DKK4* in M918T tumors included in our study. Deregulation of the Wnt pathway results in the development of cancer and other diseases, and Wnt/β-catenin signaling and JNK noncanonical pathways are implicated in RET signaling, which is activated in MTC.

Deregulation of the Wnt pathway specifically associated with *RET*^{M918T} MTC could open new perspectives for treatment.

The most interesting results among the M918T group were the over-expression of *LOXL2* (GEO accession number GSE32662) and *PROM1*. *LOXL2* (lysyl oxidase-like 2) activates Snail/E-cadherin and Src kinase/Focal adhesion kinase (Src/FAK) pathways, and is associated with tumor cell invasion. *LOXL2* is linked to epithelial-mesenchymal transition (EMT), which leads to metastasis and lower survival rates in epithelial and neuroendocrine tumors (Peinado 2005, 2008; Peng et al. 2009; Ruckert et al. 2010). Increased expression of genes associated with EMT has been previously observed in MEN2B MTCs (Jain et al. 2004b).

PROM1 was the gene most significantly over-expressed among the MTCs^{M918T} included in our series of primary tumors. *PROM1* was recently reported by Zhu *et al.* (Zhu 2010) to be a cancer stem cell marker in MZ-CRC-1 cell lines harboring a M918T *RET* mutation. Since MTCs bearing the M918T *RET* mutation are resistant to treatment, a high *PROM1* expression might be related to resistance to therapy. In this regard, high expression of *PROM1* is associated with neural crest-derived stem cells, and slowly differentiating cancer stem cells have been proven to be resistant to irradiation and cytotoxic drugs (Zhu 2010). To our knowledge, ours is the first study based on primary tumors pointing to a *PROM1* over-expression associated with the M918T mutation. Another study recently showed an association of poor prognosis with a high expression of *PROM1* in medulloblastoma tumors, suggesting that it might be a potential prognostic marker (Raso et al. 2011).

Immunohistochemical assessment of GFRA1 and PROM1 in the 71 FFPE MTCs revealed a tendency towards association of the M918T group with PROM1 over-expression. Furthermore, after silencing *PROM1* with two different siRNAs, we observed decreased levels of *PROM1* mRNA which led to an increased number of apoptotic nuclei. This significant correlation between silencing of *PROM1* and apoptosis, together with our profiling data led us to conclude that *PROM1* is a specific biomarker for the M918T *RET* mutation, and its targeting seems feasible and might lead to

apoptotic cell death. In this regards, GO biological function analyses using FatiGO/Babelomics revealed that important processes such as anti-apoptotic functions, proliferation, migration, cell cycle and adhesion were highly associated with the M918T group. Pathway enrichment analysis of the M918T group using GSEA software pointed to signaling cascades mainly involved in tumor invasion and metastasis (NFκB, interleukin, cytokine, p38MAPK, Wnt, JAK/Stat, Notch, MAPK or cell adhesion), which agrees with what would be expected on the grounds of the clinical behaviour of M918T-related MTCs. Among these pathways, the Notch pathway is known to play an important role in the normal development of neuroendocrine cells, including the calcitonin producing C-cells of the thyroid (Cook 2010).

In summary, we identified specific biomarkers related to different genetic conditions by means of expression analysis. The over-expression of *LOXL2* and *DKK4*, involved in cell adhesion pathway and the EMT process, or the Wnt pathway respectively, as well the fact of a decrease in *PROM1* expression was associated with an increased number of apoptotic nuclei, open new therapeutic possibilities to improve MTC management.

Conflict of Interest

The authors have no conflict of interest to declare.

Acknowledgments

This work was supported in part by the Fundación Mutua Madrileña (project AP2775/2008 to MR), the Fondo de Investigaciones Sanitarias (project PI080883 to MR), the Spanish Ministry of Science and Innovation MICINN (BFU2010-17628 to ME), and by grants 2009SGR794, RD06/0020/1034 and the programa de intensificación de la investigación, Instituto Carlos III. Agnieszka Maliszewska and Aguirre de Cubas are predoctoral fellows of the "la Caixa"/CNIO international PhD program. Lucía Inglada-Pérez is predoctoral fellow of the CIBERER. Luis Javier Leandro-Garcia is a predoctoral fellow of the Fondo de Investigaciones Sanitarias. Esmeralda Castelblanco holds a predoctoral fellowship from Fundació Alicaia Cuello de Merigó, and AGAUR 2010FI-B01057. Tumor samples were obtained with the support of the Spanish National Tumor Bank Network, the Red Nacional de Biobancos (RD09/0076/00047), the Biobank of the Virgen del Rocío Hospital (RD09/0076/00085), the Surgical Pathology Department of Medical and Surgical Sciences, Padova, Italy, the Xarxa Catalana de Bancs de Tumors, the Tumor Bank Platform of RTICC and the Hospital Arnau de Vilanova.

MZ-CRC-1 cells were a generous gift of Dr. Robert F. Gagel (M.D. Anderson Cancer Center, University of Texas).

References

Figure Legends:

Figure 1. Unsupervised clustering of hybridized frozen MTC series. Partial heat map showing two principal branches after applying unsupervised clustering to the 49 MTCs. The first branch was enriched with MTC^{M918T} cases and the second with familial MTC cases, mostly with RET^{634} mutation. Color bar, green and red, represents relative under- and over expression levels respectively. MTC cases were named using ID case and extensions as: S_918 (sporadic MTC with somatic M918T *RET* mutation), F_634 (familial MTC with 634 *RET* mutation) and S_WT (sporadic MTC with no *RET* mutation).

Figure 2A. Differential expression analysis of $MTCs^{M918T}$ *vs* $MTCs^{WT}$ using the GEPAS package. The first 100 genes with a false discovery rate (FDR) <0.05 are shown, including information about t statistic.

Figure 2B. Differential expression analysis of $MTCs^{M918T}$ *vs* $MTCs^{634}$ using the GEPAS package. The first 100 genes with a false discovery rate (FDR) <0.05 are shown, including information about t statistic.

Figure 3. Top panel: Knockdown efficacy of two different siRNAs against human PROM1. MZ-CRC-1 cells were nucleofected with either buffer or the indicated siRNAs against PROM1 (PROM1.1 and PROM1.2). Three days later PROM1 expression was assessed by real time RT-PCR. **Bottom panel**: Silencing of PROM1 causes apoptotic death of MZ-CRC-1 cells. Cells were nucleofected as above and three days later the number of nuclei showing apoptotic morphology was scored.

Figure 1.

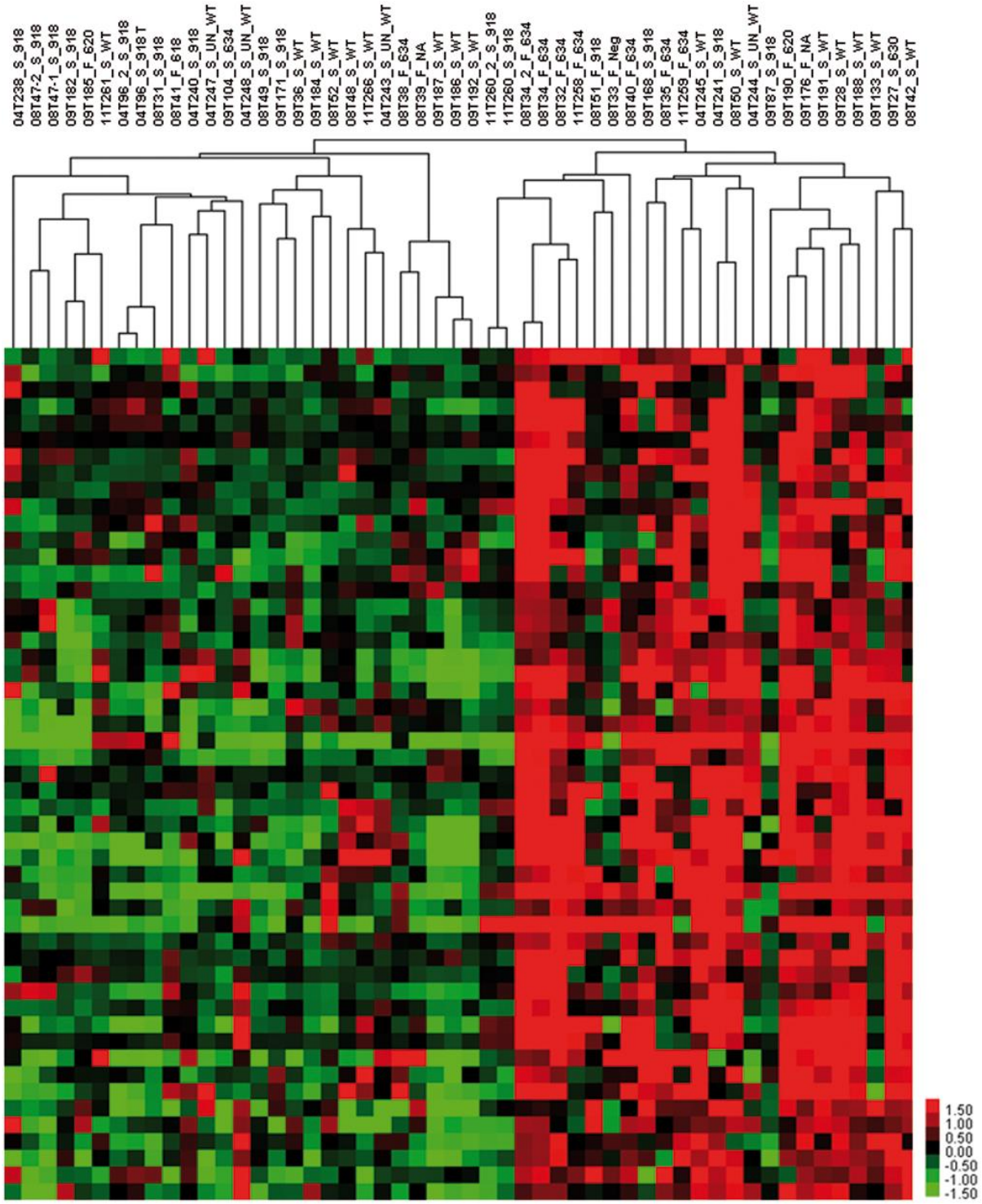
04T238_S_918
08T47-2_S_918
08T47-1_S_918
09T182_S_918
09T185_F_620
11T261_S_WT
04T96_2_S_918
04T96_S_918 T
08T31_S_918
08T41_F_618
04T240_S_918
04T247_S_UN_WT
09T104_S_634
04T248_S_UN_WT
08T49_S_918
09T171_S_918
09T36_S_WT
09T184_S_WT
08T52_S_WT
08T48_S_WT
11T266_S_WT
04T243_S_UN_WT
08T38_F_634
08T39_F_NA
09T187_S_WT
09T186_S_WT
09T192_S_WT
11T260_2_S_918
11T260_S_918
08T34_2_F_634
08T34_F_634
08T32_F_634
11T258_F_634
08T51_F_918
08T33_F_Neg
08T40_F_634
09T168_S_918
08T35_F_634
11T259_F_634
04T245_S_WT
04T241_S_918
08T50_S_WT
04T244_S_UN_WT
09T87_S_918
09T190_F_620
09T176_F_NA
09T191_S_WT
09T28_S_WT
09T188_S_WT
09T133_S_WT
09T27_S_630
08T42_S_WT
1.50
1.00
0.50
0.00
-0.50
-1.00
-1.50

Figure 2A.

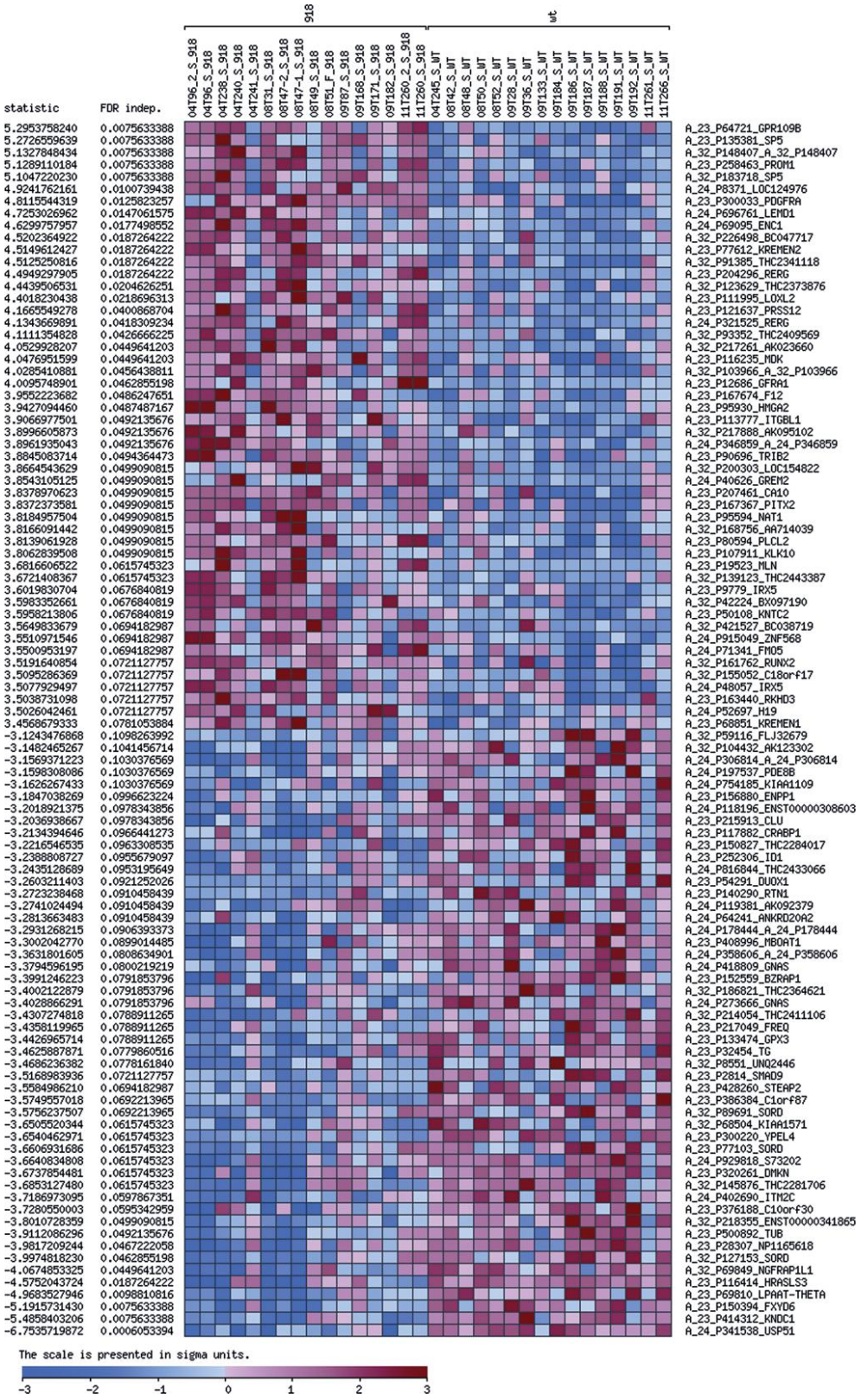
918
wt
04T96_2_S_918
04T96_S_918
04T238_S_918
04T240_S_918
04T241_S_918
08T31_S_918
08T47-2_S_918
08T47-1_S_918
08T49_S_918
08T51_F_918
09T87_S_918
09T168_S_918
09T171_S_918
09T182_S_918
11T260_2_S_918
11T260_S_918
04T245_S_WT
08T42_S_WT
08T48_S_WT
08T50_S_WT
08T52_S_WT
09T28_S_WT
09T36_S_WT
09T133_S_WT
09T184_S_WT
09T186_S_WT
09T187_S_WT
09T188_S_WT
09T191_S_WT
09T192_S_WT
11T261_S_WT
11T266_S_WT
statistic
FDR indep.
5.2953758240 0.0075633388 A_23_P64721_GPR109B
5.2726559639 0.0075633388 A_23_P135381_SP5
5.1327848434 0.0075633388 A_32_P148407_A_32_P148407
5.1289110184 0.0075633388 A_23_P258463_PROM1
5.1047220230 0.0075633388 A_32_P183718_SP5
4.9241762161 0.0100739438 A_24_P8371_LOC124976
4.8115544319 0.0125823257 A_23_P300033_PDGFRA
4.7253026962 0.0147061575 A_24_P696761_LEND1
4.6299757957 0.0177498552 A_24_P69095_ENC1
4.5202364922 0.0187264222 A_32_P226498_BC047717
4.5149612427 0.0187264222 A_23_P77612_KREMEN2
4.5125250816 0.0187264222 A_32_P91385_THC2341118
4.4949297905 0.0187264222 A_23_P204296_RERG
4.4439506531 0.0204626251 A_32_P123629_THC2373876
4.4018230438 0.0218696313 A_23_P111995_LOXL2
4.1665549278 0.0400868704 A_23_P121637_PRSS12
4.1343669891 0.0418309234 A_24_P321525_RERG
4.1111354828 0.0426666225 A_32_P93352_THC2409569
4.0529928207 0.0449641203 A_32_P217261_AK023660
4.0476951599 0.0449641203 A_23_P116235_MDK
4.0285410881 0.0456438811 A_32_P103966_A_32_P103966
4.0095748901 0.0462855198 A_23_P12686_GFRA1
3.9552223682 0.0486247651 A_23_P167674_F12
3.9427094460 0.0487487167 A_23_P95930_HMGA2
3.9066977501 0.0492135676 A_23_P113777_ITGBL1
3.8996605873 0.0492135676 A_32_P217888_AK095102
3.8961935043 0.0492135676 A_24_P346859_A_24_P346859
3.8845083714 0.0494364473 A_23_P90696_TRIB2
3.8664543629 0.0499090815 A_32_P200303_LOC154822
3.8543105125 0.0499090815 A_24_P40626_GREM2
3.8378970623 0.0499090815 A_23_P207461_CA10
3.8372373581 0.0499090815 A_23_P167367_PITX2
3.8184957504 0.0499090815 A_23_P95594_NAT1
3.8166091442 0.0499090815 A_32_P168756_AA714039
3.8139061928 0.0499090815 A_23_P80594_PLCL2
3.8062839508 0.0499090815 A_23_P107911_KLK10
3.6816606522 0.0615745323 A_23_P19523_MLN
3.6721408367 0.0615745323 A_32_P139123_THC2443387
3.6019830704 0.0676840819 A_23_P9779_IRX5
3.5983352661 0.0676840819 A_32_P42224_BX097190
3.5958213806 0.0676840819 A_23_P50108_KNTC2
3.5649833679 0.0694182987 A_32_P421527_BC038719
3.5510971546 0.0694182987 A_24_P915049_ZNF568
3.5500953197 0.0694182987 A_24_P71341_FMO5
3.5191640854 0.0721127757 A_32_P161762_RUNX2
3.5095286369 0.0721127757 A_32_P155052_C18orf17
3.5077929497 0.0721127757 A_24_P48057_IRX5
3.5038731098 0.0721127757 A_23_P163440_RKHD3
3.5026042461 0.0721127757 A_24_P52697_H19
3.4568679333 0.0781053884 A_23_P68851_KREMEN1
-3.1243476868 0.1098263992 A_32_P59116_FLJ32679
-3.1482465267 0.1041456714 A_32_P104432_AK123302
-3.1569371223 0.1030376569 A_24_P306814_A_24_P306814
-3.1598308086 0.1030376569 A_24_P197537_PDE8B
-3.1626267433 0.1030376569 A_24_P754185_KIAA1109
-3.1847038269 0.0996623224 A_23_P156880_ENPP1
-3.2018921375 0.0978343856 A_24_P118196_ENST00000308603
-3.2036938667 0.0978343856 A_23_P215913_CLU
-3.2134394646 0.0966441273 A_23_P117882_CRABP1
-3.2216546535 0.0963308535 A_23_P150827_THC2284017
-3.2388808727 0.0955679097 A_23_P252306_ID1
-3.2435128689 0.0953195649 A_24_P816844_THC2433066
-3.2603211403 0.0921252026 A_23_P54291_DUOX1
-3.2723238468 0.0910458439 A_23_P140290_RTN1
-3.2741024494 0.0910458439 A_24_P119381_AK092379
-3.2813663483 0.0910458439 A_24_P64241_ANKRD20A2
-3.2931268215 0.0906393373 A_24_P178444_A_24_P178444
-3.3002042770 0.0899014485 A_23_P408996_MBOAT1
-3.3631801605 0.0808634901 A_24_P358606_A_24_P358606
-3.3794596195 0.0800219219 A_24_P418809_GNAS
-3.3991246223 0.0791853796 A_23_P152559_BZRAP1
-3.4002122879 0.0791853796 A_32_P186821_THC2364621
-3.4028866291 0.0791853796 A_24_P273666_GNAS
-3.4307274818 0.0788911265 A_32_P214054_THC2411106
-3.4358119965 0.0788911265 A_23_P217049_FREQ
-3.4426965714 0.0788911265 A_23_P133474_GPX3
-3.4625887871 0.0779860516 A_23_P32454_TG
-3.4686236382 0.0778161840 A_32_P8551_UNQ2446
-3.5168983936 0.0721127757 A_23_P2814_SMAD9
-3.5584986210 0.0694182987 A_23_P428260_STEAP2
-3.5749557018 0.0692213965 A_23_P386384_C1orf87
-3.5756237507 0.0692213965 A_32_P89691_SORD
-3.6505520344 0.0615745323 A_32_P68504_KIAA1571
-3.6540462971 0.0615745323 A_23_P300220_YPEL4
-3.6606931686 0.0615745323 A_23_P77103_SORD
-3.6640834808 0.0615745323 A_24_P929818_S73202
-3.6737854481 0.0615745323 A_23_P320261_DMKN
-3.6853127480 0.0615745323 A_32_P145876_THC2281706
-3.7186973095 0.0597867351 A_24_P402690_ITM2C
-3.7280550003 0.0595342959 A_23_P376188_C10orf30
-3.8010728359 0.0499090815 A_32_P218355_ENST00000341865
-3.9112086296 0.0492135676 A_23_P500892_TUB
-3.9817209244 0.0467222058 A_23_P28307_NP1165618
-3.9974818230 0.0462855198 A_32_P127153_SORD
-4.0674853325 0.0449641203 A_32_P69849_NGFRAP1L1
-4.5752043724 0.0187264222 A_23_P116414_HRASLS3
-4.9683527946 0.0098810816 A_23_P69810_LPAAT-THETA
-5.1915731430 0.0075633388 A_23_P150394_FXYD6
-5.4858403206 0.0075633388 A_23_P414312_KNDC1
-6.7535719872 0.0006053394 A_24_P341538_USP51
The scale is presented in sigma units.
-3
-2
-1
0
1
2
3

Figure 2B.

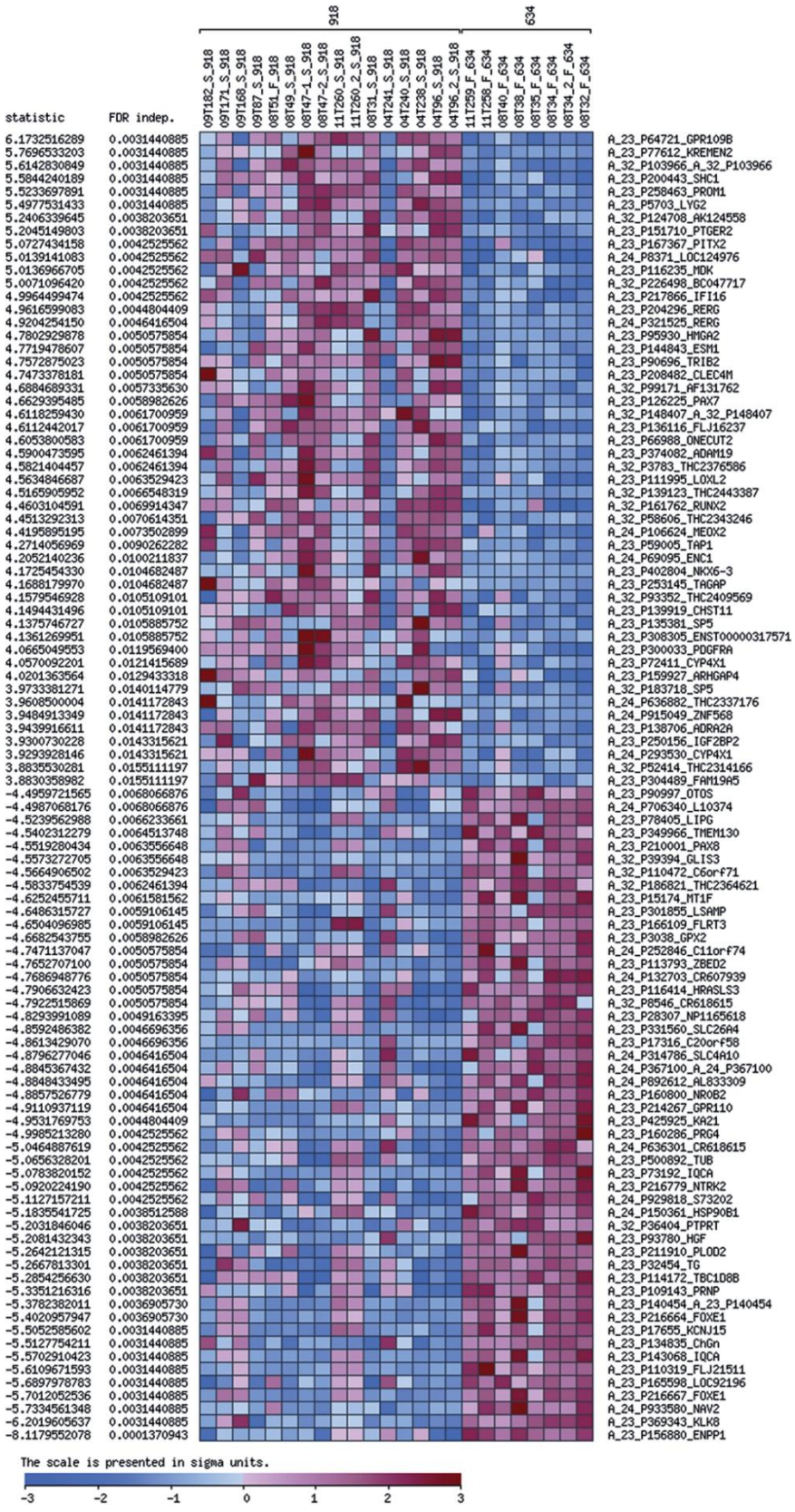
918
634
09T182_S_918
09T171_S_918
09T168_S_918
09T87_S_918
08T51_F_918
08T49_S_918
08T47-1_S_918
08T47-2_S_918
11T260_S_918
11T260_2_S_918
08T31_S_918
04T241_S_918
04T240_S_918
04T238_S_918
04T96_S_918
04T96_2_S_918
11T259_F_634
11T298_F_634
08T40_F_634
08T38_F_634
08T35_F_634
08T34_F_634
08T34_2_F_634
08T32_F_634
statistic
FDR indep.
6.1732516289 0.0031440885 A_23_P64721_GPR109B
5.7696533203 0.0031440885 A_23_P77612_KREMEN2
5.6142830849 0.0031440885 A_32_P103966_A_32_P103966
5.5844240189 0.0031440885 A_23_P200443_SHC1
5.5233697891 0.0031440885 A_23_P258463_PROM1
5.4977531433 0.0031440885 A_23_P5703_LYG2
5.2406339645 0.0038203651 A_32_P124708_AK124558
5.2045149803 0.0038203651 A_23_P151710_PTGER2
5.0727434158 0.0042525562 A_23_P167367_PITX2
5.0139141083 0.0042525562 A_24_P8371_LOC124976
5.0136966705 0.0042525562 A_23_P116235_MDK
5.0071096420 0.0042525562 A_32_P226498_BC047717
4.9964499474 0.0042525562 A_23_P217866_IFI16
4.9616599083 0.0044804409 A_23_P204296_RERG
4.9204254150 0.0046416504 A_24_P321525_RERG
4.7802929878 0.0050575854 A_23_P95930_HMGA2
4.7719478607 0.0050575854 A_23_P144843_ESM1
4.7572875023 0.0050575854 A_23_P90696_TRIB2
4.7473378181 0.0050575854 A_23_P208482_CLEC4M
4.6884689331 0.0057335630 A_32_P99171_AF131762
4.6629395485 0.0058982626 A_23_P126225_PAX7
4.6118259430 0.0061700959 A_32_P148407_A_32_P148407
4.6112442017 0.0061700959 A_23_P136116_FLJ16237
4.6053800583 0.0061700959 A_23_P66988_ONECUT2
4.5900473595 0.0062461394 A_23_P374082_ADAM19
4.5821404457 0.0062461394 A_32_P3783_THC2376586
4.5634846687 0.0063529423 A_23_P111995_LOXL2
4.5165905952 0.0066548319 A_32_P139123_THC2443387
4.4603104591 0.0069914347 A_32_P161762_RUNX2
4.4513292313 0.0070614351 A_32_P58606_THC2343246
4.4195895195 0.0073502899 A_24_P106624_MEOX2
4.2714056969 0.0090262282 A_23_P59005_TAP1
4.2052140236 0.0100211837 A_24_P69095_ENC1
4.1725454330 0.0104682487 A_23_P402804_NKX6-3
4.1688179970 0.0104682487 A_23_P253145_TAGAP
4.1579546928 0.0105109101 A_32_P93352_THC2409569
4.1494431496 0.0105109101 A_23_P139919_CHST11
4.1375746727 0.0105885752 A_23_P135381_SP5
4.1361269951 0.0105885752 A_23_P308305_ENST00000317571
4.0665049553 0.0119569400 A_23_P300033_PDGFRA
4.0570092201 0.0121415689 A_23_P72411_CYP4X1
4.0201363564 0.0129433318 A_23_P159927_ARHGAP4
3.9733381271 0.0140114779 A_32_P183718_SP5
3.9608500004 0.0141172843 A_24_P636882_THC2337176
3.9484913349 0.0141172843 A_24_P915049_ZNF568
3.9439916611 0.0141172843 A_23_P138706_ADRA2A
3.9300730228 0.0143315621 A_23_P250156_IGF2BP2
3.9293928146 0.0143315621 A_24_P293530_CYP4X1
3.8835530281 0.0155111197 A_32_P52414_THC2314166
3.8830358982 0.0155111197 A_23_P304489_FAM19A5
-4.4959721565 0.0068066876 A_23_P90997_OTOS
-4.4987068176 0.0068066876 A_24_P706340_L10374
-4.5239562988 0.0066233661 A_23_P78405_LIPG
-4.5402312279 0.0064513748 A_23_P349966_TMEM130
-4.5519280434 0.0063556648 A_23_P210001_PAX8
-4.5573272705 0.0063556648 A_32_P39394_GLIS3
-4.5664906502 0.0063529423 A_32_P110472_C6orf71
-4.5833754539 0.0062461394 A_32_P186821_THC2364621
-4.6252455711 0.0061581562 A_23_P15174_MT1F
-4.6486315727 0.0059106145 A_23_P301855_LSAMP
-4.6504096985 0.0059106145 A_23_P166109_FLRT3
-4.6682543755 0.0058982626 A_23_P3038_GPX2
-4.7471137047 0.0050575854 A_24_P252846_C11orf74
-4.7652707100 0.0050575854 A_23_P113793_ZBED2
-4.7686948776 0.0050575854 A_24_P132703_CR607939
-4.7906632423 0.0050575854 A_23_P116414_HRASLS3
-4.7922515869 0.0050575854 A_32_P8546_CR618615
-4.8293991089 0.0049163395 A_23_P28307_NP1165618
-4.8592486382 0.0046696356 A_23_P331560_SLC26A4
-4.8613429070 0.0046696356 A_23_P17316_C20orf58
-4.8796277046 0.0046416504 A_24_P314786_SLC4A10
-4.8845367432 0.0046416504 A_24_P367100_A_24_P367100
-4.8848433495 0.0046416504 A_24_P892612_AL833309
-4.8857526779 0.0046416504 A_23_P160800_NR0B2
-4.9110937119 0.0046416504 A_23_P214267_GPR110
-4.9531769753 0.0044804409 A_23_P425925_KA21
-4.9985213280 0.0042525562 A_23_P160286_PRG4
-5.0464887619 0.0042525562 A_24_P636301_CR618615
-5.0656328201 0.0042525562 A_23_P500892_TUB
-5.0783820152 0.0042525562 A_23_P73192_IQCA
-5.0920224190 0.0042525562 A_23_P216779_NTRK2
-5.1127157211 0.0042525562 A_24_P929818_S73202
-5.1835541725 0.0038512588 A_24_P150361_HSP90B1
-5.2031846046 0.0038203651 A_32_P36404_PTPRT
-5.2081432343 0.0038203651 A_23_P93780_HGF
-5.2642121315 0.0038203651 A_23_P211910_PLOD2
-5.2667813301 0.0038203651 A_23_P32454_TG
-5.2854256630 0.0038203651 A_23_P114172_TBC1D8B
-5.3351216316 0.0038203651 A_23_P109143_PRNP
-5.3782382011 0.0036905730 A_23_P140454_A_23_P140454
-5.4020957947 0.0036905730 A_23_P216664_FOXE1
-5.5052585602 0.0031440885 A_23_P17655_KCNJ15
-5.5127754211 0.0031440885 A_23_P134835_ChGn
-5.5702910423 0.0031440885 A_23_P143068_IQCA
-5.6109671593 0.0031440885 A_23_P110319_FLJ21511
-5.6897978783 0.0031440885 A_23_P165598_LOC92196
-5.7012052536 0.0031440885 A_23_P216667_FOXE1
-5.7334561348 0.0031440885 A_24_P933580_NAV2
-6.2019605637 0.0031440885 A_23_P369343_KLK8
-8.1179552078 0.0001370943 A_23_P156880_ENPP1
The scale is presented in sigma units.
-3
-2
-1
0
1
2
3

Figure 3.

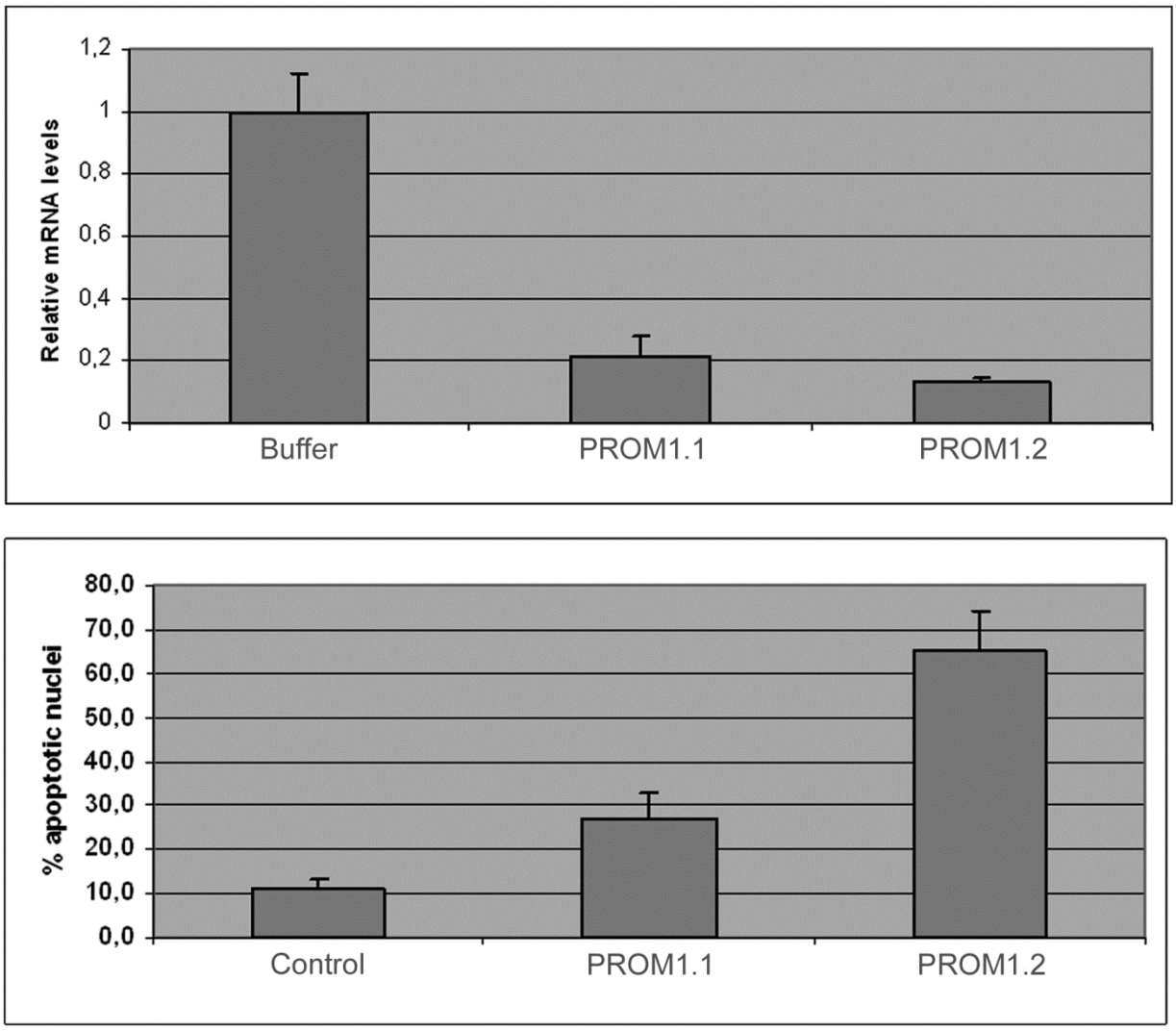
Relative mRNA levels
1,2
1
0,8
0,6
0,4
0,2
0
Buffer
PROM1.1
PROM1.2
% apoptotic nuclei
80,0
70,0
60,0
50,0
40,0
30,0
20,0
10,0
0,0
Control
PROM1.1
PROM1.2

Supplementary Information legends:

Supplemantary Figure 1A. RT-qPCR with Taqman probes of *GFRA1*, *LOXL2*, *GAL*, *PROM1* and *DKK4* expression in an independent frozen MTC validation series.

Supplementary Figure 1B. RT-qPCR with Taqman probes of *LOXL2* and *PROM1* expression in an independent FFPE MTC validation series.

Supplementary Table 1. Clinical and genetic information of the frozen MTC series.

Supplementary table 2A. Genetic information of the TMA-1.

Supplementary Table 2B. General and genetic information of the tissues included in TMA-2 .

Supplementary Table 3. FFPE MTC series for independent validation through RT-qPCR using TaqMan probes.

Supplementary Table 4A. Gene Set Enrichment Analysis (GSEA) of MTC^{M918T} *vs* MTC^{634}. Enriched pathways in the M918T group.

Supplementary Table 4B. Gene Set Enrichment Analysis (GSEA) of MTC^{M918T} *vs* MTC^{WT}. Enriched pathways in the M918T group.

Supplementary Table 5. FatiGO/Babelomics analysis of GO biological processes. Statistically significant results for genes of the M918T group included in the Agilent Whole Human Genome Microarray 4x44K. Biological processes associated with malignant behavior are shown in bold.

Supplementary Table 6. Biocarta pathways in the M918T group of genes included in the Agilent Whole Human Genome Microarray 4x44K. Significant Biocarta terms (pvalue<0.05) from FatiGO analysis are shown.

Supplemantary Figure 1A.

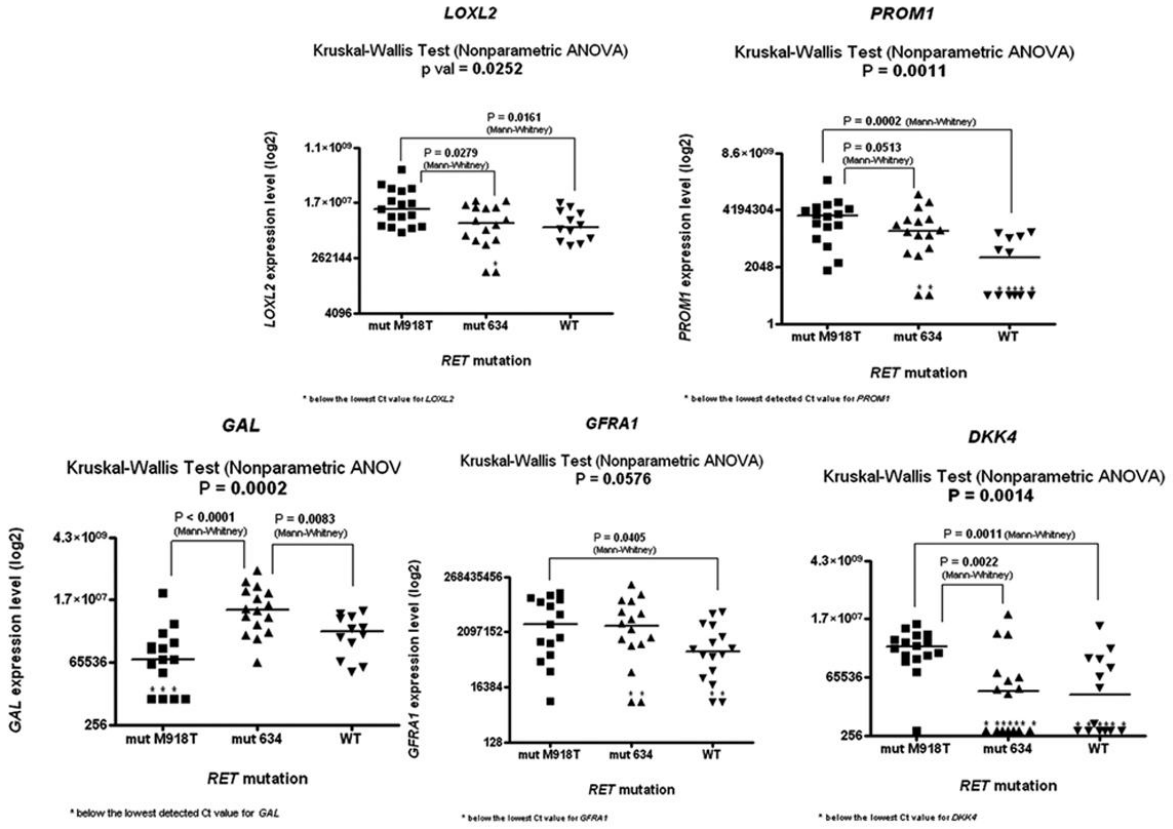

Supplemantary Figure 1B.

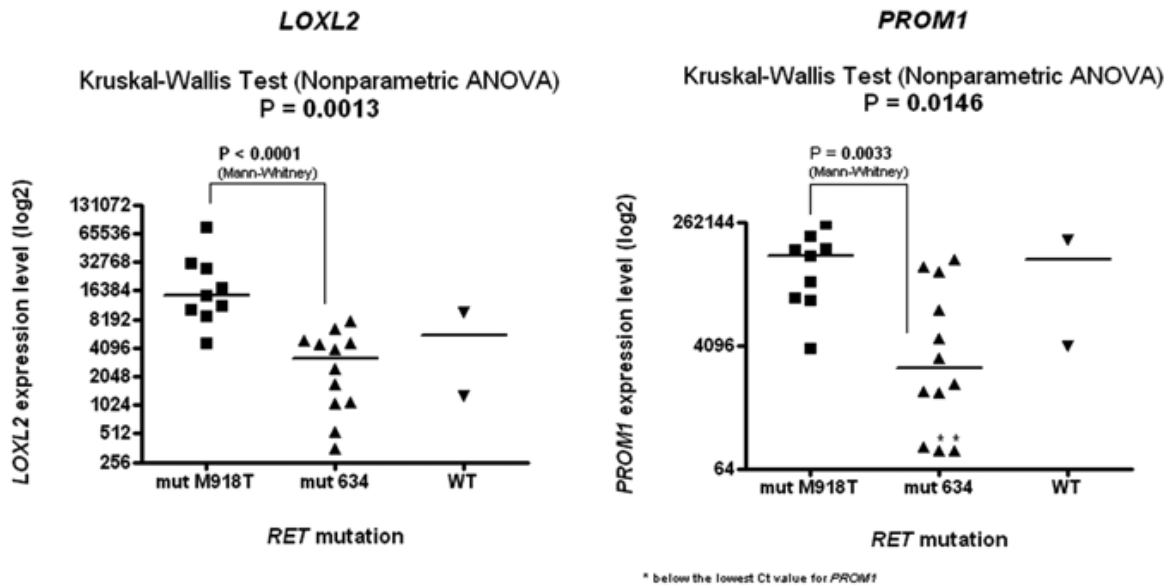

Supplementary table 1.

№	ID	Array*	MTC†	Gender	Year of birth	Antec.	Germline mutation	Somatic mutation	Classification
1	08T32	yes	FAM	F	1936	no	C634R	-	¨634¨
2	08T35	yes	FAM	F	1986	yes	C634R	-	¨634¨
3	08T38	yes	FAM	M	1966	yes	C634R	-	¨634¨
4	08T40	yes	FAM	M	1957	yes	C634R	-	¨634¨
5	11T258	yes	FAM	F	1988	yes	C634S	-	¨634¨
6	11T259	yes	FAM	M	1943	yes	C634S	-	¨634¨
7	08T34	yes	FAM	M	1973	yes	C634Y	-	¨634¨
8	09T185	yes	FAM	F	1955	yes	C620G	-	-
9	09T190	yes	FAM	F	1965	yes	C620G	-	-
10	08T41	yes	FAM	M	1968	yes	C618S	-	-
11	08T33	yes	FAM	F	1936	yes	E 11, 10 Neg	-	-
12	08T39	yes	FAM	M	1944	yes	NA	NA	-
13	09T176	yes	FAM	M	1967	yes	NA	-	-
14	08T51	yes	FAM	F	1976	no	M918T	-	¨918¨
15	04T238	yes	S	M	1944	no	Neg	M918T	¨918¨
16	04T240	yes	S	M	1924	no	Neg	M918T	¨918¨
17	04T241	yes	S	F	1979	no	Neg	M918T	¨918¨
18	04T96	yes	S	M	1949	no	Neg	M918T	¨918¨
19	08T31	yes	S	M	1949	no	Neg	M918T	¨918¨
20	08T47-1	yes	S	F	1948	no	Neg	M918T	¨918¨
21	08T47-2	yes	S	F	1948	no	Neg	M918T	¨918¨
22	08T49	yes	S	M	1968	no	Neg	M918T	¨918¨
23	09T87	yes	S	F	1949	no	Neg	M918T	¨918¨
24	09T168	yes	S	M	1961	no	Neg	M918T	¨918¨
25	09T171	yes	S	M	1938	no	Neg	M918T	¨918¨
26	09T182	yes	S	M	1979	no	Neg	M918T	¨918¨
27	11T260	yes	S	F	1929	no	Neg	M918T	¨918¨
28	08T50	yes	S	F	1944	no	Neg	Neg	¨WT¨
29	04T245	yes	S	M	1926	no	Neg	Neg	¨WT¨
30	09T28	yes	S	M	1968	no	Neg	Neg	¨WT¨
31	09T36	yes	S	M	1958	no	Neg	Neg	¨WT¨
32	09T133	yes	S	M	1939	no	Neg	Neg	¨WT¨
33	11T261	yes	S	F	1953	no	Neg	Neg	¨WT¨
34	11T266	yes	S	M	1955	no	Neg	Neg	¨WT¨
35	09T184	yes	S	F	2001	no	Neg	E-16 Neg	¨WT¨
36	09T186	yes	S	F	1946	no	Neg	E-16 Neg	¨WT¨
37	09T187	yes	S	M	1920	no	Neg	E-16 Neg	¨WT¨
38	09T188	yes	S	M	1941	no	Neg	E-16 Neg	¨WT¨
39	09T191	yes	S	M	1937	no	Neg	E-16 Neg	¨WT¨
40	09T192	yes	S	F	1959	no	Neg	E-16 Neg	¨WT¨
41	08T48	yes	S	F	1951	unknown	E 11, 10 Neg	E 11, 10 Neg	¨WT¨
42	08T42	yes	S	F	1963	no	E 11, 10 Neg	E 11, 10 Neg	¨WT¨

43	04T243	yes	S	F	1922	no	Neg	unkown	¨WT¨
44	04T244	yes	S	F	1942	no	Neg	unkown	¨WT¨
45	04T247	yes	S	M	1937	no	Neg	unkown	¨WT¨
46	08T52	yes	S	F	1936	no	Neg	unkown	¨WT¨
47	04T248	yes	S	M	1954	unknown	unkown	unkown	¨WT¨
48	09T104	yes	S	M	1944	no	Neg	C634R	-
49	09T27	yes	S	M	1963	no	Neg	C630G	-
50	09T266	no	FAM	F	1979	yes	C634Y	-	¨634¨
51	11T262	no	FAM	F	1970	yes	C634Y	-	¨634¨
52	11T263	no	FAM	M	1963	yes	C634Y	-	¨634¨
53	11T265	no	FAM	M	1972	yes	C634Y	-	¨634¨
54	09T264	no	FAM	F	1947	unknown	C634Y	-	¨634¨
55	09T265	no	FAM	F	1966	yes	C634Y	-	¨634¨
56	11T50	no	FAM	F	1970	yes	C634S	-	¨634¨
57	11T65	no	FAM	F	1969	yes	C634R	-	¨634¨
58	11T66	no	FAM	F	1993	yes	C634R	-	¨634¨
59	09T170	no	S	M	1958	no	Neg	M918T	¨918¨
60	09T178	no	S	M	1947	no	Neg	M918T	¨918¨
61	11T264	no	S	M	1962	no	Neg	M918T	¨918¨
62	04T235	no	S	F	1938	no	E 11, 10 Neg	Neg	¨WT¨
63	04T242	no	S	M	1933	no	Neg	Neg	¨WT¨
64	04T246	no	S	M	1933	no	Neg	-	¨WT¨
65	09T180	no	S	F	1971	no	Neg	E-16 Neg	¨WT¨
66	09T181	no	S	M	1942	no	Neg	E-16 Neg	¨WT¨
67	09T195	no	S	F	1958	unknown	E 11, 10 Neg	Neg	¨WT¨
68	09T213	no	S	F	1944	no	E 11, 10 Neg	Neg	¨WT¨

* Indicate if the sample was or not hybridized onto Agilent Whole Genome 4X44K Array. Those not used for hybridization purposes, were used for independent validation through RT-qPCR using TaqMan probes.
† Indicate the familial or the sporadic nature of the tumor, according to germline or somatic *RET* mutation status, as well as the existence of personal or familiar antecedents.
Abbreviations. Gender: F, female; M, male; Antec- antecedents (personal or familiar); NA- not available; Neg – negative; E-10, E-11, E-16 : exon 10, exon 16 and exon 11, respectively. FAM- Familial, S-Sporadic

Supplementary table 2A.

Nº	ID	Tumor/tissue	Somatic mutation	Germinal mutation	Normal thyroid	Classification
1	02T184	MTC	-	C618F		not used
2	03T123	MTC	-	C618F		not used
3	03T146	MTC	-	C618F		not used
4	03T113	MTC	-	C634R		¨634¨
5	03T114.3	MTC	-	C634R	yes	¨634¨
6	03T222.2	MTC	-	C634R		¨634¨
7	03T92	MTC	-	C634R		¨634¨
8	01T233	MTC	-	C634W	yes	¨634¨

9	03T124.3	MTC	-	C634W	yes	¨634¨
10	03T125	MTC	-	C634W		¨634¨
11	03T116	MTC	-	C634Y		¨634¨
12	03T127.2	MTC	-	C634Y		¨634¨
13	03T128.2	MTC	-	C634Y		¨634¨
14	03T81	MTC	-	C634Y		¨634¨
15	03T82	MTC	-	C634Y	yes	¨634¨
16	03T83	MTC	-	S891A	yes	not used
17	01T180	MTC	M918T	Neg	yes	¨918¨
18	02T367	MTC	M918T	Neg		¨918¨
19	03T104	MTC	M918T	Neg		¨918¨
20	03T120	MTC	M918T	Neg		¨918¨
21	03T22.B	MTC	M918T	Neg		¨918¨
22	03T272	MTC	M918T	Neg		¨918¨
23	03T85	MTC	M918T	Neg		¨918¨
24	03T89	MTC	M918T	Neg		¨918¨
25	03T91	MTC	M918T	Neg	yes	¨918¨
26	02T326	MTC	C618R	Neg		not used
27	03T247	MTC	C620F	Neg		not used
28	03T122	MTC	C634R	Neg		not used
29	03T147	MTC	C634S	Neg		not used
30	04T288	MTC	A883F	Neg		not used
31	03T121	MTC	E 10, 11, 15, 16 neg	Neg		¨WT¨
32	02T402	MTC	E 10, 11, 15, 16 neg	Neg		¨WT¨
33	03T138.1	MTC	E 10, 11, 15, 16 neg	Neg	yes	¨WT¨
34	01T189	MTC	E 10, 16 neg	Neg		¨WT¨
35	03T144	MTC	E 15, 16 neg	Neg		¨WT¨
36	03T117	MTC	E 11, 16 neg	Neg		¨WT¨
37	03T118	MTC	E 11, 16 neg	Neg		¨WT¨
38	03T119	MTC	E 11, 16 neg	Neg		¨WT¨
39	03T95	MTC	E 11, 16 neg	Neg		¨WT¨
40	03T90	MTC	E 11, 16 neg	Neg	yes	¨WT¨
41	03T84	MTC	E 16 neg	Neg		¨WT¨
42	03T88	MTC	E 16 neg	Neg		¨WT¨
43	03T94.2	MTC	E 16 neg	Neg	yes	¨WT¨
44	01T93.1	MTC	E 16 neg	Neg	yes	¨WT¨
45	03T93.1	MTC	E 16 neg	Neg	yes	¨WT¨
46	03T96	MTC	E 16 neg	Neg		¨WT¨
47	01T203	MTC	E 16 neg	NA	yes	¨WT¨
48	02T315	MTC	Neg	Neg		¨WT¨
50	03T271.2	MTC	Neg	Neg		¨WT¨
51	03T87	MTC	Neg	Neg		¨WT¨
52	01T64	MTC	Neg	Neg		¨WT¨
53	01T65	MTC	Neg	Neg		¨WT¨
54	03T145	MTC	NA	Neg		not used
55	03T273	MTC	NA	Neg		not used
57	07T42	PDTC				control
58	07T43.1	PTC				control
59	07T45.1	PTC				control

60	07T49.1	PTC				control
61	MC	medulla cortex				control
62	Pl	placenta				control

Abbreviations. NA- not available; Neg – negative; E-10, E-11, E-15, E-16 : exon 10, exon 11, exon 15 and exon 16, respectively.

Supplementary Table 2B.

Nº	ID case	Tumor	Somatic mutation	Germline mutation	Normal thyroid	Classification
1	08T32	MTC	-	C634R	yes	¨634¨
2	08T35	MTC	-	C634R	yes	¨634¨
3	08T40	MTC	-	C634R	yes	¨634¨
4	08T34	MTC	-	C634Y	yes	¨634¨
5	08T36*	MTC	-	C634Y	yes	¨634¨
6	08T37*	MTC	-	C634R	yes	¨634¨
7	08T49	MTC	M918T	Neg	yes	¨918¨
8	08T31	MTC	M918T	Neg	no	¨918¨
9	04T96	MTC	M918T	Neg	no	¨918¨
10	08T47-2	MTC	M918T	Neg	no	¨918¨
11	08T48	MTC	WT	E 10, 11 Neg	yes	¨WT¨
12	08T41	MTC	WT	E 10, 11 Neg	yes	¨WT¨
13	08T50	MTC	WT	E 10, 11 Neg	yes	¨WT¨
14	08T33	MTC	Unkown	E 10, 11 Neg	yes	¨WT¨
15	08T39	MTC	Unkown	Unkown	yes	not used
16	4020462	Hürthle cell neoplasm				control
17	06B873	FTC				control

*tumors not hybridized due to lack of RNA.

Abbreviations. FTC- Follicular Thyroid Carcinoma; Neg – negative.

Supplementary Table 3.

Nº	ID case	Gender	Year of birth	MTC*	*RET* mutation	Classification
1	03T124.3	M	1978	Familial	C634W	¨634¨
2	03T128.2	F	1944	Familial	C634Y	¨634¨
3	03T116	F	1973	Familial	C634Y	¨634¨
4	01T233	M	1982	Familial	C634Y	¨634¨
5	03T125	F	1952	Familial	C634W	¨634¨
6	03T127.1	M	1948	Familial	C634Y	¨634¨
7	03T092	F	1917	Familial	C634R	¨634¨
8	03T114.3	M	1958	Familial	C634Y	¨634¨
9	03T113	M	1948	Familial	C634R	¨634¨
10	03T081	M	1960	Familial	C634Y	¨634¨

11	03T082	F	1965	Familial	C634Y	¨634¨
12	03T222.2	F	1959	Familial	C634R	¨634¨
13	03T104	F	1962	Sporadic	M918T	¨918¨
14	03T091	F	1954	Sporadic	M918T	¨918¨
15	03T085	F	1937	Sporadic	M918T	¨918¨
16	01T180	F	1949	Sporadic	M918T	¨918¨
17	02T367	M	1928	Sporadic	M918T	¨918¨
18	03T120	F	1931	Sporadic	M918T	¨918¨
19	03T272	M	1948	Sporadic	M918T	¨918¨
20	03T089	M	1949	Sporadic	M918T	¨918¨
21	06T001	F	1961	Sporadic	M918T	¨918¨
22	02T402	M	1951	Sporadic	Negative	WT
23	03T121	M	1952	Sporadic	Negative	WT

* Indicate the familial or the sporadic nature of the tumor, according to germline or somatic *RET* mutation status, as well as the existence of personal or familiar antecedents.
Abbreviations. Gender: F, female; M, male;

Supplementary Table 4A.

BIOCARTA PATHWAY NAME	NES	NOM p-val*	FDR q-val†
TCRPATHWAY	1,766	0,002	0,053
NKTPATHWAY	1,830	0,000	0,055
HIVNEFPATHWAY	1,784	0,002	0,056
INFLAMPATHWAY	1,768	0,005	0,058
ATRBRCAPATHWAY	1,788	0,005	0,060
STEMPATHWAY	1,833	0,004	0,066
DEATHPATHWAY	1,732	0,005	0,066
NO2IL12PATHWAY	1,793	0,006	0,068
NTHIPATHWAY	1,709	0,011	0,077
NFKBPATHWAY	1,845	0,000	0,079
BCRPATHWAY	1,678	0,011	0,086
IL1RPATHWAY	1,688	0,009	0,086
RELAPATHWAY	1,667	0,017	0,087
LAIRPATHWAY	1,640	0,013	0,103
CASPASEPATHWAY	1,849	0,004	0,110
DCPATHWAY	1,906	0,000	0,115
TH1TH2PATHWAY	1,605	0,024	0,127
TNFR1PATHWAY	1,576	0,030	0,151
CTLA4PATHWAY	1,556	0,041	0,155
IL12PATHWAY	1,562	0,038	0,155
NKCELLSPATHWAY	1,531	0,032	0,175
FMLPPATHWAY	1,513	0,033	0,189
AMIPATHWAY	1,484	0,057	0,212
TNFR2PATHWAY	1,476	0,063	0,212

ERYTHPATHWAY	1,489	0,054	0,215
ETSPATHWAY	1,443	0,070	0,234
P38MAPKPATHWAY	1,414	0,052	0,237
CSKPATHWAY	1,446	0,071	0,239
WNTPATHWAY	1,422	0,069	0,240
CCR5PATHWAY	1,415	0,068	0,243
IL2PATHWAY	1,405	0,078	0,243
CYTOKINEPATHWAY	1,425	0,068	0,244
MAPKPATHWAY	1,447	0,021	0,246
KEGG PATHWAY NAME	**NES**	**NOM p-val***	**FDR q-val†**
NATURAL KILLER CELL MEDIATED CYTOTOXICITY	2,276	0,000	0,001
P53 SIGNALING PATHWAY	2,142	0,000	0,002
TYPE I DIABETES MELLITUS	2,067	0,000	0,002
ASTHMA	1,917	0,000	0,010
CYTOKINE-CYTOKINE RECEPTOR INTERACTION	1,880	0,000	0,012
APOPTOSIS	1,837	0,000	0,016
NATURAL KILLER CELL MEDIATED CYTOTOXICITY	1,802	0,000	0,022
HEMATOPOIETIC CELL LINEAGE	1,801	0,000	0,019
CELL CYCLE	1,794	0,000	0,018
ONE CARBON POOL BY FOLATE	1,777	0,004	0,019
DNA REPLICATION	1,765	0,005	0,020
TOLL-LIKE RECEPTOR SIGNALING PATHWAY	1,732	0,005	0,027
T CELL RECEPTOR SIGNALING PATHWAY	1,629	0,009	0,063
JAK-STAT SIGNALING PATHWAY	1,520	0,042	0,105
B CELL RECEPTOR SIGNALING PATHWAY	1,519	0,021	0,140
LEUKOCYTE TRANSENDOTHELIAL MIGRATION	1,506	0,014	0,145
NOTCH SIGNALING PATHWAY	1,505	0,030	0,135
PATHOGENIC ESCHERICHIA COLI INFECTION-EHEC	1,485	0,021	0,148
PYRIMIDINE METABOLISM	1,461	0,009	0,166
COMPLEMENT AND COAGULATION CASCADES	1,458	0,029	0,159

* NOM p-value is the significance of the normalized enrichment score (NES); †FDR q-val is the false discovery rate (FDR), the estimated probability that a gene set with a given NES represents a false positive finding; The GSEA analysis report highlights enriched gene sets with an FDR of less than 25%.

Supplementary Table 4B.

BIOCARTA PATHWAY NAME	**NES**	**NOM p-val***	**FDR q-val†**
CYTOKINEPATHWAY	2,153	0,000	0,000
COMPPATHWAY	2,139	0,000	0,001
DCPATHWAY	2,090	0,000	0,005
LAIRPATHWAY	2,020	0,000	0,008
INFLAMPATHWAY	1,998	0,000	0,007
NKTPATHWAY	1,990	0,000	0,006
ERYTHPATHWAY	1,931	0,002	0,014
STEMPATHWAY	1,797	0,004	0,053
NKCELLSPATHWAY	1,715	0,015	0,100
GCRPATHWAY	1,697	0,013	0,105

FMLPPATHWAY	1,651	0,008	0,132
RAC1PATHWAY	1,611	0,025	0,164
CXCR4PATHWAY	1,593	0,019	0,172
TH1TH2PATHWAY	1,590	0,024	0,164
IL1RPATHWAY	1,527	0,030	0,233
SPPAPATHWAY	1,517	0,037	0,233
KEGG PATHWAY NAME	**NES**	**NOM p-val***	**FDR q-val†**
COMPLEMENT AND COAGULATION CASCADES	2,430	0,000	0,000
ASTHMA	2,160	0,000	0,001
TYPE I DIABETES MELLITUS	2,118	0,000	0,001
PROTEASOME	1,923	0,000	0,013
HEMATOPOIETIC CELL LINEAGE	1,772	0,000	0,045
PORPHYRIN AND CHLOROPHYLL METABOLISM	1,771	0,002	0,037
CYTOKINE-CYTOKINE RECEPTOR INTERACTION	1,732	0,000	0,047
PATHOGENIC ESCHERICHIA COLI INFECTION	1,728	0,000	0,042
PYRIMIDINE METABOLISM	1,698	0,000	0,047
P53 SIGNALING PATHWAY	1,680	0,002	0,049
ANDROGEN AND ESTROGEN METABOLISM	1,673	0,002	0,047
PENTOSE AND GLUCURONATE INTERCONVERSIONS	1,664	0,013	0,047
NICOTINATE AND NICOTINAMIDE METABOLISM	1,607	0,018	0,071
CELL CYCLE	1,603	0,004	0,068
MAPK SIGNALING PATHWAY	1,614	0,012	0,092
TOLL-LIKE RECEPTOR SIGNALING PATHWAY	1,550	0,004	0,098
APOPTOSIS	1,500	0,007	0,132
DNA REPLICATION	1,498	0,030	0,126
ARGININE AND PROLINE METABOLISM	1,493	0,039	0,124
CELL ADHESION MOLECULES (CAMS)	1,445	0,041	0,153
RENIN-ANGIOTENSIN SYSTEM	1,433	0,074	0,174
PARKINSON'S DISEASE	1,398	0,080	0,210
GAP JUNCTION	1,389	0,031	0,212
LONG-TERM DEPRESSION	1,360	0,031	0,244
CITRATE CYCLE (TCA CYCLE)	1,355	0,095	0,242

*NOM p-value is the significance of the normalized enrichment score (NES); †FDR q-val is the false discovery rate (FDR), the estimated probability that a gene set with a given NES represents a false positive finding. The GSEA analysis report highlights enriched gene sets with an FDR of less than 25%. Pathways are ranked by the FRD q-value.

Supplementary Table 5.

Nº	Term (GO)	M918T gene list	odds_ratio_log	pvalue	adj_pvalue
1	muscle organ development (GO:0007517)	*FAM65B,TNNI3,SPIB,MEOX2,EZH2,PAX7*	1,92	3,85E-04	2,88E-02
2	organ morphogenesis (GO:0009887)	*TNNI3,SPIB,CDH13,HOXC8,TNF,PDGFRA,CHST11, MEOX2,ONECUT2,RUNX2,PITX2,SHC1*	1,78	3,23E-06	1,50E-03
3	tissue development (GO:0009888)	*TNNI3,SPIB,IKZF1,TNF,CHST11,NRTN,MEOX2, ONECUT2,RUNX2,EZH2,PAX7*	1,67	2,08E-05	4,36E-03

4	negative regulation of cytokine production (GO:0001818)	*SPIB,TNF,CIDEA*	3,08	4,68E-04	3,26E-02
5	chondrocyte differentiation (GO:0002062)	*SPIB,CHST11,RUNX2*	3,04	5,24E-04	3,33E-02
6	myeloid leukocyte differentiation (GO:0002573)	*SPIB,IKZF1,TNF,RELB,IFI16*	3,01	8,59E-06	2,10E-03
7	DNA metabolic process (GO:0006259)	*SPIB,FANCI,PDGFRA,ESCO2,CIDEA,TYMS,SHC1,TERT*	1,55	5,13E-04	3,33E-02
8	DNA replication (GO:0006260)	*SPIB,PDGFRA,TYMS,SHC1,TERT*	1,95	1,01E-03	4,83E-02
9	protein amino acid phosphorylation (GO:0006468)	*SPIB,NEK2,GSG2,TNF,PIM2,TRIB2,ADRA2A,STK17B, PDGFRA,SHC1*	1,43	3,05E-04	2,70E-02
10	**anti-apoptosis (GO:0006916)**	***SPIB,CDH13,TNF,IL2RB,PIM2,PAX7,TERT***	**2,31**	**1,24E-05**	**2,79E-03**
11	induction of apoptosis (GO:0006917)	*SPIB,TNF,CASP4,STK17B,BID,CIDEA,IFI16*	2,15	3,18E-05	5,82E-03
12	cellular component movement (GO:0006928)	*SPIB,CDH13,TNF,ADRA2A,PDGFRA,NRTN,ONECUT2 ,MTSS1*	1,44	1,07E-03	4,94E-02
13	cytoskeleton organization (GO:0007010)	*SPIB,NEK2,CXCL1,ADRA2A,ARHGAP4,MTSS1,SHC1*	1,61	8,24E-04	4,26E-02
14	**cell cycle (GO:0007049)**	***SPIB,NEK2,GSG2,TNF,PIM2,FANCI,GAS2L1,ESCO2, HMGA2***	**1,34**	**1,04E-03**	**4,92E-02**
15	**cell adhesion (GO:0007155)**	***SPIB,SIRPG,CDH13,SDK1,TNF,ONECUT2,CLEC4M, MTSS1,SHC1,LOXL2***	**1,41**	**3,68E-04**	**2,83E-02**
16	leukocyte adhesion (GO:0007159)	*SPIB,TNF,CLEC4M*	3,14	3,93E-04	2,88E-02
17	enzyme linked receptor protein signaling pathway (GO:0007167)	*SPIB,CDH13,STAP1,PDGFRA,CHST11,CIDEA,NRTN ,ONECUT2,RUNX2,MTSS1,SHC1*	2,19	1,64E-07	1,60E-04
18	**transmembrane receptor protein tyrosine kinase signaling pathway (GO:0007169)**	***SPIB,CDH13,STAP1,PDGFRA,NRTN,RUNX2,MTSS1, SHC1***	**2,25**	**4,62E-06**	**1,50E-03**
19	**transforming growth factor beta receptor signaling pathway (GO:0007179)**	***SPIB,CHST11,CIDEA,ONECUT2***	**2,56**	**3,56E-04**	**2,83E-02**
20	**protein kinase cascade (GO:0007243)**	***SPIB,GSG2,TNF,ADRA2A,STK17B,NRTN,HMGA2,SHC 1***	**1,67**	**2,41E-04**	**2,28E-02**
21	**Rho protein signal transduction (GO:0007266)**	***SPIB,CDH13,ADRA2A,ARHGAP4***	**2,24**	**1,12E-03**	**4,95E-02**
22	pattern specification process (GO:0007389)	*SPIB,MFNG,RAX,HOXC8,MEOX2,PAX7,PITX2*	2,16	2,99E-05	5,82E-03
23	**aging (GO:0007568)**	***SPIB,SHC1,TERT,LOXL2***	**2,33**	**8,30E-04**	**4,26E-02**
24	positive regulation of cell proliferation (GO:0008284)	*SPIB,SIRPG,CDH13,TNF,ADRA2A,PDGFRA,RUNX2,SH C1*	1,91	5,07E-05	7,81E-03
25	negative regulation of cell proliferation (GO:0008285)	*SPIB,SIRPG,CDH13,CXCL1,TNF,RERG*	1,73	1,00E-03	4,83E-02
26	apoptotic mitochondrial changes (GO:0008637)	*SPIB,PIM2,BID*	3,21	3,26E-04	2,73E-02
27	negative regulation of metabolic process (GO:0009892)	*SPIB,IKZF1,HOXC8,TNF,IGF2BP2,CIDEA,RUNX2,HMG A2*	1,43	1,09E-03	4,94E-02
28	positive regulation of metabolic process (GO:0009893)	*SPIB,IKZF1,CDH13,TNF,IL2RB,PDGFRA,ONECUT2,RU NX2,SHC1*	1,38	7,97E-04	4,24E-02

29	regulation of signal transduction (GO:0009966)	*SPIB,CDH13,TNF,DKK4,TRIB2,ADRA2A,CHST11,CIDEA ,ONECUT2, RUNX2,HMGA2,SHC1*	1,68	8,33E-06	2,10E-03
30	negative regulation of signal transduction (GO:0009968)	*SPIB,DKK4,CHST11,CIDEA,ONECUT2,RUNX2,HMGA2*	2,42	6,16E-06	1,80E-03
31	positive regulation of cell death (GO:0010942)	*SPIB,TNF,CASP4,STK17B,BID,CIDEA,IFI16*	1,83	2,27E-04	2,28E-02
32	peptide transport (GO:0015833)	*SPIB,CPLX3,TNF,TAP1,CLEC4M*	2,67	4,07E-05	6,61E-03
33	**cell-cell adhesion (GO:0016337)**	***SPIB,SIRPG,CDH13,TNF,CLEC4M,SHC1***	**1,93**	**3,66E-04**	**2,83E-02**
34	regulation of cell-cell adhesion (GO:0022407)	*SPIB,SIRPG,TNF*	3,26	2,85E-04	2,61E-02
35	positive regulation of cell-cell adhesion (GO:0022409)	*SPIB,SIRPG,TNF*	3,75	7,30E-05	1,02E-02
36	cell projection assembly (GO:0030031)	*SPIB,CDH13,ONECUT2,MTSS1*	2,39	6,52E-04	3,74E-02
37	myeloid cell differentiation (GO:0030099)	*SPIB,IKZF1,TNF,RELB,IFI16*	2,28	2,40E-04	2,28E-02
38	**regulation of cell adhesion (GO:0030155)**	***SPIB,SIRPG,CDH13,TNF,ONECUT2***	**2,45**	**1,08E-04**	**1,27E-02**
39	**positive regulation of cell migration (GO:0030335)**	***SPIB,CDH13,PDGFRA,ONECUT2***	**2,51**	**4,32E-04**	**3,08E-02**
40	cellular response to DNA damage stimulus (GO:0034984)	*SPIB,FANCI,ESCO2,CIDEA,IFI16,TYMS*	1,73	9,90E-04	4,83E-02
41	**regulation of growth (GO:0040008)**	***SPIB,IKZF1,CDH13,ESM1,HMGA2,RERG,SHC1***	**1,99**	**8,81E-05**	**1,17E-02**
42	**regulation of cell proliferation (GO:0042127)**	***SPIB,SIRPG,CDH13,CXCL1,TNF,ADRA2A,PDGFRA,CHST11,RUNX2,RERG,PTGER2,SHC1***	**1,76**	**3,91E-06**	**1,50E-03**
43	vitamin D biosynthetic process (GO:0042368)	*SPIB,TNF*	4,07	7,38E-04	4,06E-02
44	odontogenesis of dentine-containing tooth (GO:0042475)	*SPIB,PDGFRA,RUNX2*	2,83	9,42E-04	4,75E-02
45	regulation of apoptosis (GO:0042981)	*SPIB,CDH13,TNF,IL2RB,PIM2,CASP5,CASP4,STK17B,CHST11,BID,CIDEA,PAX7,IFI16,TERT*	1,94	8,91E-08	1,45E-04
46	positive regulation of apoptosis (GO:0043065)	*SPIB,TNF,CASP4,STK17B,BID,CIDEA,IFI16*	1,84	2,08E-04	2,25E-02
47	**negative regulation of apoptosis (GO:0043066)**	***SPIB,CDH13,TNF,IL2RB,PIM2,CHST11,CIDEA,PAX7,TERT***	**2,13**	**3,18E-06**	**1,50E-03**
48	regulation of programmed cell death (GO:0043067)	*SPIB,CDH13,TNF,IL2RB,PIM2,CASP5,CASP4,STK17B,CHST11,BID,CIDEA,PAX7,IFI16,TERT*	1,93	9,90E-08	1,45E-04
49	positive regulation of programmed cell death (GO:0043068)	*SPIB,TNF,CASP4,STK17B,BID,CIDEA,IFI16*	1,84	2,17E-04	2,27E-02
50	negative regulation of programmed cell death (GO:0043069)	*SPIB,CDH13,TNF,IL2RB,PIM2,CHST11,CIDEA,PAX7,TERT*	2,12	3,44E-06	1,50E-03
51	positive regulation of DNA replication (GO:0045740)	*SPIB,PDGFRA,SHC1*	3,06	4,96E-04	3,30E-02
52	positive regulation of cell adhesion (GO:0045785)	*SPIB,SIRPG,CDH13,TNF*	2,84	1,27E-04	1,43E-02
53	smooth muscle cell proliferation (GO:0048659)	*SPIB,CDH13,TNF,SHC1*	2,89	1,06E-04	1,27E-02
54	regulation of smooth muscle cell proliferation	*SPIB,CDH13,TNF,SHC1*	2,93	9,23E-05	1,17E-02

	(GO:0048660)				
55	positive regulation of smooth muscle cell proliferation (GO:0048661)	*SPIB,CDH13,TNF,SHC1*	3,19	3,44E-05	5,92E-03
56	skeletal system morphogenesis (GO:0048705)	*SPIB,HOXC8,PDGFRA,CHST11,RUNX2*	2,58	5,97E-05	8,74E-03
57	cytokine secretion (GO:0050663)	*SPIB,TNF,CIDEA*	3,02	5,53E-04	3,37E-02
58	regulation of developmental process (GO:0050793)	*SPIB,IKZF1,CDC42SE1,CDH13,TNF,IL2RB,PIM2,CHST11,CIDEA,RUNX2,EZH2,PAX7,TERT*	1,67	4,49E-06	1,50E-03
59	cartilage development (GO:0051216)	*SPIB,CHST11,RUNX2,PAX7*	2,59	3,22E-04	2,73E-02
60	negative regulation of protein transport (GO:0051224)	*SPIB,TNF,CIDEA*	2,91	7,49E-04	4,06E-02
61	positive regulation of cellular component movement (GO:0051272)	*SPIB,CDH13,PDGFRA,ONECUT2*	2,44	5,50E-04	3,37E-02
62	centrosome separation (GO:0051299)	*SPIB,NEK2*	4,16	6,34E-04	3,71E-02
63	negative regulation of amino acid transport (GO:0051956)	*SPIB,TNF*	3,85	1,10E-03	4,94E-02
64	palate development (GO:0060021)	*SPIB,PDGFRA,MEOX2*	3,06	4,96E-04	3,30E-02
65	limb development (GO:0060173)	*SPIB,RAX,CHST11,MEOX2*	2,39	6,70E-04	3,77E-02
66	positive regulation of calcidiol 1- (GO:0060559)	SPIB,TNF	4,16	6,34E-04	3,71E-02

Supplementary Table 6.

№	Term (Biocarta Pathway)	M918T gene list	odds_ratio_log	pvalue	adj_pvalue
1	Angiotensin II mediated activation of JNK Pathway via Pyk2 dependent signaling (h_At1rPathway)	*SPIB,SHC1*	3,302	3,07E-03	2,57E-02
2	BCR Signaling Pathway (h_bcrPathway)	*SPIB,SHC1*	3,028	5,06E-03	3,28E-02
3	Bioactive Peptide Induced Signaling Pathway (h_biopeptidesPathway)	*SPIB,SHC1*	3,202	3,68E-03	2,57E-02
4	CBL mediated ligand-induced downregulation of EGF receptors (h_cblPathway)	*SPIB,PDGFRA*	4,168	6,78E-04	2,11E-02
5	Cadmium induces DNA synthesis and proliferation in macrophages (h_cdMacPathway)	*SPIB,TNF*	3,945	9,89E-04	2,11E-02
6	Apoptotic Signaling in Response to DNA Damage (h_chemicalPathway)	*SPIB,BID*	3,682	1,56E-03	2,12E-02
7	Cytokine Network (h_cytokinePathway)	*SPIB,TNF*	3,762	1,36E-03	2,12E-02
8	Induction of apoptosis through DR3 and DR4/5 Death Receptors (h_deathPathway)	*SPIB,BID*	3,156	4,01E-03	2,66E-02
9	Phospholipids as signalling intermediaries (h_edg1Pathway)	*SPIB,PDGFRA*	3,302	3,07E-03	2,57E-02
10	EGF Signaling Pathway (h_egfPathway)	*SPIB,SHC1*	3,414	2,52E-03	2,57E-02
11	EPO Signaling Pathway (h_epoPathway)	*SPIB,SHC1*	3,682	1,56E-03	2,12E-02
12	Role of Erk5 in Neuronal Survival (h_erk5Pathway)	*SPIB,SHC1*	3,849	1,17E-03	2,11E-02
13	Fc Epsilon Receptor I Signaling in Mast Cells (h_fcer1Pathway)	*SPIB,SHC1*	2,845	7,06E-03	4,17E-02
14	Growth Hormone Signaling Pathway (h_ghPathway)	*SPIB,SHC1*	3,202	3,68E-03	2,57E-02

15	Adhesion and Diapedesis of Granulocytes (h_granulocytesPathway)	*SPIB,TNF*	3,945	9,89E-04	2,11E-02
16	Calcium Signaling by HBx of Hepatitis B virus (h_HBxPathway)	*SPIB,SHC1*	5,149	1,53E-04	1,04E-02
17	Role of ERBB2 in Signal Transduction and Oncology (h_her2Pathway)	*SPIB,SHC1*	3,251	3,37E-03	2,57E-02
18	HIV-I Nef (h_HivnefPathway)	*SPIB,TNF,BID*	2,949	6,98E-04	2,11E-02
19	Stress Induction of HSP Regulation (h_hsp27Pathway)	*SPIB,TNF*	3,945	9,89E-04	2,11E-02
20	IGF-1 Signaling Pathway (h_igf1Pathway)	*SPIB,SHC1*	3,539	2,01E-03	2,38E-02
21	Multiple antiapoptotic pathways from IGF-1R signaling lead to BAD phosphorylation (h_igf1rPathway)	*SPIB,SHC1*	3,302	3,07E-03	2,57E-02
22	Signal transduction through IL1R (h_il1rPathway)	*SPIB,TNF*	3,202	3,68E-03	2,57E-02
23	IL 2 signaling pathway (h_il2Pathway)	*SPIB,IL2RB,SHC1*	4,025	3,87E-05	1,02E-02
24	Cytokines and Inflammatory Response (h_inflamPathway)	*SPIB,TNF*	3,302	3,07E-03	2,57E-02
25	Insulin Signaling Pathway (h_insulinPathway)	*SPIB,SHC1*	3,539	2,01E-03	2,38E-02
26	Integrin Signaling Pathway (h_integrinPathway)	*SPIB,SHC1*	3,156	4,01E-03	2,66E-02
27	Keratinocyte Differentiation (h_keratinocytePathway)	*SPIB,TNF*	2,879	6,63E-03	4,01E-02
28	NF-kB Signaling Pathway (h_nfkbPathway)	*SPIB,TNF*	3,682	1,56E-03	2,12E-02
29	Nerve growth factor pathway (NGF) (h_ngfPathway)	*SPIB,SHC1*	3,357	2,79E-03	2,57E-02
30	p38 MAPK Signaling Pathway (h_p38mapkPathway)	*SPIB,SHC1*	3,202	3,68E-03	2,57E-02
31	PDGF Signaling Pathway (h_pdgfPathway)	*SPIB,PDGFRA,SHC1*	3,773	7,48E-05	1,02E-02
32	Regulation of transcriptional activity by PML (h_pmlPathway)	*SPIB,TNF*	3,849	1,17E-03	2,11E-02
33	Links between Pyk2 and Map Kinases (h_pyk2Pathway)	*SPIB,SHC1*	3,302	3,07E-03	2,57E-02
34	Acetylation and Deacetylation of RelA in The Nucleus (h_RELAPathway)	*SPIB,TNF*	4,168	6,78E-04	2,11E-02
35	SODD/TNFR1 Signaling Pathway (h_soddPathway)	*SPIB,TNF*	4,301	5,43E-04	2,11E-02
36	Sprouty regulation of tyrosine kinase signals (h_spryPathway)	*SPIB,SHC1*	3,762	1,36E-03	2,12E-02
37	TNF/Stress Related Signaling (h_stressPathway)	*SPIB,TNF*	3,608	1,78E-03	2,30E-02
38	T Cell Receptor Signaling Pathway (h_tcrPathway)	*SPIB,SHC1*	2,879	6,63E-03	4,01E-02
39	Chaperones modulate interferon Signaling Pathway (h_tidPathway)	*SPIB,TNF*	4,301	5,43E-04	2,11E-02
40	TNFR1 Signaling Pathway (h_tnfr1Pathway)	*SPIB,TNF*	3,251	3,37E-03	2,57E-02
41	TPO Signaling Pathway (h_TPOPathway)	*SPIB,SHC1*	3,357	2,79E-03	2,57E-02
42	Trka Receptor Signaling Pathway (h_trkaPathway)	*SPIB,SHC1*	3,849	1,17E-03	2,11E-02
43	VEGF, Hypoxia, and Angiogenesis (h_vegfPathway)	*SPIB,SHC1*	3,202	3,68E-03	2,57E-02
44	Wnt/LRP6 Signalling (h_wnt-lrp6Pathway)	*SPIB,KREMEN2*	5,149	1,53E-04	1,04E-02
45	IL-2 Receptor Beta Chain in T cell Activation (h_il2rbPathway)	*IL2RB,SHC1*	2,879	6,63E-03	4,01E-02
46	Erk1/Erk2 Mapk Signaling pathway (h_erkPathway)	*PDGFRA,SHC1*	3,251	3,37E-03	2,57E-02

Appendix III

Other publications

1. Cancer Res. 2012 Jul 17. [Epub ahead of print]

The hematologic-specific β-tubulin VI exhibits genetic variability influencing paclitaxel toxicity.

Leandro-García LJ, Leskelä S, Inglada-Perez L, Landa I, de Cubas AA, Maliszewska A, Comino-Méndez I, Letón R, Gómez-Graña A, Torres R, Ramírez JC, Alvarez S, Rivera J, Martinez C, Lozano ML, Cascon A, Robledo M and Rodríguez-Antona C.

Cellular microtubules composed of α-β-tubulin heterodimers that are essential for cell shape, division and intracellular transport are valid targets for anticancer therapy. However, not all the conserved but differentially expressed members of the β-tubulin gene superfamily have been investigated for their role in these settings. In this study, we examined roles for the hematologic isoform β-tubulin VI and functional genetic variants in the gene. β-tubulin VI was highly expressed in blood cells with a substantial interindividual variability (7-fold variation in mRNA). We characterized DNA missense variations leading to Q43P, T274M and R307H, and a rare nonsense variant, Y55X. Since variations in the hematologic target of microtubule binding drugs might alter their myelosuppressive action, we tested their effect in cell lines stably expressing the different β-tubulin VI full length variants, finding that the T274M change significantly decreased sensitivity to paclitaxel-induced tubulin polymerization. Furthermore, patients treated with paclitaxel and carrying β-tubulin VI T274M exhibited a significant reduction in thrombocytopenia than wild-type homozygous patients (P=0.031). Together, our findings define β-tubulin VI as a hematologic isotype with significant genetic variation in humans that may affect the myelosuppresive action of microtubule-binding drugs.

2. Clin Cancer Res. 2012 Jul 13. [Epub ahead of print]

Regulatory Polymorphisms in β-Tubulin IIa Are Associated with Paclitaxel-Induced Peripheral Neuropathy.

Leandro-García LJ, Leskelä S, Jara C, Gréen H, Avall-Lundqvist E, Wheeler HE, Dolan ME, Inglada-Perez L, Maliszewska A, de Cubas AA, Comino-Méndez I, Mancikova V, Cascón A, Robledo M, Rodríguez-Antona C.

PURPOSE: Peripheral neuropathy is the dose-limiting toxicity of paclitaxel, a chemotherapeutic drug widely used to treat several solid tumors such as breast, lung, and ovary. The cytotoxic effect of paclitaxel is mediated through β-tubulin binding in the cellular microtubules. In this study, we investigated the association between paclitaxel neurotoxicity risk and regulatory genetic variants in β-tubulin genes.

EXPERIMENTAL DESIGN: We measured variation in gene expression of three β-tubulin isotypes (I, IVb, and IIa) in lymphocytes from 100 healthy volunteers, sequenced the promoter region to identify polymorphisms putatively influencing gene expression and assessed the transcription rate of the identified variants using luciferase assays. To determine whether the identified regulatory polymorphisms were associated with paclitaxel neurotoxicity, we genotyped them in 214 patients treated with paclitaxel. In addition, paclitaxel-induced cytotoxicity in lymphoblastoid cell lines was compared with β-tubulin expression as measured by Affymetrix exon array.

RESULTS: We found a 63-fold variation in β-tubulin IIa gene (TUBB2A) mRNA content and three polymorphisms located at -101, -112, and -157 in TUBB2A promoter correlated with increased mRNA levels. The -101 and -112 variants, in total linkage disequilibrium, conferred TUBB2A increased transcription rate. Furthermore, these variants protected from paclitaxel-induced peripheral neuropathy [HR, 0.62; 95% confidence interval (CI), 0.42-0.93; P = 0.021, multivariable analysis]. In addition, an inverse correlation between TUBB2A and paclitaxel-induced apoptosis (P = 0.001) in lymphoblastoid cell lines further supported that higher TUBB2A gene expression conferred lower paclitaxel sensitivity.

CONCLUSIONS: This is the first study showing that paclitaxel neuropathy risk is influenced by polymorphisms regulating the expression of a β-tubulin gene.

3. Hum Pathol. 2012 Jul;43(7):1103-12. Epub 2011 Dec 29.

Thyroid paraganglioma. Report of 3 cases and description of an immunohistochemical profile useful in the differential diagnosis with medullary thyroid carcinoma, based on complementary DNA array results.

Castelblanco E, Gallel P, Ros S, Gatius S, Valls J, De-Cubas AA, Maliszewska A, Yebra-Pimentel MT, Menarguez J, Gamallo C, Opocher G, Robledo M, Matias-Guiu X.

Thyroid paraganglioma is a rare disorder that sometimes poses problems in differential diagnosis with medullary thyroid carcinoma. So far, differential diagnosis is solved with the help of some markers that are frequently expressed in medullary thyroid carcinoma (thyroid transcription factor 1, calcitonin, and carcinoembryonic antigen). However, some of these markers are not absolutely specific of medullary thyroid carcinoma and may be expressed in other tumors. Here we report 3 new cases of thyroid paraganglioma and describe our strategy to design a diagnostic immunohistochemical battery. First, we performed a comparative analysis of the expression profile of head and neck paragangliomas and medullary thyroid carcinoma, obtained after complementary DNA array analysis of 2 series of fresh-frozen samples of paragangliomas and medullary thyroid carcinoma, respectively. Seven biomarkers showing differential expression were selected (nicotinamide adenine dinucleotide dehydrogenase 1 alpha subcomplex, 4-like 2, NDUFA4L2; cytochrome c oxidase subunit IV isoform 2; vesicular monoamine transporter 2; calcitonin gene-related protein/calcitonin; carcinoembryonic antigen; and thyroid transcription factor 1) for immunohistochemical analysis. Two tissue microarrays were constructed from 2 different series of paraffin-embedded samples of paragangliomas and medullary thyroid carcinoma. We provide a classifying rule for differential diagnosis that combines negativity or low staining for calcitonin gene-related protein (histologic score, <10) or calcitonin (histologic score, <50) together with positivity of any of NADH dehydrogenase 1 alpha subcomplex, 4-like 2; cytochrome c oxidase subunit IV isoform 2; or vesicular monoamine transporter 2 to predict paragangliomas, showing a prediction error of 0%. Finally, the immunohistochemical battery was checked in paraffin-embedded blocks from 4 examples of thyroid paraganglioma (1 previously reported case and 3 new cases), showing also a prediction error of 0%. Our results suggest that the comparative expression profile, obtained by complementary DNA arrays, seems to be a good tool to design immunohistochemical batteries used in differential diagnosis.

4. Oncogene. 2011 Dec 12. doi: 10.1038/onc.2011.556. [Epub ahead of print]

Sprouty1 is a candidate tumor-suppressor gene in medullary thyroid carcinoma.

Macià A, Gallel P, Vaquero M, Gou-Fabregas M, Santacana M, Maliszewska A, Robledo M, Gardiner JR, Basson MA, Matias-Guiu X, Encinas M.

Medullary thyroid carcinoma (MTC) is a malignancy derived from the calcitonin-producing C-cells of the thyroid gland. Oncogenic mutations of the Ret proto-oncogene are found in all heritable forms of MTC and roughly one half of the sporadic cases. However, several lines of evidence argue for the existence of additional genetic lesions necessary for the development of MTC. Sprouty (Spry) family of genes is composed of four members in mammals (Spry1-4). Some Spry family members have been proposed as candidate tumor-suppressor genes in a variety of cancerous pathologies. In this work, we show that targeted deletion of Spry1 causes C-cell hyperplasia, a precancerous lesion preceding MTC, in young adult mice. Expression of Spry1 restrains proliferation of the MTC-derived cell line, TT. Finally, we found that the Spry1 promoter is frequently methylated in MTC and that Spry1 expression is consequently decreased. These findings identify Spry1 as a candidate tumor-suppressor gene in MTC.

5. Nat Genet. 2011 Jun 19;43(7):663-7. doi: 10.1038/ng.861.

Exome sequencing identifies MAX mutations as a cause of hereditary pheochromocytoma.

Comino-Méndez I, Gracia-Aznárez FJ, Schiavi F, Landa I, Leandro-García LJ, Letón R, Honrado E, Ramos-Medina R, Caronia D, Pita G, Gómez-Graña A, de Cubas AA, Inglada-Pérez L, Maliszewska A, Taschin E, Bobisse S, Pica G, Loli P, Hernández-Lavado R, Díaz JA, Gómez-Morales M, González-Neira A, Roncador G, Rodríguez-Antona C, Benítez J, Mannelli M, Opocher G, Robledo M, Cascón A.

Hereditary pheochromocytoma (PCC) is often caused by germline mutations in one of nine susceptibility genes described to date, but there are familial cases without mutations in these known genes. We sequenced the exomes of three unrelated individuals with hereditary PCC (cases) and identified mutations in MAX, the MYC associated factor X gene. Absence of MAX protein in the tumors and loss of heterozygosity caused by uniparental disomy supported the involvement of MAX alterations in the disease. A follow-up study of a selected series of 59 cases with PCC identified five additional MAX mutations and suggested an association with malignant outcome and preferential paternal transmission of MAX mutations. The involvement of the MYC-MAX-MXD1 network in the development and progression of neural crest cell tumors is further supported by the lack of functional MAX in rat PCC (PC12) cells and by the amplification of MYCN in neuroblastoma and suggests that loss of MAX function is correlated with metastatic potential.

6. Mol Endocrinol. 2010 Dec;24(12):2382-91. Epub 2010 Oct 27.

Research resource: Transcriptional profiling reveals different pseudohypoxic signatures in SDHB and VHL-related pheochromocytomas.

López-Jiménez E, Gómez-López G, Leandro-García LJ, Muñoz I, Schiavi F, Montero-Conde C, de Cubas AA, Ramires R, Landa I, Leskelä S, Maliszewska A, Inglada-Pérez L, de la Vega L, Rodríguez-Antona C, Letón R, Bernal C, de Campos JM, Diez-Tascón C, Fraga MF, Boullosa C, Pisano DG, Opocher G, Robledo M, Cascón A.

The six major genes involved in hereditary susceptibility for pheochromocytoma (PCC)/paraganglioma (PGL) (RET, VHL, NF1, SDHB, SDHC, and SDHD) have been recently integrated into the same neuronal apoptotic pathway where mutations in any of these genes lead to cell death. In this model, prolyl hydroxylase 3 (EglN3) abrogation plays a pivotal role, but the molecular mechanisms underlying its inactivation are currently unknown. The aim of the study was to decipher specific alterations associated with the different genetic classes of PCCs/PGLs. With this purpose, 84 genetically characterized tumors were analyzed by means of transcriptional profiling. The analysis revealed a hypoxia-inducible factor (HIF)-related signature common to succinate dehydrogenase (SDH) and von Hippel-Lindau (VHL) tumors, that differentiated them from RET and neurofibromatosis type 1 cases. Both canonical HIF-1α and HIF-2α target genes were overexpressed in the SDH/VHL cluster, suggesting that a global HIF deregulation accounts for this common profile. Nevertheless, when we compared VHL tumors with SDHB cases, which often exhibit a malignant behavior, we found that HIF-1α target genes showed a predominant activation in the VHL PCCs. Expression data from 67 HIF target genes was sufficient to cluster SDHB and VHL tumors into two different groups, demonstrating different pseudo-hypoxic signatures. In addition, VHL-mutated tumors showed an unexpected overexpression of EglN3 mRNA that did not lead to significantly different EglN3 protein levels. These findings pave the way for more specific therapeutic approaches for malignant PCCs/PGLs management based on the patient's genetic alteration.

7. Horm Metab Res. 2009 Sep;41(9):672-5. Epub 2009 Apr 2.

Rationalization of genetic testing in patients with apparently sporadic pheochromocytoma/paraganglioma.

Cascón A, López-Jiménez E, Landa I, Leskelä S, Leandro-García LJ, Maliszewska A, Letón R, de la Vega L, García-Barcina MJ, Sanabria C, Alvarez-Escolá C, Rodríguez-Antona C, Robledo M.

Hereditary susceptibility to pheochromocytoma (PCC) and paraganglioma (PGL) represents a very complex genetic scenario. It has been reported that the absence of familial antecedents of the disease does not preclude the existence of a mutation affecting any of the five major susceptibility genes. In fact, 11-24% of apparently sporadic cases (without familial or syndromic antecedents) harbor an unexpected germline mutation, but we do not know what is happening in "truly apparently" sporadic patients (i.e., apparently sporadic cases diagnosed with only one tumor). In the present study, we have analyzed 135 apparently sporadic patients developing a single tumor for the five major susceptibility genes: VHL, RET, SDHB, SDHC, and SDHD. Fourteen percent of cases were found to harbor a germline mutation, and only 2.2% of patients were older than 45 years at onset. By taking into account the tumor location and a threshold age at onset of 45 years, we propose a rational scheme for genetic testing. Analyzing VHL and RET genes would be recommended only in young patients developing a single PCC. On the other hand, genetic testing of SDHD should be done in all patients developing an extra-adrenal tumor before the age of 45, and SDHC could be the responsible gene in cases developing a single head and neck tumor, independently of age. Finally, the analysis of SDHB should always be performed because of its association to malignancy and the low penetrance of mutations affecting this gene.

8. Electrochemistry Communications 11 (2009) 664–667.

DNA surface nanopatterning by selective reductive desorption from polycrystalline gold electrode.

Henry OYF, Maliszewska A, O'Sullivan CK.

Selective electrochemical desorption was employed to pattern polycrystalline gold electrodes with thiolated DNA. The sacrificial thiol 3-mercaptopropionic acid (3-MPA) was selectively desorbed from the crystallographic plane Au(111) to revealed bare gold domains, surrounded by SAMs of 3-MPA present on the adjacent low index planes Au(110) and Au(100). Thiolated DNA sequences were further immobilized on the revealed Au(111) and the hybridisation efficiency towards complementary and non-complementary sequences evaluated. All derivatisation steps were followed by cyclic voltammetry and faradaic electrochemical impedance spectroscopy. Successful hybridisation resulted in large drops in resistance to charge transfer, attributed to the extension of the DNA surface duplex into solution resulting in an increased diffusion of electrochemical probes to the electrode surface. The results demonstrated the feasibility of the method to generate a DNA sensor able to efficiently discriminate between complementary and non-complementary sequences with good reproducibility.

9. J Org Chem. 2007 Mar 30;72(7):2682-5. Epub 2007 Mar 1.

Synthesis of alpha-phosphorylated alpha,beta-unsaturated imines and their selective reduction to vinylogous and saturated alpha-aminophosphonates.

Palacios F, Vicario J, Maliszewska A, Aparicio D.

An efficient synthesis of α,β-unsaturated imines derived from α-aminophosphonates is achieved through aza-Wittig reaction of P-trimethyl phosphazenes with β,γ-unsaturated α-ketophosphonates. Selective 1,2-reduction of such 1-azadienes affords β,γ-unsaturated α-aminophosphonates, phosphorylated analogs of vinylglycines, which are hydrogenated to yield saturated α-aminophosphonate derivatives.